

DTIC FILE COPY

2

AD-A220 070

# WATER HEAT PIPE FROZEN STARTUP AND SHUTDOWN TRANSIENTS WITH INTERNAL TEMPERATURE, PRESSURE AND VISUAL OBSERVATION

T. Reinarts, et al



Texas A&M University  
College Station, TX 77843

February 1990

Final Report

Approved for public release; distribution is unlimited.

DTIC  
LECTE  
APR 02 1990  
E D

Weapons Laboratory  
Air Force Systems Command  
Kirtland Air Force Base, NM 87117-6008

90 04 02 055

This final report was prepared by Texas A&M University, College Station, Texas, under Contract F29601-84-K-0078, Job Order 57972308 with the Weapons Laboratory, Kirtland Air Force Base, New Mexico. First Lieutenant Donald A. Verrill (TA) was the Laboratory Project Officer-in-Charge.

When Government drawings, specifications, or other data are used for any purpose other than in connection with a definitely Government-related procurement, the United States Government incurs no responsibility or any obligation whatsoever. The fact that the Government may have formulated or in any way supplied the said drawings, specifications, or other data, is not to be regarded by implication, or otherwise in any manner construed, as licensing the holder, or any other person or corporation; or as conveying any rights or permission to manufacture, use, or sell any patented invention that may in any way be related thereto.

This report has been authored by a contractor of the United States Government. Accordingly, the United States Government retains a nonexclusive, royalty-free license to publish or reproduce the material contained herein, or allow others to do so, for the United States Government purposes.

This report has been reviewed by the Public Affairs Office and is releasable to the National Technical Information Service (NTIS). At NTIS, it will be available to the general public, including foreign nationals.

If your address has changed, if you wish to be removed from our mailing list, or if your organization no longer employs the addressee, please notify WL/TA, Kirtland AFB, NM 87117-6008 to help us maintain a current mailing list.

This technical report has been reviewed and is approved for publication.



DONALD A. VERRILL  
1Lt, USAF  
Project Officer

FOR THE COMMANDER



FRANCIS J. JANKOWSKI  
Acting Chief  
Space Nuclear Power Systems Branch



ERNEST D. HERRERA  
Lt Col, USAF  
Chief, Applied Technology Division

DO NOT RETURN COPIES OF THIS REPORT UNLESS CONTRACTUAL OBLIGATIONS OR NOTICE ON A SPECIFIC DOCUMENT REQUIRES THAT IT BE RETURNED.

# REPORT DOCUMENTATION PAGE

Form Approved  
OMB No. 0704-0188

Public reporting burden for this collection of information is estimated to average 1 hour per response, including the time for reviewing instructions, searching existing data sources, gathering and maintaining the data needed, and completing and reviewing the collection of information. Send comments regarding this burden estimate or any other aspect of this collection of information, including suggestions for reducing this burden, to Washington Headquarters Services, Directorate for Information Operations and Reports, 1215 Jefferson Davis Highway, Suite 1204, Arlington, VA 22202-4302, and to the Office of Management and Budget, Paperwork Reduction Project (0704-0188), Washington, DC 20503.

<b>1. AGENCY USE ONLY (Leave blank)</b>		<b>2. REPORT DATE</b> February 1990	<b>3. REPORT TYPE AND DATES COVERED</b> Final Report - Sep 84-May 89
<b>4. TITLE AND SUBTITLE</b> WATER HEAT PIPE FROZEN STARTUP AND SHUTDOWN TRANSIENTS WITH INTERNAL TEMPERATURE, PRESSURE AND VISUAL OBSERVATIONS		<b>5. FUNDING NUMBERS</b> PE: 62601F PR: 5797 TA: 23 WU: 08 C: F29601-84-K-0078	
<b>6. AUTHOR(S)</b> Reinarts, T.; DeHart, M.; Peery, J.; Best, F.			
<b>7. PERFORMING ORGANIZATION NAME(S) AND ADDRESS(ES)</b> Texas A&M University College Station, Texas 77843		<b>8. PERFORMING ORGANIZATION REPORT NUMBER</b>	
<b>9. SPONSORING / MONITORING AGENCY NAME(S) AND ADDRESS(ES)</b> Weapons Laboratory Kirtland AFB, NM 87117-6008		<b>10. SPONSORING / MONITORING AGENCY REPORT NUMBER</b>  WL-TR-89-59	
<b>11. SUPPLEMENTARY NOTES</b>			
<b>12a. DISTRIBUTION / AVAILABILITY STATEMENT</b>  Distribution Statement A		<b>12b. DISTRIBUTION CODE</b>	
<b>13. ABSTRACT (Maximum 200 words)</b> Three sets of experiments were performed to analyze the transient nature of heat pipes and possible failures. The first set studied the entrainment phenomenon and suggests that entrainment starts in a form not readily observable by other than visual means. The second set used a specially designed heat pipe with a rectangular cross section, flat mesh-type wick, and a clear top through which internal mechanisms of heat pipe operation could be seen. These served as scoping experiments for the third set. The third set measured vapor space temperatures, wick/liquid temperatures, and internal pressure. A normal start-up experiment, and experiment with step changes in input power levels, including previously unexpected pressure transients and two frozen start-ups, a step decrease in power input to the evaporator, and a steady-state run with decreasing secondary coolant temperature were performed. In addition to the experiments, a multinodal, implicit, finite difference model was developed to stimulate heat pipe rapid transients. The mass, momentum, and energy conservation equations generate the velocity, pressure, and temperature profiles. The temperature profiles differed significantly from the experimental data, but the pressure and velocity profiles agree well with existing theory.			
<b>14. SUBJECT TERMS</b> Heat Pipe Transient Analysis Heat Pipe Entrainment		Pressure Transients Frozen Startup	<b>15. NUMBER OF PAGES</b> 338 <b>16. PRICE CODE</b>
<b>17. SECURITY CLASSIFICATION OF REPORT</b> Unclassified	<b>18. SECURITY CLASSIFICATION OF THIS PAGE</b> Unclassified	<b>19. SECURITY CLASSIFICATION OF ABSTRACT</b> Unclassified	<b>20. LIMITATION OF ABSTRACT</b>

## SUMMARY

Three different sets of experiments have been performed to analyze the transient nature of heat pipes and failures that may occur in those transients. The first studied the entrainment phenomenon and indicated that this phenomenon occurs at higher velocities than previously suspected. In a glass-walled model of a heat pipe, air was blown over wetted wick material in order to determine the onset of entrainment. Results suggest that entrainment actually starts in a form not readily observable by other than visual means.

The second set of experiments used a specially designed heat pipe with a rectangular cross section, flat mesh-type wick and a clear top through which internal mechanisms of heat pipe operation could be observed. The transient conditions observed were startup and load change. Thermocouples on the outside of the pipe and inside the vapor space were used to study temperature profiles during operation, and a data acquisition system was used to concurrently display and record all measurements as the experiments ran. The heat pipe operated in a manner consistent with theory. Results of the experimental work indicate that certain transient modes of operation can cause failure where not predicted by steady-state theory.

In the third set of transient experiments, vapor space temperatures, wick/liquid temperatures, and internal pressure were measured. A normal startup experiment was performed, as was an experiment with step changes in input power levels. Two frozen startups were then performed. In another experimental series, the pipe was brought to steady-state conditions with a power input of 25 W, and the secondary coolant temperature was lowered until the heat pipe working fluid froze and the evaporator wick dried out. Finally, data were obtained on a step decrease in power input to the evaporator.

These unique data on frozen heat pipes, including previously unexpected pressure transients, show there are many parameters to be considered in frozen startups of a heat pipe, including the power input, secondary coolant temperature, and amount of working fluid in the wick. In both of these frozen startups, the data indicate that normal operation was not achieved.

In addition to the experimental work, a multinodal, implicit, finite difference

model, Heat Pipe Transient Analysis Code (HPTAC), has been developed to simulate heat pipe rapid transients. The mass, momentum, and energy conservation equations are employed to generate the velocity, pressure, and temperature profiles in a heat pipe. A lumped capacitance exponential model for stored energy is used in order to achieve a solution for the thermal hydraulic phenomena associated with a heat pipe. The numerical model is compared to data from the second series of experimental heat pipes. The temperature profiles generated by the numerical model differ significantly from the experimental data, but the pressure and velocity profiles agree well with existing theory.

<b>Accession For</b>	
NTIS GRA&I	<input checked="" type="checkbox"/>
DTIC TAB	<input type="checkbox"/>
Unannounced	<input type="checkbox"/>
Justification	
By _____	
Distribution/	
Availability Codes	
Dist	Avail and/or Special
A-1	



## TABLE OF CONTENTS

	Page
Section 1: Introduction.....	1
1.1 Introduction.....	1
1.2 Literature Review.....	3
1.3 Heat Pipe Theory.....	6
1.4 Report Organization.....	14
Section 2 : Entrainment Experiments.....	15
2.1 Introduction.....	15
2.2 Experimental Setup.....	15
2.3 Experimental Procedures.....	16
2.4 Results and Discussion.....	17
2.5 Summary.....	21
Section 3 : Heat Pipe Scoping Experiments.....	22
3.1 Introduction.....	22
3.2 Experimental Setup.....	22
3.3 Experimental Procedures.....	36
3.4 Results and Discussion.....	39
3.5 Summary.....	66

Section 4 : Heat Pipe Experiments.....	68
4.1 Experimental Setup.....	68
4.2 Experimental Procedures.....	91
4.3 Results and Discussion.....	92
4.4 Summary.....	146
Section 5 : Modeling Work.....	147
5.1 Heat Pipe Model Development.....	147
5.2 Application of the Model .....	187
5.3 Summary.....	206
Section 6 : Conclusions and Recommendations.....	213
References.....	218
Appendix A HABL Computer Code Listing.....	223
Appendix B HPIPE Computer Code Listing.....	233
Appendix C Hp-TK1 BASIC File Listing.....	242
Appendix D Data Collection Batch File.....	252
Appendix E Computer Code Listing.....	255
Appendix F Energy Equation Term Definitions.....	317
Appendix G Nomenclature.....	321

## LIST OF FIGURES

	Page
Figure 1. General Schematic of a Wicked Heat Pipe	7
Figure 2. Working Drawings of the Experimental Heat Pipe	8
Figure 3. The Change in the Radius of Curvature of Menisci in Different Sections of a Heat Pipe	9
Figure 4. Liquid and Vapor Phase Pressure Profiles in a Heat Pipe Where Partial Pressure Recovery Occurs in the Vapor Phase	11
Figure 5. Apparatus for Entrainment Observation	16
Figure 6. Air Flow Over a Slightly Wrinkled Wetted Wick	18
Figure 7. Proposed Form of Entrainment Inception	19
Figure 8. Predicted and Measured Velocities for Entrainment	20
Figure 9. Dimensions of the Experimental Heat Pipe	23
Figure 10. Schematic Diagram of the System Layout	24
Figure 11. Thermocouple Placement in the Heat Pipe	27
Figure 12. Operation Versus Conduction at 100 W	41
Figure 13. Operation Versus Conduction at 250 W	42
Figure 14. Evaporator, Adiat, and Condenser Temperatures for Run 3	46
Figure 15. Evaporator Temperature Versus Time for Run 5	48
Figure 16. Adiat Temperature Versus Time for Run 5	49
Figure 17. Condenser Temperature Versus Time for Run 5	50
Figure 18. Vapor Temperature Versus Time for Run 3	51
Figure 19. Temperature Profile at Heat Pipe Outer Wall During Start-up	54
Figure 20. Temperature Profile in Vapor Channel During Start-up	55
Figure 21. Evaporator, Adiat, and Condenser Temperature for Run 2	57

	Page
Figure 22. Evaporator Temperature Versus Time for Run 4	58
Figure 23. Condenser and Adiabatic Temperatures for Run 4	59
Figure 24. Vapor Temperature Versus Time for Run 4	60
Figure 25. Evaporator, Adiabatic, and Condenser Temperatures for Run 7	61
Figure 26. Vapor Channel Temperatures for Run 7	62
Figure 27. Vapor Channel Temperatures Near Time of Transient (Run 7)	64
Figure 28. Condenser Pressure Near Time of Transient (Run 7)	65
Figure 29. Overall Experiment Layout	70
Figure 30. Overall Side View of Heat Pipe	71
Figure 31. Placement of Instrumentation (Except K Thermocouples)	73
Figure 32. Placement of K Thermocouples	74
Figure 33. Heat Pipe Channel Cross Section	75
Figure 34. Condenser and Evaporator Cross Sections	76
Figure 35. Cross-sectional View of Adiabatic Shoulder Holes	78
Figure 36. Cross-sectional View of Insulation in Adiabatic	81
Figure 37. View of Heat Pipe Outer Wall Shoulder Thermocouple	82
Figure 38. View of Vapor Space Thermocouples	83
Figure 39. Pressure Transducer Calibration Setup	85
Figure 40. Pressure Transducer Calibration Data	86
Figure 41. Differential Temperature Calibration Setup	89
Figure 42. Differential Temperature Calibration Data	90
Figure 43. Location of Instrumentation (except K thermocouples) 100 W	94
Figure 44. Location of K Thermocouples 100 W	95
Figure 45. Liquid/Wick and Vapor Space Thermocouples For 100 W	96
Figure 46. Outer Wall Measurements For 100 W	97

	Page
Figure 47. Location of Instrumentation (except K thermocouples) 0-50-100-200-250	101
Figure 48. Location of K Thermocouples 0-50-100-200-250	102
Figure 49. Liquid/Wick and Vapor Space Thermocouples 0-50 W	103
Figure 50. Outer Wall Measurements for 0-50 W	104
Figure 51. Pressure for 0-50 W	105
Figure 52. Liquid/Wick and Vapor Space Thermocouples for 50-100 W	109
Figure 53. Outer Wall Measurements for 50-100 W	110
Figure 54. Liquid/Wick and Vapor Space Thermocouples for 100-200 W	111
Figure 55. Outer Wall Measurements for 100-200 W	112
Figure 56. Power 100-200 W	113
Figure 57. Location of Instrumentation (except K thermocouples)	116
Figure 58. Location of K Thermocouples	117
Figure 59. Liquid/Wick and Vapor Space Thermocouples For Frozen Start-up 1	118
Figure 60. Enlargement of Figure 59	119
Figure 61. Outer Wall Measurements for Frozen Start-up 1	120
Figure 62. Enlargement of Outer Wall Thermocouples for Frozen Start-up 1	121
Figure 63. Diagram of Ice Formations	125
Figure 64. Location of Instrumentation (except K thermocouples) for Frozen 2	129
Figure 65. Location of K Thermocouples for Frozen 2	130
Figure 66. Liquid/Wick and Vapor Space Thermocouples for Frozen Start-up 2	131
Figure 67. Outer Wall Measurements For Frozen Start-Up 2	132
Figure 68. Vapor Space Temperatures for 25 W With Decreasing Secondary Coolant	137

	Page
Figure 69. Outer Aluminum Wall Temperatures for 25 W With Decreasing Secondary Coolant	138
Figure 70. Vapor Space Temperatures for 25 W with Decreasing Secondary Coolant Temperature	139
Figure 71. Outer Aluminum Wall Temperatures for 25 W with Decreasing Secondary Coolant Temperature	140
Figure 72. Vapor Space and Liquid Space for Downpower from 250 W	143
Figure 73. Outer Aluminum Wall Temperatures for Downpower from 250 W	144
Figure 74. Power Removed By Secondary Coolant for Downpower from 250 W	145
Figure 75. Nodal Scheme for the Heat Pipe Numerical Model	148
Figure 76. Vapor Control Volume for the Mass Conservation Equation	150
Figure 77. Liquid Control Volume for the Mass Conservation Equation	153
Figure 78. Vapor Control Volume for Axial Momentum	160
Figure 79. Liquid Control Volume for Axial Momentum	162
Figure 80. Outer Wall Region Control Volume for the Energy Equation	169
Figure 81. Inner Wall Region Control Volume for the Energy Equation	172
Figure 82. Liquid-wick Region Control Volume for the Energy Equation	175
Figure 83. Vapor Region Control Volume for the Energy Equation	179
Figure 84. Matrix Generated by the Energy Equation	185
Figure 85. Flow Chart Illustrating the Solution Scheme	186
Figure 86. Computed Outer Wall Temperature Profiles for Various Fluid Charges Compared with Experimental Data for a Power Input of 250 W	193
Figure 87. Computed Outer Wall Temperature Profiles for Various Fluid Charges Compared with Experimental Data for a Power Input of 100 W	194

	Page
Figure 88. Heat Pipe Temperatures at Different Radial Locations for a Power Input of 250 W and a Fluid Charge of 100 ml	197
Figure 89. Heat Pipe Temperatures at Different Radial Locations for a Power Input of 250 W and a Fluid Charge of 180 ml	198
Figure 90. Liquid and Vapor Pressure Profiles for a Power Input of 250 W and a Fluid Charge of 100 ml	200
Figure 91. Liquid and Vapor Pressure Profiles for a Power Input of 250 W and a Fluid Charge of 180 ml	201
Figure 92. Vapor Velocity Profile for a Power Input of 250 W and a Fluid Charge of 100 ml	202
Figure 93. Liquid Velocity Profile for a Power Input of 250 W and a Fluid Charge of 100 ml	203
Figure 94. Vapor Velocity Profile for a Power Input of 250 W and a Fluid Charge of 180 ml	204
Figure 95. Liquid Velocity Profile for a Power Input of 250 W and a Fluid Charge of 180 ml	205
Figure 96. Outer Wall Temperature Profiles for a Power Input of 250 W and a Fluid Charge of 100 ml	207
Figure 97. Outer Wall Temperature Profiles for a Power Input of 250 W and a Fluid Charge of of 180 ml	208
Figure 98. Liquid Temperature Profiles for a Power Input of 250 W and a Fluid Charge of 100 ml	209
Figure 99. Liquid Temperature Profiles for a Power Input of 250 W and a Fluid Charge of 180 ml	210
Figure 100. Vapor Temperature Profiles for a Power Input of 250 W and a Fluid Charge of 100 ml	211
Figure 101. Vapor Temperature Profiles for a Power Input of 250 W and a Fluid Charge of 180 ml	212

## LIST OF TABLES

	Page
Table 1. Resistance to Energy Transport for Regions of a Typical Water Heat Pipe	10
Table 2. Thermocouple Placement Along the Heat Pipe	28
Table 3. Operating Conditions for Startup from Zero Power	45
Table 4. Equilibrium Temperatures for 100- and 250-W Runs	52
Table 5. Outer Aluminum Wall Temperatures Observed and Predicted	114
Table 6. Summary of the Equations used in the Heat Pipe Model Solution	182
Table 7. Initial Conditions and Thermal Constants	189
Table 8. Important Parameters Used or Calculated in the Numerical Model	192

## 1.0 INTRODUCTION

An understanding of transient conditions in a heat pipe is dependent on a more complete understanding of the phenomena occurring inside the heat pipe during the transient. This project attempts to help further that understanding by performing a series of transient heat pipe experiments that include simultaneous measurements of the vapor space and liquid/wick temperatures and vapor space pressures, in addition to visual observation of the inner workings of the heat pipe channel through one clear wall. Outer wall temperatures and power input and output values are also recorded. This information would be useful to help develop and verify a computer model of heat pipe transients. In the introductory section of this section the direction and relevance of and the motivation for the work to be discussed in later chapters is presented. This is followed by a literature review of the historical background of heat pipes and the work already performed in the attempt to understand transient heat pipe operation. The theory of heat pipe operation as it is currently understood is then described. This description includes the operating principles and operating limits of a heat pipe. Finally, the organization of the remainder of the report is summarized at the end of the section.

### 1.1 Introduction

A wicked heat pipe consists of liquid and vapor in a closed void-capillary system which is divided into an evaporator, an adiabatic and a condenser section. When the evaporator section is heated, liquid evaporates, increasing the gas region vapor content and pressure, and causing the vapor-liquid interface there to recede into the capillary structure. The vapor travels to the condenser section due to this pressure gradient and condenses in this lower temperature region. The liquid is then returned to the heated end by capillary forces.

Heat pipe performance is sufficiently well understood in steady-state regimes to allow satisfactory heat pipe design. However, heat pipe designs are generally conservative due to uncertainties in modeling the heat pipe performance under transient conditions<sup>1</sup> (start-up, shutdown, and rapid power changes). Heat pipe

design can be the limiting factor in an energy transport and rejection system. The hydrodynamic ability of a heat pipe to operate through transients depends upon the available capillary forces, which are opposed by friction and acceleration pressure losses.

Heat pipes play an increasingly important role in thermal systems due to their ability to passively transport large quantities of thermal energy over considerable distances with essentially no temperature drop. Heat pipes have been used at Los Alamos National Laboratory to maintain specimens in irradiation cells at constant temperatures while being irradiated.<sup>2</sup> NASA has a continuing program studying the use of heat pipes to carry energy away from the leading edges of hypersonic vehicles traveling through air, such as the space shuttle upon reentry from orbit.<sup>3</sup> Because of their light weight and mechanical simplicity, heat pipes are going to play an important role in the thermal management systems of many spacecraft.<sup>4</sup>

The application of heat pipes to a space environment will necessitate new approaches to the design of heat pipes. Obviously, these heat pipes will have to operate under zero-gravity conditions, or microgravity at best. However, since terrestrial heat pipes have been shown to operate without gravity assistance and can work against gravity, the absence of gravity can be accounted for and have little effect on normal operation; this has been verified experimentally.<sup>5,6</sup> Due to the nature of space technology, heat pipes will have to be designed to be as light as possible while maintaining high reliability; this will require a thorough understanding of their operational modes, both during steady-state and transient operation.

Clearly, to be able to achieve optimal design, a more thorough understanding of heat pipes during all modes of operation must be attained. Modeling accuracy must be improved, based on the results of experimental studies of heat pipe performance under transient conditions.

The purpose of this study is to gain a better understanding of the transient thermal hydraulic behavior of a screened wick heat pipe by using a simplified evaporation/condensation model which will investigate the response of the vapor and liquid regions during heat pipe transients. This will be compared with a series of heat pipe transient experiments including, but not limited to, normal start-ups from zero power, rapid power level changes, and frozen start-ups.

## 1.2 Literature Review

The history of heat pipes began with a patent by R. D. Gaugler<sup>7</sup> in 1942 while he was working for General Motors Corporation. His patent deals with the use of evaporation, condensation and liquid pumping by capillary forces in order to cause absorption of heat. His invention did not receive much attention until 1963, when G. M. Grover<sup>8</sup> of the Los Alamos National Laboratory patented a device similar to Gaugler's and included a limited discussion on theory and experiments with a sodium heat pipe. At this point, an extensive program was initiated at Los Alamos National Laboratory to investigate heat pipe phenomena. In 1964, the first paper on heat pipes was submitted by G. M. Grover<sup>9</sup> along with T. P. Cotter and G. F. Erickson to the Journal of Applied Physics describing the theory and significance of a device they termed a "heat pipe." Cotter went deeper into the theory of the heat pipe operation in a 1965 Los Alamos report.<sup>10</sup>

Closely following Grover's publication, the study of liquid metal heat pipes was initiated by P.D. Dunn at the United Kingdom's Atomic Energy Laboratory and H. Nue and C. A. Busse at the Joint Nuclear Research Center in Ispra, Italy.<sup>11</sup> Busse's early work centered on the operating limits of heat pipes.<sup>12</sup> The value of heat pipes had been recognized, and heat pipe experimentation and research picked up. The potential for space applications was recognized, and soon J. E. Deverall and J. E. Kemme<sup>6</sup> developed a water-charged stainless-steel heat pipe for satellite use. In 1967, this design was launched into earth orbit and performed successfully while in orbit.

By this time, primarily through the work of Cotter, the steady-state theory of the heat pipe was well developed, and experimentation with various permutations of the original design was carried out worldwide.<sup>11</sup> The first text about heat pipes<sup>13</sup> by D. Chisholm was published in 1971. P. D. Dunn and D. A. Reay<sup>11</sup> published the first comprehensive text of heat pipe history, design, theory, and applications. They recognized that the worst transient that could be experienced by a heat pipe is a step change to the input power at the evaporator, based on work by W. Bienert and P. J. Brennan<sup>14</sup> in the study of transient performance of variable conductance heat pipes.

Mathematical models have been developed by many researchers since the

invention of the heat pipe for both transient and steady-state modes. In 1972, C. C. Roberts and K. T. Feldman<sup>15</sup> developed a model to predict the performance of heat pipes with partially saturated wicks. This model employed a detailed steady-state analysis for the pressure drops in a water heat pipe and reported that the results of the study concurred with recession theory. In 1978, Y. Kanolani<sup>16</sup> developed a numerical model that predicts the steady-state temperature distribution inside an axially grooved heat pipe wall for various heat input and output modes. The model determines the heat transport limit and optimum fluid charge for a given operating condition. In 1981, S. Drouilhet and J. Buchlin<sup>17</sup> investigated the use of variable conductance heat pipes in an air-to-air heat exchanger. A computer code based on a quasi-analytic solution was used to determine the temperature profiles in the heat exchanger under steady-state operation. In 1979, a hydrodynamic model for heat pipe performance, HPIPE, was developed by F. C. Prenger.<sup>18</sup> This program can be used to optimize designs and calculate performance limits for a variety of heat pipe geometries. In addition, the program calculates the axial temperature and pressure profiles for steady-state operation.

D. C. Kane<sup>19</sup>, in 1980, investigated the steady-state operation of a vertically oriented gas-loaded variable conductance heat pipe using a one-dimensional (1-D) analytic model. A set of ten highly nonlinear differential equations was collapsed into two nonlinear differential equations and solved using a fourth order Runge Kutta scheme to accurately describe the transport process. In 1980, a finite element formulation was developed by W. A. Davis<sup>20</sup> to solve the steady-state two-dimensional (2-D) conduction heat transfer equation for the condenser wall section of an internally finned rotating heat pipe. The computer code predicts the maximum heat transfer possible from a given fin design. This model indicated that a sawtooth profile is preferable to spacing between fins. In 1981, H. J. Su<sup>21</sup> studied heat transfer in porous media with fluid phase changes and developed a 1-D steady-state theory which demonstrates the functional dependence of heat pipe operation on liquid saturation gradient, capillary pressure, permeability, fluid viscosity, latent heat, heat flux and gravity. In 1983, A. F. Kleinholz<sup>22</sup> developed a mathematical model to study the effects of various condenser geometries on the heat transfer rate. He found very little difference in the overall heat transfer between triangular and rectangular fins for rotating

axially finned condensers. In addition, the results indicated a reduction in the heat transfer rate with increasing condenser film thickness. In 1983, G. A. McLennan<sup>23</sup> developed a computer code for the simulation of heat pipe operation. The ANL/HTP computer code simulates heat pipe performance and temperature distributions under steady-state conditions.

The amount of work dealing with transient heat pipe model development is limited. A model predicting the transient behavior of low temperature heat pipes was developed by Colwell<sup>4</sup> in 1977. In this model, a three-dimensional (3-D) temperature distribution is solved by an explicit method. The temperature in the vapor region is treated as one node and a 1-D momentum equation is employed for the liquid region. Shukla<sup>24</sup>, in 1980, developed a transient model to predict the response of a gas controlled heat pipe. His model, however, deals primarily with the vapor dynamics between the working fluid and the control gas, and does not include phase changes in the evaporator wick. Chang<sup>25</sup>, in 1981, developed an improved model for the transient response of low temperature heat pipes. The model incorporates a 3-D treatment of the energy equation; however, the vapor region is again given as one node. A 1-D momentum equation is used to predict the motion of the liquid phase. The model allows for variation of thermal properties. The nodal temperatures are calculated using an alternating directions implicit method. Chang then designed, constructed, and operated a low temperature heat pipe using Freon-11 as the working fluid. Chang reported no difficulty in transient operation when far from the critical point of the working fluid, but operation in that region could cause evaporator dryout. Chang did not test at freezing temperatures.

Researchers in the Soviet Union have been experimentally studying the dynamics of heat pipe transient response. V.I. Tolubinski et al.<sup>26</sup> have studied the behavior of liquid metal heat pipes during start-up and with step changes in input power. They have found that operational failure can occur due to dryout in the evaporator, even at low power levels. L. L. Vasiliev and S. V. Konev<sup>27</sup> have studied the transient response of cryogenic and low temperature heat pipes, and suggest that existing theory of transient operation of heat pipes is insufficient to explain observed experimental results. Cenker et al.<sup>28</sup> performed similar work in the study of cryogenic heat pipes during start-up and step changes in input power. They also suggested that further work in both the experimental and

theoretical studies of heat pipe transient behavior is necessary.

In his 1985 Ph. D. dissertation<sup>29</sup>, J. Beam studied the heat transfer of a heat pipe in the start-up mode both experimentally and theoretically, and proposed a limiting start-up rate in heat pipes due to the hydrodynamics of the working fluid, which he was able to show experimentally and predict with a numerical model.

Tilton et al.,<sup>30</sup> in 1985 and 1986 investigated the transient response of a liquid metal heat pipe when an adverse thermal load was applied to the condenser section. Their analysis was both experimental and analytical.

Most recently, in a report to NASA in 1987, Colwell<sup>31</sup> described a code to model the start-up of a heat pipe that has an alkali-metal as the working fluid originally in a frozen state. The model follows the melting process of the frozen substance, and after assuming that the conditions are such that the pipe will reach a steady-state, follows the transient to that steady-state. The model was for a heat pipe that would be in place at the leading edges of reentry vehicles and hypersonic aircraft.

The following paragraphs outline heat pipe theory so that the relevance of the present work can be more fully understood.

### 1.3 Heat Pipe Theory

A heat pipe is a closed thermal hydraulic device designed for thermal energy transport. The physical laws governing the operation of a heat pipe are complex although the operating concepts are simple.

A heat pipe can be regarded as a closed cavity which is heated at one location and cooled at another. A typical heat pipe design is shown in Figure 1. Along the wall of a wicked heat pipe is a type of porous structure. The most common porous structures are screen materials and axial grooves. A working fluid in the liquid phase fills the porous structure and is held there by surface tension. The volume not occupied by the porous structure and liquid phase of the working fluid is considered the vapor space of the heat pipe. A water heat pipe with a rectangular cross section, clear top, and screen wick is analyzed in this study and is illustrated in Figure 2.

A heat pipe transports energy when either the evaporator is heated or the condenser is cooled. Most heat pipes begin operation with the heating of the

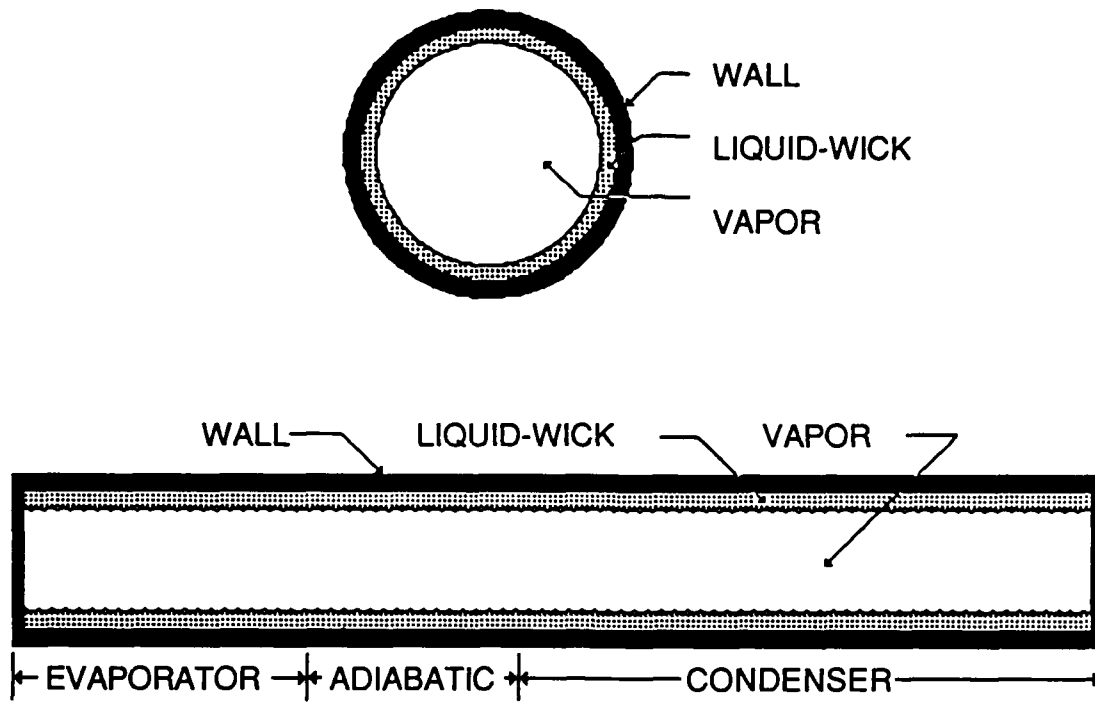
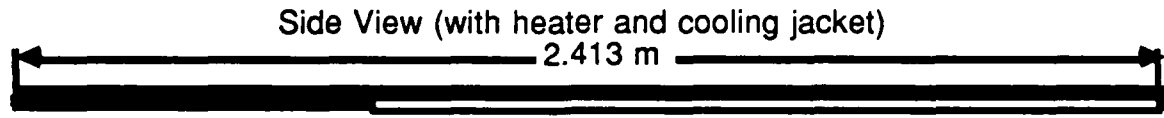


Figure 1. General Schematic of a Wicked Heat Pipe

evaporator. Hence, discussion of heat pipe operation will begin with this scenario.

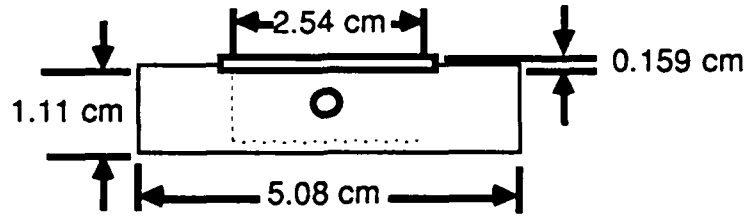
The process by which a heat pipe transfers energy is based on two-phase flow where energy and mass transfer occur between the phases. The mass transfer is due to evaporation/convection and also to pressure differences generated by capillary forces. The energy transfer is primarily due to the latent heat of evaporation carried by the evaporating or condensing medium. When the evaporator is heated, evaporation of the working fluid causes the liquid to recede into the wick structure and the vapor pressure to rise. The recession results in a smaller radius of curvature in the evaporator wick as seen in Figure 3. The increased vapor pressure causes a velocity profile to be generated in the vapor region. Energy is then carried into the condenser section by convective energy transport in the vapor phase. The vapor, upon reaching the condenser section,



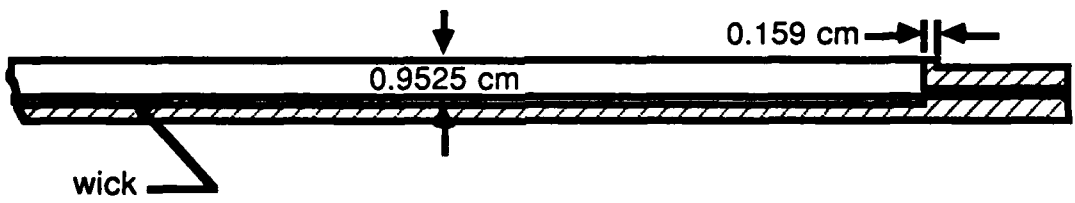
Heater (55.88 cm)

Condenser (1.651 m)

End View (condenser)



Side View (condenser end)



Top View

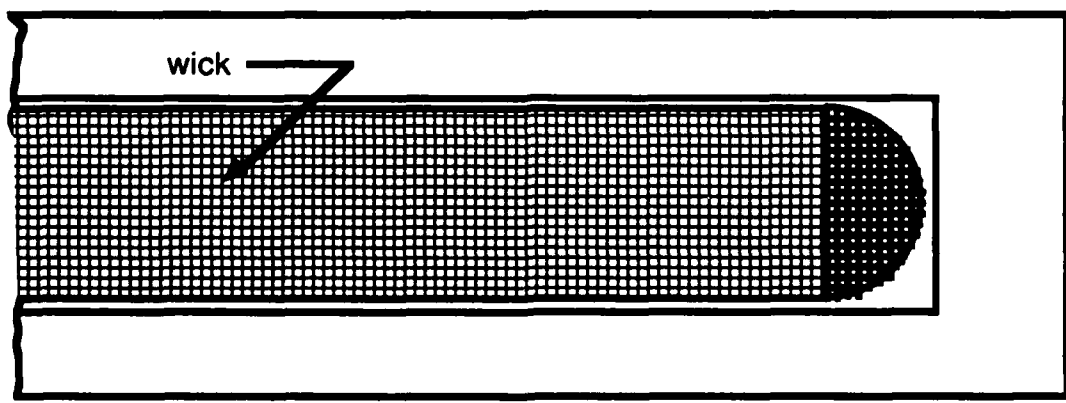


Figure 2. Working Drawings of the Experimental Heat Pipe

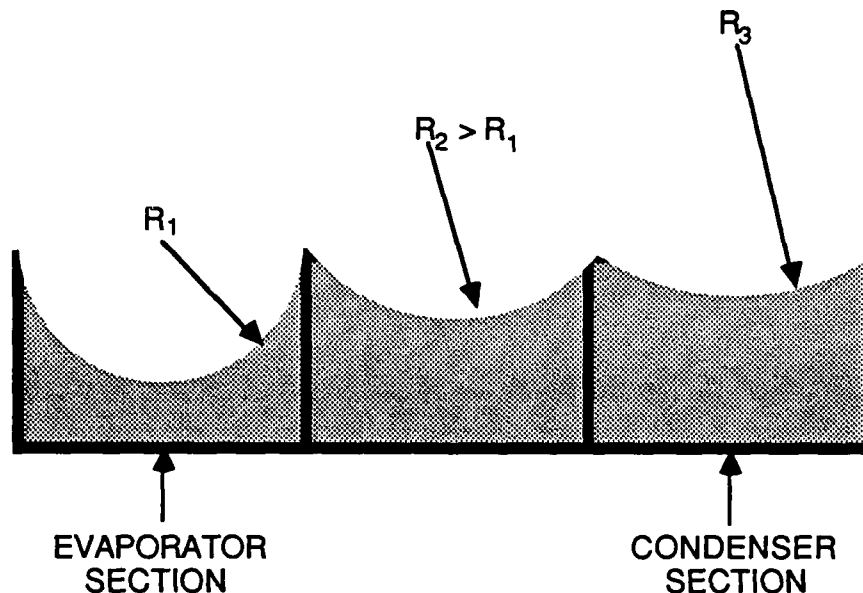


Figure 3. The Change in the Radius of Curvature of Menisci  
in Different Sections of a Heat Pipe

condenses on the cooler liquid in the wick structure and increases the radius of curvature in that region. The radius of curvature in the condenser region, now being larger than the radius of curvature in the evaporator region, causes capillary forces to return the liquid from the condenser to the evaporator. This sequence of events occurs with almost no temperature drop along the length of the heat pipe and continues until the heat source is removed or the heat pipe exceeds an operating limit.

Although heat transfer is very efficient in a heat pipe, several temperature drops do exist. Energy can be supplied to or removed from a heat pipe by conduction, convection, or radiation. In each case, a resistance to energy transport exists in the heat pipe wall, liquid-wick structure, vapor-liquid interface, and vapor channel. In most heat pipe systems, the largest temperature drop

occurs from the heat source to the heat pipe wall. Asselman and Green<sup>32</sup> report an estimate of the resistance/cm<sup>2</sup> of a heat pipe to energy transport for the regions of a typical water heat pipe; these values are shown in Table 1. It should be noted that these values are not generic to water heat pipe designs. Different designs can cause the largest resistance to occur in different regions of a heat pipe. The values given in Table 1 are those expected from a production-type heat pipe.

Table 1. Resistance to Energy Transport for Regions of a Typical Water Heat Pipe

RESISTANCE/ cm <sup>2</sup> *	K/W
Heat Source to Wall (Evaporator)	10 <sup>3</sup> - 10
Wall (Evaporator)	10 <sup>-1</sup>
Wick/ Liquid (Evaporator)	10
Liquid-Vapor (Evaporator)	10 <sup>-5</sup>
Vapor	10 <sup>-8</sup>
Liquid-Vapor (Condenser)	10 <sup>-5</sup>
Wick-Liquid (Condenser)	10
Wall (Condenser)	10 <sup>-1</sup>
Wall to Heat Rejection (Condenser)	10 <sup>3</sup> - 10

\* The cm<sup>2</sup> refers to the cross-sectional area through which energy is being transported.

Heat pipe operation is determined to a large extent by pressure drops that occur in the pipe. A typical pressure profile is shown in Figure 4. The vapor pressure is highest at the beginning of the evaporator section and decreases to the adiabatic section due to acceleration and friction pressure drops. The

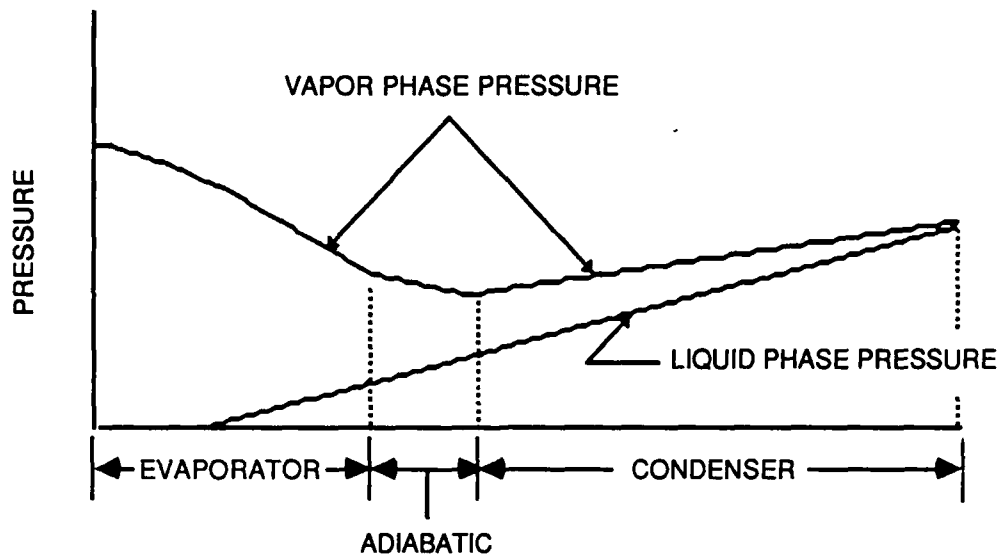


Figure 4. Liquid and Vapor Phase Pressure Profiles in a Heat Pipe Where Partial Pressure Recovery Occurs in the Vapor Phase

pressure continues to drop through the adiabatic section primarily due to friction forces. In the condenser, friction forces result in a pressure drop component while acceleration forces cause a pressure rise component. The combined effects can result in either a net pressure rise or drop depending upon the velocity, geometry, and viscosity of the vapor. The return of the liquid from the condenser to the evaporator results in a pressure drop. The pressure drop is due primarily to friction forces since the velocity is too small to create any significant acceleration pressure loss or gain. A heat pipe has five distinct steady-state operating limits<sup>11</sup>: capillary, boiling, viscous, sonic, and entrainment. The following paragraphs briefly describe each of these.

The capillary limit is a function of the maximum capillary pumping head. The following development is typical of that presented in most heat pipe theory texts.<sup>11</sup> The maximum capillary pumping head is given by

$$\Delta P_{c \max} = \frac{2\sigma}{r_{\text{crit}}} \quad (1)$$

where  $\sigma$  = the surface tension of the working fluid  
 $r_{crit}$  = the minimum radius of curvature and is given for wire meshes as

$$r_{crit} = \frac{w+d}{2}$$

where  $w$  = width of pore  
 $d$  = wire diameter.

The maximum capillary pumping head must be greater than or equal to the pressure drops due to friction, acceleration, and gravitation in both the vapor and liquid regions. This inequality may be written as

$$\Delta P_{c\ max} \geq \Delta P_l + \Delta P_v + \Delta P_g \quad (2)$$

where

$\Delta P_l$  = liquid pressure drop  
 $\Delta P_v$  = vapor pressure drop  
 $\Delta P_g$  = gravitational pressure drop.

The capillary limit is the point at which the pressure drops exceed the available head.

The boiling limit is the point at which boiling occurs in the wick. Boiling generally occurs at high radial heat fluxes in the evaporator. This can result in a loss of energy transport ability in the pipe due to bubbles or vapor pockets generated in the wick which decrease the flow area, increase the pressure drop, and thus reduce liquid return to the whole evaporator.<sup>33</sup>

The viscous limit occurs at low operating temperatures, when the high viscosity of the vapor causes greater pressure losses than the capillary head is capable of overcoming.

The sonic limit occurs when the vapor velocity reaches the sonic value for the given operating conditions. A shock front will be formed and a substantial pressure loss will occur in the vapor. The heat pipe is still capable of operating at this point, albeit with reduced capability, unless the pressure drop exceeds the maximum capillary pumping power, in which case the evaporator will dry out.

Entrainment is a result of high vapor velocities. At high velocities, miniscule waves are formed at the surface of the liquid in the wick. Droplets from the top of these waves are torn off and returned to the condenser by the vapor flow. Small amounts of entrainment will reduce the effectiveness of the heat pipe, but operation is still possible. However, when entrainment occurs on a large scale, liquid is prevented from returning to the evaporator, and dry out occurs.

The parameter usually used in predicting the onset of entrainment is the dimensionless Weber Number,  $We$ . The Weber Number is the ratio of the inertial forces of the moving vapor and the surface tension forces of the liquid in the wick.<sup>11</sup> That is,

$$We = \frac{\rho_v V^2 l}{\sigma} \quad (3)$$

where  $\rho_v$  = density of the vapor  
 $V$  = average velocity of the vapor  
 $l$  = characteristic length associated with the mesh spacing in the wick  
 $\sigma$  = liquid surface tension

Many investigators<sup>11, 34, 35, 36</sup> have assumed that the Weber Number is equal to unity at the beginning of entrainment, and adjusted the characteristic length or added a correction so that  $We = 1$  when entrainment was observed. However, it is not apparent that liquid drops should be entrained in the counterflowing vapor at the point where steady-state inertial and viscous forces just balance; turbulent fluctuations may be important. It would be more convenient, therefore, to define the characteristic length in terms of the actual mesh size of the wick, and then experimentally determine the value of  $We$  at which entrainment occurs. Thus, the characteristic length can be represented by the center-to-center spacing of the wick, i.e., the width of the pore opening plus the diameter of the wire.

In the design of heat pipes, it is essential that operating limits are not exceeded. In the past, heat pipe designs have relied on steady-state analysis to avoid the operating limits. These limits, however, can also occur during transient operations (start-up, shutdown, rapid power changes, etc.). This has

caused transient heat pipe modeling to become an increasingly important subject.

#### 1.4 Report Organization

In this section, the relevance and direction of and motivation for doing this study of the transient heat pipe have been discussed. A literature review of the history of the heat pipe and the work already performed in the areas of transient heat pipe modeling and experimentation were then presented. This was followed by a review of heat pipe operating principles and operational limits. Sections 2 through 4 will describe the experimental thrust of this study. Each of these chapters describes a separate series of experiments and will have five sections. The first is an introduction to the work of the section followed by a description of the experimental setup used. Next the experimental procedures employed are described, followed by the results and a discussion of the results for the series of experiments. The fifth section gives a summary of the section.

Section 2 explains the analysis of the entrainment limit and the problems associated with it in the transient heat pipe. Section 3 describes the rapid transient experiments performed, both from zero power to another power level and from one steady-state power level to another. Section 4 discusses a set of improvements to the experiments of Section 3, first confirming that the changed apparatus acts as a heat pipe, then analyzing power increases from an operating state, and then going over a set of experiments performed at or near the freezing point of the working fluid of the heat pipe, including two start-ups from the frozen state. Data on the cooling of the pipe from an operating state, shutdown, wick rewetting, wick dry out, and partial wick dry out are also analyzed in Section 4.

Section 5 discusses the modeling side of this report. After an introduction there are three subsections to this section. The first subsection describes the model used. This is followed by a discussion of the verification and application of this model. Finally, the third subsection gives a summary of the section.

Section 6 summarizes the report, draws conclusions, and makes recommendations for future work.

## 2.0 ENTRAINMENT EXPERIMENTS

### 2.1 Introduction

In an attempt to understand the entrainment limit as it affects heat pipe transients, an experiment was constructed to find the vapor velocities at which entrainment will occur. In this experiment a heat pipe was simulated by having forced air blown over four different wetted wicks of mesh sizes 18X18, 40X40, 80X80, and 100X100 per inch. Beneath the wick was a channel to allow for the passage of liquid and on top of the channel was a glass wall to allow for visual observations. The air velocity at which entrainment was first visually observed for each of the mesh sizes was measured by a hot wire anemometer and recorded and plotted against the characteristic length for the mesh size. When compared to the predicted velocities for entrainment, the measured values appeared to be significantly larger, although liquid flow instabilities in the wick occurred at or near the air velocities predicted by theory.

### 2.2 Experimental Setup

The entrainment experiments involved the use of a simulated heat pipe into which high pressure air could be blown and expanded through an entry length so that a region of uniform velocity and pressure could be observed. A metal block was milled, as shown in Figure 5, such that a wick could be supported with a water channel beneath it and vapor flow channel above it. The top of the block was sealed with glass, so that the wick could be observed. The wick sat on a piece of sheet metal, and the the channel beneath it allowed any excess water in the wick to run off. One end of the block was sealed except for the high pressure air inlet, while the other end of the vapor channel was left open. The entire block was 0.2032 m long, and preliminary experiments showed that the entrance region of nonuniform flow was less than 0.1016 m in length. A hot wire anemometer was used at the outlet of the block to determine the average vapor velocity at the exit.

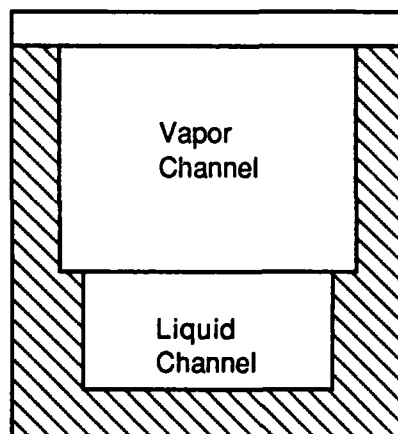
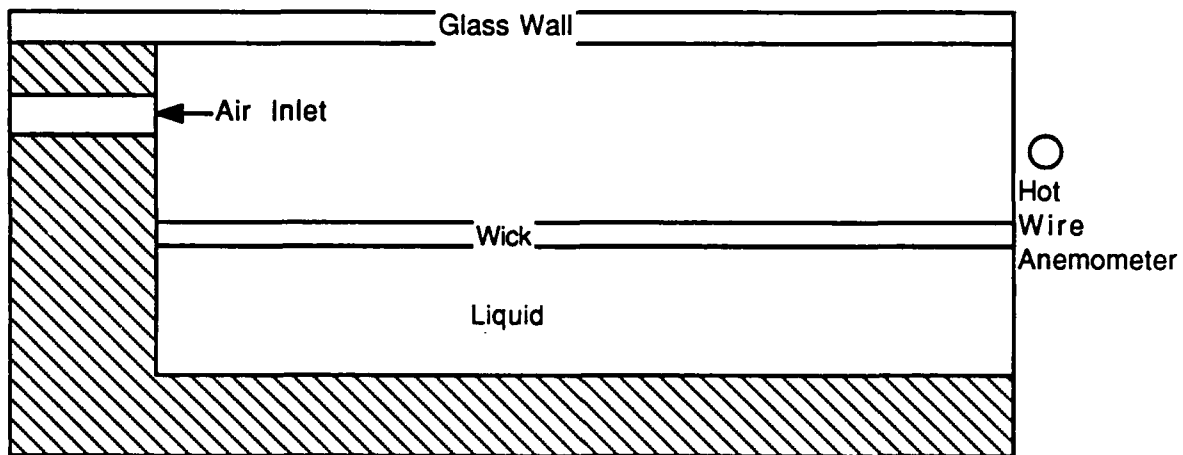


Figure 5. Apparatus for Entrainment Observation

### 2.3 Experimental Procedures

In trying to observe entrainment, the last 0.0762 m of the wick in the channel was wetted, and the mass flow rate of the air was slowly increased. The first group of these experiments were performed with the wick material cut and laid on the sheet metal support in the block. It was found that wrinkles perpendicular to the direction of flow existed in the material. These wrinkles were very small and not readily observable at first; however, the wrinkles were large when compared

to the characteristic length of the pores. As air flowed over the wrinkles, water was pulled out of the wick at the downstream end of the wrinkle. This is shown in Figure 6.  $V_1 = 0$  is the case of no air flow over the wick.  $V_2$  and  $V_3$  are velocities where  $V_2 < V_3$ . The magnitude of  $V_2$  and  $V_3$  are dependent on the size of the wrinkles in the wick. Once velocity  $V_3$  was attained, water droplets began to be carried out of the channel without ever returning to the wick.

To eliminate the early inception of entrainment due to these wrinkles, a piece of hardware was devised that would stretch the screen wicks and reduce the magnitude of the wrinkles. This allowed testing of the properties of the screen mesh itself. When wrinkles were present, although they could not be seen by just looking closely at the wick, they could be seen when water was pulled out of the wick because the water would form a long, narrow puddle outlining the back side of the wrinkle and running across the width of the channel.

Once the desired experimental conditions were established, a hot wire anemometer measured the average air velocity at the outlet of the channel. The wick was first wetted as described previously, and the air mass flow rate into the channel was slowly increased until entrainment was first observed. At this point, the air velocity was measured. This procedure was performed for four different mesh sizes : 18X18, 40X40, 80X80, and 100X100 meshes per inch.

## 2.4 Results and Discussion

In the study of the wrinkled wicks, it was determined that water was pulled out of the downwind side of the wrinkles by a low pressure region due to the expansion of the air stream. This is illustrated in Case 2 of Figure 6. As the mainstream velocity is increased further, the water is pulled farther and farther out of the wick, until a point is reached where surface tension forces are overcome by shear forces. This may be, but is not necessarily, the point where the forces balance. Extending this to the microscopic level of the wick itself, as shown in Figure 7, it is conceivable that the same phenomenon could occur as a gas flows over a flat wick. For no gas flow, the liquid in the wick would have a natural meniscus shape. As air begins to flow over the wick, a low pressure region will develop on the downwind side of each wire in the wick, and liquid will be drawn up that side of the pore. In addition, the reverse will happen on the leading edge

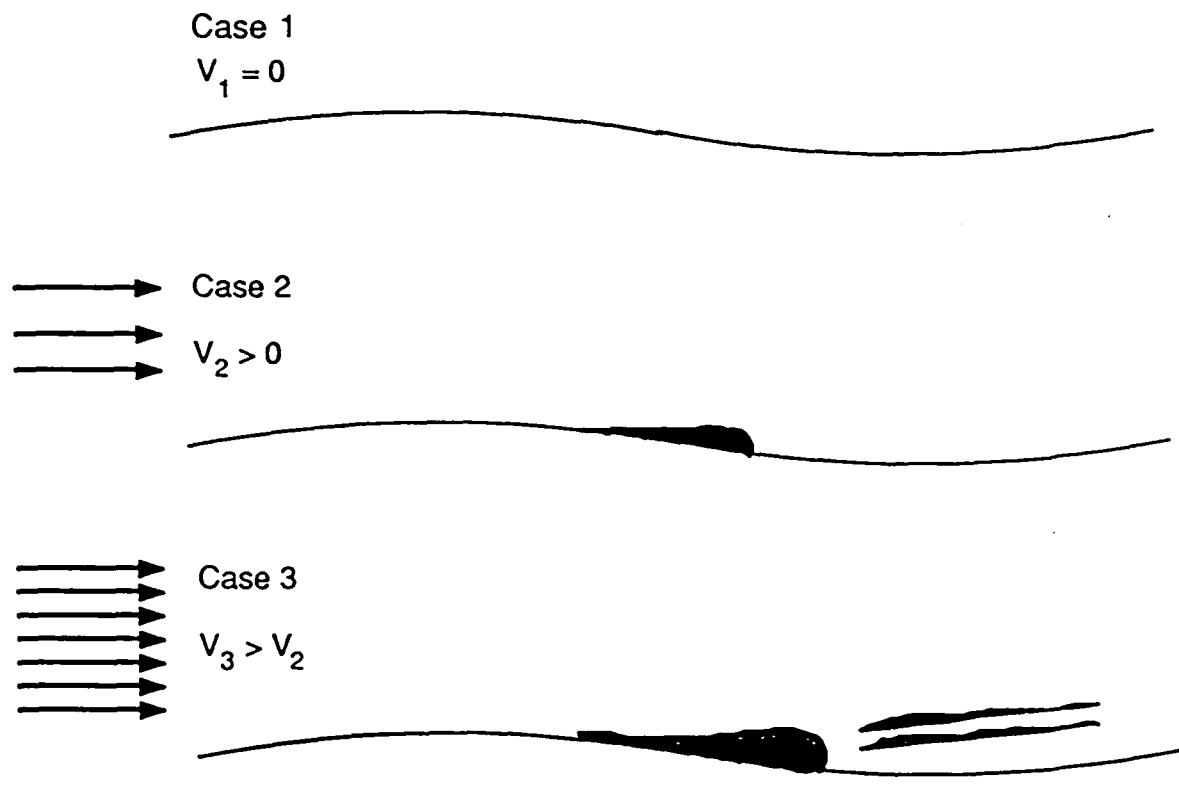


Figure 6. Air Flow Over a Slightly Wrinkled Wetted Wick

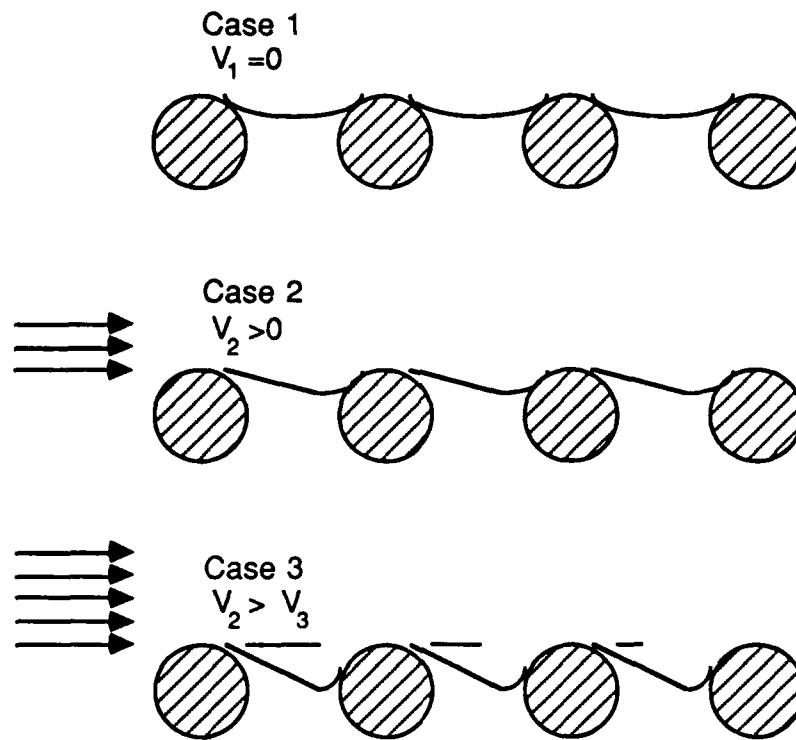
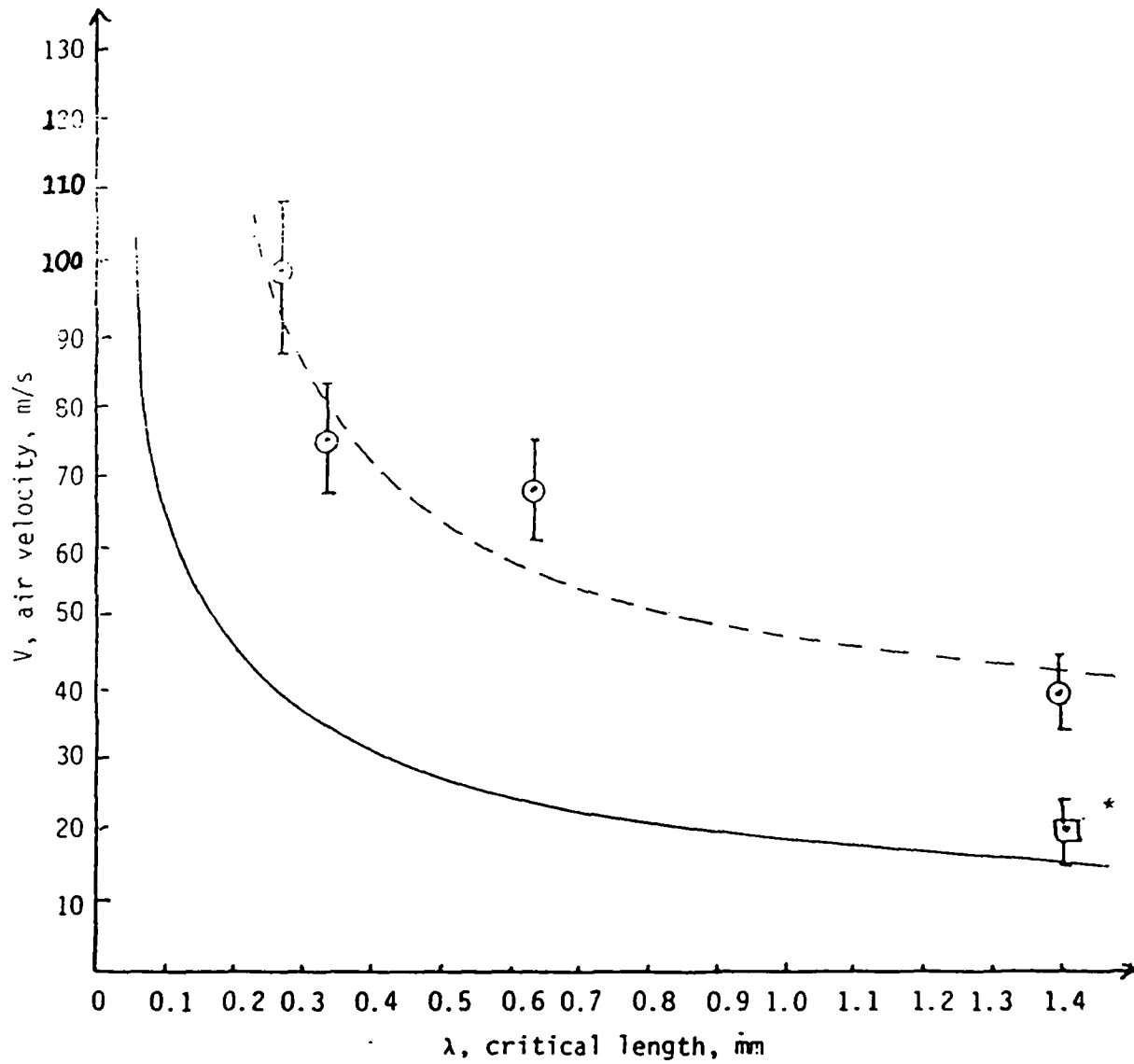


Figure 7. Proposed Form of Entrainment Inception

of each wire, causing a high pressure region which forces liquid down from the leading edge. Finally, when the gas velocity reaches the critical point, liquid is entrained in the vapor.

From the measurements of the mean air velocity required to entrain liquid and carry it out of the channel, velocity was plotted as a function of the critical length ( the mesh center to mesh center spacing) for the various wicks tested. This is shown as the dashed line in Figure 8. Also shown on Figure 8 is the predicted value of velocity (solid line) for a given characteristic length using the criterion that the Weber Number,  $We$ , is equal to one. It can easily be seen that the onset of entrainment as determined by the transport of water droplets down a channel occurs at much higher velocities than can be expected for a Weber Number of one at the inception of entrainment.

When working with the 18X18 mesh, it was possible to observe individual pores. As the mean air velocity approached the value predicted by the Weber Number correlation, the water in the pore could be seen to be unstable, meaning



\*nonentrained fluid motion

Figure 8. Predicted and Measured Velocities for Entrainment

that motion could be seen by reflection off the meniscus surface. After the predicted velocity was exceeded, it could be seen that liquid was moving downwind while still remaining in the wick. The pattern of movement was apparently random; the liquid in any individual pore could remain in place for quite a while, and then suddenly move down the wick a distance of one to three pores, then come to a stop and stay in the new location a few seconds before moving again. Increasing the velocity resulted in less time between jumps, until a velocity was attained that would actually entrain the drop. This velocity corresponds to the point on the dashed line of Figure 8.

These experiments indicate that a Weber Number of one can be used to predict the params for which the liquid flow in the wick becomes unstable, but further measurements are needed to determine the Weber Number for which liquid is physically removed from the wick. It is possible, however, that the reversal of flow in the wick without removal of liquid from the wick could be the actual inception of the entrainment limit.

## 2.5 Summary

A set of experiments was designed and performed to analyze the onset of entrainment in a heat pipe to further the understanding of the effect of entrainment on the transient heat pipe. The experiments simulated a heat pipe by having a controlled mass flow rate of air blown through a heat pipe channel that was covered by glass. The air was forced over a wick which had a liquid passage channel beneath it. Mesh sizes of 18X18, 40X40, 80X80, and 100X100 per inch were used. The air velocities at which entrainment was first visually observed were measured by a hot wire anemometer, plotted against the characteristic length of the wick, and compared with the velocities of the inception of entrainment predicted by theory. Those velocities measured in the experiment were significantly higher than those predicted by theory. However, liquid flow instabilities in the wick occurred at or near the air velocities predicted by the Weber Number.

## 3.0 HEAT PIPE SCOPING EXPERIMENTS

### 3.1 Introduction

This chapter discusses the design and transient testing of a heat pipe with a rectangular cross section, flat mesh-type wick, and a glass wall through which internal mechanisms of heat pipe operation could be observed. Thermocouples located on the outside of the unit attached to one metal wall and inside the vapor space close to the glass wall were used to study temperature profiles during operation, and a data acquisition system was used to concurrently display and record all measurements. The heat pipe operated in a manner consistent with theory. However, results of these experiments indicate that certain transient modes of operation can cause failure where not predicted by steady-state theory. There were some problems with the data collection and hardware of these experiments. The data collected by the outer wall thermocouples indicated larger temperature drops than expected. Also, the glass cover was subject to cracking under high temperatures and stresses. These major problems, as well as other minor problems, were overcome as discussed in Section 4.

### 3.2 Experimental Setup

To conduct a comprehensive study of the various conditions limiting heat pipe transient operation, a heat pipe has been constructed which was designed to operate with water as the working fluid in the power and temperature regions where failure is predicted by theory. The unique features of this design are a square cross section and a glass wall through which the actual mechanisms of transient phenomena may be observed as they occur. Its peripherals include a vacuum pump, a pressure transducer and indicator, thermocouples on the outer wall of the main body and on the inner wall of the glass cover inside the vapor channel, and an IBM PC and analog to digital (A/D) converters for data collections and manipulation. Figure 9 shows the major dimensions of the heat pipe. Figure 10 is a schematic diagram of the system layout.

Prior to the design of this heat pipe, a similar heat pipe was designed,

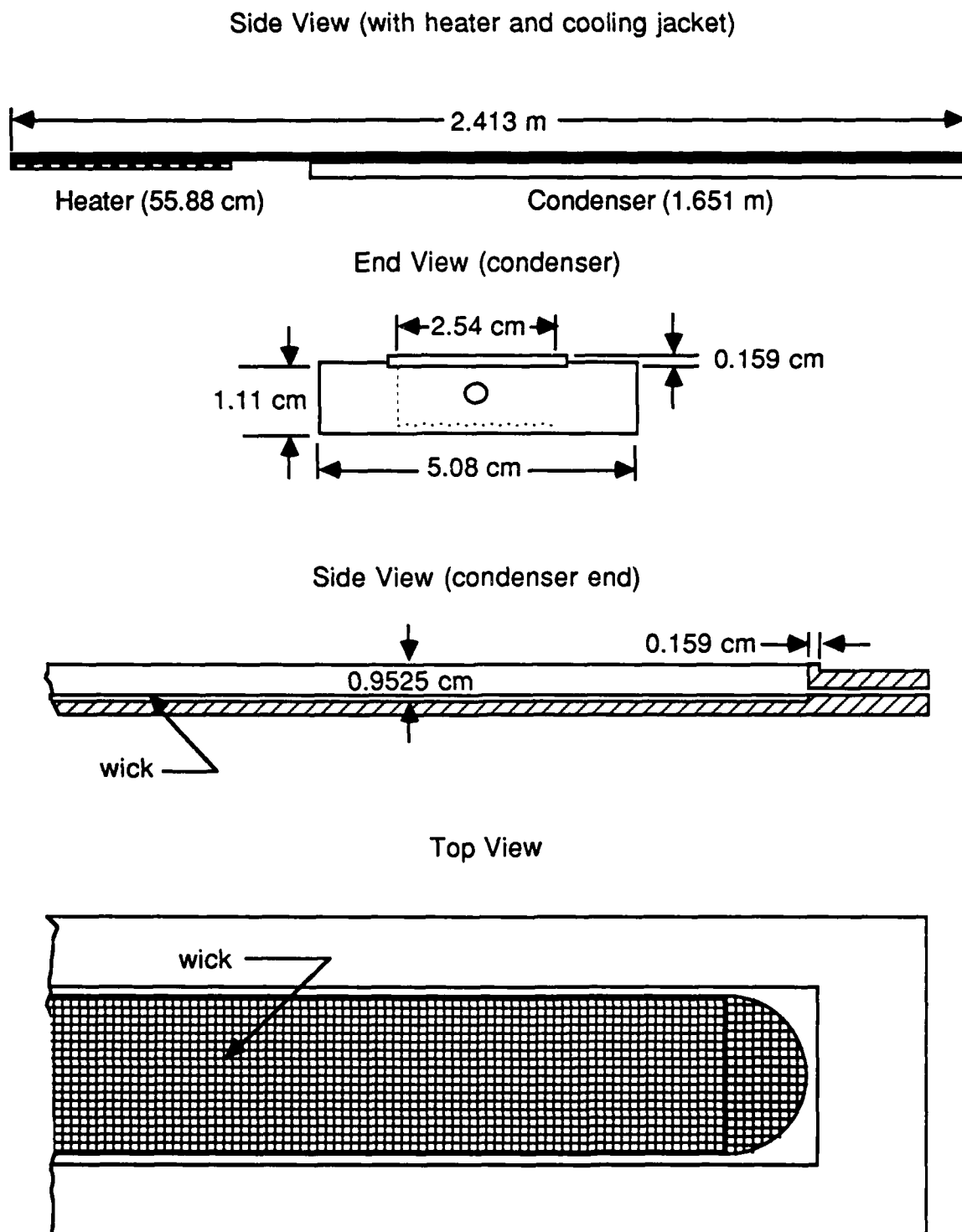


Figure 9. Dimensions of the Experimental Heat Pipe

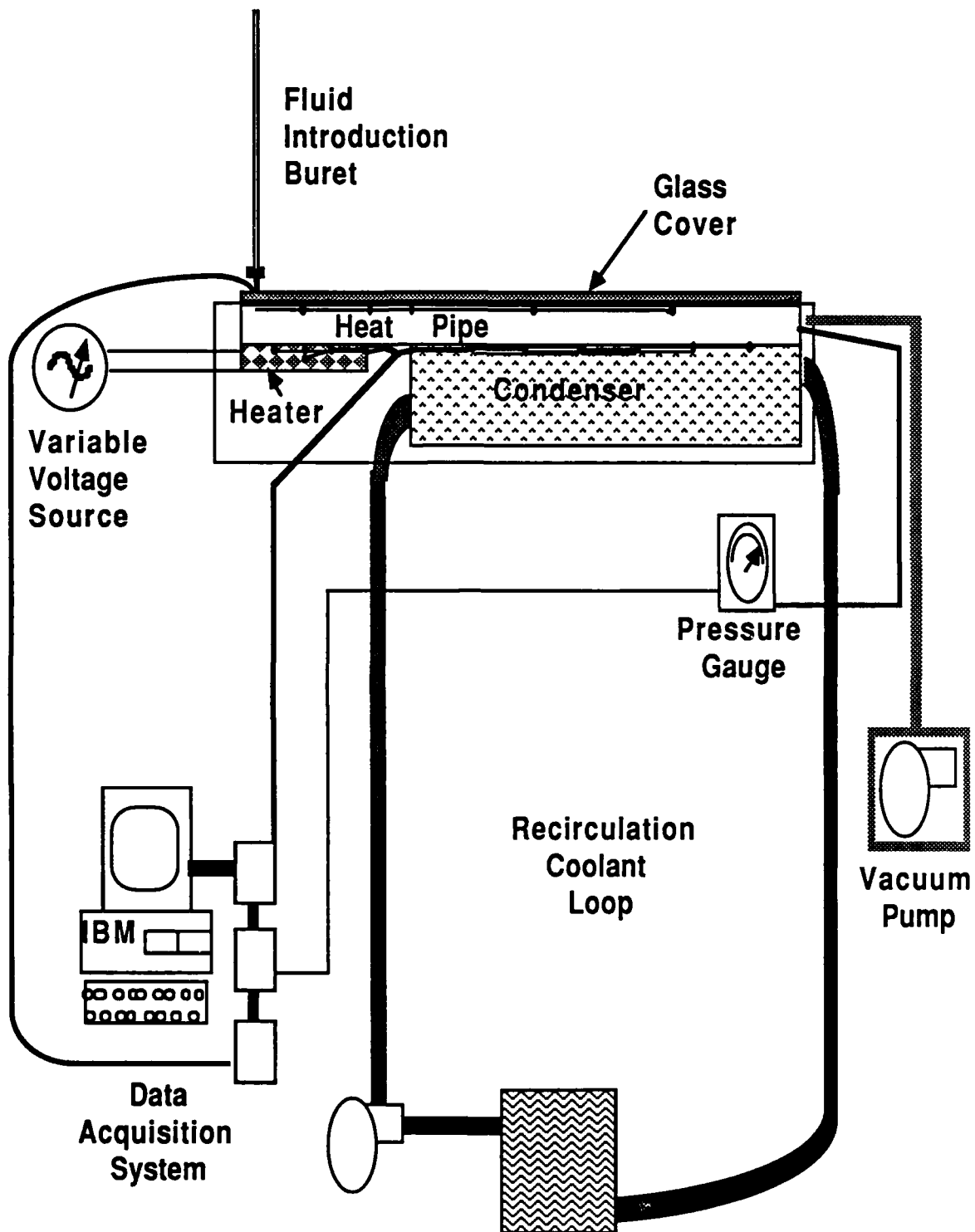


Figure 10. Schematic Diagram of the System Layout

constructed, and operated, also using water as the working fluid. This previous unit was built as a first attempt to operate a heat pipe in which the inner workings would be visible, and served as a basis for the current design. Its strong points were incorporated into the new design, while its faults were corrected. This first unit was milled from aluminum stock, with a 2.5-cm<sup>2</sup> cross section flow channel 100 cm in length. It had a 15-cm evaporator region, a 25-cm adiabat and a 60-cm condenser. The heat pipe was cooled by a water jacket on the bottom wall of the condenser. Thermocouples were cemented to the outside of the bottom wall along the entire length of the unit, and a tube was run along the length of the flow channel inside the heat pipe through which a thermocouple could be moved to any location along the length. There were two taps through the wall at the end of the evaporator to which a vacuum line and a pressure transducer were mounted. The heater was constructed of nickel-chromium wire wrapped around the metal stock, and sealed inside an epoxy with a high temperature rating and high thermal conductivity.

This original design was shown to operate as a heat pipe, but had several serious design flaws. The most significant of these was that the large channel area resulted in a very large vapor flow area relative to the amount of liquid in the wick, so a high vapor velocity could not be obtained in the heat pipe. This flaw was exacerbated by the fact that the heater used could not provide a very large energy input (75 W max) through the walls of the evaporator. Calculations, which will be explained in more detail later in this section, indicated that sonic, capillary, and entrainment limits could not be approached. In addition, during operation, noncondensable gases were produced and carried to the condenser by the vapor flow in that direction. Since the vacuum line was connected to the evaporator end, these gases could not be drawn off. Finally, problems with gaskets at the aluminum/glass interface when trying to evacuate the heat pipe necessitated a whole new approach to the design of this interface.

The heat pipe designed and constructed for the research of this section (shown in Figure 9), while based on the same concept as the original pipe, has changed considerably in appearance. The flow channel is now 238.8 cm in length and has a rectangular cross section 2.54 cm wide and 0.953 cm high with no wick. As wicking material is added to the channel, the vapor flow area is correspondingly decreased. The body is milled from a single piece of aluminum

stock. The evaporator is 56.5 cm in length, the adiabatic region is 17.8 cm long, and the remaining 164.5 cm is the condenser. The condenser region is cooled by a water jacket, similar to the previous system, except that all the gaskets, internal fittings and tubing were required to be able to withstand temperatures down to  $-40^{\circ}\text{C}$  without failure; this was to allow the use of low temperature coolant in the water jacket. Thermocouples were fitted to the outside of the bottom wall (Figure 11) as with the previous design, but no tube was used inside the flow channel because of the flow disturbances it would cause in such a small flow area. However, five small (30 gauge) thermocouples were attached to the underside of the glass cover, for the study of vapor behavior during normal operating conditions with relatively low vapor velocities, where small disturbances in the flow field would not be as significant as they would be in entrainment studies. The locations of these thermocouples are shown in Figure 11. The outer wall thermocouples are identified by letter designations A through M, while the vapor channel thermocouples are given letters O through S. The location of each thermocouple with respect to the distance from the beginning of the evaporator is given in Table 2.

The vacuum and pressure transducer fittings were connected to one tap at the far end of the condenser region. A strip-type heater was acquired with a power rating of 1500 W and surface dimensions the same as those of the base wall of the evaporator.

### 3.2.1 Heat Pipe Axial Heatflux Limitations (HAHL) Computer Code

The computer code H AHL is a program written in BASIC for the Commodore 64 computer, and is listed in Appendix A. The purpose of H AHL was to determine the axial energy flux required to attain each of the operational limits for a heat pipe of a given design and operating temperature. "Operational limits" in this case describes the viscous, sonic, entrainment, and capillary limits experienced by heat pipes. The code contains property data for water based on numerical fits.<sup>37</sup> For a given operating temperature, pressure can be calculated, assuming two-phase equilibrium. From this, H AHL calculates the specific volume and dynamic viscosity for each of the two phases, the surface tension of the liquid, and the latent heat of vaporization for water. The user then inputs the design

(all dimensions in cm)

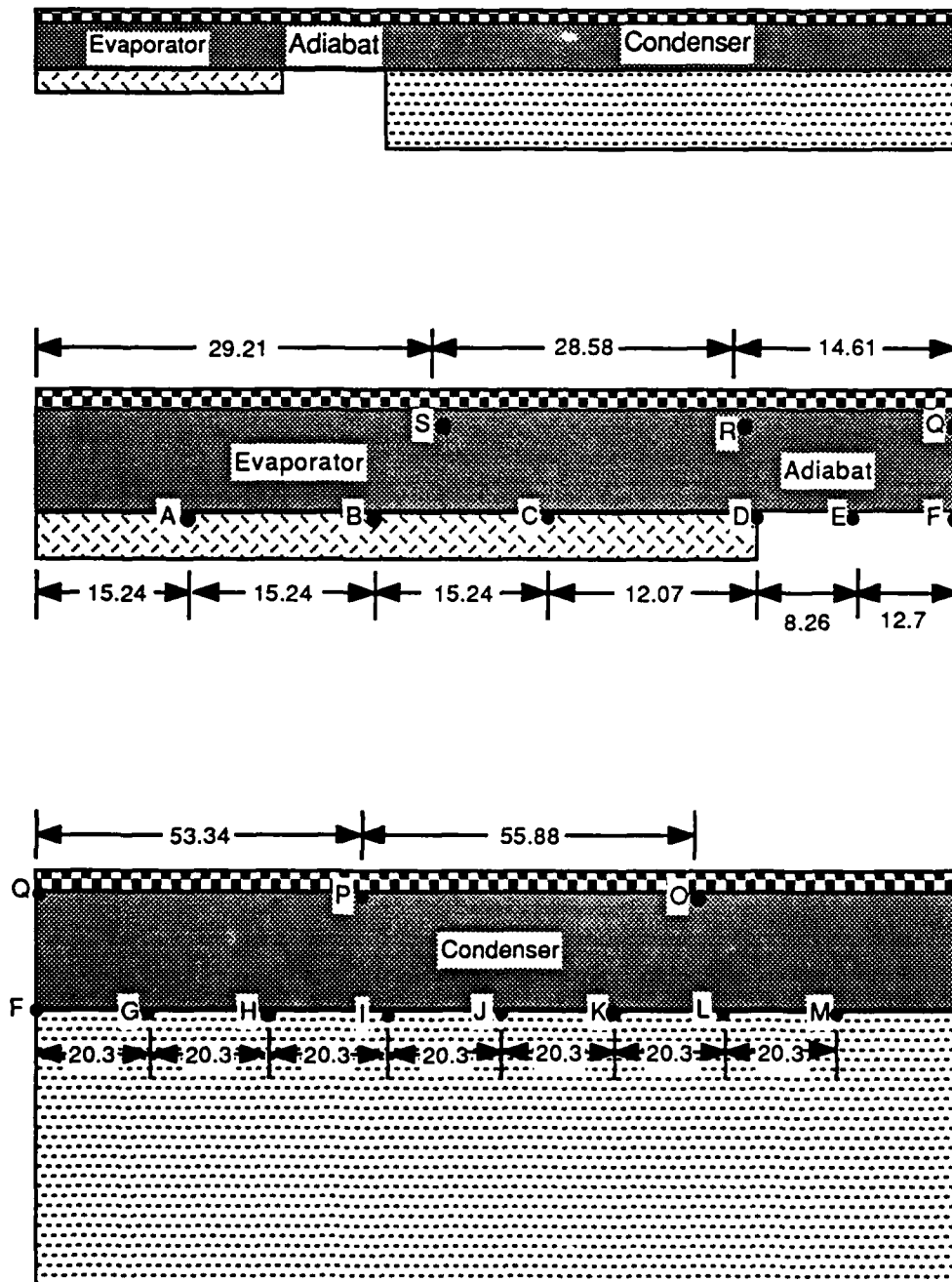


Figure 11. Thermocouple Placement in the Heat Pipe

Table 2. Thermocouple Placement Along the Heat Pipe

Outer Wall Thermocouple	Location (meters)	Vapor Thermocouple	Location (meters)
A	0.1524	S	0.2921
B	0.3048	R	0.5779
C	0.4572	Q	0.7239
D	0.5779	P	1.2573
E	0.6604	O	1.8161
F	0.7874		
G	0.9906		
H	1.1938		
I	1.3970		
J	1.6002		
K	1.8034		
L	2.0066		
M	2.2098		

criteria for a proposed design, i.e., evaporator, adiabat, and condenser lengths, mesh spacing, permeability of the wick material, vapor and liquid flow areas, etc. The code takes this information and converts it to the form and units required for the limiting heat flux equations. The user is then allowed to input various operating temperatures, and the code will compute the energy flux corresponding to each of the aforementioned limits for each input temperature. Thus, by calculating the limits over a range of temperatures, the maximum operational heat transfer rates for a particular design are known. HAHL's results were benchmarked using H<sup>T</sup>PIPE<sup>18</sup>, a heat pipe computer program written at Los Alamos National Laboratory. The results of this comparison showed that HAHL predicts the same limits as H<sup>T</sup>PIPE within a few percent, which was more than adequate for the purpose of designing the heatpipe described here. HAHL was written instead of using H<sup>T</sup>PIPE because it would be easier and less expensive to use and modify for a rectangular cross section design, and because H<sup>T</sup>PIPE

calculates much more information and to a greater degree of accuracy than was needed for this work.

HAHL computes the entrainment limit from an equation given by Dunn and Reay<sup>11</sup>:

$$q_e^* = \left( \frac{2\pi\rho_v L^2 \sigma_l}{z} \right)^{\frac{1}{2}} \quad (4)$$

where  $q_e^*$  = limiting heat flux for entrainment,  
 $\rho_v$  = density of the vapor,  
 $L$  = latent heat of vaporization of water,  
 $\sigma_l$  = surface tension of the liquid,  
and  $Z$  = characteristic length for the wick.

The characteristic length for the wick is approximately equal to the center-to-center wire spacing in the wick.

The expression for the capillary limit comes from Chi<sup>34</sup>, and is rather more complicated than the above equation. Chi's formulation calculates the vapor pressure drop along the heat pipe in terms of vapor properties and the size of the flow channel. There are four possible cases for the vapor depending on whether the flow is laminar or turbulent and whether the Mach number indicates compressible or incompressible flow. The correct case is determined depending on operating conditions and the appropriate equation is used. The code then calculates the pressure drop in the liquid as a function of the liquid's properties and the size of the flow channel and the wick. Assuming the radii of the menisci are at a minimum in the evaporator, a pressure balance can be made between the capillary pumping pressure and the pressure losses of the liquid and vapor. When the losses are equal to the capillary head, the maximum axial heat flux exists. This part of the program is iterative, as it must determine the heat flux at which the pressures balance for a solution. Since the equations assume the best possible capillary head at the limit, they may overpredict the capillary limit.

Viscous and sonic limits are calculated by analytically determined correlations presented in Dunn and Reay.<sup>11</sup> The viscous limit is given by:

$$\dot{q}_v = \left( \frac{r_v^2 L \rho P}{16 \mu l} \right)^{\frac{1}{2}} \quad (5)$$

where  $r_v$  = effective radius of the vapor channel,  
 $L$  = latent heat of vaporization for water,  
 $\rho$  = density of the vapor,  
 $P$  = pressure of the vapor,  
 $\mu$  = dynamic viscosity of the vapor,  
and  $l$  = effective length of the heat pipe.

The effective length of the heat pipe is the sum of the length of the adiabat plus half the length each of both the evaporator and the condenser. The sonic limit is given by:

$$\dot{q}_s = 1.159 L (\rho P)^{\frac{1}{2}} \quad (6)$$

where  $L$ ,  $\rho$  and  $P$  are as defined above. These are rough estimates for these limits, but were sufficient for the purpose of this design.

Prior to running the code, certain constraints were already placed on the design: the heater section could be no more than 0.57785 m in length and 0.0508 m in width, the overall length could not exceed 3.048 m to make the glass cover easy to make and to handle, and the operating temperatures must remain well below 100°C so that internal vapor pressure would remain less than the external air pressure. These are just a few of the constraints. Based on all the constraints, various conceptual designs were tested. The results showed that the dimensions and characteristics of the final design should enable the heat pipe to reach and exceed all of the limiting heat fluxes with an extra margin for error.

### 3.2.2 Main Body

The main body of the heat pipe was milled from a 0.0191 X 0.0508 X 3.6576 m bar of 6061 T6 aluminum to the specifications shown in Figure 9. Aluminum was used because it allowed easy milling and was inexpensive. While stainless steel would have undoubtedly been a superior material, the cost in milling,

drilling and tapping such a material would have been prohibitive. It was felt that the problems due to the reaction of water with aluminum inside the heat pipe would be minimal, since the unit was not designed to operate more than a few hours continuously.

The active region of the heat pipe is 2.3876 m in length and 0.0095 m deep. The upper surface was milled such that there would be a 0.0016-m lip around the main channel. This lip was originally designed as a retainer for a 0.0032-m-tall square gasket. It was later found that an O-ring facilitated a better seal, and no design changes would be required, so the gasket was replaced by the O-ring. Forty-eight holes were drilled and tapped along the length of the main body to allow 2.4130- X 0.0508-m sheets of 0.0032-m aluminum to be bolted to the sides, flush with the upper surface of the main body. The purpose of these walls was twofold. First, they served as structural support for the main body to keep it from bending when a vertical force was applied. Second, they served as the walls for the water jacket in the condenser and the insulating jacket around the heater in the evaporator. A bottom piece was manufactured for both the evaporator and the condenser, both of which were bolted to the bottom of the walls. End pieces were also made for the condenser and all connections in the water jacket were gasketed to avoid leakage.

### 3.2.3 Evaporator

The evaporator is 56.5 cm in length and uses as an energy source a commercially available strip heater, which is also 56.5 cm in length and 5.1 cm in width. A high temperature, high thermal conductivity epoxy was used to bond the heater to the wall of the heat pipe to prevent air gaps and to avoid the possibility of local hot spots at the contact points of the heater. The heater is constructed of high quality coiled nickel-chromium resistor wire, uniformly spaced along the length and width of the heater. The wires are embedded in a highly compressed refractory material which is enclosed in an iron sheath. It has a maximum working temperature of 149°C, and a maximum continuous power rating of 1500 W. The output can be pushed up as high as 1750 W for short periods of time.

The three sides of the heater not in direct contact with the wall of the heat pipe are insulated with 1 inch of ceramic block, trimmed to fit around the heater.

This insulation is rated for temperatures up to 1260°C, and thus cannot be ignited by the heater. The evaporator section of the heat pipe is further insulated by packed fiberglass insulation, and is contained inside a 0.1524- X 0.1524-m three-sided wooden box in which the entire heat pipe is encased. There are four thermocouples in the evaporator, attached to the outside wall of the heat pipe. The fourth thermocouple is at the adiabat end of the evaporator. The other three are spaced as shown in Figure 11. All of these thermocouples are Type J (iron-constantan), and are permanent fixtures since removal would require complete disassembly of the unit.

#### 3.2.4 Adiabat

The adiabatic section of the heat pipe is 17.8 cm in length. The sides and base of the adiabatic section are insulated with a foam-type insulating material which was sprayed underneath the heat pipe and allowed to fill the wooden box on three sides. The foam expanded to fill any voids as it hardened and excess material at the top was removed. All thermocouple wires from both the condenser and the evaporator were fed through the adiabatic section and out through a gap in the aluminum casing beneath that section. The coolant inlet for the water jacket also enters the unit through this gap. The adiabatic section has one thermocouple of its own, located in the center of the region, and shares one each with both the evaporator and the condenser where they meet the adiabat.

#### 3.2.5 Condenser

The condenser, 164.5 cm in length, is cooled by a coolant flowing in a jacket below the bottom wall of the pipe. There are seven evenly spaced thermocouples along the length of the condenser, as shown in Figure 11. The ends of the thermocouples are cemented to the wall and then are covered with cement. The wires are run inside plastic tees and a rubber hose to ensure that they do not come in contact with the liquid flowing through the cooling jacket. All fittings and gaskets were selected based on their ability to withstand the low temperatures that could be experienced with a low temperature coolant used when freezing the heat pipe. The only penetration through the aluminum body of

the heat pipe into the flow channel is at the end of the condenser farthest from the adiabatic section. This is to allow the attachment of the vacuum line.

The water jacket can be operated in either of two modes. The open loop mode uses tap water, which flows through the coolant jacket once and then is dumped. This method is used primarily for flushing out the condenser after other fluids have been run through it, or when running the condenser at room temperature will suffice. The second mode of operation is the closed loop mode. In this case, a pump is used to pump fluid from a reservoir, through the condenser and then back to the reservoir. The pump is a magnetically coupled centrifugal pump so that the low temperatures near the impeller have no conduction path into the motor housing. Cooling the motor shaft to such low temperatures could cause either the motor to seize or the shaft to shear. In both cases, the fluid passes through a flowmeter so that an approximate indication of the flow rate is given. Upon leaving the flowmeter, but prior to entering the cooling jacket, the fluid flows by a thermocouple, which is also connected to an analog to digital (A/D) signal conversion board for data collection. The unit was designed so that the condenser would be essentially isothermal ( $\Delta T < 1^\circ\text{C}$  across the condenser for 1500 W input and 3 gal/min flow rate of water).

### 3.2.6 Glass Cover

The glass cover for the heat pipe measures 2.4130 X 0.0508 m, and is 0.0064 m in thickness. The cover is separated from the aluminum body of the heat pipe by a 0.0032-m-diameter, 4.8768-m-long neoprene O-ring. The glass cover has a single penetration, which is on the major axis, 0.0508 m from one end. Through this hole, a 50-ml buret is attached via a rubber grommet. The buret is to allow addition of a measured amount of working fluid to the inner channel of the heat pipe after the glass cover has been secured and the inner channel evacuated.

Five type K (chromel-alumel) thermocouples are attached to the glass. The tip of each thermocouple is bent down into the vapor channel approximately 0.0032 m. The wires run along the surface of the glass and exit the vacuum chamber through the rubber grommet which supports the buret. These thermocouples were not originally included in the design for it was felt that the

flow disturbances they would cause in the case of high vapor velocities when approaching entrainment and sonic limits would be detrimental. However, in the study of the response of a heat pipe near nominal operating conditions, such high vapor velocities would not be encountered.

Before sealing the heat pipe all surfaces are thoroughly cleaned to remove excess grease left from previous work and any other contaminants. Then the O-ring is uniformly greased with a low temperature vacuum grease. It is then laid on top of the aluminum body around the outside of the retaining lip. The glass cover is set on top of the O-ring and then clamped down. The vacuum pump is started and the glass is pulled down by the vacuum. The clamps are then removed from the glass and the O-ring is pushed all the way up against the retaining lip from the outside. The vacuum pump remains on until the lowest pressure possible is attained.

### 3.2.7 External Equipment

As mentioned previously, real-time acquisition of large amounts of data was made possible by the use of an IBM PC/XT for data acquisition and storage, and interfacing with analog to digital hardware and software from MetraByte Corporation. The supplied software was used as an example to write a BASIC routine for data conversion, display, and storage. A listing of this code, called HTPIPE, is given in Appendix B.

The purpose of the A/D hardware is to take a voltage reading and convert it to a signal which can be accepted by the microcomputer and have a digital representation inside the machine. The hardware consists of two parts: the analog input expansion submultiplexer (MetraByte model EXP-16) and the A/D converter and timer (MetraByte model DASH-8). The EXP-16 is located external to the computer, and sends signals via a flat ribbon cable. All type J thermocouples are connected to one EXP-16, which can accept up to 16 different inputs. The five type K thermocouples are attached to a second board. The pressure transducer is connected to a third unit. The gain setting requirement differs for each type of sensor, and thus each type requires its own EXP-16 with the board gain set to its appropriate value. Each board has its own user selected gain setting, which applies to all 16 connections on the board, so that an

appropriately amplified signal can be transmitted to the DASH-8. Type J thermocouples require a gain setting of 100, type K a gain of 50, while the pressure transducer output supplies a sufficiently strong signal by itself and requires a gain setting of 0.5. These three boards are connected in series. The DASH-8 can support up to 8 boards in series.

The DASH-8 is connected directly to the chassis of the computer, in one of the free ports inside the machine. This is the unit that actually does all of the work. It selects a board and input location on that board as instructed by the software. It measures the amplified voltage from the EXP-16 and converts this to a digital value. The software then divides the value by the gain corresponding to that board and processes the information as described above.

The use of the MetraByte hardware and software results in some loss of accuracy because of the limited number of bits for transmission of voltage data, and due to linear interpolation between tabulated temperature values for discrete voltage values. This results in an accuracy under best conditions of 0.3°C, and readings tend to be randomly distributed within this limit around the temperature that the thermocouple would normally indicate based on a direct voltage measurement. Electronic background noise will make this error even worse. Values for temperatures reported in this work should be considered to have an associated error of 0.3° unless otherwise noted.

The use of the data acquisition system allowed the collection of large amounts of data, with a complete set of readings taken within a small fraction of a second, and a new set taken only a second or two later. This allowed a detailed analysis of rapid transients after they occurred - transients which may be too fast for the experimenter to observe and record. It also served to free the experimenter to visually observe any internal mechanisms as they occurred. Finally, the information displayed and continuously updated on the CRT monitor provided an essentially real-time update of the operating conditions of the heat pipe, so that the experimenter could tell the status of the unit at any time.

The code HPIPE performs several functions. First, it instructs the A/D converter to look for a reading on a particular board and slot. Then it stores the digital representation of the voltages measured by the A/D conversion hardware from both the thermocouples and the pressure meter and divides by the appropriate gain. It then does a table look-up to find the voltage range in which

the measured value falls, and uses an interpolation routine to approximate the corresponding value of temperature for thermocouples and pressure for the pressure transducer. The table look-up was supplied by MetraByte for the thermocouples, and was created based on figures supplied by the manufacturer for the pressure meter. The converted data is then stored in virtual memory along with the time the reading was taken. A virtual memory region of 50 kilobytes is reserved for this information; once this amount is filled, the data are written on a floppy disk and the virtual memory is cleared to be refilled. The converted data are also displayed on the screen with an option to see each reading, or every nth reading as specified by the user. The conversion process is relatively fast, and the entire process takes approximately one second prior to printing to the screen. The screen print itself takes approximately one second. It is more efficient, therefore, to print to the screen once for every five to ten readings; refreshing the visual display any faster would be superfluous and hinder the rate of data collection. Also, a data collection rate any greater than once per second would be of little use as it would use too large a storage space and would not yield any more meaningful data since the response times of the thermocouples and of the pressure transducer are both on the order of a large fraction of a second to seconds, depending on the rate of temperature change.

### 3.3 Experimental Procedures

Prior to beginning the transient study, it was necessary to confirm proper operation as a heat pipe to assure that energy removal from the evaporator was not merely due to convection losses in the air or conduction losses along the length of the bar. The following subsection describes the procedure used to confirm operation as a heat pipe. Once verification of proper operation was completed, thermocouples were installed inside the heat pipe vapor space to allow a better determination of the operational status of the unit. The study of transient behavior was then initiated. The concluding subsection of this section describes the experimental methodology of these studies.

### 3.3.1 Operation as a Heat Pipe

In shakedown testing, the heat pipe was primarily run in a thermosyphon mode, that is, operated with a gravity assist and no wick. To run as a heat pipe required that it be able to operate with no gravity assist (horizontally), or to work opposing gravity (evaporator elevated above the condenser). In either case, capillary pumping would be required for continuous operation at power. To demonstrate that it could be operated as a heat pipe, the unit was loaded with four layers of 400-mesh/in stainless steel wick, sealed, and evacuated by the methods described in the previous chapter. The working fluid was distilled water. The condenser was cooled by once-through-flow tap water at room temperature. Coolant temperature for these runs stayed at  $21 \pm 1^\circ\text{C}$ . The coolant flow was started well ahead of the planned start-up time to allow the entire heat pipe to come to thermal equilibrium. This was necessary because room temperature was somewhat less than the tap water temperature; introduction of warmer water to the pipe (initially at room temperature) would cause a warming of the condenser relative to the rest of the pipe. Thus, coolant flow was started at least an hour before start-up so that the entire pipe could come to equilibrium with the coolant temperature. Observation of the outer wall thermocouples allowed a precise determination as to when the bar reached an equilibrium temperature.

To test the capabilities of the unit to dissipate energy when not operating as a heat pipe, energy was input at the evaporator with no fluid present in the inner chamber of the heat pipe so heat transfer could only occur by conduction through the bar, with energy removal due to flow through the condenser and some free convection losses at the ends of the pipe. To prevent damage to the heat pipe due to high temperatures, a maximum of 250 W from the heater was allowed. The heater was first set at 100 W and the unit was allowed to come to steady-state. The power input was then raised to 250 W and equilibrium was allowed to reestablish itself. The data acquisition system was concurrently storing all the thermocouple and pressure data. The heater was turned off and the heat pipe was allowed to return to room temperature. Distilled water (250 ml) was added to the heat pipe, and dissolved gases were drawn off through the vacuum system. The unit was brought to equilibrium at 62-W power input, and remained there for 10 min, during which time the vacuum line was opened for

short periods to allow removal of any additional noncondensable gases present. The unit was then taken to 100 W and allowed to equilibrate. The energy input rate was then increased to 250 W, and the heat pipe was allowed to stabilize at this condition. As before, the data acquisition system was measuring, converting and storing all thermocouple and pressure data as the experiment ran. The results of these measurements and a discussion of their significance will be presented later in this section.

### 3.3.2 Transient Measurements

As mentioned in the literature review, there are many who suspect that the worst transient experienced by a heat pipe is a rapid change in power. It was therefore felt that emphasis should be placed on the observation of heat pipe performance under these conditions. For the work of this section, most measurements were made to study the mechanics of start-up behavior. A single measurement of transition from one power level to another was made before a major equipment malfunction prohibited further measurements from being taken before rebuilding the pipe.

In performing start-up experiments, the heat pipe was loaded with four layers of 20-mesh/in aluminum wick, for a total wick thickness of approximately 0.0032 m (a larger mesh size was used in an attempt to enhance the probability of transient failure). A fluid charge of 215 ml of water was added to the inner chamber after sealing and evaluating the chamber. The outgassing procedure described previously was used to remove any dissolved or generated gases. As with the previous measurements, the heat pipe was allowed to come to equilibrium with its surroundings and with the coolant before any start-up was attempted. The glass cover was covered by several layers of fiberglass insulation to reduce convection from the glass; portions of the insulation could be removed to observe inner workings of the pipe. Once thermal equilibrium was established, the data collection routine on the computer was started and the heater was turned on at a preselected power level. The heat pipe was allowed to follow its own course without any other outside interference, other than temporarily moving portions of the insulation for visual observations. The unit was then allowed to come to equilibrium at its new operating level, as judged by observation of the

rate of change of the heat pipe temperatures. In the case of transient failure, the energy input remained on until temperatures approached those which could cause physical damage to the heat pipe itself. When the heater was shut off, the data acquisition process was terminated; no attempt was made to follow the behavior of the pipe as it returned to initial conditions. Several runs were made, with power inputs of 100 and 250 W.

In the power transition study, the heat pipe was prepared in exactly the same manner as for start-ups. The heater was turned on at 100 W and allowed to come to equilibrium. The power was then raised to 250 W and equilibrium was allowed to reestablish. Other than the power-up from an operational equilibrium, the procedure for this experiment was identical to that of the start-up experiments.

### 3.4 Results And Discussion

This subsection is divided into three major parts. The first presents a comparison of the normal steady-state operation of the heat pipe versus operation with conduction energy transport in the body in the absence of working fluid. Following this, the results of the start-ups from zero power are presented. A total of five start-ups are presented: three start-ups with a 100-W energy input, and two with 250 W. A detailed discussion, dealing with the behavior of the heat pipe under start-up conditions, accompanies these results. Finally, the last subsection deals with the results of a power increase from one operating state to another.

#### 3.4.1 Steady-state Operation

Upon completion of cleaning and assembly with two layers of 400-mesh/in stainless steel wick, the heat pipe was sealed and evacuated, charged with 150 ml of water, started up with a 100-W power input, and allowed to come to steady-state. This procedure was then repeated for a 250-W power input. Plots were made of the steady-state temperature profile measured along the heat pipe outer wall for both the conduction (no working fluid) and operating (working fluid present) cases. The data were plotted for each power level; these are shown in Figure 12 for 100 W and Figure 13 for 250 W. Both figures clearly show a much

lower temperature profile in the evaporator during operation as a heat pipe compared with the alternative case when energy transport was by conduction along the wall of the pipe.

Since the condenser was cooled by a once-through-flow of water at room temperature, and since the flow rate was sufficient to guarantee no measurable temperature rise along the length of the condenser, the condenser can be considered to be an infinite isothermal heat sink. Thus, if the heat pipe is considered to be a semi-infinite slab with a uniform thickness of 0.0032 m, heated along the first 0.5652 m, insulated for the next 0.1461 m (no energy gain or loss), and with the remaining length maintained at room temperature, then based on the following conduction analysis one would expect a temperature distribution similar in shape to that shown.

Solving Fourier's heat conduction equation for a 1-D bar and assuming the conditions given above gives a second-order temperature distribution in the evaporator and a linear temperature distribution in the adiabatic region. Both Figures 12 and 13 show this kind of pattern. The slight decrease in temperature at the left side of both curves for the conduction-only case is due to the fact that the ends of the heat pipe were not insulated so there was some energy loss due to free convection at the end of the evaporator.

When the heat pipe was operated with a working fluid at a power level of 100 W, three temperature regions were clearly seen. The thermocouples on the evaporator outer wall showed approximately the same temperature all along the length of the evaporator. Similarly, the condenser remained isothermal. Only one thermocouple is dedicated to the adiabatic section, and is located at its center. This thermocouple showed an outer wall temperature about 7°C warmer than that of the condenser, and about 25°C cooler than the evaporator. These temperatures are consistent with heat pipe operation as explained below.

For steady-state heat pipe operation, the two-phase mixture inside the pipe should be essentially isothermal. When the measurements shown in Figures 11 and 12 were made, the heat pipe did not have thermocouples mounted inside the vapor channel. Thus, it was not possible to measure the vapor temperature directly. The determination of isothermal operation had to be made indirectly by measuring the temperature of the outer wall of the heat pipe. Despite the

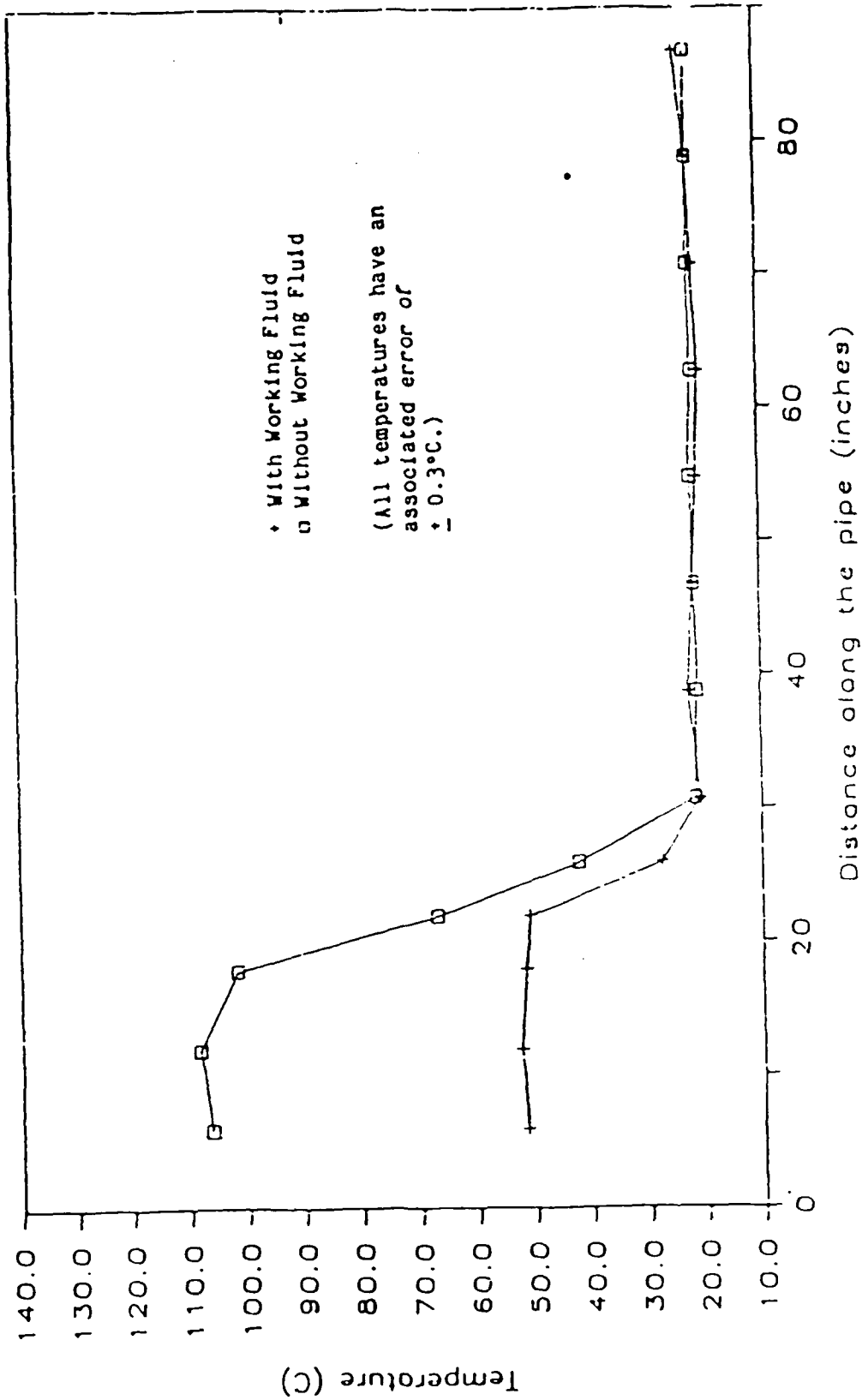


Figure 12. Operation Vs. Conduction at 100 W

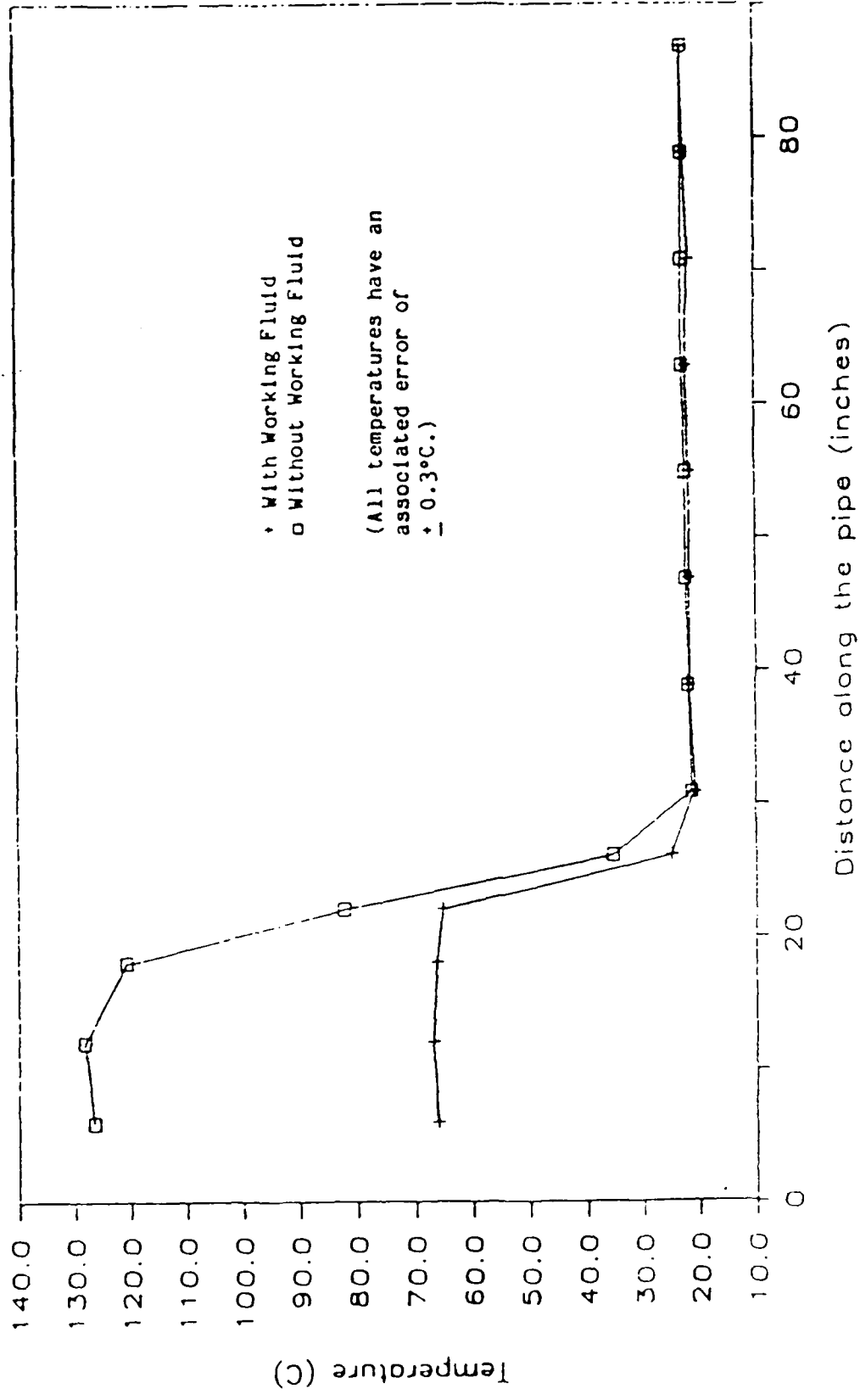


Figure 13. Operation Vs. Conduction at 250 W

isothermal operation of the internals of the heat pipe, temperature variations exist along the length of the pipe due to the temperature gradient caused by conduction through the wall in the transverse direction. Assuming that all energy input through the evaporator is rejected through the condenser, i.e., neglecting losses, then:

$$Q_{in} = Q_{out} \quad (7)$$

or in terms of the energy flux,

$$q'' A |_{\text{evaporator}} = q'' A |_{\text{condenser}} \quad (8)$$

Since the condenser is approximately three times the length of the evaporator and both are the same width, the area of the condenser is three times the area of the evaporator, and  $q''_{\text{evaporator}}$  must be three times greater than  $q''_{\text{condenser}}$ . Applying the 1-D heat conduction equation to the wall of the heat pipe,

$$q'' = -k \frac{dT}{dx} \quad (9)$$

Assuming a constant thermal conductivity, the temperature gradient in the wall is proportional to the energy flux. Since the wall separating the inside of the heat pipe from the thermocouples is of uniform thickness, the temperature change across the wall would be expected to be proportional to the energy flux through the wall. Since  $q'' = 0$  through the adiabatic region wall, there should be no temperature gradient through this wall, and the outside wall reading should be the same as the inner wall (neglecting axial conduction). Therefore, for the 100-W case, the temperature difference between the evaporator and the adiabatic section should be three times the magnitude of the difference between the condenser and the adiabatic section, and should have the opposite sign because the heat transfer occurs in opposite directions for each section. Since the condenser is 7°C below the adiabatic temperature and the evaporator is 25°C above the adiabatic temperature, this is indeed the case.

Operation of the heat pipe at 250 W demonstrates similar behavior, except

that the adiabatic temperature is closer to the condenser temperature than expected. This is perhaps due to the fact that axial conduction (conduction down the length of the pipe) cannot be neglected at higher energies. In addition, the supporting shoulders of the heat pipe were neglected when the heat pipe was assumed to be a 0.0032-m-thick semi-infinite slab. Since the sides of the pipe were neglected while they represent most of the mass of the heat pipe itself, the slab approximation is weak and simple modeling is not sufficient. However, as this is not within the scope of this research, a more detailed analysis will not be developed here. What is important is that the results show that the heat pipe does operate in the manner for which it was designed, as predicted by theory, and can therefore be used to study heat pipe transient phenomena.

#### 3.4.2 Start-up from Zero Power

A total of six different runs were made from zero power to fixed power levels. Table 3 is a summary of the conditions for each run. Runs 1 through 5 behaved as expected during operation, as will be shown, making a smooth transition from steady-state at zero power and room temperature to a new power level and corresponding equilibrium temperature.

During runs 1 and 2, electrical interference from an unidentified source resulted in a smaller signal to noise ratio (SNR) than was achieved in the ensuing measurements. While the trends in both temperature and pressure are clearly seen when the results are plotted, the error associated with each reading is larger ( $\pm 1^\circ\text{C}$ ) than for the later runs. In addition, the failure of a floppy disk used for recording data from run 2 resulted in the loss of data for the last half of the transient; however, visual observation of the data output to the computer CRT during the transient indicated normal behavior similar to that seen in runs 1,3,4, and 5. Due to the lack of data, only a guess can be made at run 2 equilibrium temperatures, based on the first 3000 s of operation.

Looking first at the 100-W start-ups, Figure 14 shows the variation of evaporator, adiabat, and condenser temperatures with time, beginning when the heater was turned on ( $t = 0$  s). Since the temperature profile along the outer wall of the evaporator remained essentially flat, as will be shown later, the evaporator temperature is represented in this figure by only one thermocouple, thermocouple

Table 3. Operating Conditions for Startup from Zero Power

Run Number	Input Power (W)	Room Temperature (°C)	Coolant Temperature (°C)
1	100	24-25	27.5-28.1
2	250	24-25	27.9-28.2
3	100	22-23	28.1-28.6
4	250	23-24	27.4-27.9
5	100	22-24	27.4-28.0

B, which is located approximately at the center of the evaporator. Thermocouple E, located at the center of the adiabat, was dedicated to the outer wall of the adiabat, so it alone was used to determine adiabat outer wall temperature. As with the evaporator, an isothermal profile allows the use of one thermocouple, G, located 8 in from the condenser inlet, to represent the condenser outer wall temperature.

All three runs to 100 W show the same exponential behavior, approaching a maximum temperature of approximately 50°C after 5000-6000 s. It is important to note that the temperature rise does not start at  $t = 0$ , but many seconds later. Due to the stored energy effects in both the heater and the body of the heat pipe, a short time delay is seen at the far left part of the curve representing the evaporator temperature. Such a delay would be expected in both the condenser and adiabat as well, enhanced by the delay time associated with conduction back out of the heat pipe through the wall. However, the fluctuations in thermocouple readings around a mean value appear to be large enough to hide such behavior. The time required before the outer wall of the heat pipe senses energy from the heater is a measure of the ability of this system to simulate a step input of power. As the

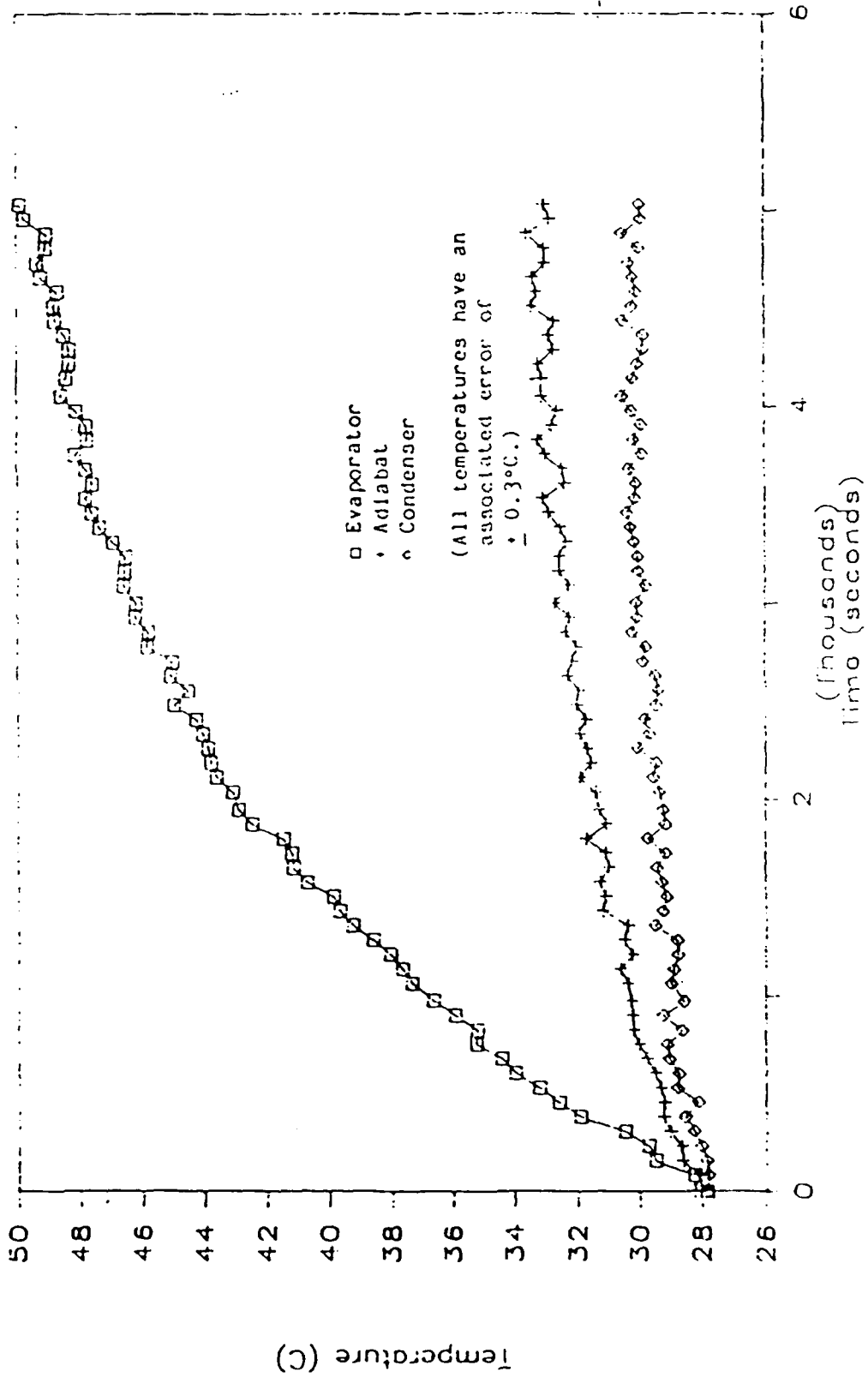


Figure 14. Evaporator, Adiabatic and Condenser Temperatures for Run 3

response time is on the order of a minute for a 100-W input, this represents a poor step function, and the heat pipe is perhaps moving through a quasi-steady-state start-up.

Figures 15, 16, and 17 show the evaporator, adiabat, and condenser temperatures respectively as a function of time for run 5. Again, the exponential rise and approach to an equilibrium temperature noted in Figure 14 can be clearly seen. In these figures, the "knee" prior to reaction to the energy input can also be seen.

It is easy to determine equilibrium temperatures for the adiabat and condenser from these figures: the adiabat outer wall levels off at a temperature of about 33.3°C, while the condenser comes to equilibrium at 30.3°C. The mean coolant temperature over the time of the run was 27.9°C. All temperatures have an associated error of  $\pm 0.3^\circ\text{C}$ .

Measurement of the vapor temperature with time for any of the five vapor channel thermocouple locations results in exactly the same shape as shown in the previous figures. Figure 18 shows the behavior as measured by thermocouple P at the evaporator-adiabat interface during run 3. The equilibrium temperature (after 6000 s) came to 32.3°C. Equilibrium temperatures for the evaporator, adiabat, condenser, and vapor channel (thermocouples B, E, G, and P) are given in Table 4 below. It can be seen that temperatures are similar in each region for all three runs at 100 W with the exception of the evaporator in run 1. This could be caused by a slight difference in room temperature or other uncontrolled conditions. In any case, the variation is not extreme.

Several observations on the steady-state performance of the heat pipe for runs 1, 3, and 5 may be made on the basis of the results presented in Table 3. First, the outer wall temperature of the heat pipe decreases from the evaporator, through the adiabat and to the condenser region. However, the outer wall temperature decrease along the pipe is 20°C, larger than would be expected for a 100-W power input. In addition, the temperature difference between the evaporator outer wall and the evaporator vapor temperature is 18°C, while the temperature difference between the condenser vapor temperature and the condenser outer wall is 2.3°C. Due to the 3:1 ratio in the areas of the condenser and evaporator, a 3:1 ratio would be expected in the outer wall to vapor temperature differences in the evaporator and condenser regions. The reason for

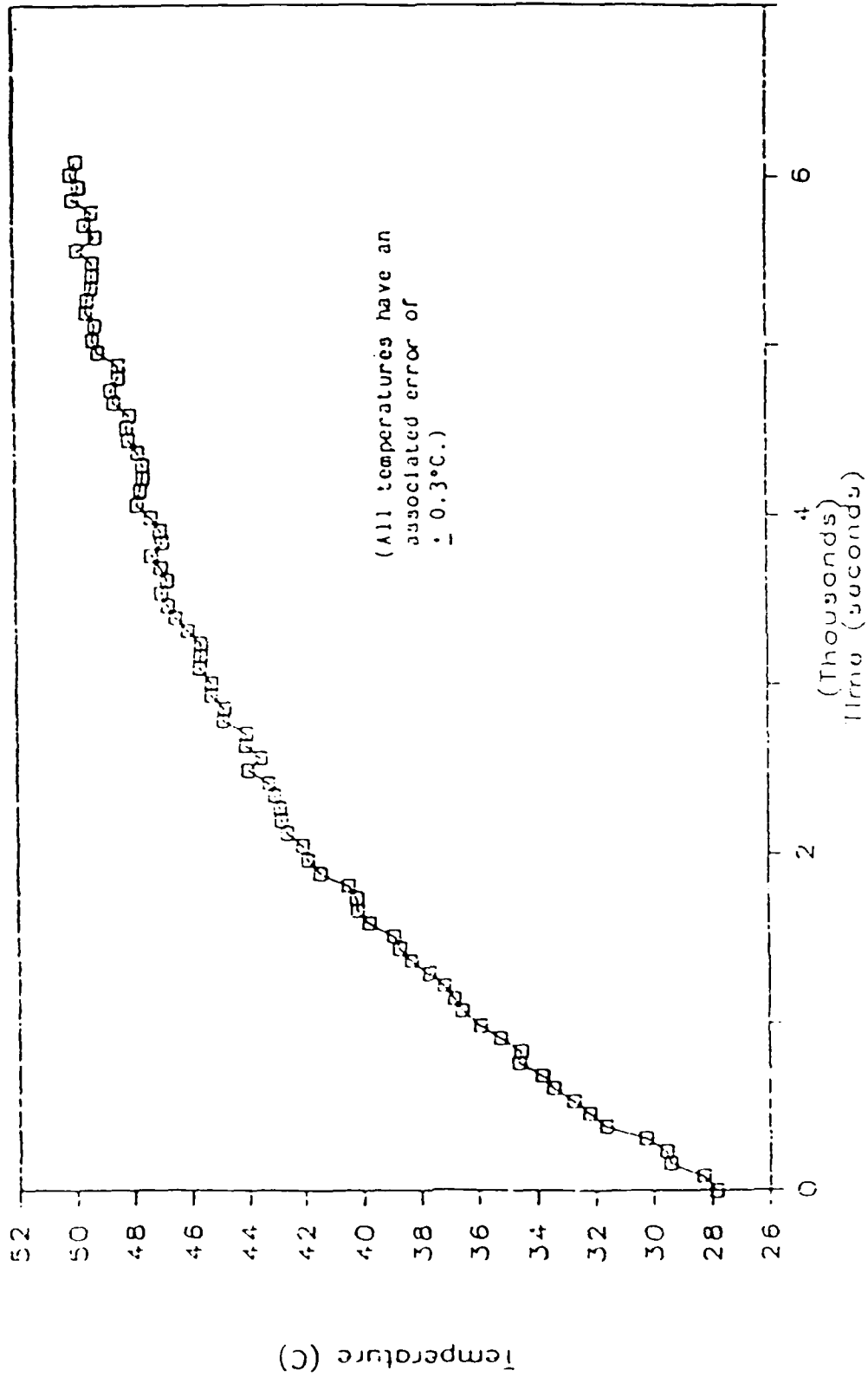


Figure 15. Evaporator Temperature Versus Time for Run 5

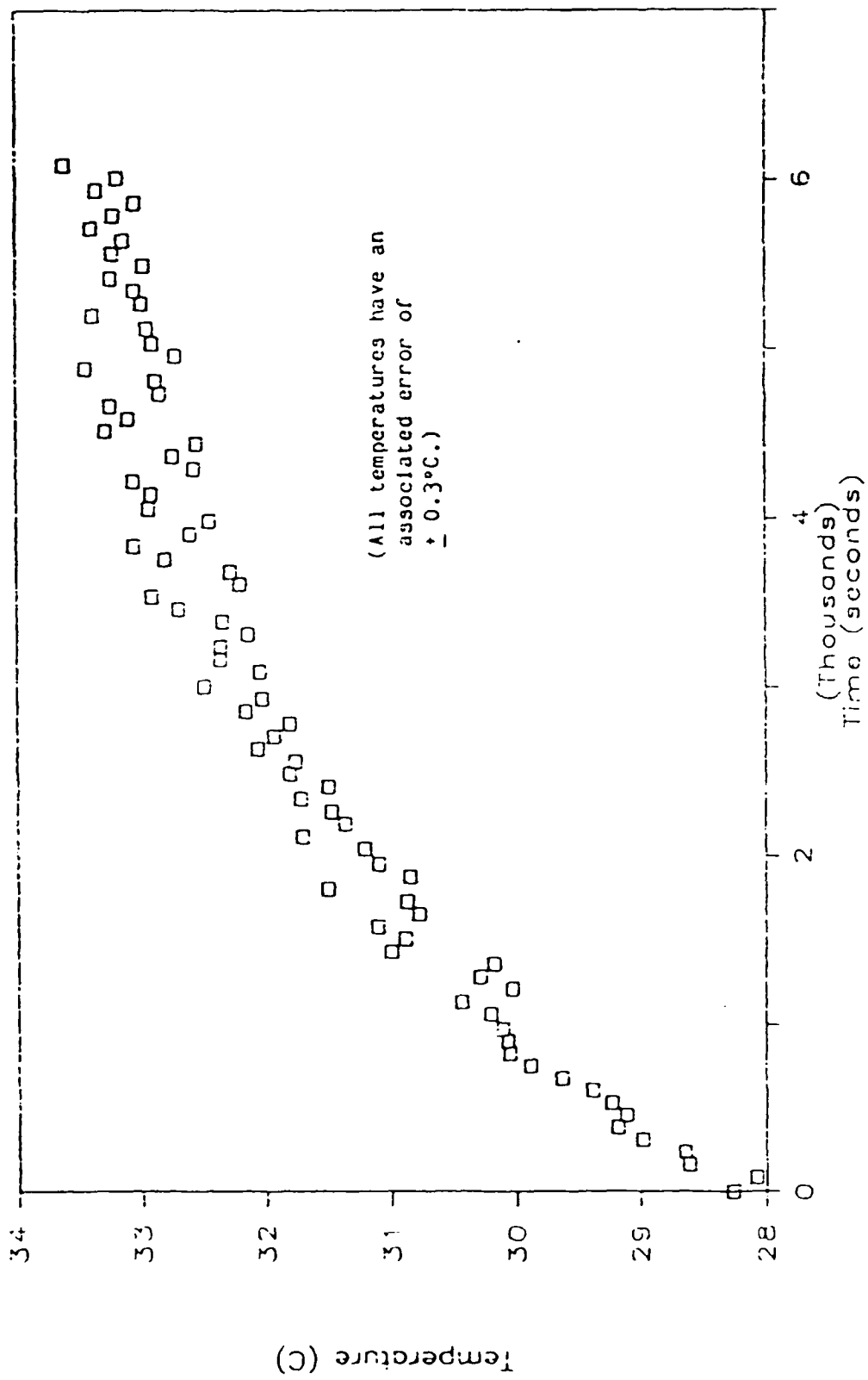


Figure 16. Adiabatic Temperature Versus Time for Run 5

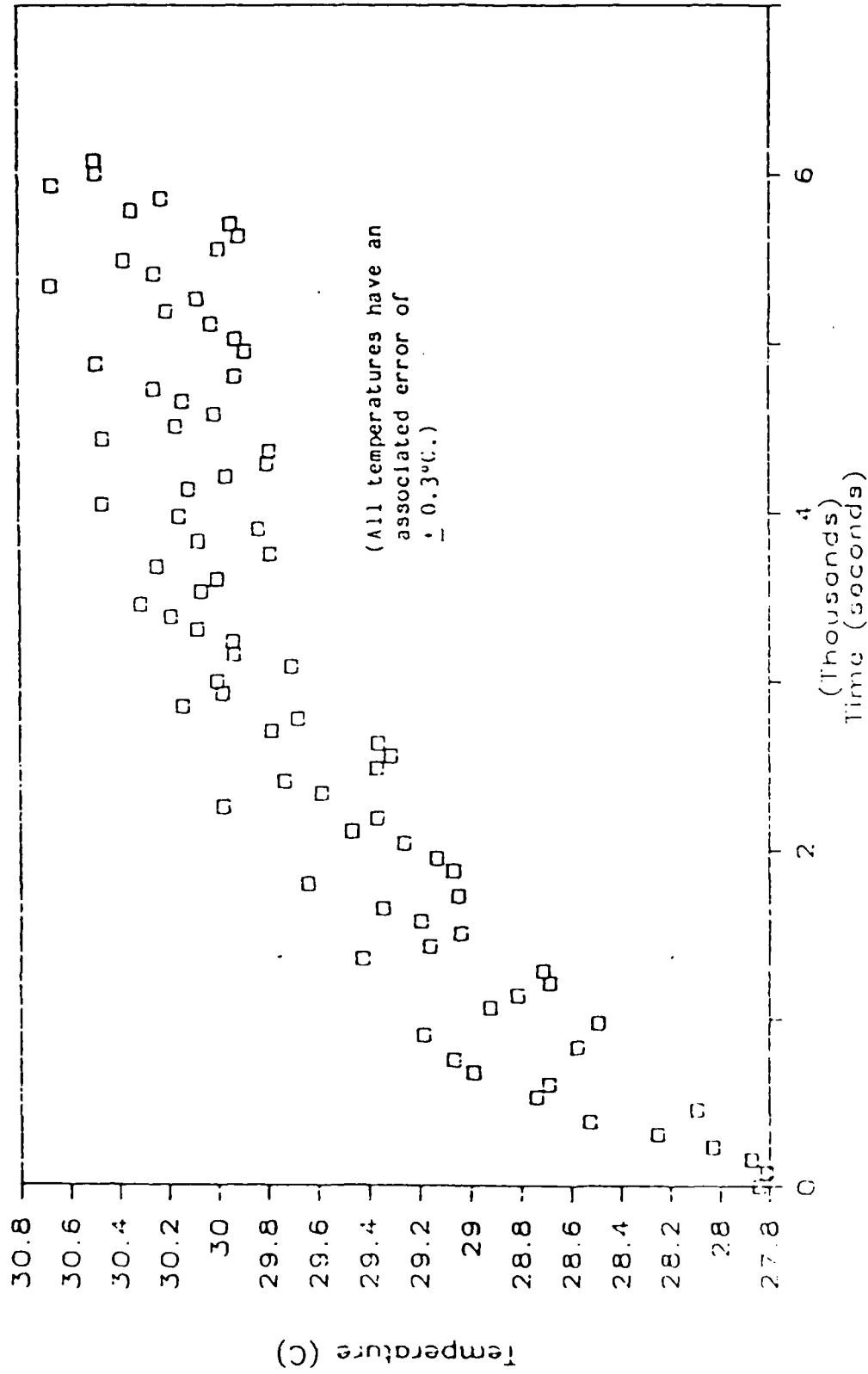


Figure 17. Condenser Temperature Versus Time for Run 5

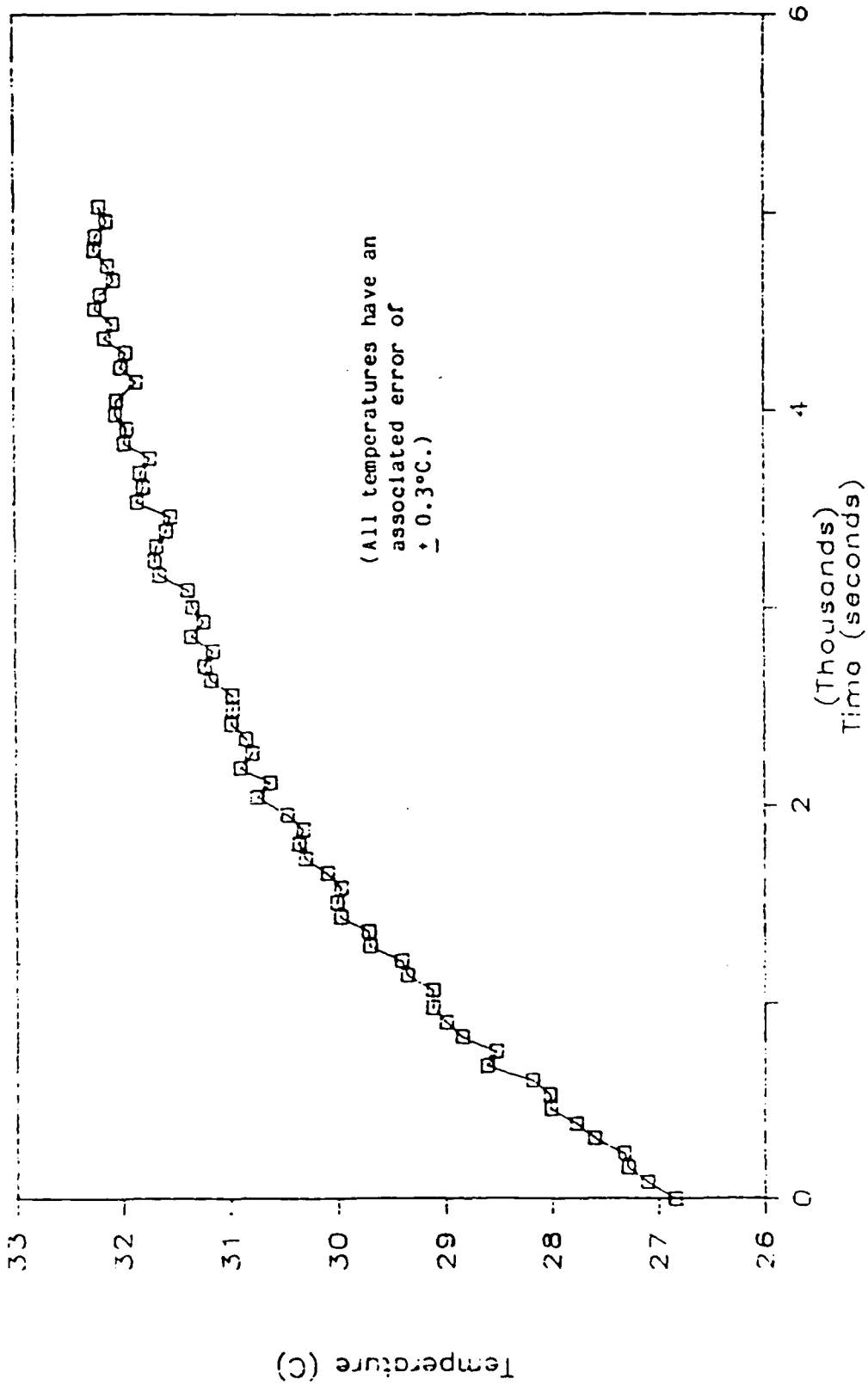


Figure 18. Vapor Temperature Vs. Time For Run 3

Table 4. Equilibrium Temperatures for 100- and 250-W Runs

Run Number	Power (Watts)	Evaporator $T_{eq}$ (°C)	Adiabat $T_{eq}$ (°C)	Condenser $T_{eq}$ (°C)	Vapor Channel $T_{eq}$ (°C)
1	100	53.0-55.0	33.0-35.0	29.0-31.0	31.0-33.0
3	100	50.2-50.8	32.7-30.3	29.7-30.3	32.0-32.6
5	100	49.7-50.3	33.0-33.6	30.0-30.6	32.2-32.8
2	250	70	40	30	35
4	250	68.7-69.3	37.9-38.5	31.2-31.8	36.8-37.4

this discrepancy is not known.

Second, the adiabat outer wall temperature seems to be somewhat hotter than one would expect. Liquid traveling from the condenser to the evaporator should be near the vapor channel temperature and the adiabat should therefore be at vapor channel temperature or lower. However, the measured adiabat outer wall temperature is higher than the vapor liquid temperature. Conduction through the wall and shoulders of the pipe from the hot evaporator to the cooler adiabat is presumed to be the cause of this anomaly. This interpretation means that evaporation is taking place in part or all of the adiabat as well as in the evaporator.

The final comment on runs 1, 3, and 5 from Table 4 deals with the comparison of these results with the results shown in Figures 12 and 13. The results of Table 4 should not be compared with the results of Figures 12 and 13 because the heat pipe used significantly different wick structure and coolant temperature in the two sets of tests. Therefore, wall temperatures and the unit's performance as a whole would be different, as such a comparison indicates.

Pressure readings were also collected during run 1, but analysis of that data

gave no new information. Since the pressure tap in the heat pipe is at the far end of the condenser, the pressure indicated is the stagnation pressure of the vapor at that end of the pipe. The data indicate a pressure consistent with the equilibrium vapor pressure for the measured vapor channel temperature throughout the transient. Therefore the pressure trace has the shape of the vapor channel temperature curve with time.

As was mentioned previously, measurements show relatively isothermal conditions in the evaporator and condenser regions along the outer wall. This fact is illustrated in Figure 19, which shows "snapshots" of the temperature profile every 1000 s from  $t = 0$  to  $t = 5000$  s for run 3. Variations from the mean temperature in each region are within  $\pm 0.3^\circ\text{C}$  of that mean, and are thus within the error associated with the data collection system. The shape of the curve closely resembles the 100-W operation curve of Figure 12. Theoretically, under steady-state operation the internal volume of the heat pipe should be essentially isothermal. If a region, such as the evaporator, is subject to a uniform heat flux, then the temperature change across the wall will be axially uniform and the temperature along the outer wall will also be uniform in that region. This can be seen to be true in both Figures 12 and 19. The fact that the vapor channel is truly operating isothermally is illustrated in Figure 20, which shows the "snapshot" temperature profile of the vapor channel as measured by thermocouples O - S for run 5. Again, variations from straight line behavior are within experimental uncertainty. Returning to Figure 19, one can conclude that, since the vapor channel is isothermal and the condenser section is also isothermal, there must be a uniform heat flux through the wall of the heat pipe. This implies that energy is being removed from the vapor along the entire instrumented length of the condenser, and that condensation is occurring throughout the condenser. Uniform condensation was also suggested by visual observation of the presence of droplets of uniform size and density on the sides of the channel and on the glass cover along the length of the condenser.

Considering the 250-W start-ups, two runs were made. Data for run 2 are incomplete, but run 4 measured all thermocouple and pressure readings from start-up through equilibrium. Run 2, which is missing data after 3000 s, demonstrates that the initial start-up phases of the two runs were nearly identical. Visual observation of the data while the experiment ran and of the heat pipe itself

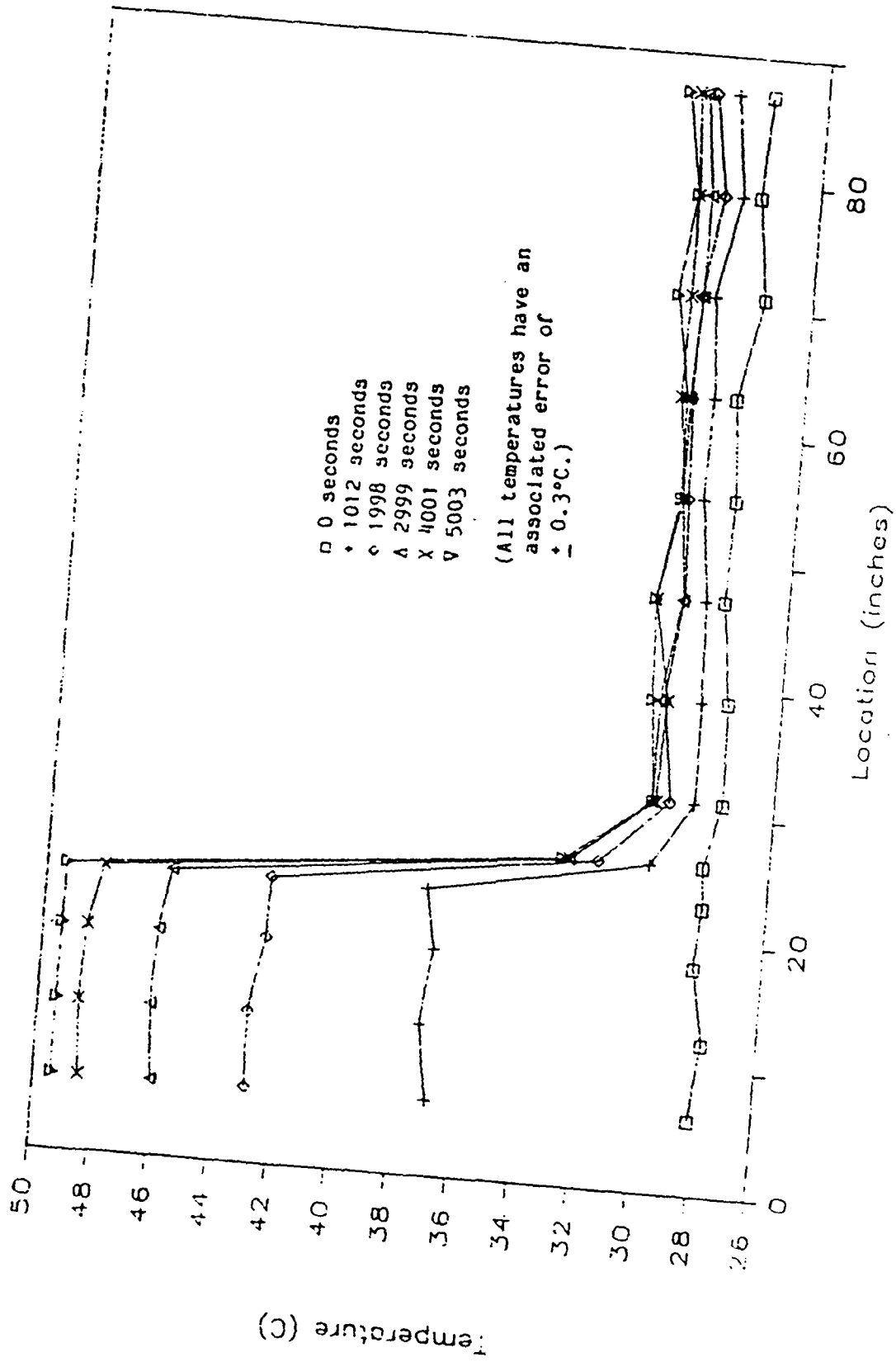


Figure 19. Temperature Profile at Heat Pipe Outer Wall During Start-up

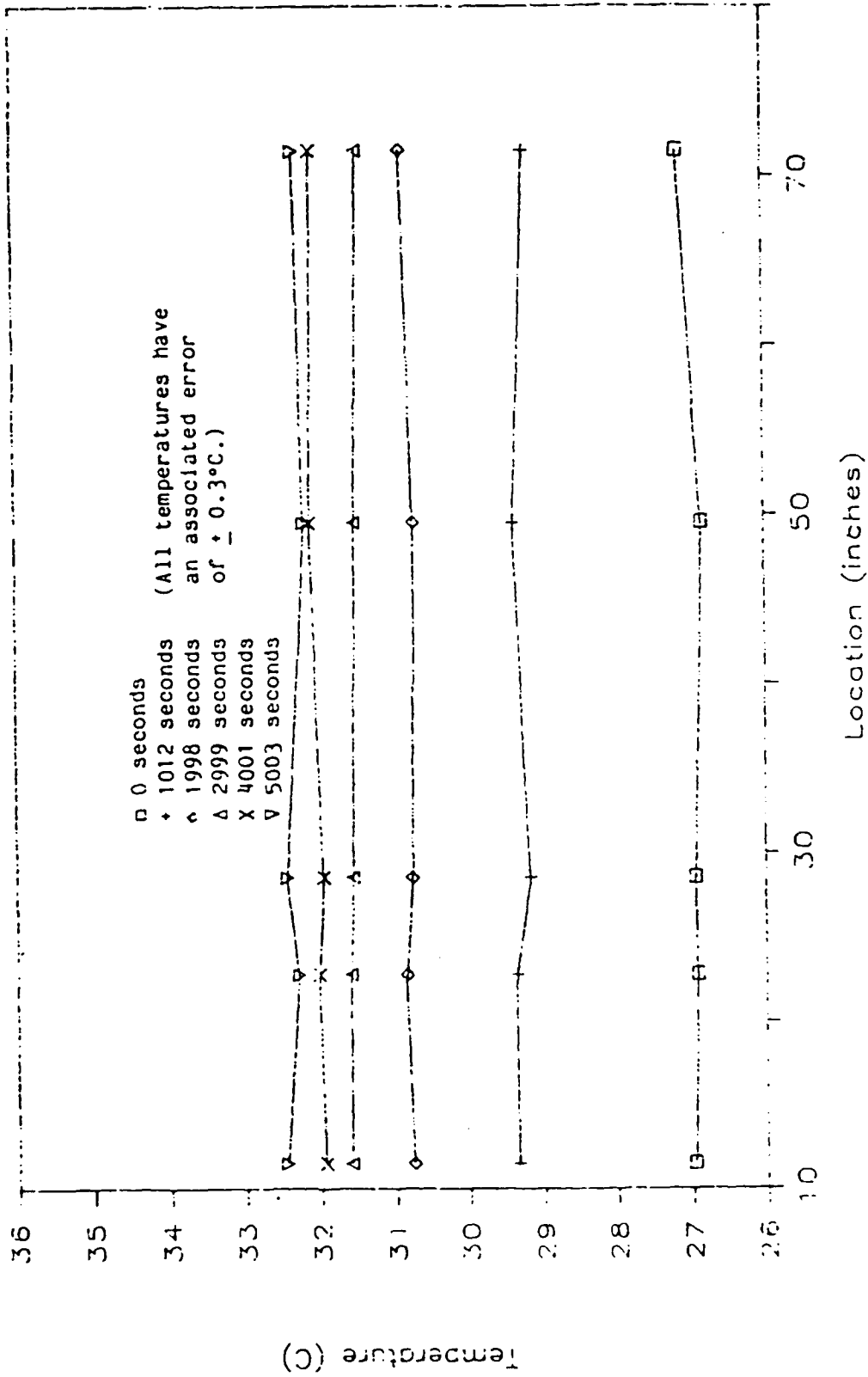


Figure 20. Temperature Profile in Vapor Space During Start-up

indicated no significant difference between the two runs. Figure 21 shows the evaporator, adiabat and condenser temperatures for data available. These data were recorded in the presence of electrical interference not encountered in the later runs, and therefore demonstrates a greater spread around the average temperatures.

The increase of temperature with time up to the equilibrium temperatures are shown for the evaporator in Figure 22 and for both the adiabat and condenser in Figure 23. The temperature inside the vapor channel is shown in Figure 24. As with the previous illustrations, these represent the readings of thermocouples B, E, G, and P in the evaporator, adiabat, condenser, and vapor channel, respectively. Other than higher equilibrium temperatures, which are summarized in Table 4, very little difference is seen between start-up behavior for 250 W compared to that for 100 W. One can see the same knee at the beginning of the start-up, followed by an exponential rise to a new equilibrium point. It appears that as with the 100-W start-up runs, temperature increases are slow enough such that the heat pipe is in a quasi-steady-state mode. The pressure data follows the temperature of the vapor channel.

### 3.4.3 Power Increase From An Operating State

The last run made in this set of experiments was an increase in power while operating at a lower power. In this case, the heat pipe was started up with an input power of 100 W. This start-up was identical to the previously observed 100-W start-ups. Once the heat pipe was at or at least very close to equilibrium conditions, the power input was increased to 250 W, and the pipe allowed to come to equilibrium. Figure 25 shows the temperature measured in the evaporator, adiabat, and condenser (thermocouples B, E, and G) from the initial start-up time until well into the second transient. Although measurements were taken well into the equilibrium stage of the 250-W response, these data offer no new insight into the transient operation of heat pipes and will not be presented. The time of interest in this study is the period immediately following the power increase. Other than the jump in temperature at the evaporator outer wall, which occurs 50 s after the increase in power, nothing especially remarkable is seen in the wall thermocouples. Figure 26 shows the readings on all five vapor channel

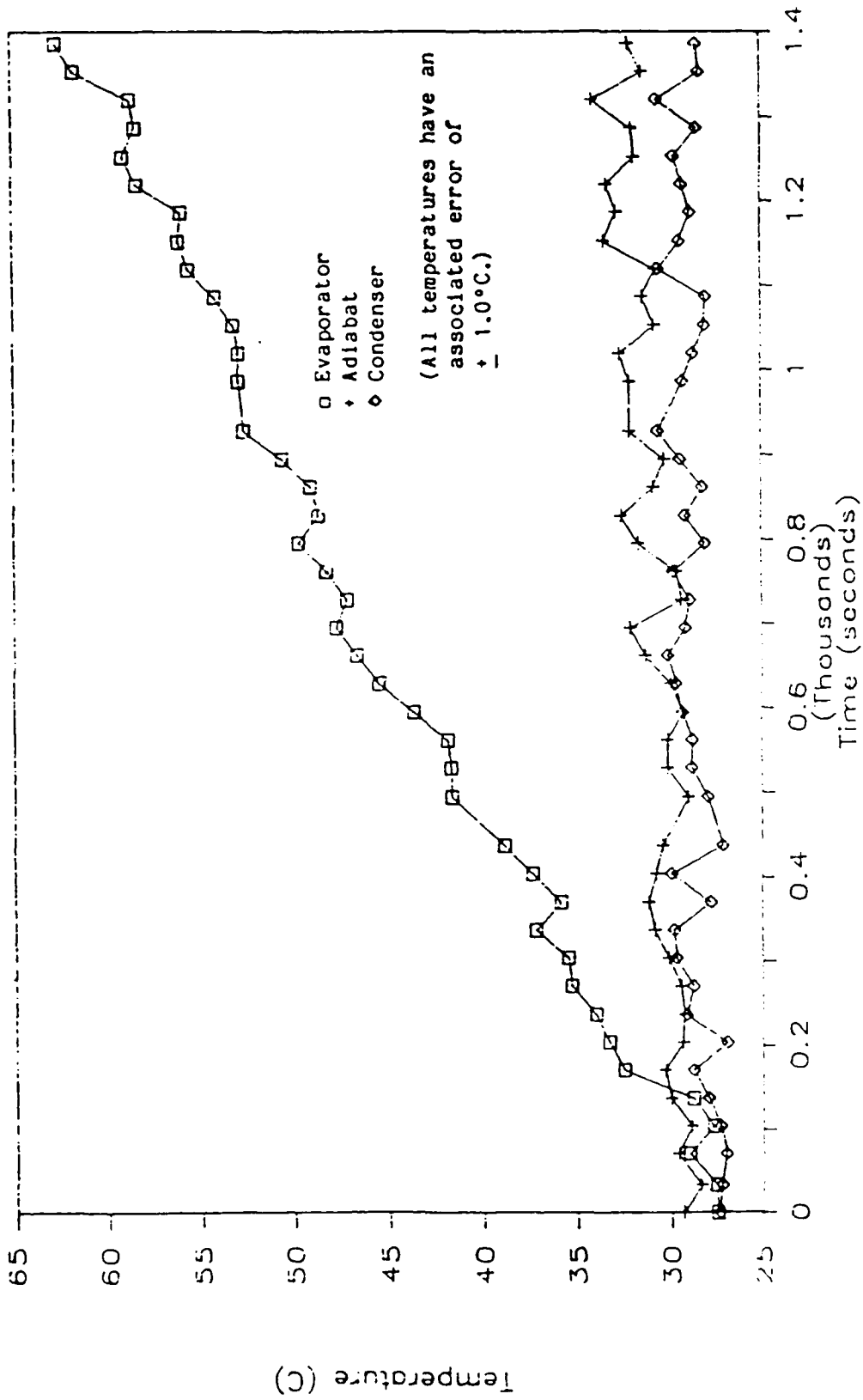


Figure 21. Evaporator, Adiabatic and Condenser Temperatures for Run 2

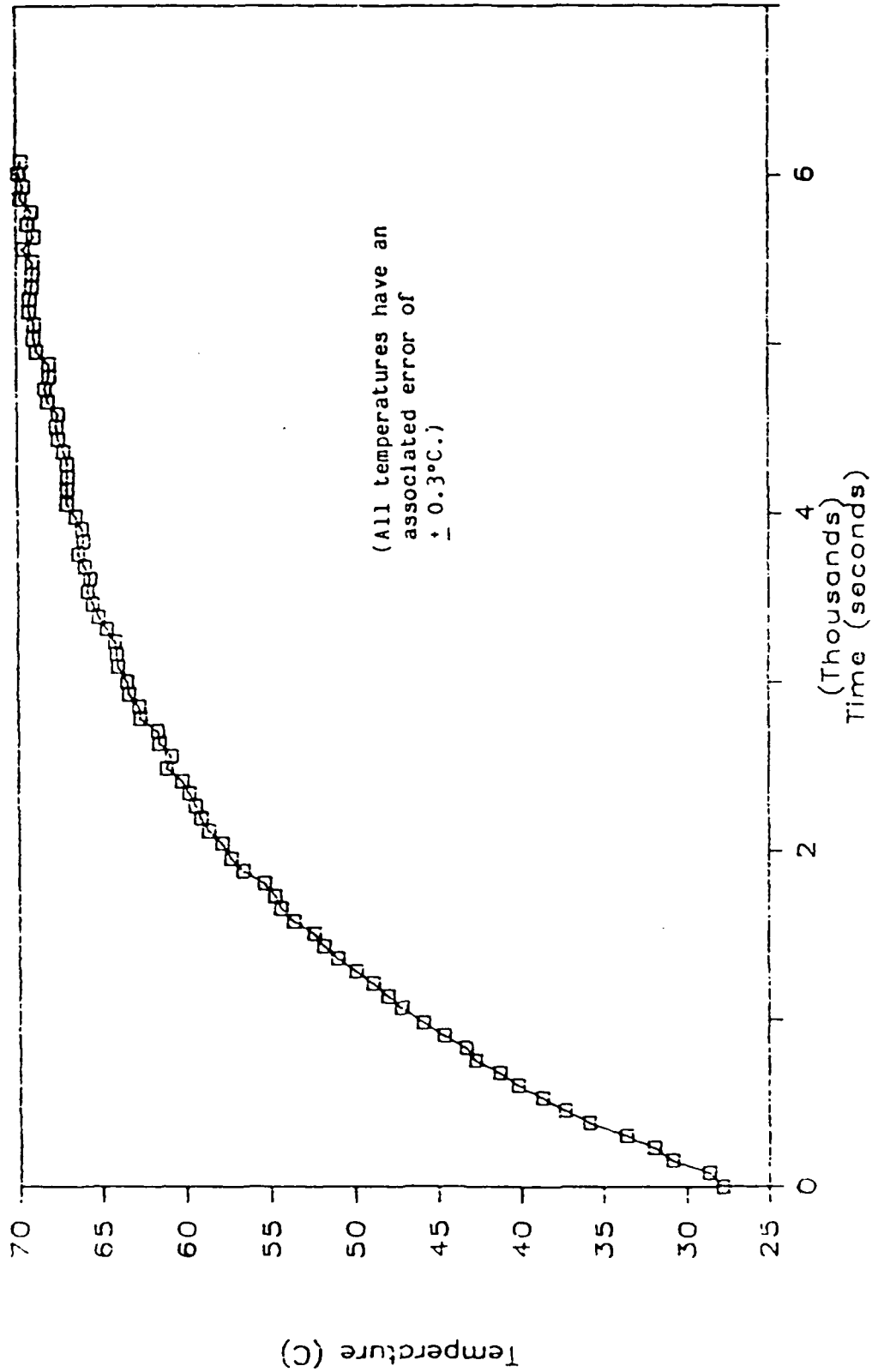


Figure 22. Evaporator Temperature Versus Time for Run 5

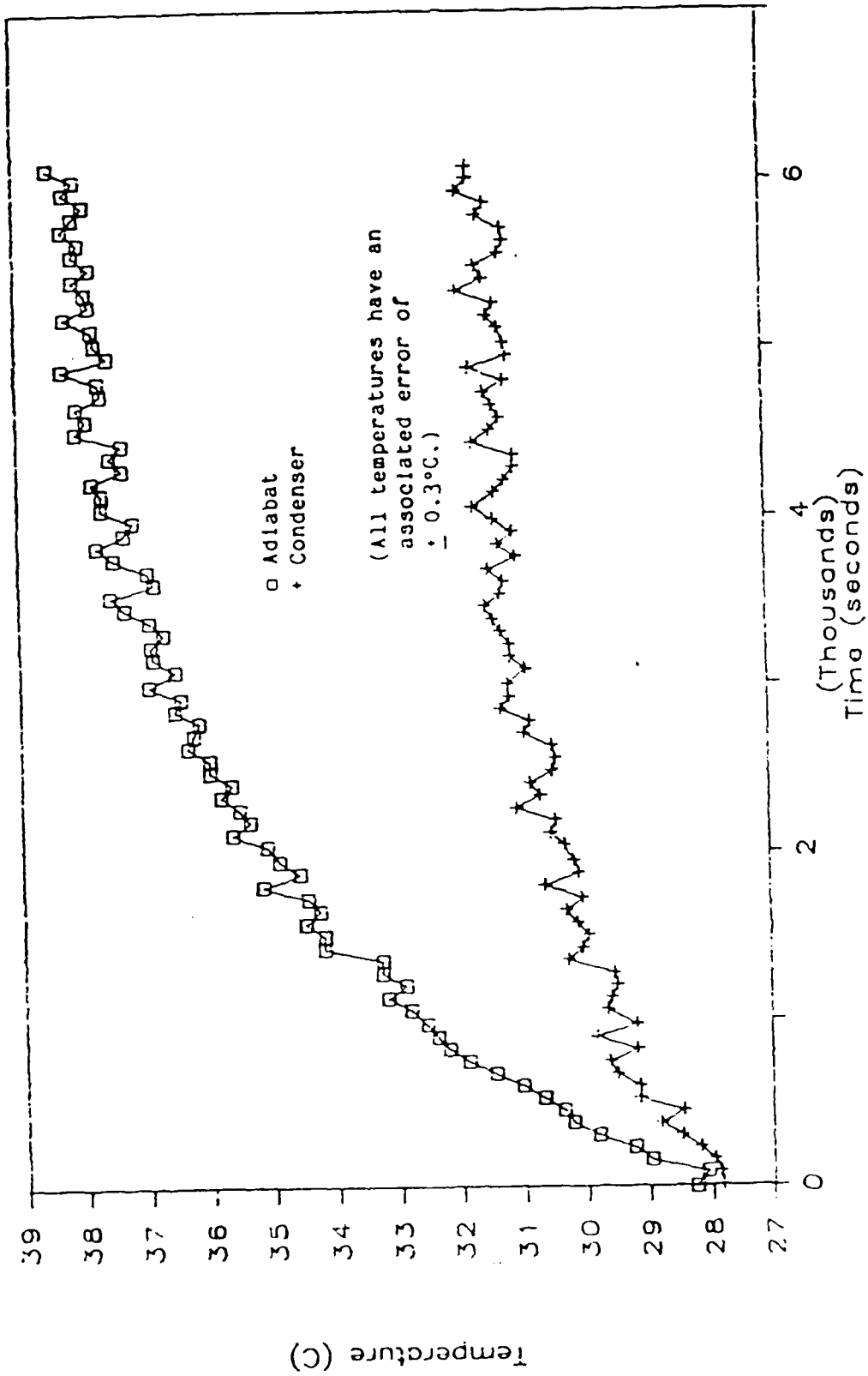


Figure 23. Condenser and Adiabatic Temperatures For Run 4

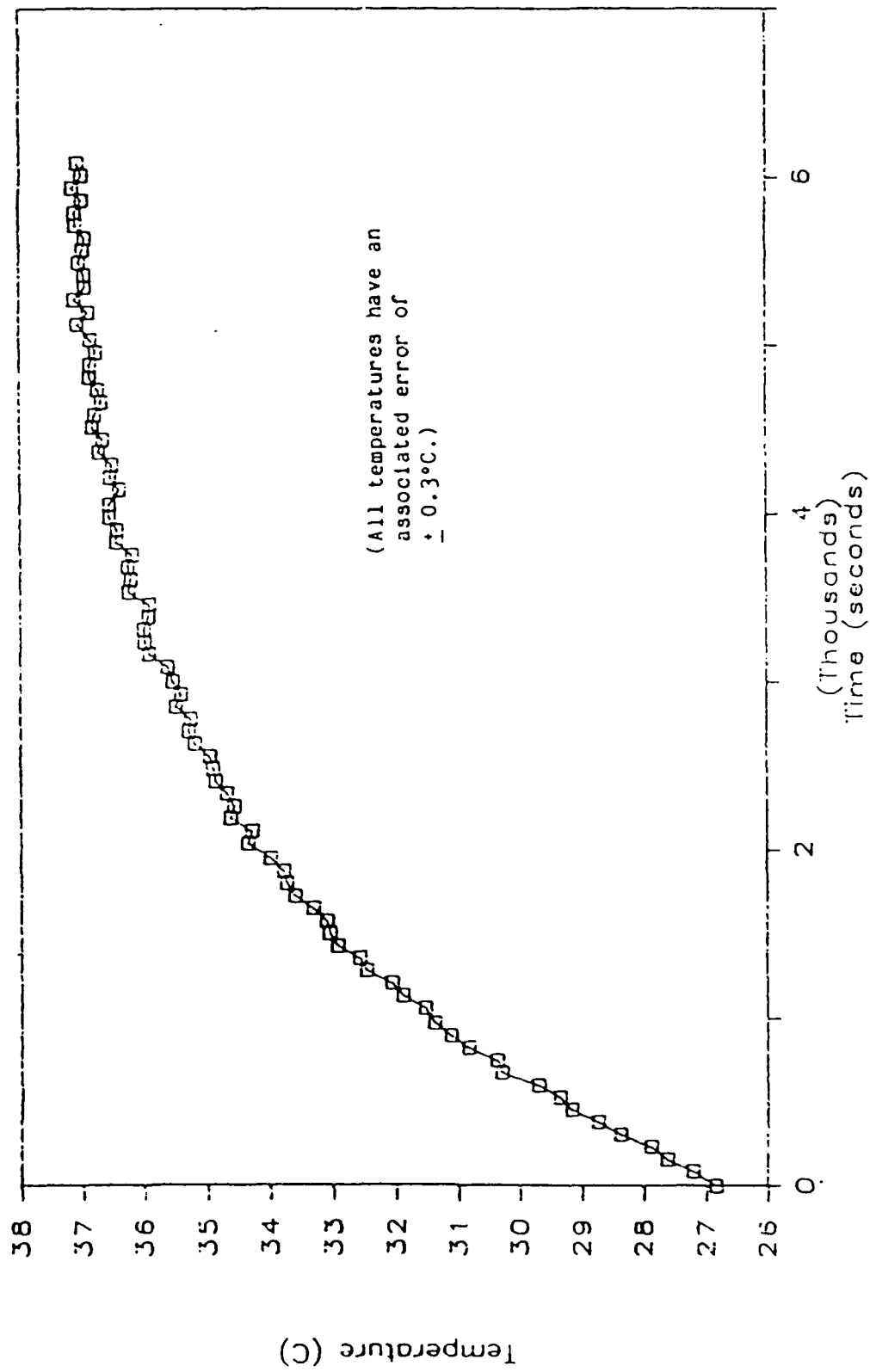


Figure 24. Vapor Temperature Versus Time For Run 4

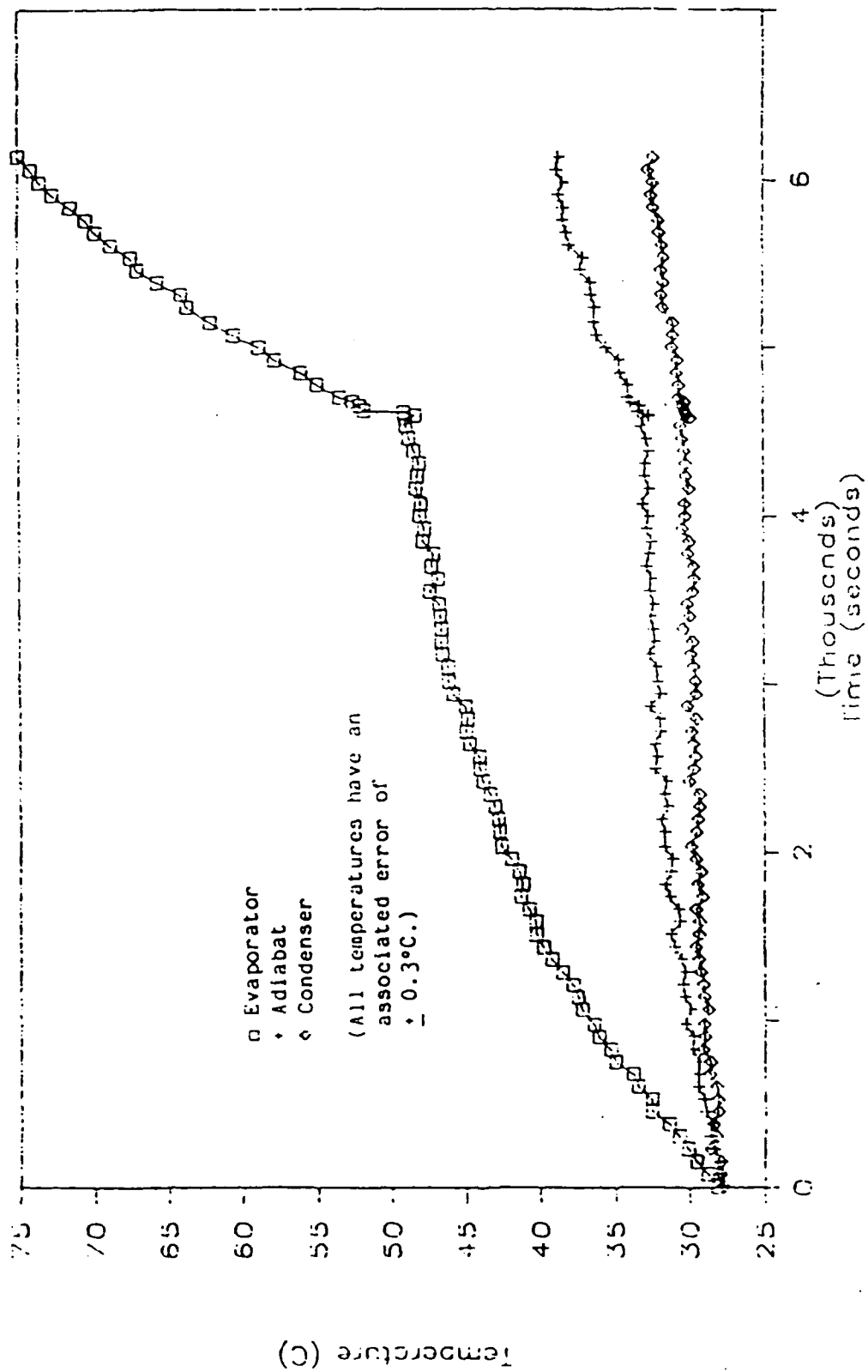


Figure 25. Evaporator, Adiabatic and Condenser Temperatures for Run 4

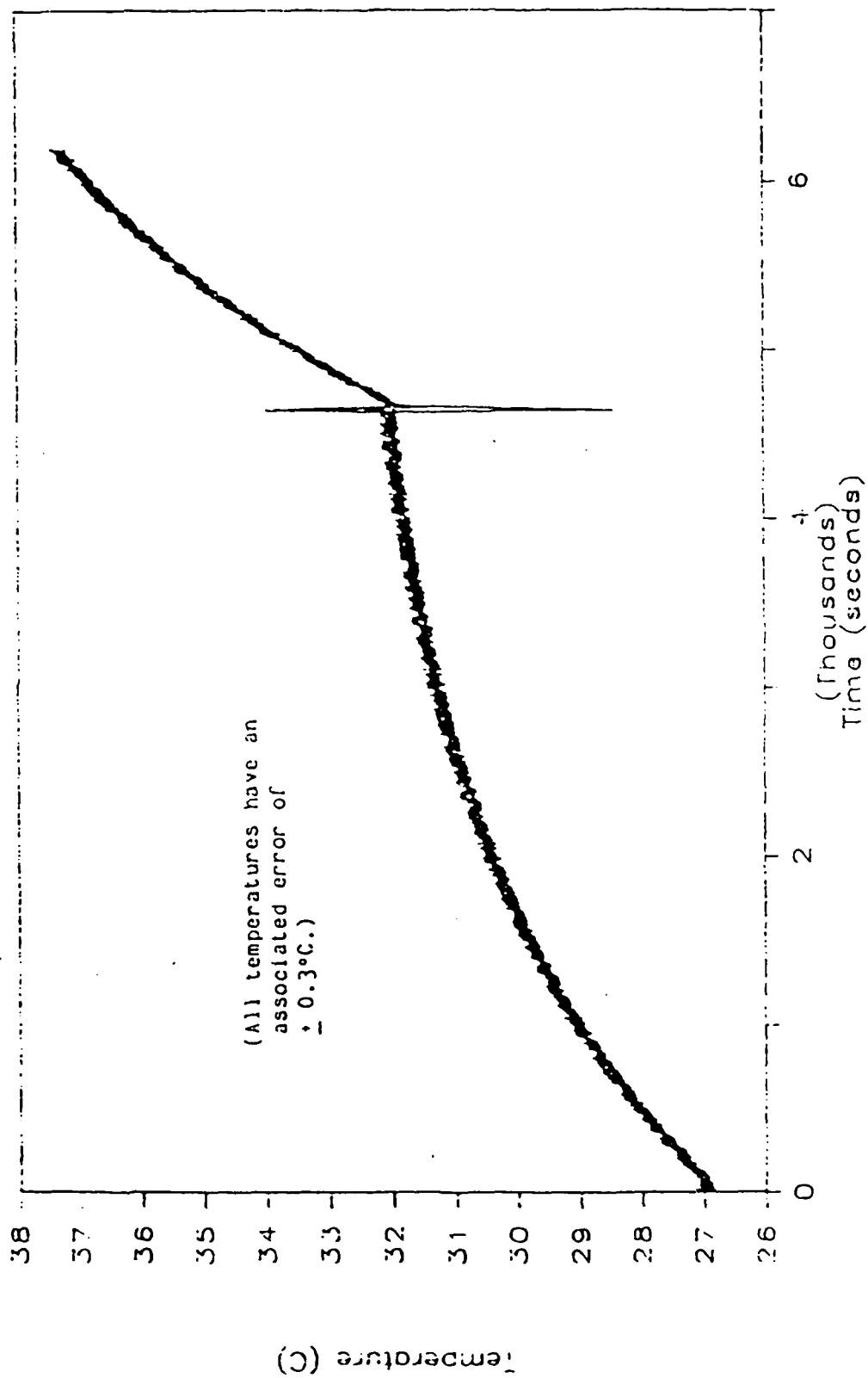


Figure 26. Vapor Temperature Versus Time For Run 7

thermocouples simultaneously and on the same time scale as that used in Figure 25. Here one can see a spike in the temperature behavior after the power increase. While the spike does follow the increase in power, it also precedes the jump in evaporator outer wall temperature and is probably caused by some occurrence inside the heat pipe and not directly by the power increase at the heater. In order to study this "spike" more closely, Figure 27 focuses on the temperature behavior indicated by the vapor channel thermocouples over a much smaller time period. The first data points just after 4590 s are close to the time at which the heater was turned on at 4593 s. Several seconds pass before any response is detected, then a sharp increase in the temperature at thermocouples S and R is sensed, along with a smaller temperature increase in the adiabat at thermocouple Q. At the same time, a temperature drop is experienced by both vapor channel thermocouples in the condenser. The pressure at the far end of the condenser was measured over the same time period, and is shown in Figure 28. It shows the drop in pressure that one would expect to accompany the temperature drop in the condenser, but it does indicate a pressure drop preceding the temperature drop in the condenser. During this period, very little could be seen of the inside of the heat pipe because of condensation on the glass cover, but there was enough visibility to establish that there was no large-scale boiling occurring. The amount of liquid in the wick could not be seen.

Due to the relatively short duration of the transient, and because the normal operation of the heat pipe was reestablished, it is not likely any kind of critical heat flux limit was approached. A more likely scenario would be a wick dryout. In this case, the power increase caused a large evaporation rate, but either the heat flux was not sufficient to start a boiling situation, or there was still sufficient liquid coming from the condenser (since the liquid was already in motion from operation at 100 W) to lower the temperature of the evaporator to prevent boiling, but not enough to prevent the liquid-vapor interface from sinking below the wick and perhaps completely drying out. This was a short-term condition, however, because liquid was returned to the evaporator eventually and the heat pipe was able to restart. As the evaporator was drying out, less liquid remained and it was thus superheated beyond the saturation temperature as it removed energy from the wall. This caused the increase in evaporator temperature seen in Figure 27. At the same time, the reduced rate of evaporation was not able to keep up with

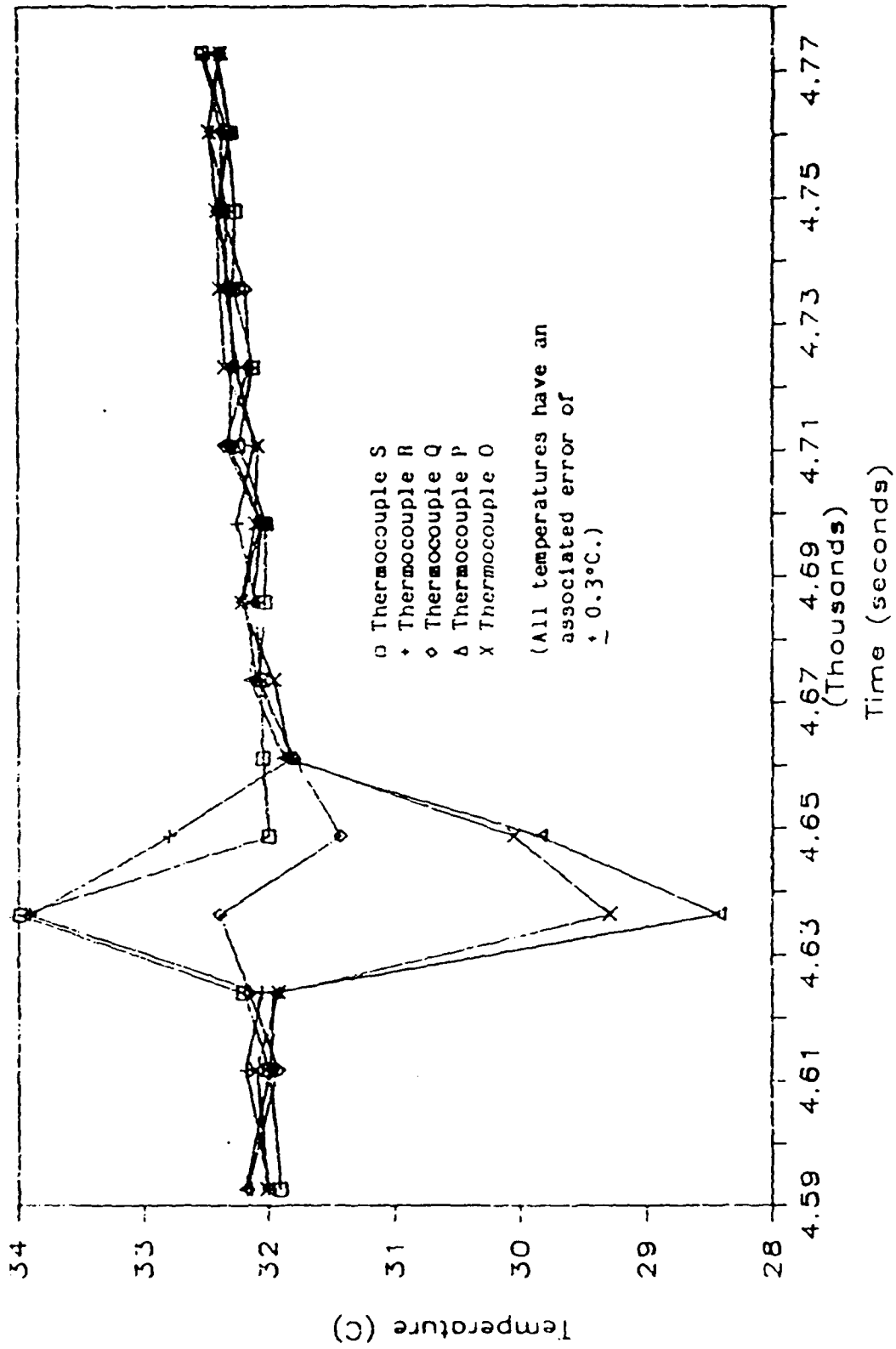


Figure 27. Vapor Temperature Versus Time Near Time of Transient (Run 7)

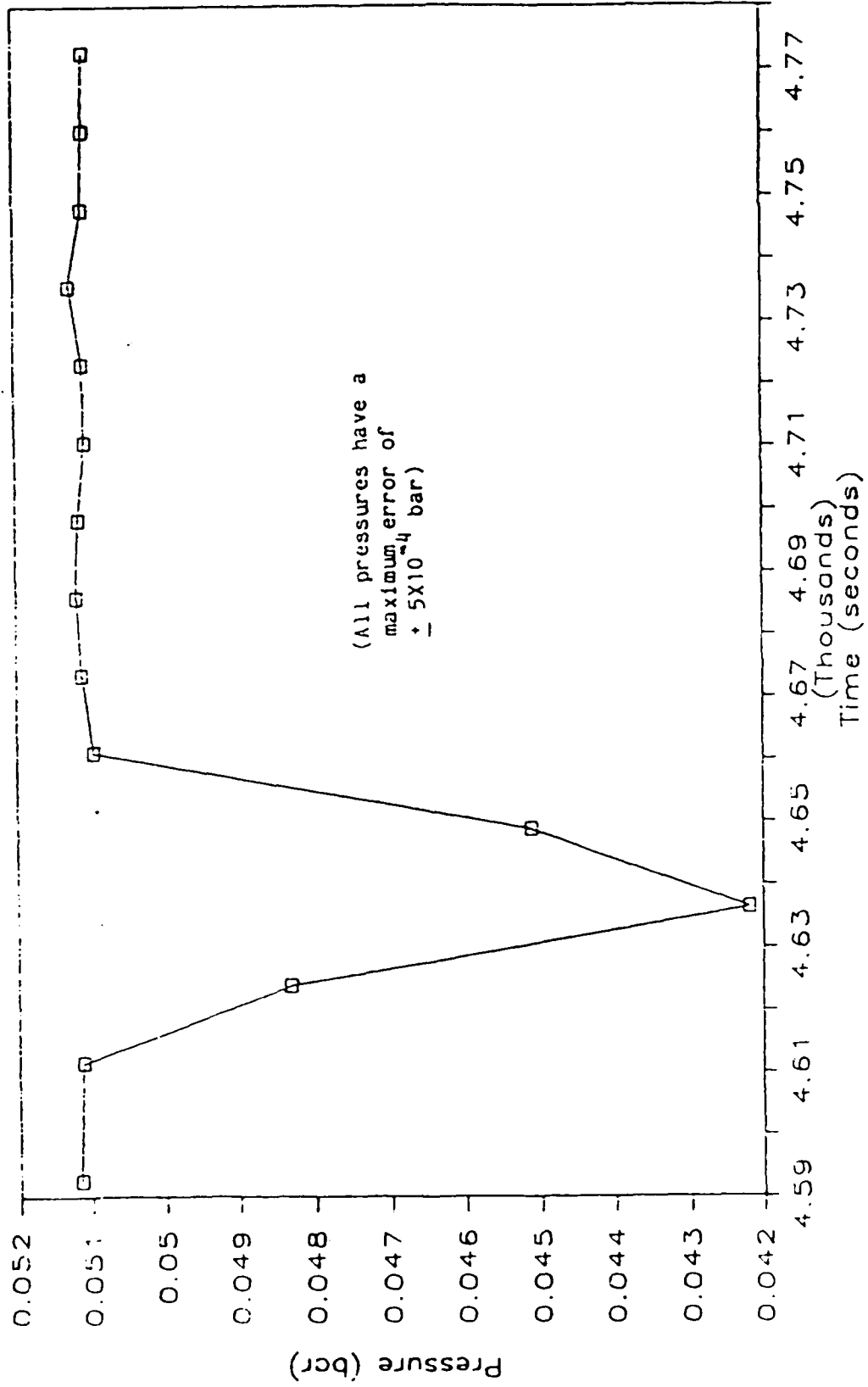


Figure 28. Condenser Pressure Near Time of Transient (Run 7)

the established rate of condensation, so a pressure drop was seen in the condenser. As the pressure dropped, the saturation temperature dropped, and so the vapor temperature in the condenser also dropped. This pressure drop was felt along the entire length of the condenser, as thermocouple Q, at the adiabat-condenser interface, experienced the same temperature drop. This thermocouple was able to sense the superheated vapor out of the evaporator, at least initially, since it first responded with a temperature rise. Based on this argument, one might expect the peak in the evaporator temperature and the dip in the condenser temperature to be somewhat out of phase and not aligned. This may have been the case. Since the data were taken with several seconds between each reading, the peaks and dips are not likely to have been at their maximum and minimum values when a reading was taken. The lines connecting the data points accenuate trends in the temperatures, but do not represent the actual path taken by the temperatures during the transient.

### 3.5 Summary

A specially designed heat pipe with a rectangular cross section, flat mesh-type wick, and a single glass wall has been conceived, designed, and tested, and used to observe the characteristics of heat pipe transient behavior under start-up and load change conditions. The flat glass wall is a unique feature in an experimental heat pipe, as it allows the study, by visual or optical means, of the internal operating characteristics of a heat pipe during steady-state and transient modes.

In summarizing the results obtained by the heat pipe described in this section, several phenomena have been observed. Start-up from ambient conditions and zero input power to 100 or 250 W is slow enough to be termed quasi-steady-state, and therefore exhibits no observed departure from expectations based on steady-state theory. Finally, transition from one operational power to another can lead to a temporary dry out and perhaps even to a permanent dry out and failure. This again may be explained by limited hydrodynamic response over a short time period before eventual recovery. Beam<sup>29</sup> also suggests such hydrodynamic limits in his experimental and analytical work studying the behavior of heat pipes under transient conditions.

The major drawbacks to this design include indicated outer wall temperature drops larger than predicted by theory for loads of 100 and 250 W, and a fragile glass wall that was susceptible to cracking under high thermal loads or high pressure. These problems, as well as other minor problems, will be analyzed and solved in the following section. Also in the following section, the data from two start-ups with initially frozen water inside the pipe will be presented, as will various other transient data.

## 4.0 HEAT PIPE EXPERIMENTS

The performance of the heat pipe and associated instrumentation described in Section 3 was analyzed and found to need improvement in several areas. A new heat pipe and instrumentation system was therefore built and a new set of experiments conducted. The system design for these experiments is very similar to that used for the experiments of the previous section, but there are some important improvements made. These improvements and the rest of the design for the experimental apparatus for the experiments of this section will be discussed first. The experiments of the previous section were essentially scoping runs for the experiments of this section, so the experimental design will be presented in more detail in this section, for both those elements of the design that have changed and those that have not. Next, in the Experimental Procedures subsection, the methods of preparing the experimental apparatus for a heat pipe run are discussed. Finally, in Results and Discussion, the data from six different runs will be presented. The first run analyzes a 0.0- to 100-W start-up and confirms the experiment is operating a heat pipe. The second run is a 0.0- 50- 100- 200- to 250-W transient. The next two runs are frozen start-ups. The fifth run is for a heat pipe that is operating at 25 W when the coolant temperature is reduced until the condenser of the pipe reaches freezing conditions. Finally, the sixth run analyzes a 250.0- to 0.0-W shutdown of the heat pipe.

### 4.1 Experimental Setup

This subsection describes the apparatus used for the experiments described later in this section. The subsection contains three parts. The first gives a brief outline of the hardware and data collection equipment used and a brief overview of the improvements on this experimental setup over that of the previous section. The second part gives a more detailed description of the hardware. The third gives more specifics about the data collection equipment used, including thermocouples, pressure transducers, data collection cards, computer hardware that converts the analog signal of the thermocouples and transducer to a digital signal, and software that retrieves this digital information and converts it to a

temperature or pressure value and stores it on a computer disk.

#### 4.1.1 System Outline and Improvements

To better understand the transient workings of a heat pipe, it is desirable to understand the inner workings of the pipe as well as the response of the outer wall. To this end, a heat pipe has been designed that allows data to be obtained both inside the channel of the heat pipe and in the outer wall. This design allows the pipe to operate at a variety of conditions while making it possible to study various failure modes of the pipe. The overall system is shown in Figure 29, and a side view of the heat pipe, heater, and secondary coolant section is shown in Figure 30. A CENCO-MEGAVAC vacuum pump is attached to the heat pipe to remove noncondensable gases. A similar vacuum pump is attached to a filter flask of water to allow degassing of the water before it is added to the heat pipe as the working fluid. This filter flask can be heated and the water inside the flask can be agitated by the magnetic stirrer and heater below it. The secondary coolant flows underneath the condenser section through a rectangular tube, a new addition to the heat pipe which is more leakproof than the previous secondary coolant jacket. The secondary coolant consists of an ethylene-glycol/water mixture circulated by a centrifugal pump. The coolant line also contains a gas trap between the pump and the coolant jacket to keep gases from collecting in the jacket and adversely affecting the energy removal from the pipe.

Attached to the condenser and evaporator outer walls are sections of aluminum plate originally intended to hold outer wall thermocouples, but these thermocouples were moved to the shoulder of the heat pipe body. A variable power electrical heater and the coolant jacket section are placed beneath this plating, as shown in Figure 30. The heater is the same as the one discussed in the previous section.

One feature that this design incorporates from the design of the previous section is the use of a clear top which makes observations of various phenomena inside the pipe possible. The material of the top was changed from glass to Lexan to eliminate the glass-cracking problem previously experienced. The Lexan is also easier to machine than glass.

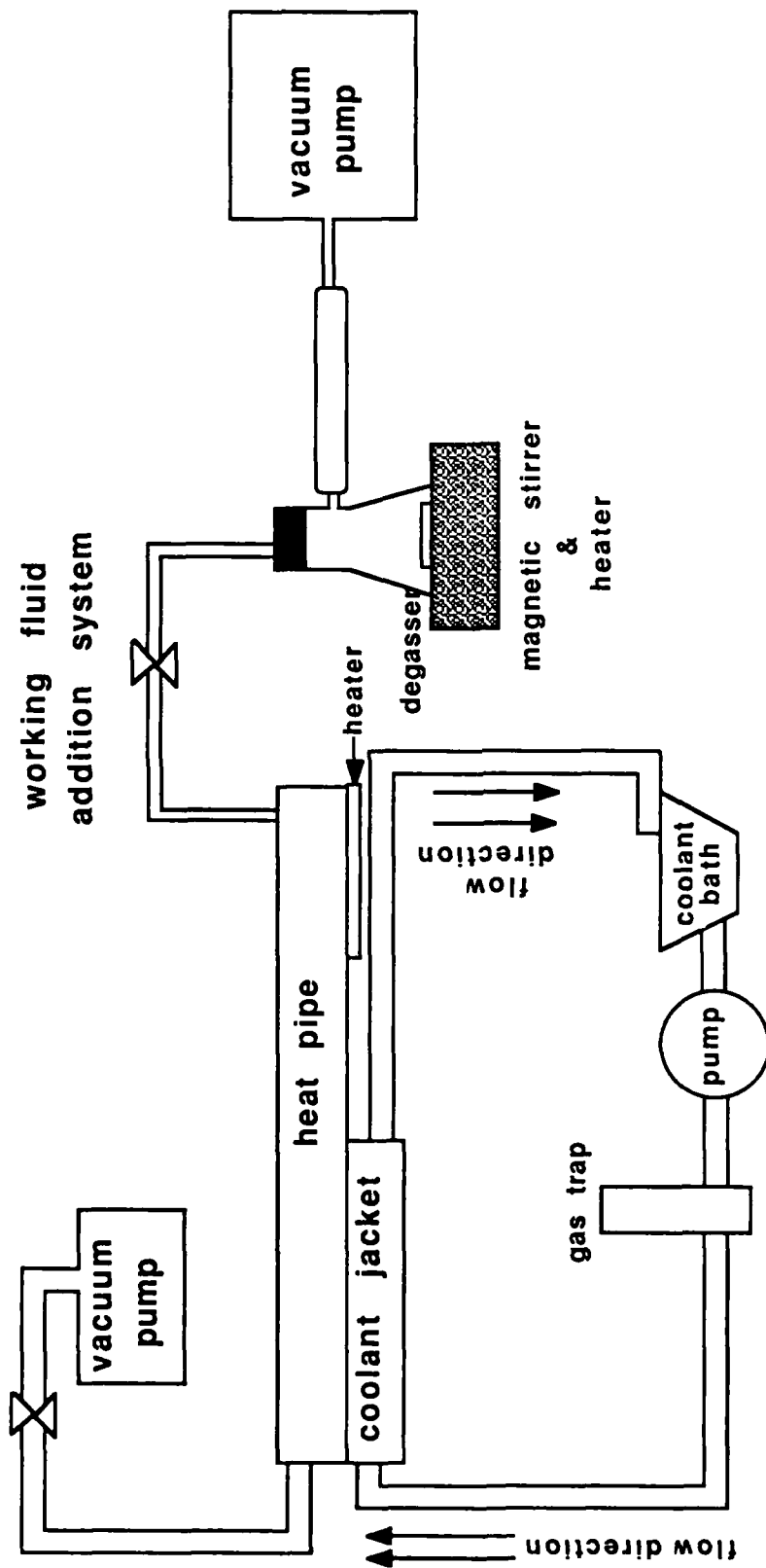


Figure 29. Overall Experiment Layout

(all dimensions in cm)

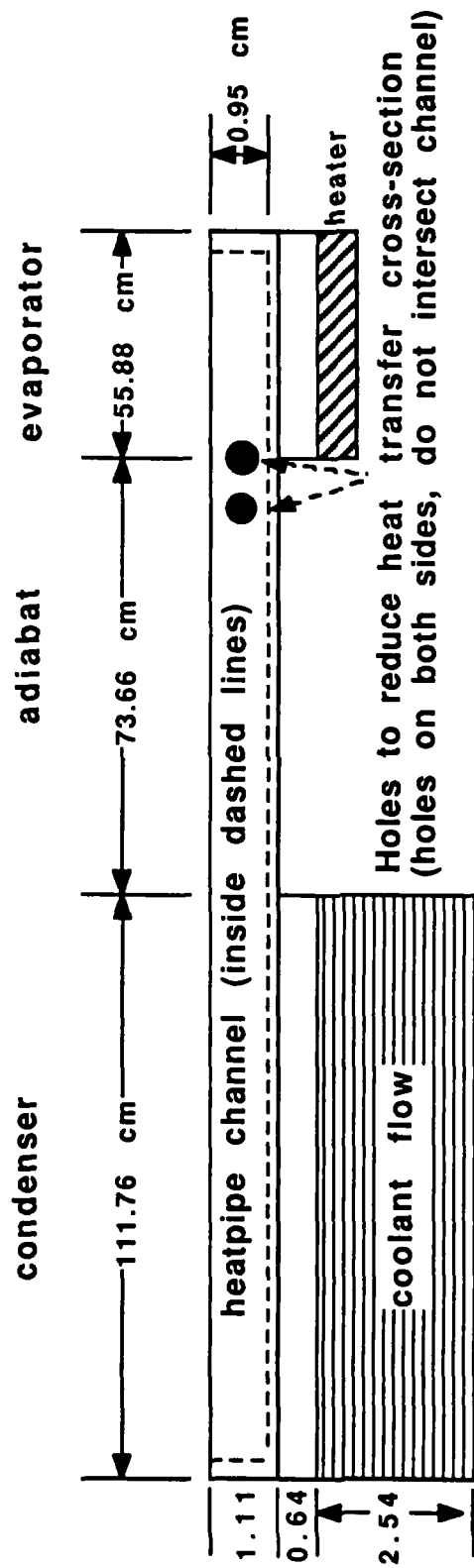


Figure 30. Overall Side View of Heat Pipe

The thermocouple arrangement of this design has the unique ability to simultaneously measure temperatures in the liquid/wick region and the vapor space and vapor space pressure. Figures 31 and 32 show sample locations for these measurements, as well as the placement for some of the outer wall thermocouples. The placement of the remainder of the outer wall thermocouples is shown in Figure 32. The vapor space, wick/liquid space and outer wall temperature measurements illustrated in Figure 31 are all taken by sheathed type T thermocouples. The vapor and wick/liquid space thermocouples enter the heat pipe channel through the Lexan cover. The outer wall thermocouples shown in Figure 31 are placed in the shoulder of the heat pipe. The outer wall temperatures shown in Figure 32 are all taken by type K thermocouples on the top of the Lexan cover underneath a layer of insulation. The temperature difference across the ethylene glycol/water coolant is measured by two type T thermocouples connected in differential form for highest accuracy. All of the thermocouples used in this experiment are different from those used in the experiments of the previous section both in style and placement. The thermocouples used here offer better accuracy over the range of temperatures for which they are used, and their new placement, described later in this subsection, also provides a more accurate temperature reading.

Pressure measurements are taken inside the channel by a Granville-Phillips Convector Vacuum Gauge. This is the same transducer used in Section 3, but the sensor is now placed directly in the vapor space of the condenser. The data are monitored in analog format as in the experiments of the previous section, on MetraByte EXP-16 cards which send the information to a MetraByte DASH-8 digitizing card so the data can be digitized and stored on floppy disks using an IBM XT personal computer.

#### 4.1.2 System Hardware

The cross section of the main channel of the heat pipe is shown in Figure 33. The channel is milled from a 0.0127 m x 0.0508 m x 2.4130 m rectangular bar of 6061 T6 aluminum. The channel itself is 0.0111 m x 0.0254 m x 2.3876 m long and has a rectangular cross section. Included in Figure 33 are the positions of the O-ring and Lexan top. The evaporator section of the pipe is 0.5588 m long,

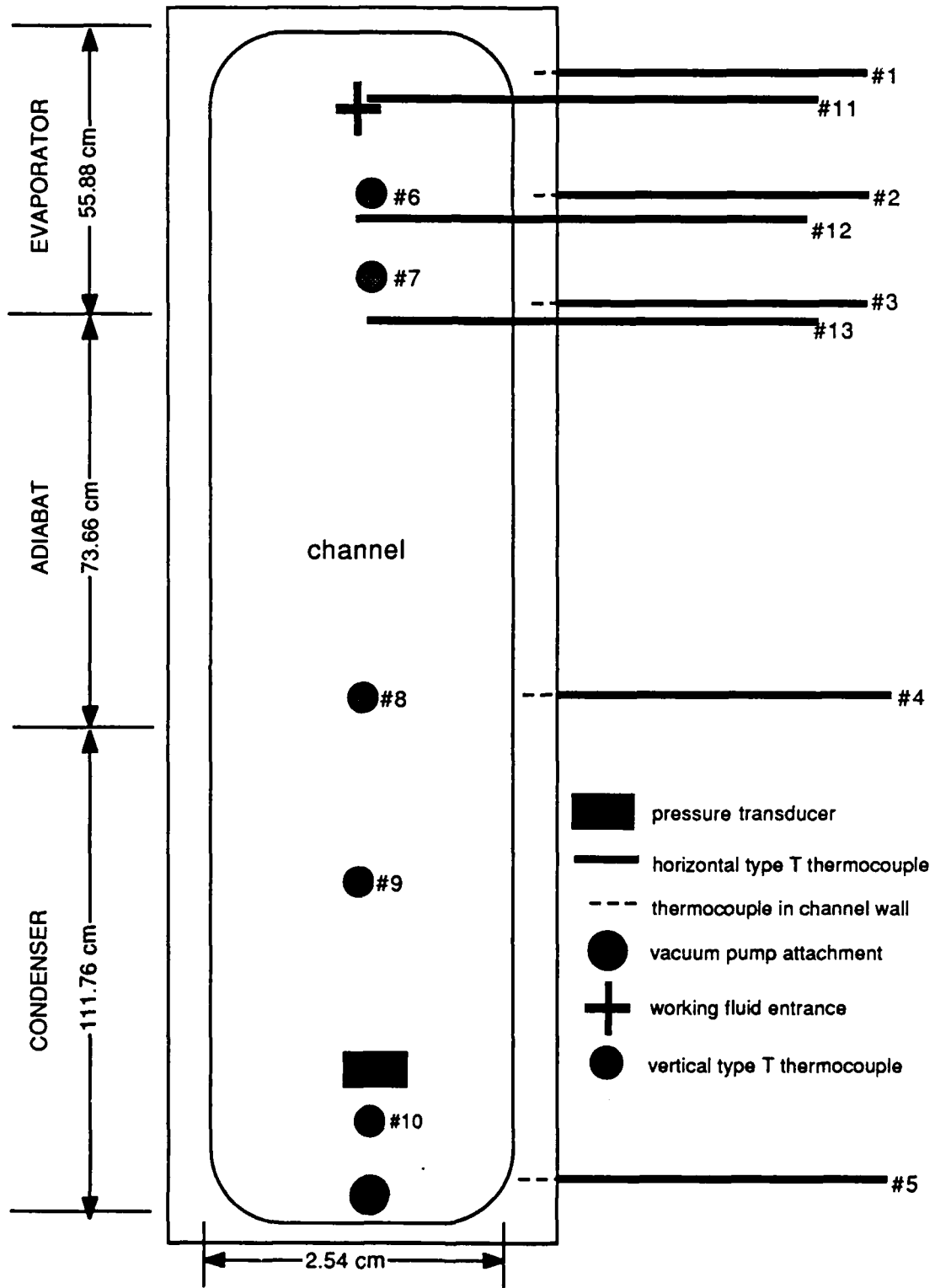


Figure 31. Location of Instrumentation (except K thermocouples)

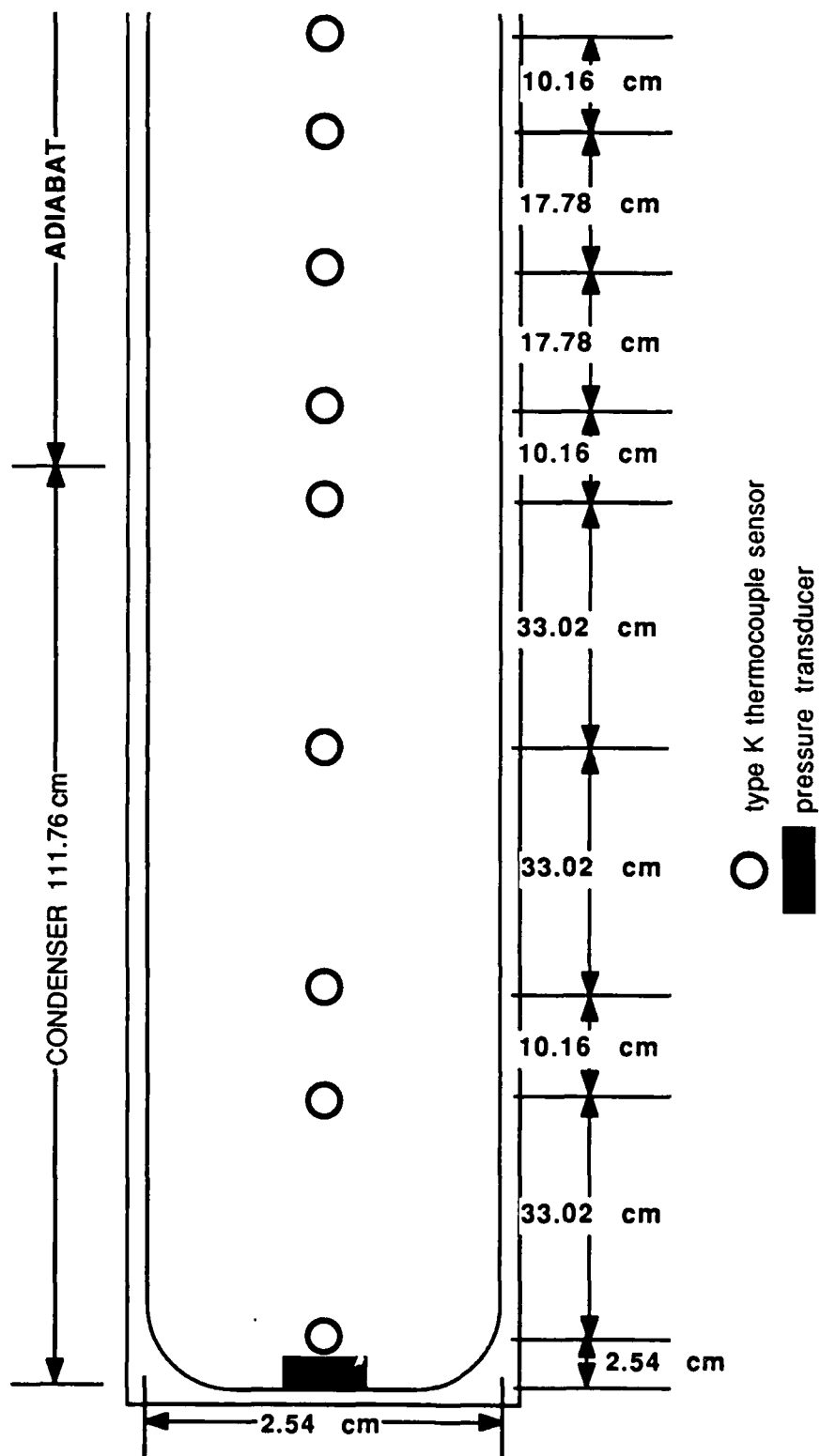


Figure 32. Placement of K Thermocouples

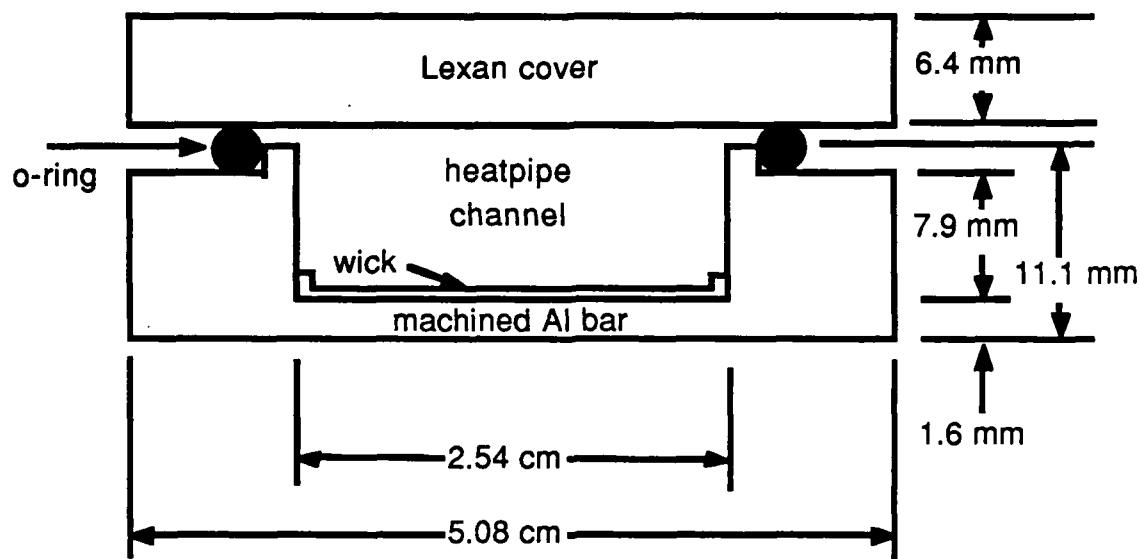


Figure 33. Heat Pipe Channel Cross Section

the condenser section is 1.1176 m in length, and the adiabatic section is 0.7366 m long.

Underneath the evaporator and condenser are 0.00635 m x 0.0254 m aluminum plates which were initially intended to allow for the placement of thermocouple probes underneath the channel. The plates are attached to the aluminum bar by screws through holes countersunk on the bottom of the plate and tapped into the shoulders of the bar on either side of the channel. Holes 0.001588 m in diameter were drilled through the sides of the plate so that when a sheathed thermocouple is placed inside the hole, the thermocouple probe lies directly underneath the center of the channel. It was subsequently determined that the small contact conductance between the plate and the bar was causing a significant temperature drop between the plate and the heat pipe outer wall, and the thermocouples were therefore shifted to the shoulder of the bar as described later.

Power is applied to the pipe through a strip heater equal in length to the evaporator which is placed underneath the evaporator and aluminum plating. A cross section of this arrangement is shown in Figure 34. The heater is surrounded on three sides by oven insulation. The heater is pressed against the

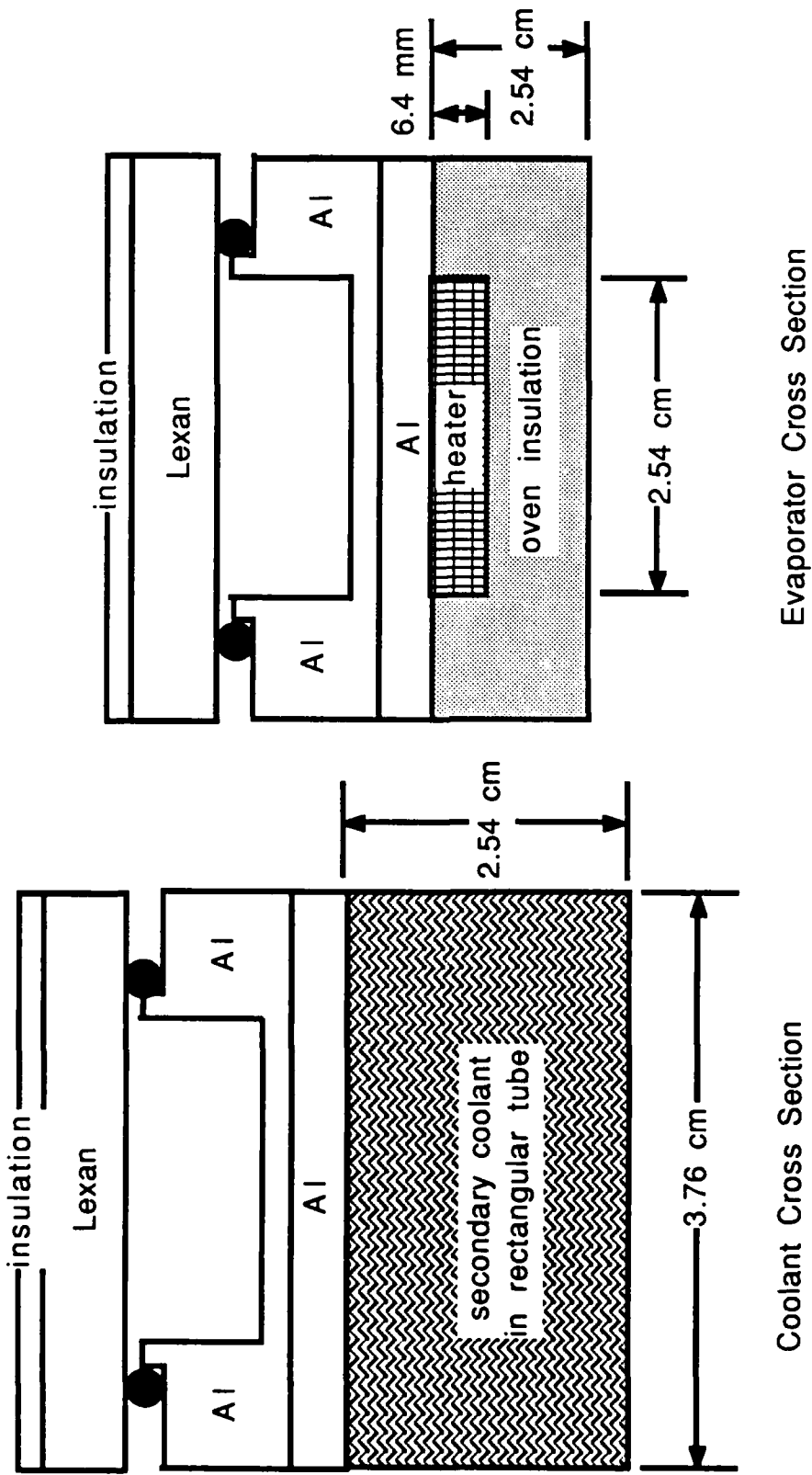


Figure 34. Condenser and Evaporator Cross Sections

aluminum plate by pressure from the surrounding oven insulation which is encased in a thin stainless steel frame. The heater consists of nickel-chromium wire spaced evenly along the length and width of the heater. The heater resistance is nearly constant over the temperatures of planned operation. The input voltage is controlled, and when the voltage input is known, the input power can easily be calculated using the equation  $P = V^2 / R$ . The resistance of the heater was measured to be  $10.5 \Omega (\pm 0.5 \Omega)$ . The maximum working temperature of the heater is  $300^\circ\text{C}$  and the maximum power input is 1500 W.

Energy is removed from the heat pipe by a secondary coolant flow underneath the condenser section of the pipe. The coolant used is a mixture of approximately 50 percent ethylene glycol and 50 percent water. This mixture was chosen so the coolant temperature could be brought below the freezing point of water (water being the working fluid of the pipe) by adding dry ice to the mixture. This makes freezing the pipe possible.

The secondary coolant passes through a section of aluminum 6063-T52 rectangular tubing 0.0508 m wide, 0.0254 m high and 1.1176 m long. The tubing is placed directly under the aluminum plate below the condenser section of the heat pipe. A cross section of this arrangement is illustrated in Figure 34. The flow enters at the end of the condenser away from the adiabat and exits at the interface between the condenser and adiabat. The fluid is pumped by a centrifugal pump that has a maximum flow rating of approximately 5 l/min.

The adiabatic section of the bar has holes drilled horizontally in the shoulders to reduce the cross section, thereby minimizing the energy conducted from the heated evaporator to the cooled condenser and also stored energy in the shoulders of the adiabatic section. Thus, the adiabat is close to being truly adiabatic. See Figure 35 for a more complete view.

Lexan was chosen for the cover primarily because it will not break or crack like glass and is easier to machine than glass. Lexan is also much more flexible and thus achieves a better fit on the O-ring. This makes it easier to obtain a vacuum seal on the heat pipe with the Lexan resting on the O-ring, which is placed around the lip which surrounds the channel on the top surface of the pipe. The O-ring placement is shown in Figure 33. Problems with Lexan include an easily scratched surface and an operating temperature lower than that for glass. With care, however, scratches can be avoided and it is never necessary for the

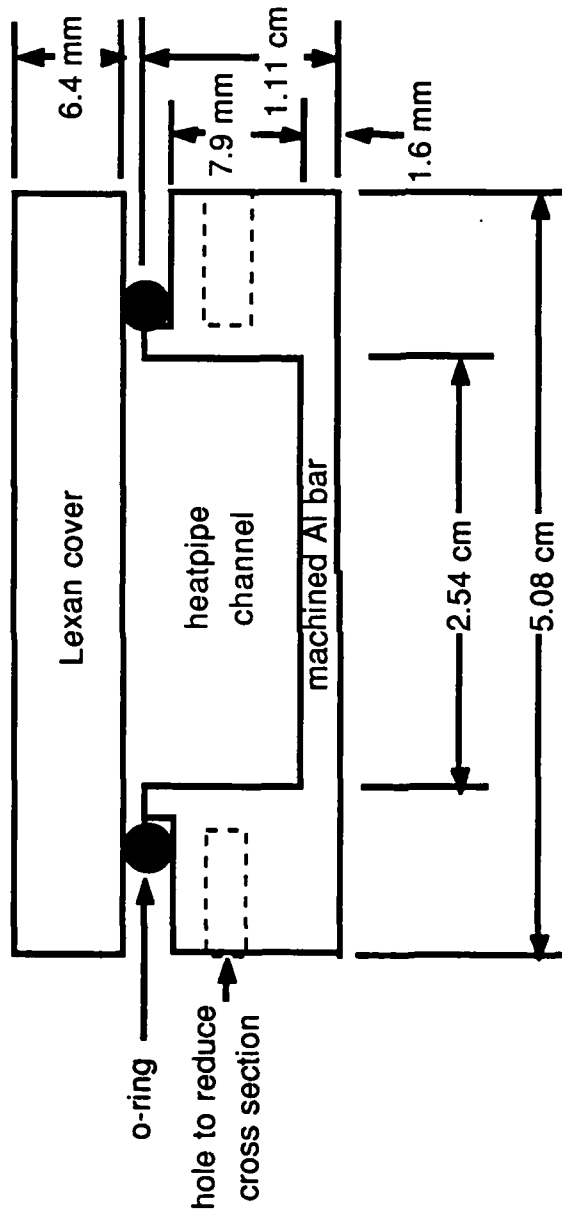


Figure 35. Cross-sectional View of Adiabatic Shoulder Holes

heat pipe to operate at temperatures high enough for the temperature limit to become important. The upper Lexan wall is 0.0254 m wide, 2.3876 m long and 0.0127 m thick.

There are two vacuum pumps used on this apparatus. Both are CENCO-MEGAVAC pumps capable of producing vacuums as low as 0.0001 mm of Hg. One is connected to the pipe through a 0.0159 m O.D. copper tube which enters the channel through the cover plate via a compression fitting with a 1/8-in NPT male piece. The penetration is at the far end of the condenser from the evaporator. This is the hole through which the noncondensable gases are removed from the pipe. In the middle of the vacuum hose is a valve that can separate the pipe from the pump. This serves two purposes. It keeps any moisture from the pipe that might be present during a run from getting into the vacuum pump and causing rust and other problems. It also eliminates possible leak sources.

The second vacuum pump is used to de-gas the working fluid before it enters the heat pipe. Before a heat pipe run begins, the working fluid is contained in a filter flask. The top of the flask is sealed with a rubber stopper, through which a 1/16-in stainless steel tube penetrates into the liquid. The other end of the tube enters the heat pipe through the Lexan top via a 1/8-in male NPT fitting attached to the tube by a Swagelok compression fitting. The attachment to the heat pipe is in the far end of the evaporator from the condenser and the fitting is screwed into a 1/8-in female NPT hole tapped into the Lexan top. Between the entrance to the flask and the entrance to the pipe is a valve that is closed except for the period when the working fluid is being added to the pipe. Through an attachment to a nipple on the flask, the vacuum pump removes the noncondensable gases prior to the start of an experiment. While the gases are being removed, the degassing is aided by agitating the fluid with a magnetic stirrer. Lower pressure in the pipe causes the flow of working fluid into the pipe. If necessary, the flask can be heated, increasing the pressure difference and facilitating the flow. Once a predetermined amount of working fluid is added, the valve is shut.

On both long sides of the heat pipe there is fiberglass insulation approximately 0.0125 m thick, and below the pipe is insulation 0.0254 m thick. The insulation encases the pipe as well as the aluminum plate, the heater and the coolant channel. The cover is insulated by foam insulation that is 0.0032 m

thick, except for the area where visual observation will be taking place. The insulation itself, except for the cover, is encased by a wooden shell. A cross-sectional view of the insulation surrounding the adiabat of the heat pipe is shown in Figure 36.

#### 4.1.3 Instrumentation and Data Collection Equipment

The thermocouples used in this experiment are of three types. The first is a type T (Copper-Constantan) thermocouple which is 0.3048 m long and has a 0.00159-m outside diameter stainless steel sheath with an exposed probe junction. The second is also a type T thermocouple with the same length and sheath, but the probe is shielded rather than exposed. The probe is ungrounded. The type T thermocouples were chosen because of their accuracy over the desired temperature ranges. The accuracy of both styles is  $\pm 0.9^{\circ}\text{C}$ . The third model of thermocouple is a type K thermocouple used to measure the outer cover plate temperature in the condenser. The outside diameter of the wires is 0.00127 m and the wires are coated with Teflon. The probe is exposed, and the accuracy is  $\pm 2.2^{\circ}\text{C}$ .

The outer wall thermocouples are mounted in one of two places: either in the shoulder of the heat pipe approximately 0.00318 m away from the channel, placed on the side of the channel as shown in Figure 37, or on the top of the Lexan cover. Those thermocouples placed in the heat pipe shoulder employ the shielded probe, and pass through the fiberglass insulation before resting in the holes drilled for them. Those on the cover employ the exposed probe T thermocouples or the K thermocouples and rest underneath the foam insulation on the cover plate. Measurements of the temperatures on the outside of the fiberglass insulation can also be taken. The exposed probe thermocouples are used, and are placed at the same height as the heat pipe channel.

Three types of data are taken inside the heat pipe channel: the pressure of the vapor space and temperatures of both the liquid/wick region and the vapor space. The vapor space temperatures are taken with exposed probe thermocouples. These thermocouples are installed so that about 0.0762 m of the sheath and the probe lie in the vapor space, as can be seen in Figure 38. This geometric arrangement is designed so that the fin effects of the external

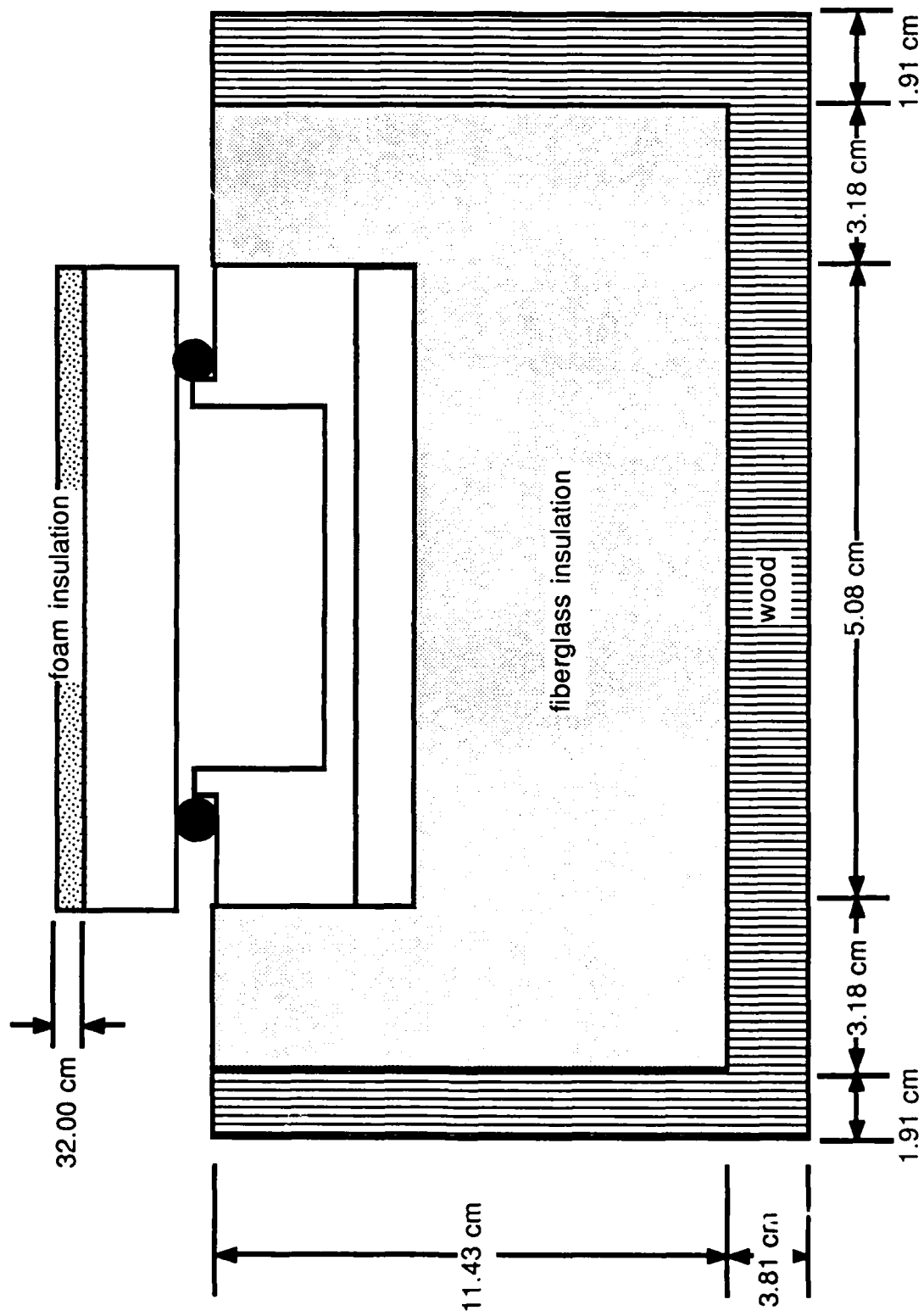


Figure 36. Cross-Sectional View of Insulation, Adiabat

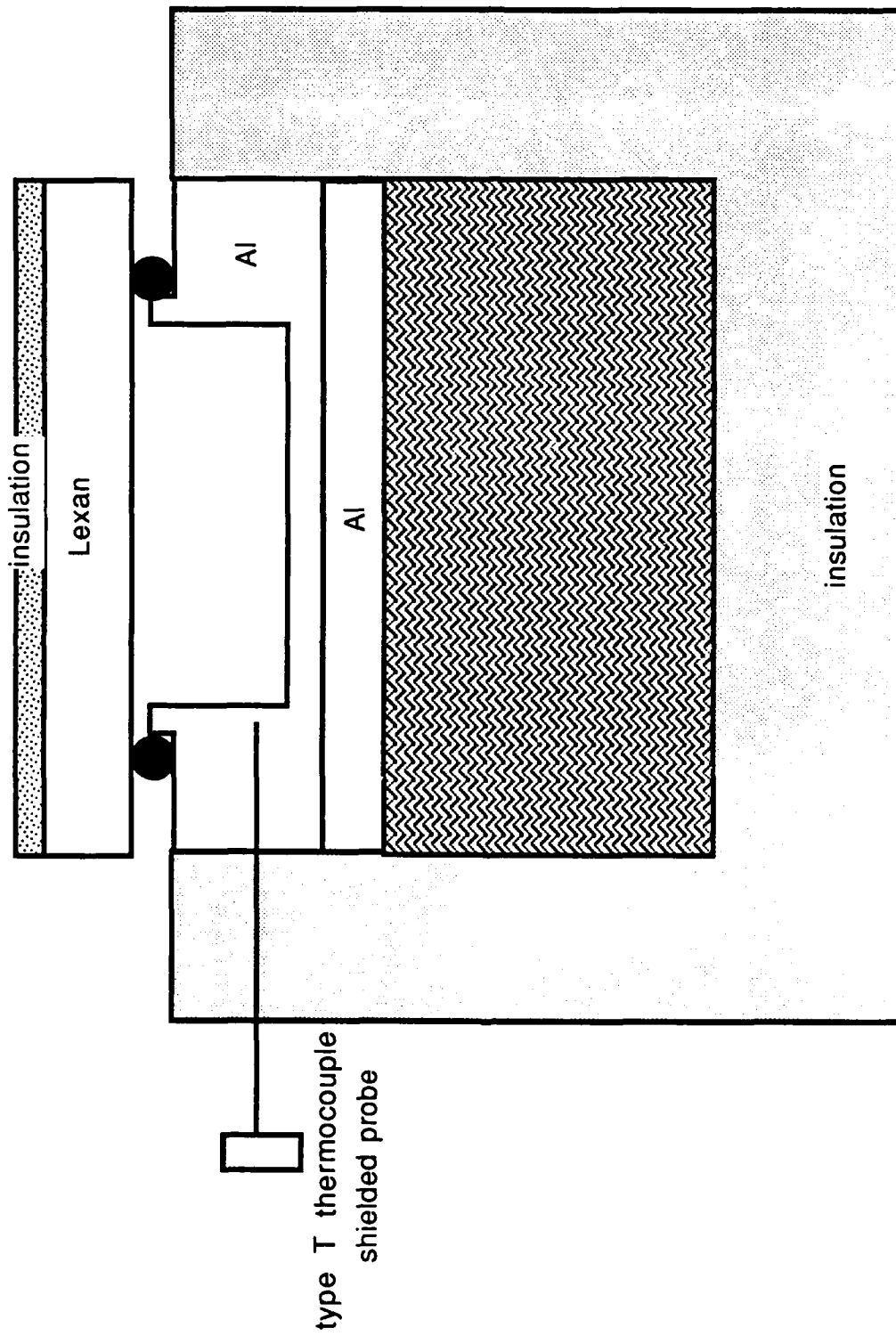


Figure 37. View of Heat Pipe Outer Wall Shoulder Thermocouple

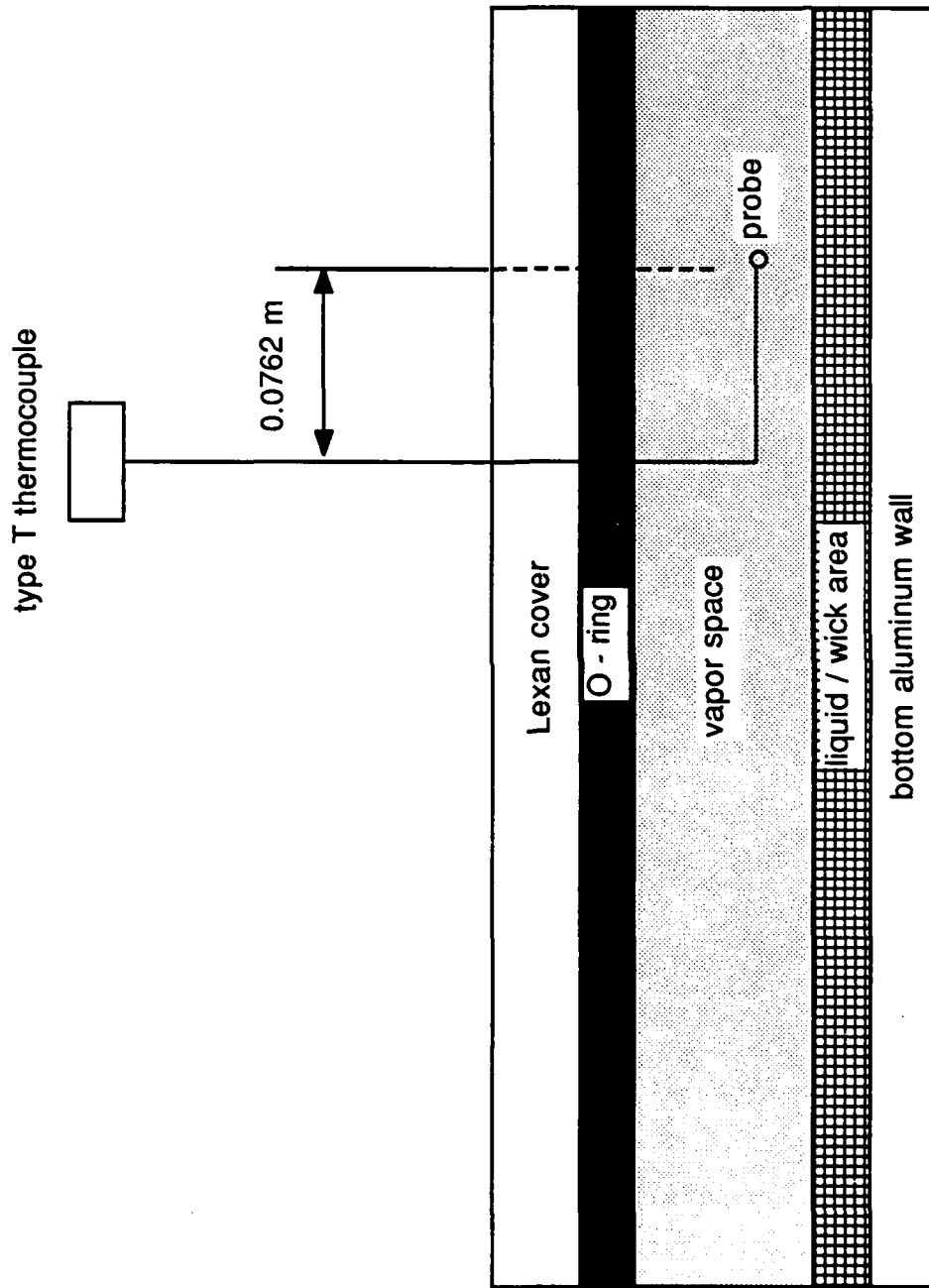


Figure 38. View of Vapor Space Thermocouples

environment on the indicated temperature are minimized. The thermocouples are held in place by a 1/16-in compression fitting with a Teflon ferrule on one end. On the other end is a 1/8-in NPT female fitting that is screwed into the Lexan top where a 1/8-in NPT male inlet is tapped.

The liquid/wick region thermocouples are essentially the same as the vapor space thermocouples in design and positioning except that the probes are left unbent and are shielded and grounded so that they actually touch the wick.

The pressure transducer system used is a Granville-Phillips Convectron Vacuum Gauge. This device was chosen because it is able to maintain an accuracy of five to eight percent over a range of pressure from milli- to kilo- torr. This is necessary since the pressure readings needed to check the seal of the heat pipe are approximately two to three orders of magnitude lower than pressures inside the pipe once the working fluid has been added and a transient has begun. The transducer itself is a Pirani gauge with a male 1/8-in NPT mount. Limits on the transducer preclude operating temperatures above 50°C due to the collection of condensation inside the gauge tube. The latter limit essentially means that when water vapor pressure is being measured, the vapor must be below room temperature. This can be accomplished by running the coolant temperature far below room temperature. If operation above room temperature becomes necessary, a valve placed between the gauge tube and the pipe can be closed. If this is done, the saturation pressure under normal conditions can be determined from the saturation temperature, since the pipe is a two-phase system.

The pressure transducer analog readout comes calibrated for N<sub>2</sub> gas, and conversion charts are available for a variety of other gases; but water vapor is not one of them, so lab calibration using the saturation properties of water had to be performed. A diagram of the calibration setup is shown in Figure 39 and the resulting plot of calibrated pressure against transducer voltage is shown in Figure 40. The calibration utilized a filter flask with water in it. A vacuum pump was attached via a vacuum hose secured by a hose clamp to the nipple of the flask. Through a hole in the rubber stopper, a type T thermocouple with a shielded probe was placed in the flask. The transducer was similarly positioned. Both the thermocouple and transducer fits in the rubber stopper were tight enough so that an acceptable seal on the flask could be made. The noncondensable gases were

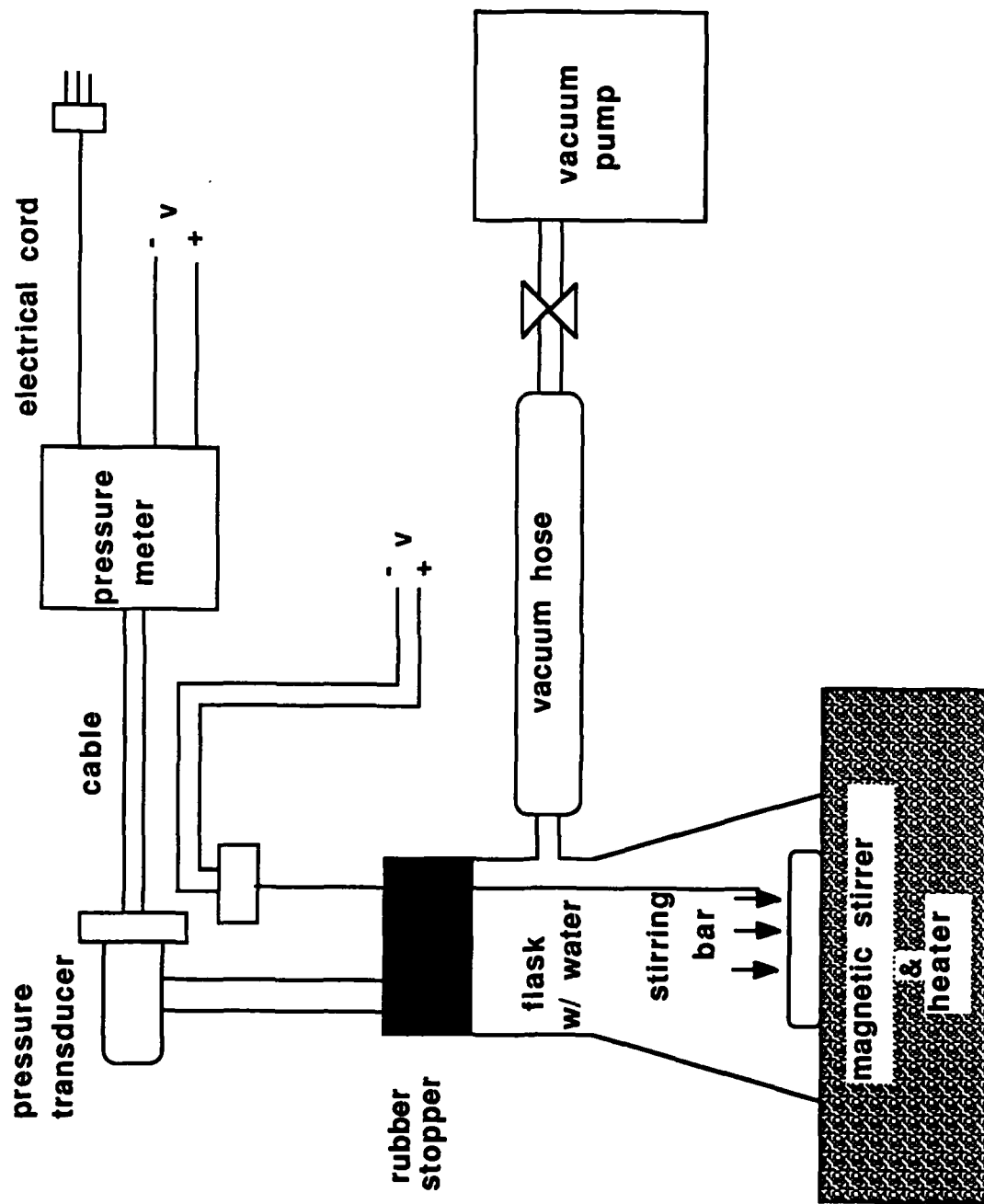


Figure 39. Pressure Transducer Calibration Setup

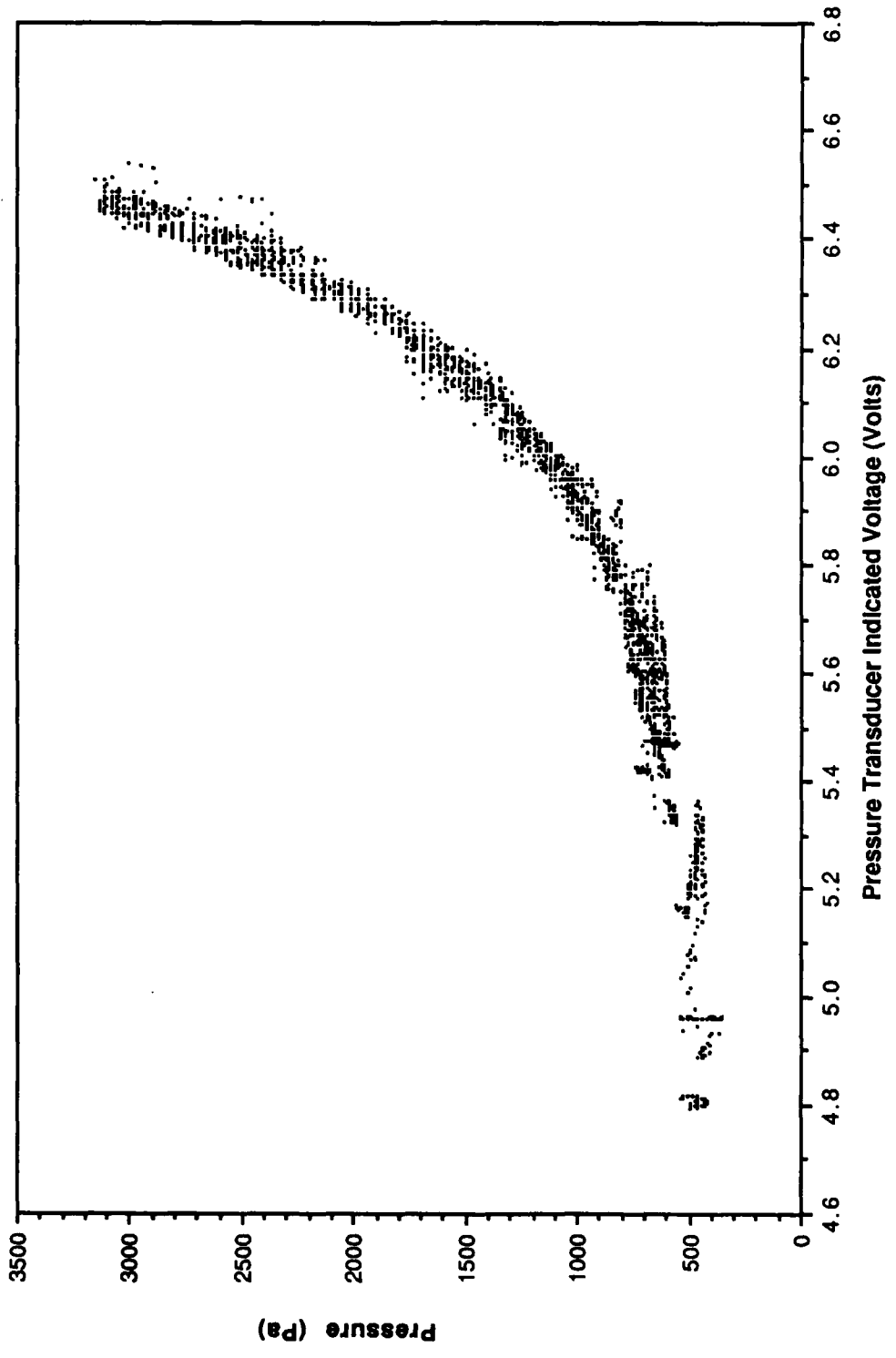


Figure 40. Pressure Transducer Calibration Data

removed from the flask by the pump with the aid of a magnetic stirrer and applied heat. When it was determined that the noncondensable gases were removed, data collection was started. Both the thermocouple temperature and pressure transducer volts were measured and recorded for a temperature range from 0.01°C (water's triple point pressure) to approximately 25°C. After the run, the thermocouple readings were converted to a corresponding pressure value. The colder temperatures were achieved by placing the flask in an ice and salt bath and using the vacuum pump to reduce pressure and hence temperature.

There are three types of data taken concerning the ethylene-glycol/water coolant: the coolant cold sink temperature, the coolant flow rate and the temperature difference measured across the coolant channel. The coolant itself is circulated by a centrifugal pump with an inlet attached to the styrofoam insulated coolant sump. After leaving the pump, the coolant enters the heat pipe cooling jacket at the condenser-adiabat interface and exits at the far end of the condenser. The coolant then flows through a hose back into the styrofoam sump. The cold sink temperature is taken by inserting an immersion thermometer into the ethylene-glycol mixture in the sump. The coolant flow rate is measured by redirecting the flow after it leaves the heat pipe into a plastic bucket with volume levels marked on the side and recording the amount of time it takes for the fluid level to reach one of the markings. The flow rate does not change appreciably for a constant coolant temperature, but when the coolant temperature changes by more than two degrees Celsius, the flow rate must be taken again.

With a known coolant flow rate, it is possible to measure the power removed from the pipe by the coolant if the temperature drop of the coolant across the condenser section of the pipe is known. It is possible to measure this temperature drop by taking the temperature at either end of the condenser section with two thermocouples and subtracting them, but there will be some error involved with both readings. The accuracy of the measurement can be improved if the same two thermocouples are connected in series so that a differential voltage across the thermocouples can be measured. With proper calibration, the differential voltage can be converted into a temperature difference, and the only error involved is that which occurs from the calibration. The thermocouples used were type T with shielded probes. The calibration was performed in the laboratory.

A diagram of the calibration setup is shown in Figure 41 and the results of

that calibration are shown in Figure 42. A third-order fit to the data is also shown in Figure 42. For the calibration, one of the thermocouples was placed in an ice water bath so that it could be kept at a constant temperature of 0°C. The other thermocouple was placed in another water bath where the temperature started at 0°C and the bulk temperature was gradually raised until a maximum temperature difference of 5°C was reached. The differential voltage was recorded and the corresponding differential temperature was measured with a type J thermocouple with a digital readout. This means that the calibration error will be at least as large as the error associated with the repeatability of the type J thermocouple. The repeatability of a thermocouple is the ability of the thermocouple to read the same temperature (of, say a constant temperature bath) each time the thermocouple probe is placed in the bath. The ability of the thermocouple to read the absolute temperature of the bath is of less interest here since a temperature difference calibration is desired. The repeatability of this thermocouple was determined to be at least 0.1°C. Therefore the error for the calibration of the differential thermocouple arrangement is also 0.1°C.

All data during a heat pipe run except the coolant flow rate and the coolant bath temperature are monitored in the form of an analog voltage signal which is converted to a digital form to allow it to be processed and stored on a personal computer. MetraByte EXP-16 cards are used to collect the voltage signals which are digitized by a MetraByte DASH-8 card before being stored via a compiled BASIC program and batch file onto a 5-1/4-in floppy disk. Complete listings of the program and batch file are in Appendices C and D.

The voltage input to the EXP-16 cards can range from millivolts to  $\pm 10$  V. Voltage gains of 1000, 200, 100, 50, 10, 2, 1, and 0.5 can then be applied before the signal is sent to the DASH-8 card, which has a maximum resolution of 2.44 mV. Higher gains can be achieved through special modifications to the EXP-16 card. The maximum allowable input to the DASH-8 card is  $\pm 5$  V. The DASH-8 card converts the analog signal into a digital signal which can be read from a BASIC program and returned to a voltage value through a known relationship between the digital and analog signal. This voltage can then be corrected for temperature effects on the thermocouples through the aid of a cold junction compensation (CJC) temperature signal provided by the EXP-16 card. The CJC circuitry provides a signal of  $+24.4$  mV/°C with a 0.0-V output at 0.0°C.

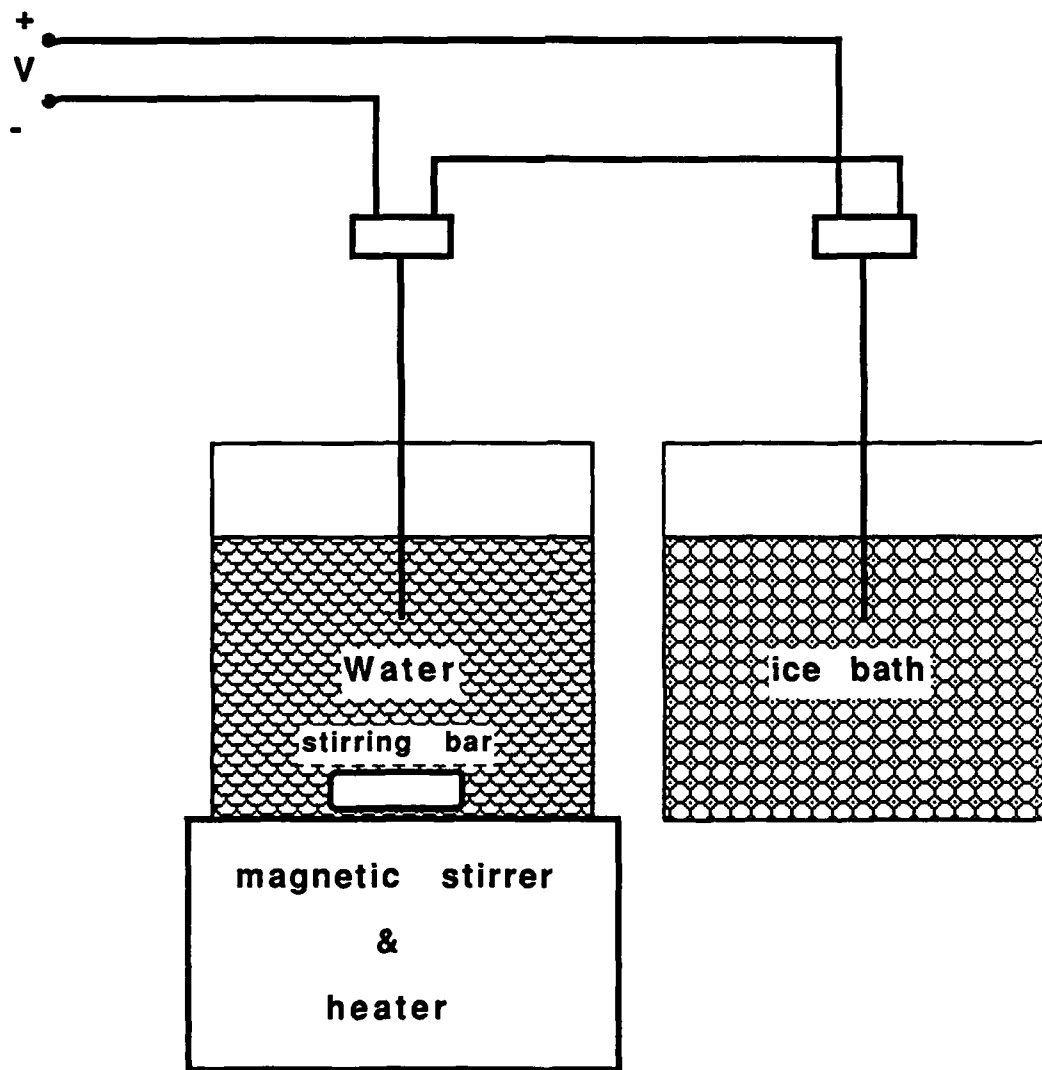


Figure 41. Differential Temperature Calibration Setup

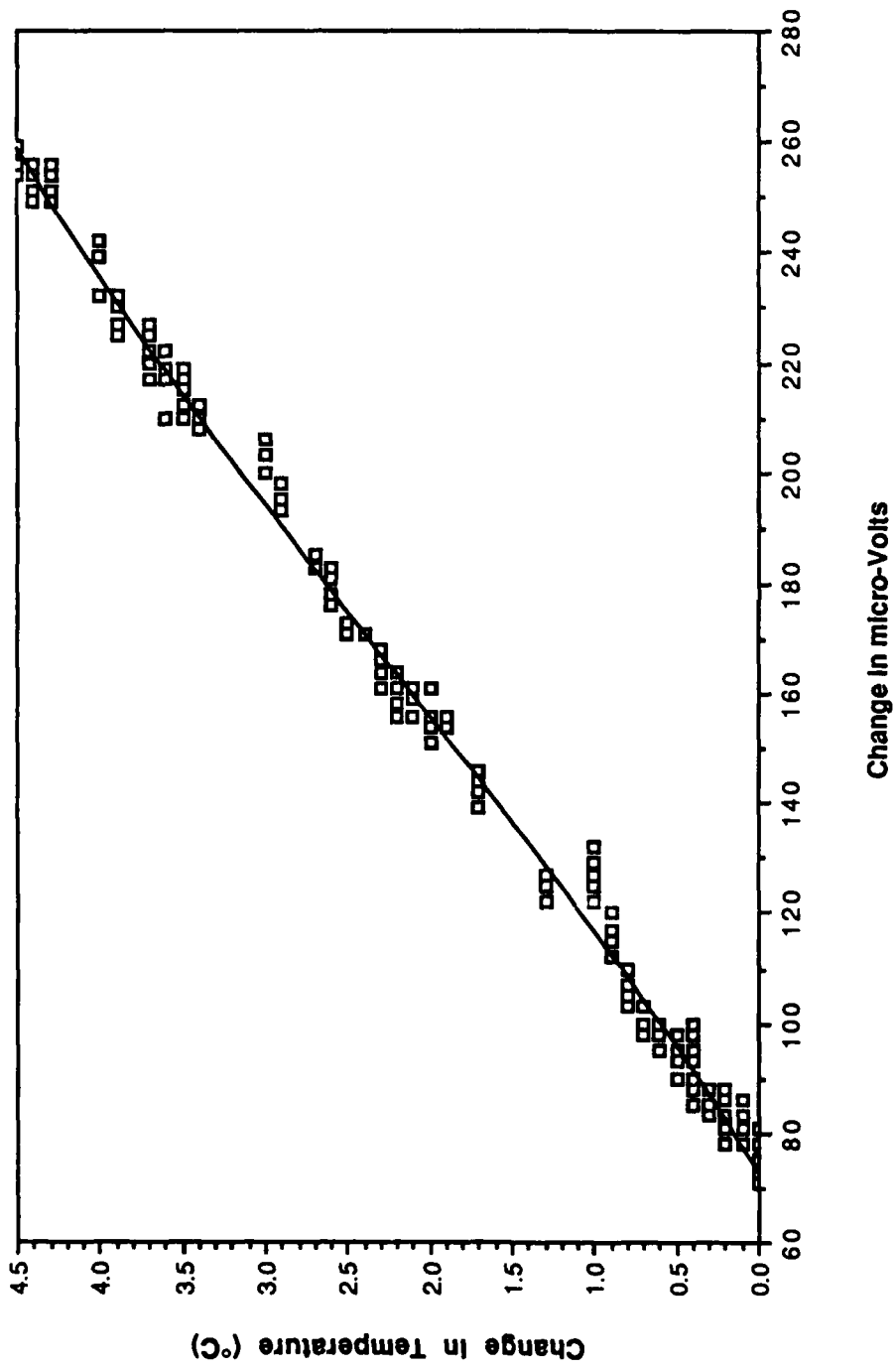


Figure 42. Differential Temperature Calibration Data

As many as eight EXP-16 cards may be used during an experiment, with up to 16 data points available on each card. For the heat pipe experiment, three EXP-16 cards were used: one for the type T thermocouples, with 15 temperatures and a CJC reading, one for the differential temperature measurement across the coolant channel, and the final one for the pressure transducer signal. All the data were stored on floppy disks.

## 4.2 Experimental Procedures

The procedural steps performed can be broken down into two categories. The first includes those steps performed before the data collection begins. The second category includes those steps performed after the data collection begins. The former are similar for every experiment and are discussed in this subsection, while the latter change from experiment to experiment and are discussed in the results and discussion subsection of this section.

A disadvantage of using an aluminum heat pipe with water as a working fluid is the long-term incompatibility of the two. Over time the aluminum oxidizes releasing hydrogen gas, but over the course of these transient experiments this is insignificant. After a day of experiments it is necessary to dismantle the pipe and clean the system. The channel, O-ring, and shoulder of the heat pipe are cleaned with acetone. The wick is then placed in the channel. Aluminum wick of mesh number 100/in is used. It covers the bottom of the channel as well as a portion of the side walls of the channel. It is held flat in place by aluminum screen with a mesh number of 16/in. It is crucial that the 100-mesh wick be flat against the channel to ensure proper wick performance during the experiments.

When cleaning the O-ring, it is important that it not be stretched. The O-ring is coated with a thin layer of Celvacene heavy vacuum grease and is placed around the channel on the clean shoulder. If the bottom side of the cover plate needs to be cleaned, liquid soap and water are used since Lexan can easily be scratched. The cover is then placed on top of the O-ring, making sure that no particles collect between it and the O-ring or between the O-ring and the aluminum. The heat pipe vacuum pump is turned on and a vacuum is pulled on the channel to a pressure of 50 millitorr or less. The leak rate is less than 0.5 torr per hour at the anticipated working pressures.

Once the pipe is at an acceptable vacuum level and seal, the ethylene-glycol/water coolant flow can be started. However, it is important to keep gases from collecting in the coolant line; so before coolant flow is started, the coolant line is flushed out with higher than normal flow rates. The flow rate the coolant pump can produce decreases with temperature; therefore it is critical that the flow rate be measured periodically to ensure good knowledge of the flow rate so that power calculations may be performed properly.

After the pipe reaches a thermal steady-state, the degassed working fluid can be added from the external flask. Once the desired amount of working fluid has been added to the pipe and the wick is wetted, data collection is begun. Several different types of experiments were performed and the procedures for them varied. The full details of these experiments and their procedures will be given in the next subsection.

#### 4.3 Results and Discussion

This subsection is divided into 6 parts. The first part describes a step increase in power to the evaporator from zero W to 100 W and follows the transient until steady-state conditions in the pipe are reached and confirms that the experimental apparatus is operating as a heat pipe at 100 W. The second part describes an experiment which had three step increases in power, with the heat pipe being allowed to reach steady-state conditions after each increase. The increases in power were from 0 to 50 W, 50 to 100 W, and 100 to 200 W. The apparatus was confirmed to be operating as a heat pipe after each of the power increases. Finally, the power was increased to 250 W, and immediately after that increase, the experiment ceased to work as a heat pipe. Also, while the pipe was approaching steady-state conditions at 50 W, there was a temporary partial dry out of the wick in the evaporator, and this will be compared with the final experiment of the previous section.

The next two parts present the data for two frozen start-ups. For each of these transients, it was first visually confirmed that the working fluid in the wick throughout the pipe was frozen. Then 100 W was applied via the heater to the evaporator. These parts of the subsection will attempt to explain what happened during each of the experiments.

The fifth part presents the data for a transient in which the heat pipe was brought to steady-state conditions with a power input of 25 W. The secondary coolant temperature was then gradually reduced until freezing conditions in the condenser caused a dry out in the evaporator. Finally, in the sixth part, data are presented on a step decrease in power from 250 to 0.0 W with an initially partially dried out evaporator. During this transient the wick rewets itself and the pipe temperatures cool down.

#### 4.3.1 Transient 1: 0-100 W

In this first experiment, the pipe had a positive tilt of  $0.6^\circ$  from the horizontal, the condenser being higher than the evaporator. The amount of working fluid added to the pipe was 100 ml. The secondary coolant sump outlet temperature at the time the step increase in power from 0.0 to 100.0 W was made was  $9^\circ\text{C}$ , where it remained ( $\pm 0.5^\circ\text{C}$ ) for the remainder of the transient. Before the transient was started, a completely wetted wick was visually verified. Also, immediately before the transient was started, the vacuum pump was briefly turned on and off to remove any noncondensable gases that may have collected. The transient ended when the internal vapor and wick/liquid temperatures of the pipe indicated steady-state conditions had been reached. The data presented for this transient cover the time from when the step increase in power is made and continue until steady-state operating conditions are confirmed.

The placement of type T thermocouples, the pressure transducer, the heat pipe vacuum attachment and the working fluid addition point are shown in Figure 43. The placement of the type K thermocouples is shown in Figure 44. Note that these K thermocouples are attached to the outer surface of the Lexan cover in the condenser and adiabat.

Figure 45 shows the temperature response of wick/liquid thermocouples 6 and 10 and vapor space thermocouple 8. Figure 46 displays the temperature data for outer aluminum wall thermocouples 2, 4, and 5. Thermocouple six is in the middle of the evaporator, thermocouple 8 is in the adiabat 0.0635 m from the adiabat/condenser interface, and thermocouple 10 is 0.2286 m from the end of the condenser away from the adiabat. Thermocouple 2 is in the middle of the evaporator, 4 is at the adiabat/condenser interface, and 5 is 0.0899 m from the

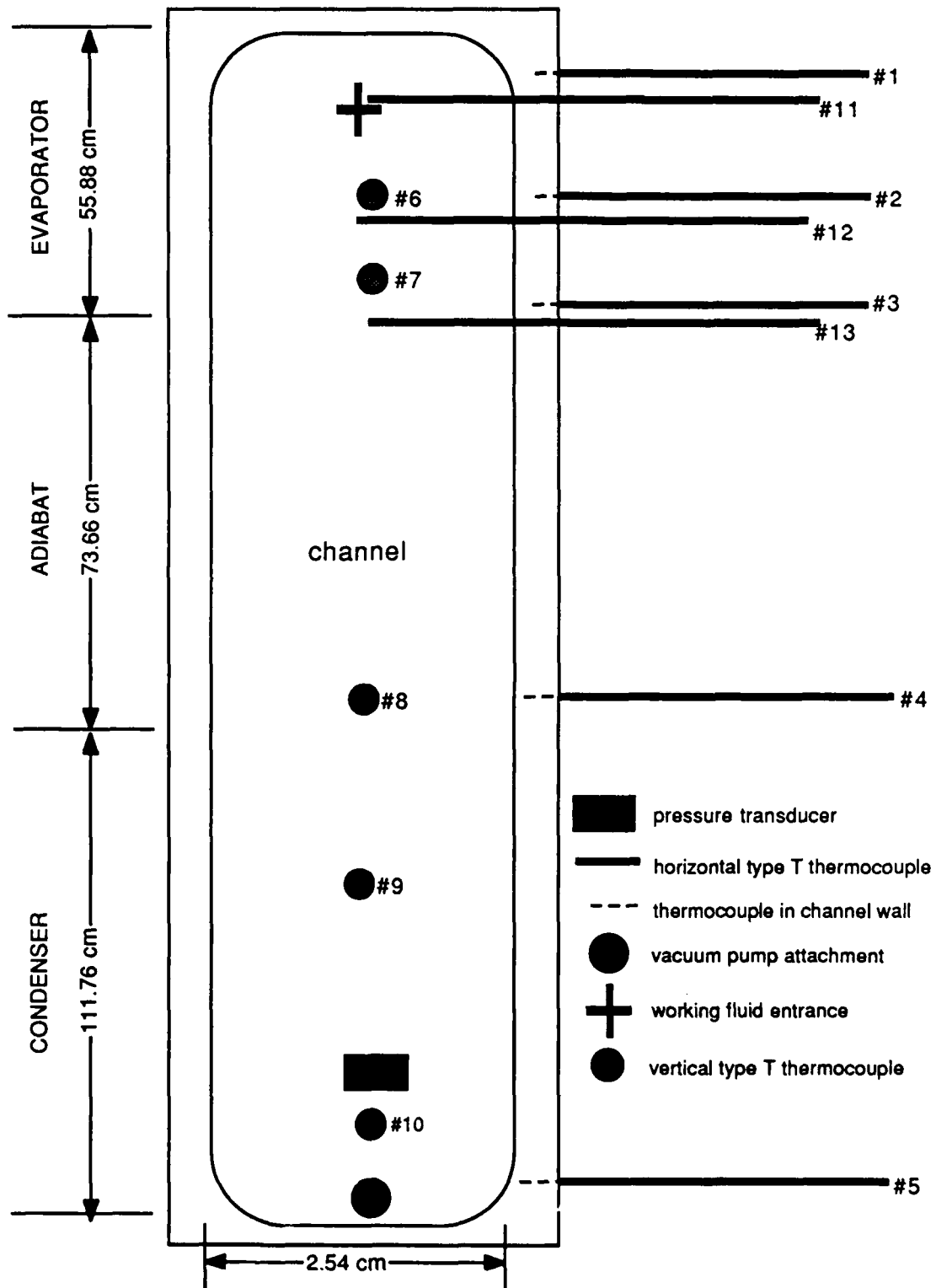


Figure 43. Location of Instrumentation (except K thermocouples) 100 W

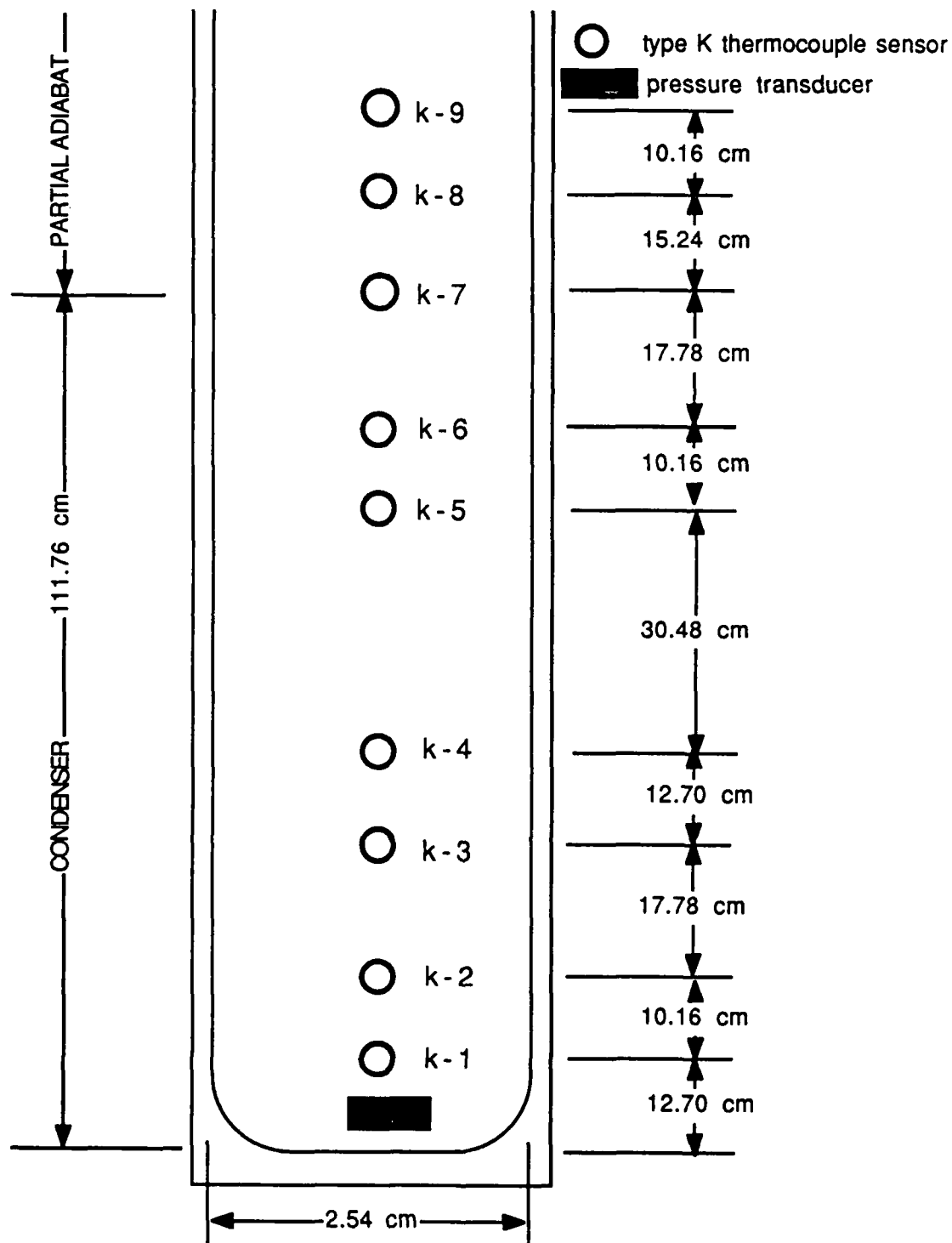


Figure 44. Location of K Thermocouples 100 W

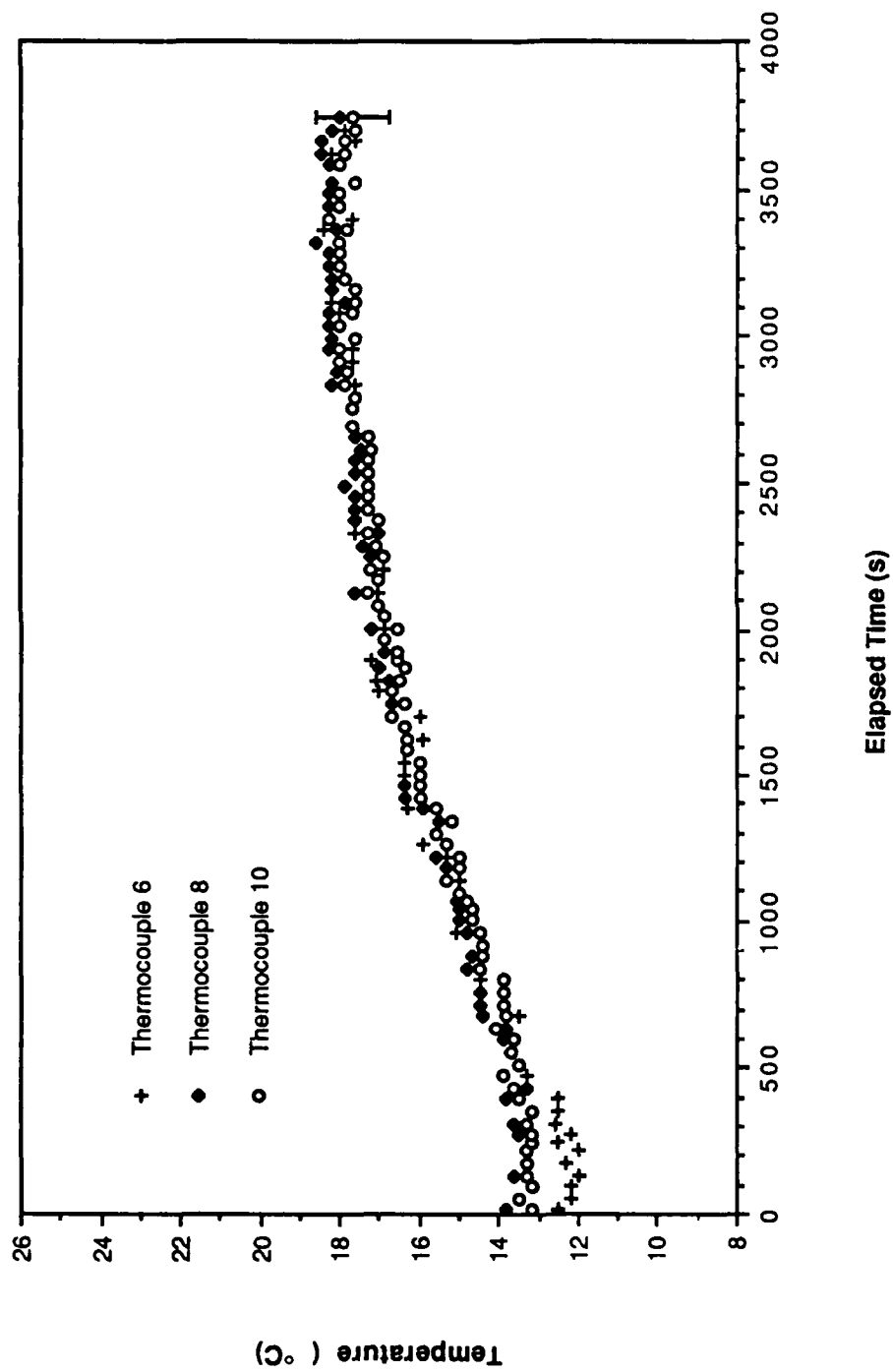


Figure 45. Liquid/Wick and Vapor Space Thermocouples for 100 W

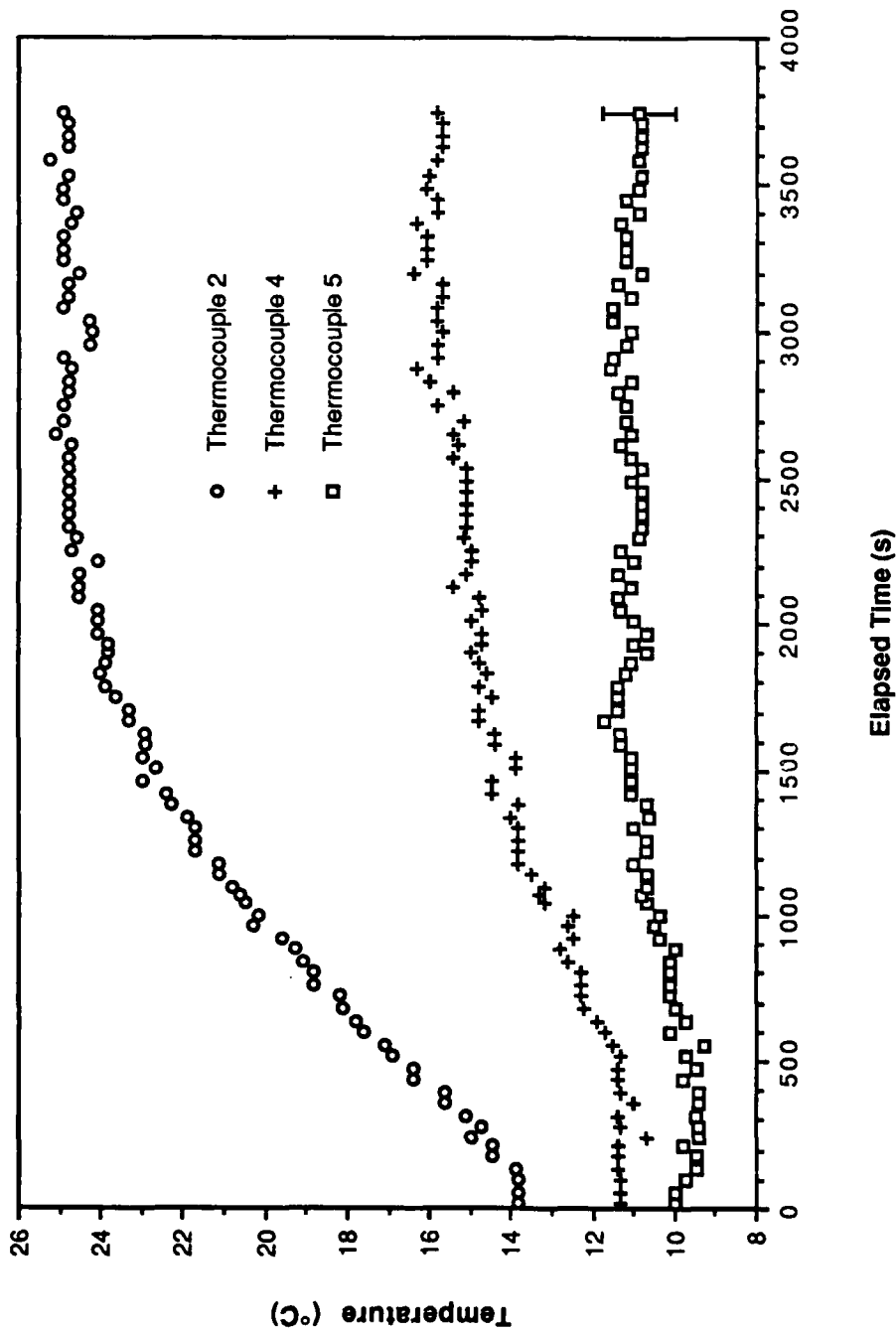


Figure 46. Outer Wall Measurements For 100 W

end of the condenser away from the adiabat.

Figure 45 shows that the temperatures of thermocouples 6, 8, and 10 are almost the same after 400 s. It is possible that the pipe was not isothermal in the internal channel before and shortly after power was applied, but once vapor generation has started in the evaporator due to a power input, the vapor will flow to the condenser due to a pressure drop caused by a slightly lower temperature in the condenser than in the evaporator. As the vapor flows over the adiabat and condenser and over the liquid returning to the evaporator in the wick, the pipe becomes nearly isothermal within a short time, as occurred in this transient. The temperature drop from the evaporator vapor space to the condenser vapor space is within the error of the thermocouples, as is the temperature drop across the liquid/vapor interface, so values for these drops were not measurable, but they must exist for the heat pipe to operate normally. The vapor space and wick/liquid temperatures should read nearly the same temperature after 400 s, which they do. These temperatures come together at 13.5°C and slowly rise until 2800 s, when steady-state conditions were reached and lasted until the experiment was terminated at 3700 s. The steady-state temperature in the pipe was 18°C.

Figure 46 shows thermocouples 2, 4 and 5 and their temperature paths. The steady-state temperatures for thermocouples 2, 4 and 5 at that point are 25°C, 16°C and 11.2°C, respectively. The temperatures for those thermocouples can be calculated if one assumes that the aluminum outer wall is essentially isothermal in a given cross section, and that there is 1-D conduction from the heater to the evaporator and from the condenser to the secondary coolant jacket. This first assumption is reasonable considering the high thermal conductivity of aluminum, and the one-dimensional assumptions are good if the insulation of the pipe is effective in preventing ambient gains or losses. Finally, since the conductivity of aluminum is so high, the only temperature drops that need to be considered are those in the evaporator wick/liquid and condenser wick/liquid sections. If equations 7, 8 and 9 are used, it can be seen that  $\Delta T_{\text{wick/liquid}} = q'' k \Delta X$ , where  $k$  is the effective conductivity of the wick/liquid section. Dunn and Reay<sup>11</sup> suggest that  $k$  can be approximated by the following equations:

$$k = ((\beta - \epsilon) / (\beta + \epsilon)) k_l \quad (10)$$

where  $\beta = (1 + k_s / k_l) / (1 - k_s / k_l) \quad (11)$

where  $k_l$  = thermal conductivity of liquid

$$= 0.603 \text{ W / m } ^\circ\text{C}$$

$k_s$  = thermal conductivity of wick

$$= 205.0 \text{ W / m } ^\circ\text{C}$$

and  $\epsilon$  = volume fraction of solid in the wick

$$= 0.71$$

Then,  $k = 3.56 \text{ W / m } ^\circ\text{C}$ .

For the evaporator wick,

$$\Delta x = 0.000229 \text{ m}$$

$$Q = 100 \text{ W}$$

$$A = 0.0145 \text{ m}^2$$

so,  $q'' = 6897 \text{ W / m}^2$

and  $\Delta T = 5.6^\circ\text{C}$ .

For the condenser wick,

$$\Delta x = 0.000229 \text{ m}$$

$$Q = 100 \text{ W}$$

$$A = 0.0284 \text{ m}^2$$

$$q'' = 3523 \text{ W / m}^2$$

and  $\Delta T = 2.7^\circ\text{C}$ .

The calculated temperature for the evaporator outer aluminum wall is  $23.6^\circ\text{C}$  compared with a measured value of  $25.2^\circ\text{C}$ , which is close when the approximate method of calculating  $k$  is considered. The calculated temperature for the condenser outer aluminum wall is  $15.3^\circ\text{C}$ . Thermocouples 4 and 5 are on opposite ends of the condenser, and indicate temperatures of 16 and  $11.2^\circ\text{C}$  respectively. Since 4 is influenced by the adiabat and 5 is at the far end of the heat pipe from the adiabat, it is difficult to get a good idea of the true condenser outer wall temperature, but that temperature would certainly be between those indicated by thermocouples 4 and 5, as the calculation above suggests.

Finally, the differential temperature measurements across the secondary coolant jacket give the power removed from the heat pipe by the coolant jacket as 100 to 110 W, which is reasonable considering the above discussion. The extra 10 W is partially explained by small ambient gains to the pipe and partially by the error involved in the power input measurements and output calibrations.

The K thermocouples on the cover plate in the condenser conveyed no additional information except to show that the buildup of noncondensable gases

during the transient was not significant. Therefore none of the K thermocouple data are shown here. The same is the case for the plot of power removed by the secondary coolant jacket and for the pressure of the condenser vapor space. The pressure changes tracked with the vapor temperatures of thermocouple 8, as expected.

#### 4.3.2 Transient 2 : 0-50-100-200-250 W

In this run the heat pipe had a positive tilt of  $0.75^\circ$  from the horizontal. The amount of working fluid added to the pipe was 100 ml. The sump temperature of the secondary coolant for the experiment was  $5^\circ\text{C} \pm 1^\circ\text{C}$ . As in the previous experiment, visual verification of a completely wetted wick was made prior to adding power to the pipe. First a step increase of power into the evaporator from 0 to 50 W was made and the pipe was allowed to reach a steady-state. A partial wick dry out and rewetting occurred in the evaporator during this part of the experiment. After steady-state was reached, the power to the evaporator was increased to 100 W, and again a steady-state was reached. The power was then increased to 200 W, steady-state conditions were again reached, and the power was increased to 250 W. Shortly after this last increase, the wick in the evaporator experienced a sustained partial dry out, and the experiment was stopped.

The placement of type T thermocouples, the pressure transducer, the heat pipe vacuum attachment and the working fluid addition point are shown in Figure 47. The placement of the type K thermocouples is shown in Figure 48. Note that these K thermocouples appear only on the outer surface of the Lexan cover in the condenser and adiabat.

The analysis of this transient will be broken up into three different parts. The first analyzes the initial input of 50 W. The second part analyzes the increase in power from 50 to 100 W, and the third analyzes the increase in power from 100 to 200 W and from 200 W to 250 W. At zero s the power to the evaporator is increased from zero to 50 W, from 50 to 100 W at 6000 s, from 100 to 200 W at 8100 s, and from 200 to 250 W at 11500 s.

The data for the first part are shown in Figures 49, 50, and 51. Figure 49 displays the vapor space and wick liquid temperatures of thermocouples 6, 7, and 9. Thermocouple 6 is placed as described in the previous section and is in the

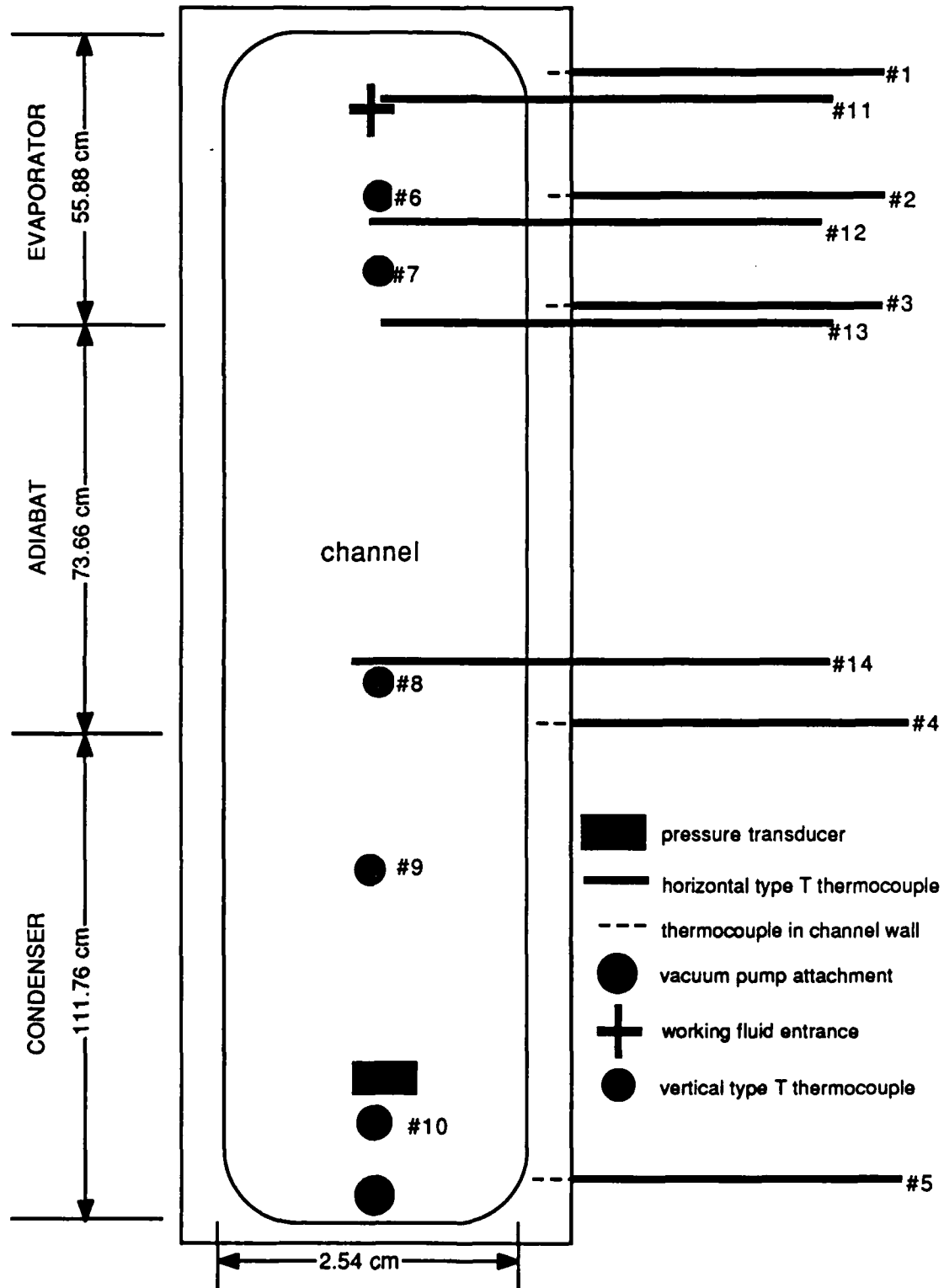


Figure 47. Location of Instrumentation (except K thermocouples)  
0-50-100-200-250

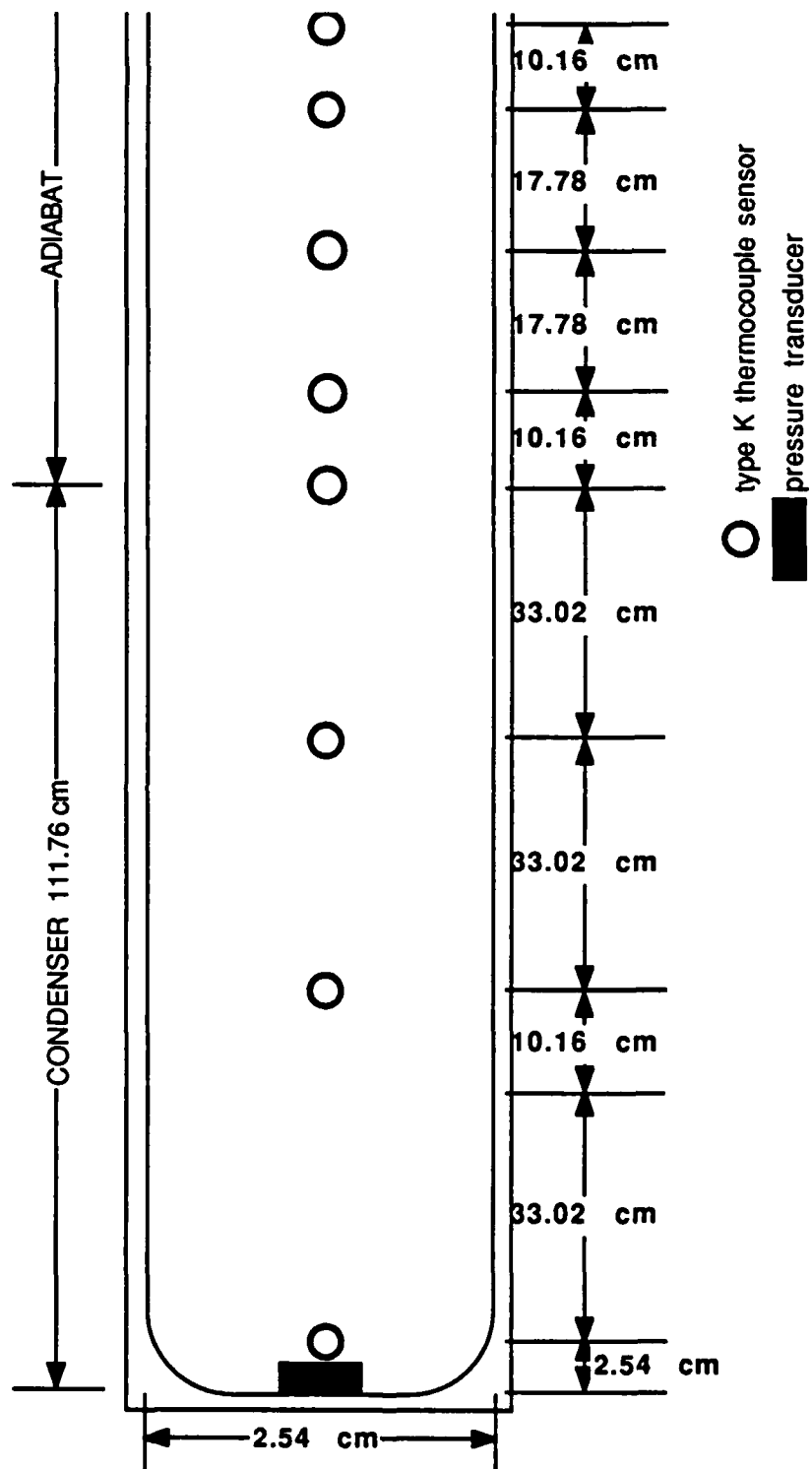


Figure 48. Location of K Thermocouples  
0-50-100-200-250

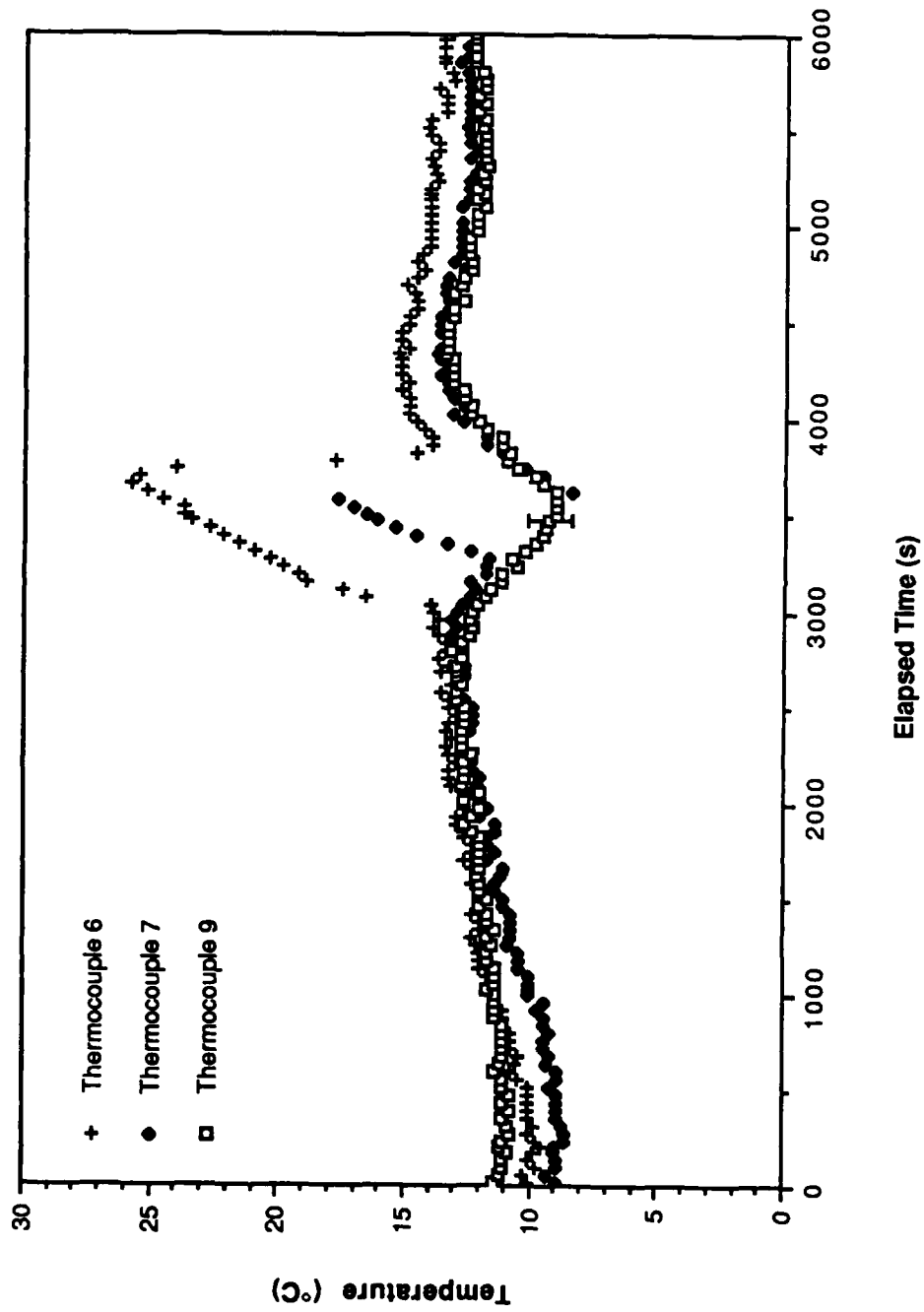


Figure 49. Liquid/Wick and Vapor Space Thermocouples 0-50 W

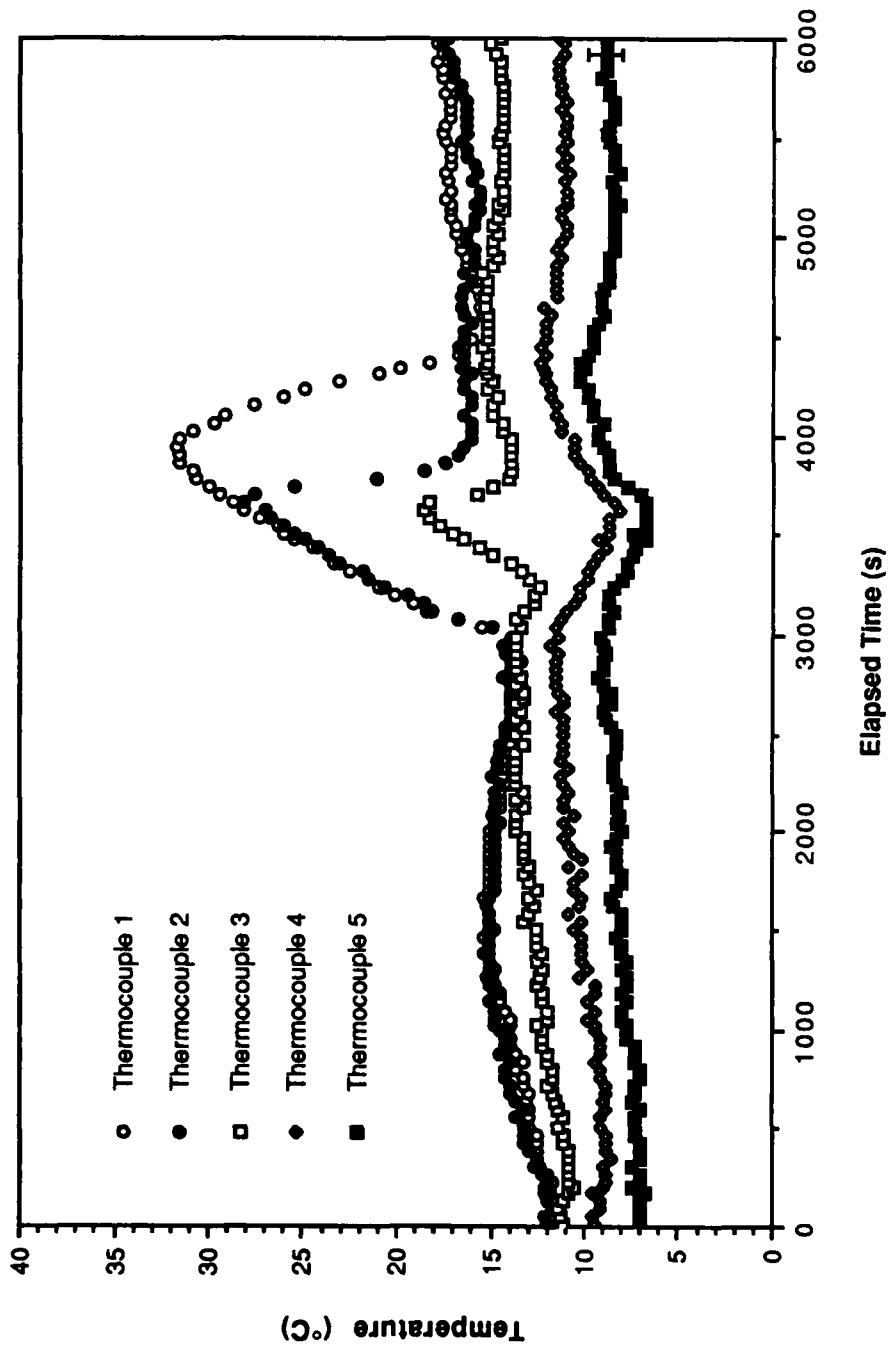


Figure 50. Outer Wall Measurements for 0-50 W

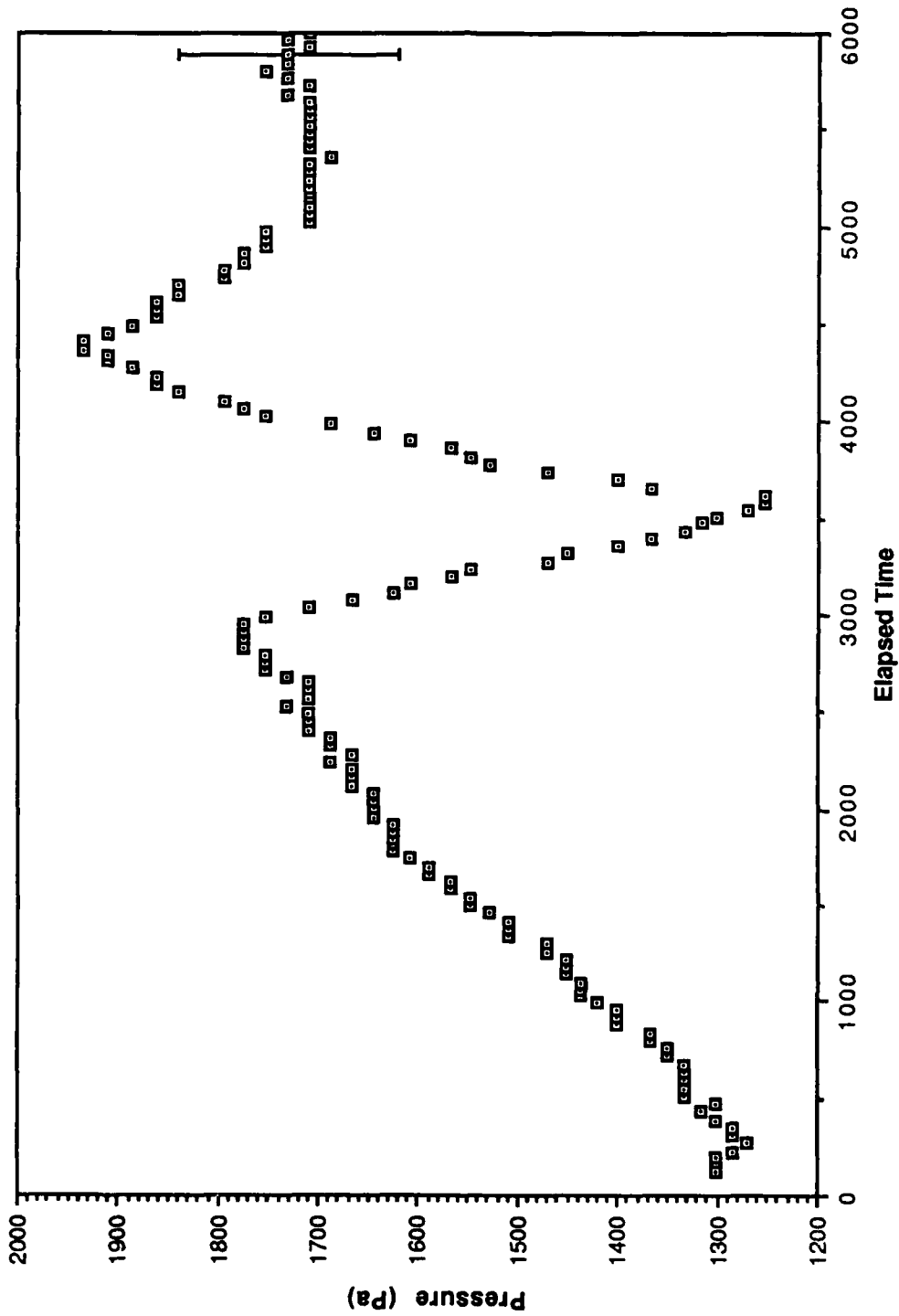


Figure 51. Pressure for 0-50 W

wick/liquid region of the evaporator. Thermocouples 7 and 9 are vapor space thermocouples with the probe of 7 being at the evaporator/adiabat interface and the probe of 9 in the center of the condenser. Figure 50 presents the outer aluminum wall temperatures of thermocouples 1 through 5. Thermocouples 2, 4, and 5 are placed as described in the previous experiment. Thermocouple 2 is in the middle of the evaporator, 4 is at the adiabat/condenser interface, and 5 is 0.0899 m from the end of the condenser away from the adiabat.. Thermocouples 1 and 3 are in the evaporator along with 2. Number 1 is 0.0254 m from the far end of the evaporator from the adiabat, and 3 is at the evaporator/adiabat interface. The data obtained from the pressure transducer are shown in Figure 51. The transducer reads the vapor space pressure in the condenser 0.0749 m from the adiabat/condenser interface.

After the 50 W is added, the transient appears to be experiencing a normal startup until 3000 s, when the temperatures of thermocouples 1, 2, and 6 increase drastically, and the temperatures of 3, 4, 5, 7, and 9 decrease noticeably. The pressure in the condenser also experiences a decrease. At about 3200 s, the temperatures of 3 and 7 stop decreasing and start increasing. Shortly after 3500 s, the condenser and adiabat temperatures stop decreasing and start to rise again at nearly the same rate at which they were decreasing between 3000 and 3500 s. These temperatures level out at about the same point they were at just before 3000 s. The evaporator temperatures start to decline after 3500 s, with the exception of thermocouple 1, and all decline at a much faster rate than the increase they experienced between 3000 and 3500 s; or in the case of thermocouple 1, between 3000 and 4000 s. They also level out at the temperature they were at just before 3000 s. Thermocouple 7 makes a rapid drop in temperature at 3500 s and actually reads the same temperature as thermocouple 9 for the rest of this part of the transient after 3500 s. Between 3800 and 4000 s, all thermocouples rise about 2°C in temperature before coming to their steady-state temperatures for this part of the transient at 5000 s, which is about 2°C below the temperature at 3800 s for all thermocouples except 1, which read 33°C at 4000 s and 13°C at 5000 s. The shape of the pressure trace is similar to that for the condenser vapor space temperatures.

The reason for the temperature excursions between 3000 and 4000 s is a dry out in the evaporator wick. This was confirmed visually. It is also apparent that the

evaporator wick rewet itself between 3600 and 4000 s. These measurements are very similar to those made in Section 3 in the discussion of the power increase from an operating state, and the description of that transient holds for this transient, although the temperature excursions here occurred over a much longer time period and the evaporator experienced a more thorough, if only temporary, dry out, with the entire evaporator wick appearing dried out at 3300 s.

The initial dry out occurs because the vaporization rate of the liquid in the evaporator is greater than the return rate of liquid in the wick to the evaporator through gravitational and capillary forces. When this occurs, the evaporator wick contains less and less liquid with time until the wick starts to dry out. This also means that there will be no new vapor generation; thus the vapor will no longer flow through the evaporator and condenser, so energy is no longer transferred to the adiabat and condenser by this means from the dried out sections of the wick, and the only energy transferred will be by conduction in the outer walls of the heat pipe. The temperatures in the areas with liquid still in the wick will thus decrease due to a proportionally greater influence from the secondary coolant. The pressures in these areas will decrease with temperature. Meanwhile, the vapor in the dried out sections will be superheating, and rapid increases in temperature will occur. The evaporator can eventually be fully dried out. The process of dry out can be reversed if the capillary and gravity effects become such that the return rate of liquid in the wick to the evaporator is enough to overcome the dry out and is equal to or greater than the rate of vaporization of the liquid in the evaporator.

The temperature hump from 3800 to 4000 s appears to be caused by the fact that the evaporator wick is not completely rewet until 4300 s, when the peak of the hump occurs. Although most of the pipe is operating normally at 3800 s, there is some additional heat input from stored energy in the pipe walls and wick caused by the high temperature in the dried out sections of the evaporator wick. This extra stored energy becomes insignificant or is fully removed after 5000 s.

The cause for this partial and temporary dry out is unknown, but it could be that the wick was not as completely wet as had been visually ascertained earlier. Although liquid appeared in or above the wick, it may not have made its way down into the pores fully enough to avoid the dry out. Once capillary pumping brought the liquid back to the evaporator, the wick was completely wet, and the

heat pipe continued operating normally. In the series of figures to follow, it will be shown that there were no more problems with wick dry out until a power level of 250 W was reached. It is also possible that the dry out occurred because a capillary limit was reached at the internal temperature of the pipe when the dry out occurred, and that the temperature of the pipe increased just enough to reduce the viscosity of the liquid and increase the capillary limit enough so the pipe could reach steady-state.

The data for the part of the transient that includes the increase in power to the evaporator from 50 to 100 W, and the achievement of steady-state conditions at 100 W, are shown in Figures 52 and 53. Figure 52 shows thermocouples 6, 7 and 9, and Figure 53 shows the temperature response of thermocouples 2, 4 and 5. The power increase occurred at 6000 s. The heat pipe appeared to reach steady-state conditions after 7400 s, with the steady-state vapor space and wick/liquid temperatures both at 16.5°C.

Figures 54, 55 and 56 represent the data for the third part of the transient, which is from 8100 to 12500 s. The power input was increased from 100 to 200 W at 8100 s, and from 200 to 250 W at 11400 s. At 12500 s, the experiment was stopped. Figure 54 shows thermocouples 6, 7 and 9, Figure 55 shows thermocouples 1, 2, 3, 4 and 5, and Figure 56 shows the power removed by the secondary coolant as calculated from the known flow rate and the temperature difference across the secondary coolant jacket measured by the differential thermocouples. The heat pipe seems to have behaved normally after the increase in power to 200 W, and reached a steady-state near 10800 s. Shortly after the increase in power to 250 W at 11400 s, however, thermocouple 1 indicates that there was a dry out in the evaporator wick when the temperature there increased dramatically. Thermocouples 2 and 3 and 6 and 7 do not show such increases, so the dry out was only partial in the evaporator, but the experiment had to be ended to protect the O-ring and Lexan cover. Figure 56 shows the power removed by the coolant jacket, and shows that the value rose from 100 to 200 W from 8100 s to 11500 s as expected. This also helps verify the power calorimetry calculations performed.

Finally, the outer aluminum wall temperatures of the adiabat and condenser predicted by the equations presented earlier are shown in Table 5 for the 50, 100, and 200 W power levels along with the measured values in the middle of the

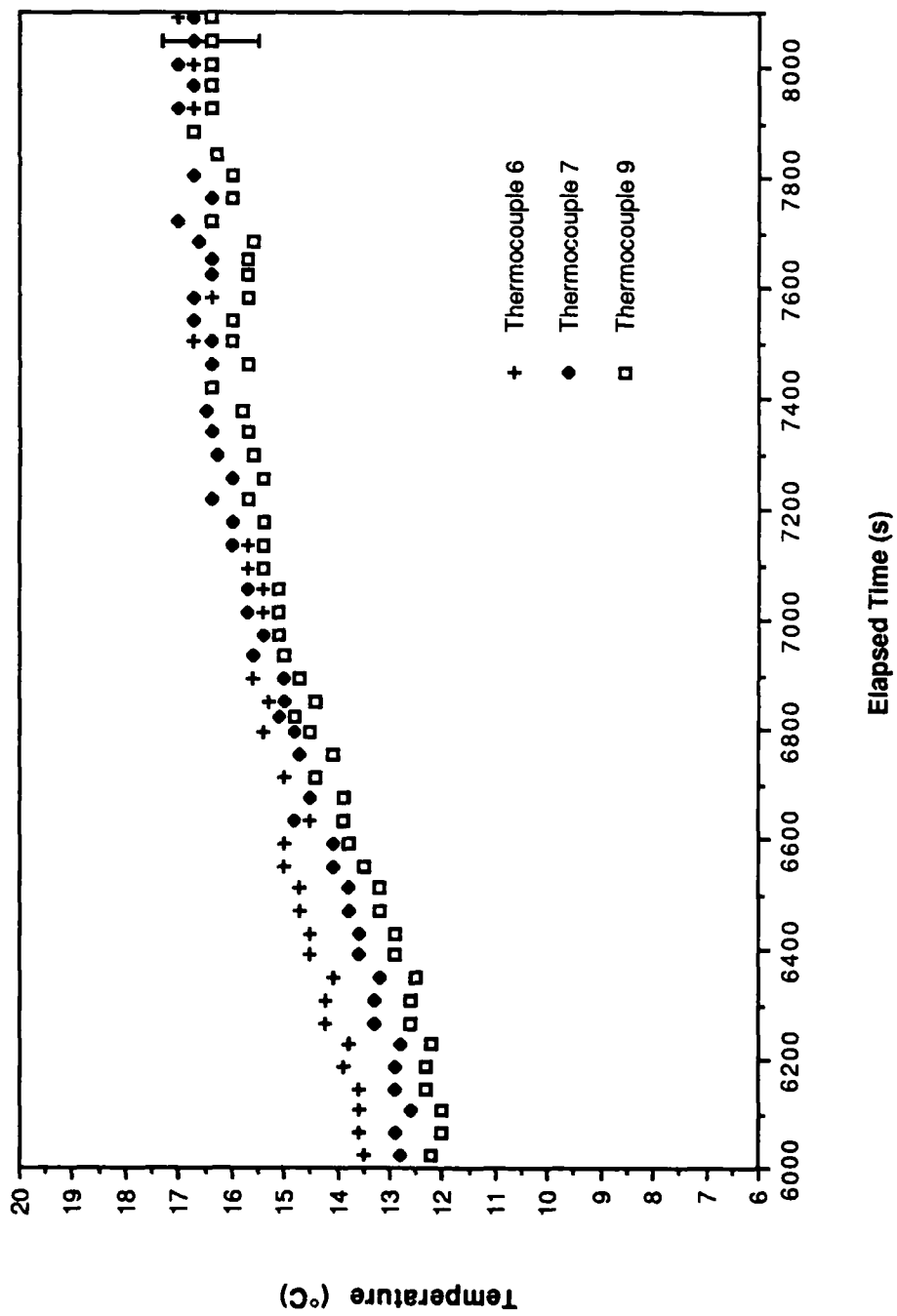


Figure 52. Liquid/Wick and Vapor Space Thermocouples for 50-100 W

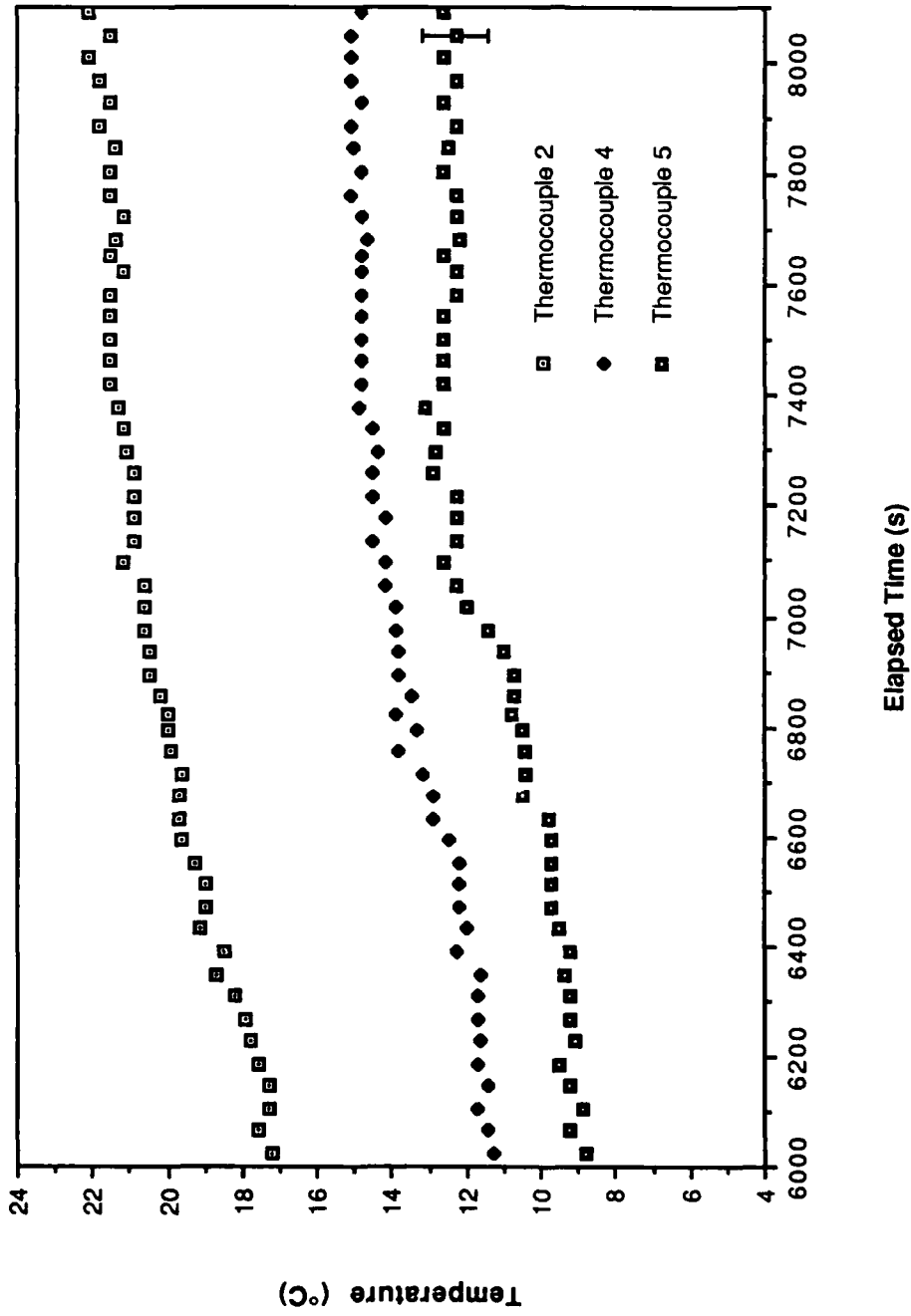


Figure 53. Outer Wall Measurements For 50-100 W

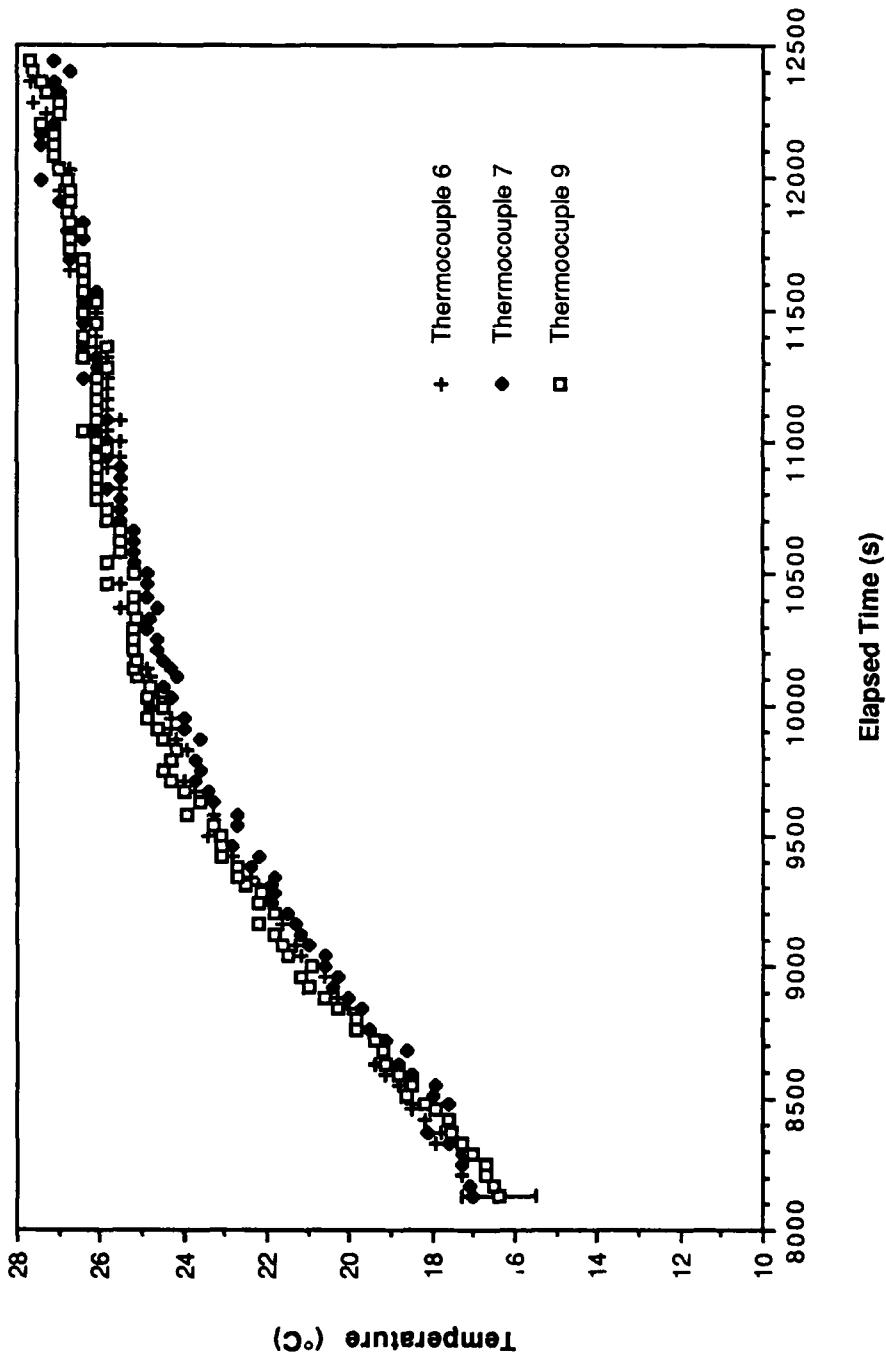


Figure 54. Liquid/Wick and Vapor Space Thermocouples For 100-200 W

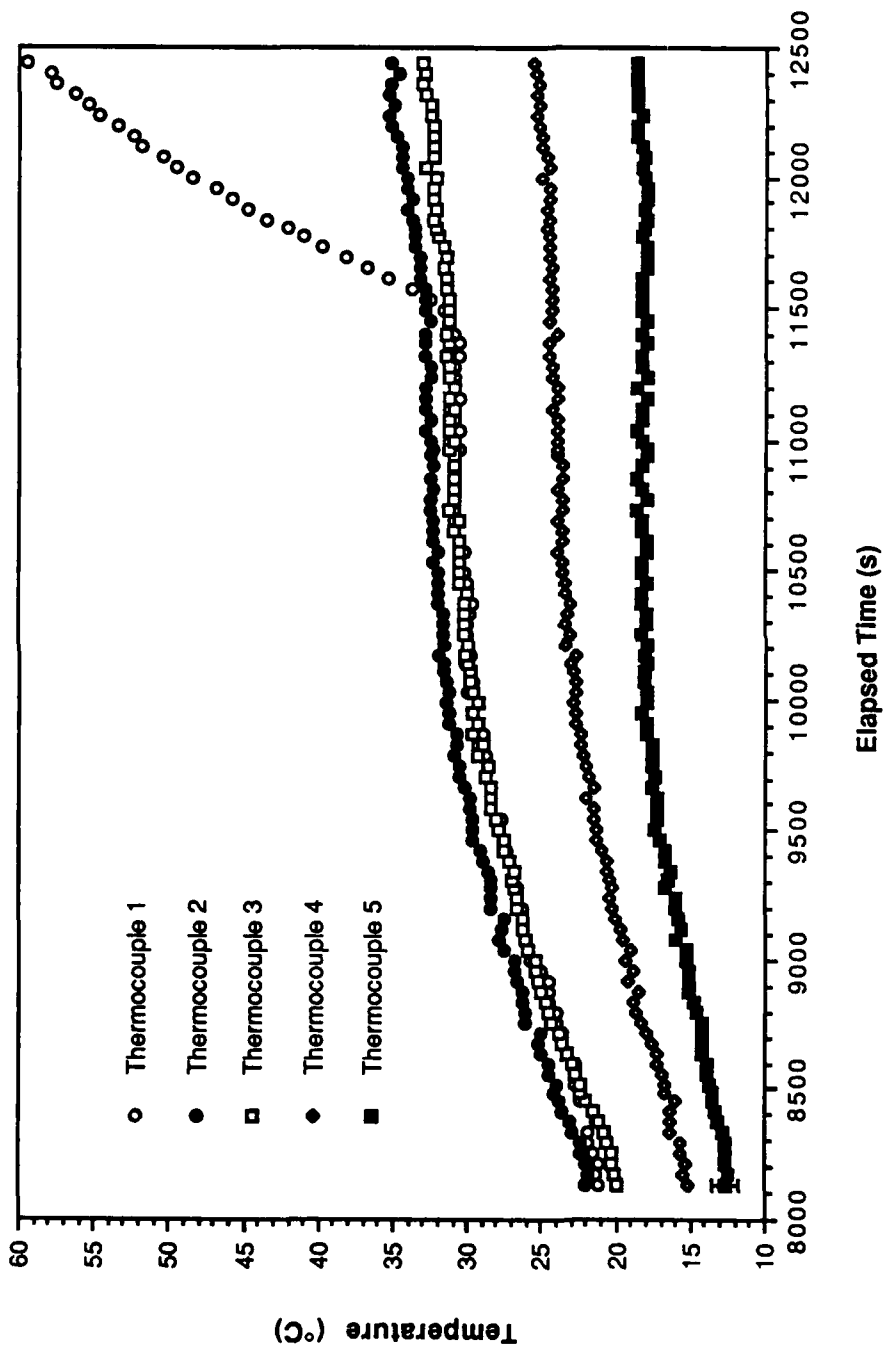


Figure 55. Outer Wall Measurements for 100-200 W

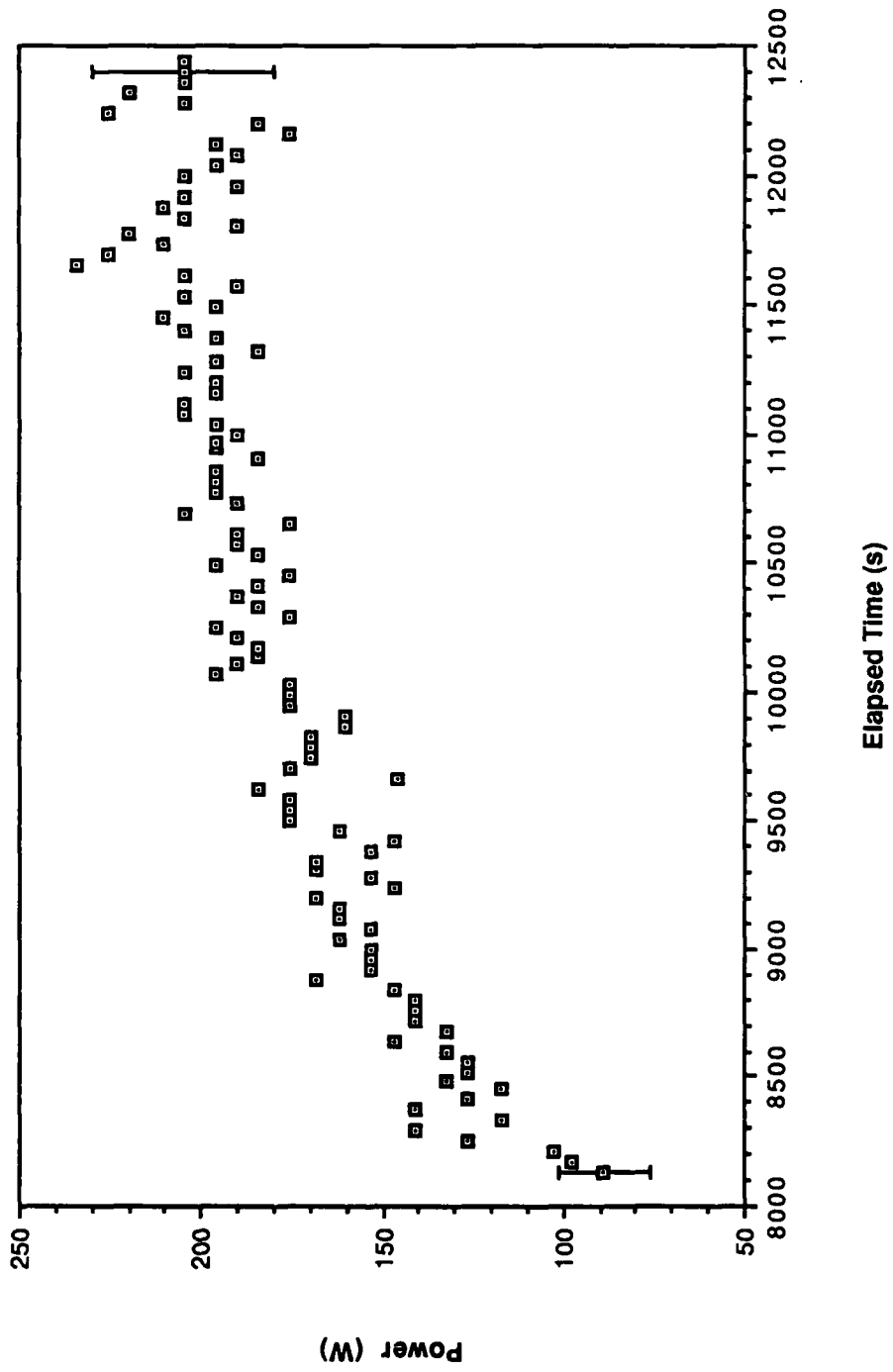


Figure 56. Power 100-200 W

Table 5. Outer Aluminum Wall Temperatures Observed and Predicted

Power (W)	Internal Temp. (°C)	Condenser Outer Wall Temperature-Far End (°C)	Condenser Outer Wall Temperature A/C Interface (°C)	Condenser Outer Wall Predicted Temperature (°C)	Evap. Outer Wall Temp. (°C)	Evap. Outer Wall Predicted (°C)
50	12.0	9.0	11.0	10.7	16.0	14.8
100	16.5	12.0	14.7	13.7	21.3	22.1
200	26.2	18.0	24.0	20.8	37.4	33.0

evaporator and on both ends of the condenser and the internal pipe temperature. The predicted and measured values are in reasonable agreement.

#### 4.3.3 Transient 3 : Frozen Start-up Number 1

In the third experiment the pipe had a positive tilt (the condenser higher than the evaporator) of  $0.6^\circ$  from the horizontal. The amount of working fluid added to the heat pipe channel was 100 ml. The coolant sump temperature at the time the working fluid was added was  $3^\circ\text{C}$ . The coolant sump temperature was reduced to  $-20^\circ\text{C}$  over a period of about 75 min. A completely frozen working fluid was then verified by observation through the clear Lexan cover in all sections of the pipe. At that point the vacuum pump was turned on to remove any noncondensable gases that may have accumulated. Five minutes later 100 W was applied to the strip heater attached to the lower side of the evaporator. When an unrecoverable wick dry out was observed in the evaporator both visually and instrumentally, and the temperatures in the outer aluminum wall surpassed  $50^\circ\text{C}$ , the power was turned off to protect the Lexan cover and O-ring. The data presented for this run represent the period of time from 90 s before the power was turned on to the time when power was turned off.

The placement of type T thermocouples, the pressure transducer, the heat pipe vacuum attachment and the working fluid addition point are shown in Figure 57. The placement of the type K thermocouples is shown in Figure 58. Note that these K thermocouples are placed only on the outer surface of the cover plate in the condenser section.

Figure 59 shows the response of thermocouples 6 and 7 during the first frozen transient. Figure 60 shows an enlarged time scale for those same two thermocouples between 600 and 1400 s. Thermocouple 6 gives a liquid/wick temperature measurement in the center of the evaporator and thermocouple 7 shows the response of the vapor space 0.0762 m into the adiabat from the condenser/adiabat interface. Figure 61 shows thermocouples 1, 2, 3, and 4 and their response throughout the transient. These are all type T thermocouples placed inside the shoulder of the heat pipe and they give the temperature response of the outer wall. Thermocouple 1 was 0.0254 m from the far end of the evaporator; thermocouple 2 was in the middle of the evaporator, at the same

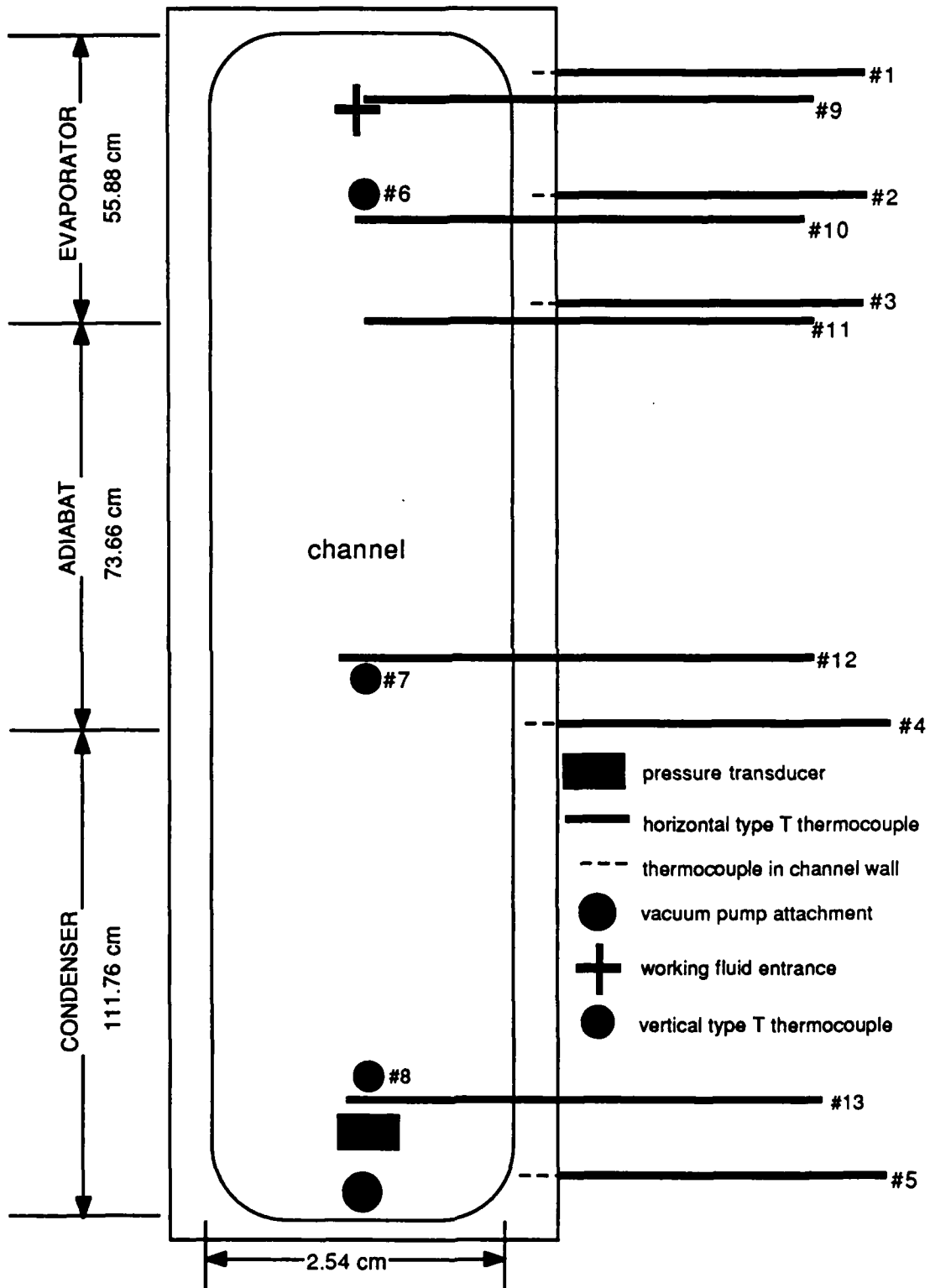


Figure 57. Location of Instrumentation (except K thermocouples)

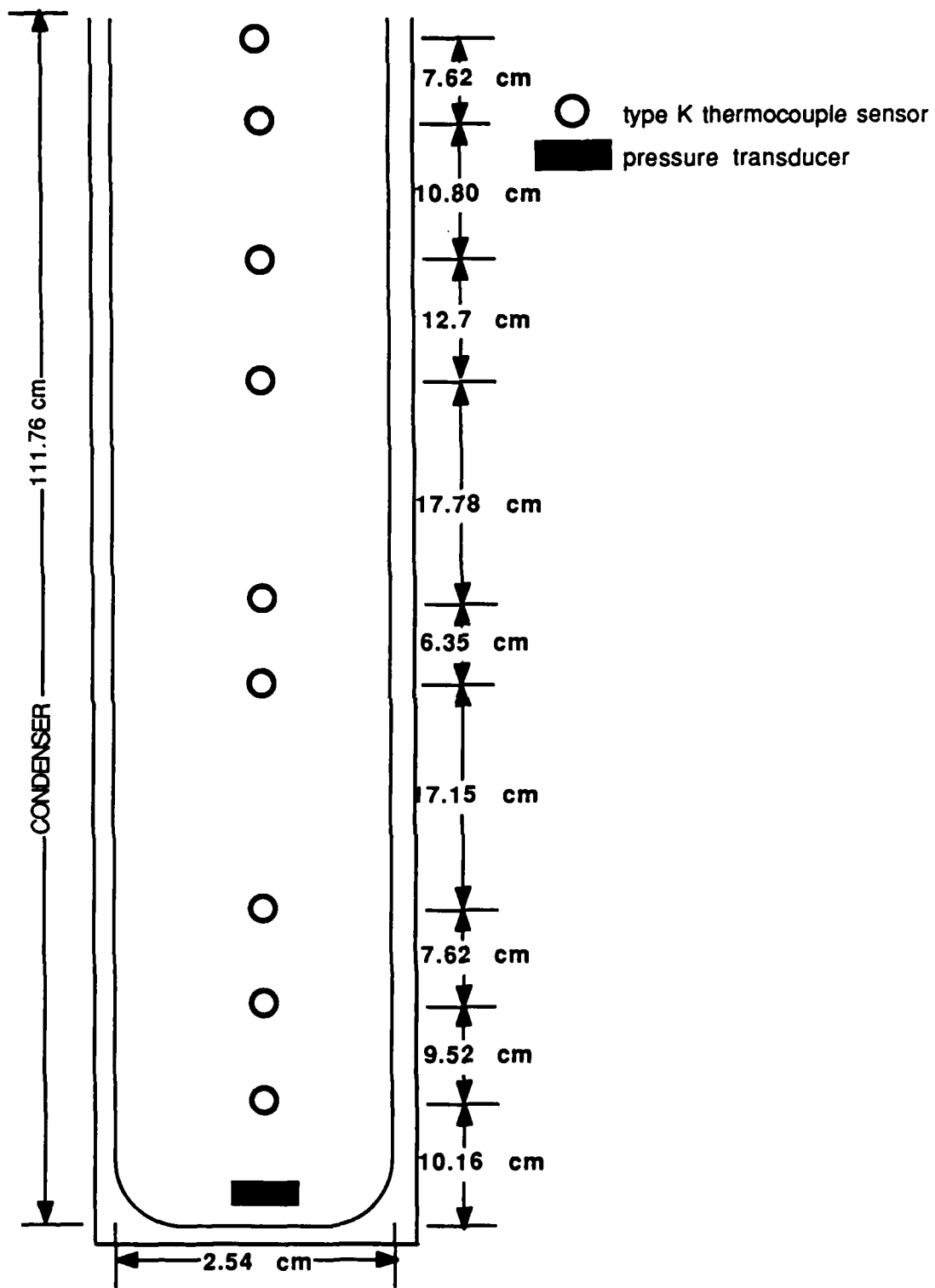


Figure 58. Location of K Thermocouples

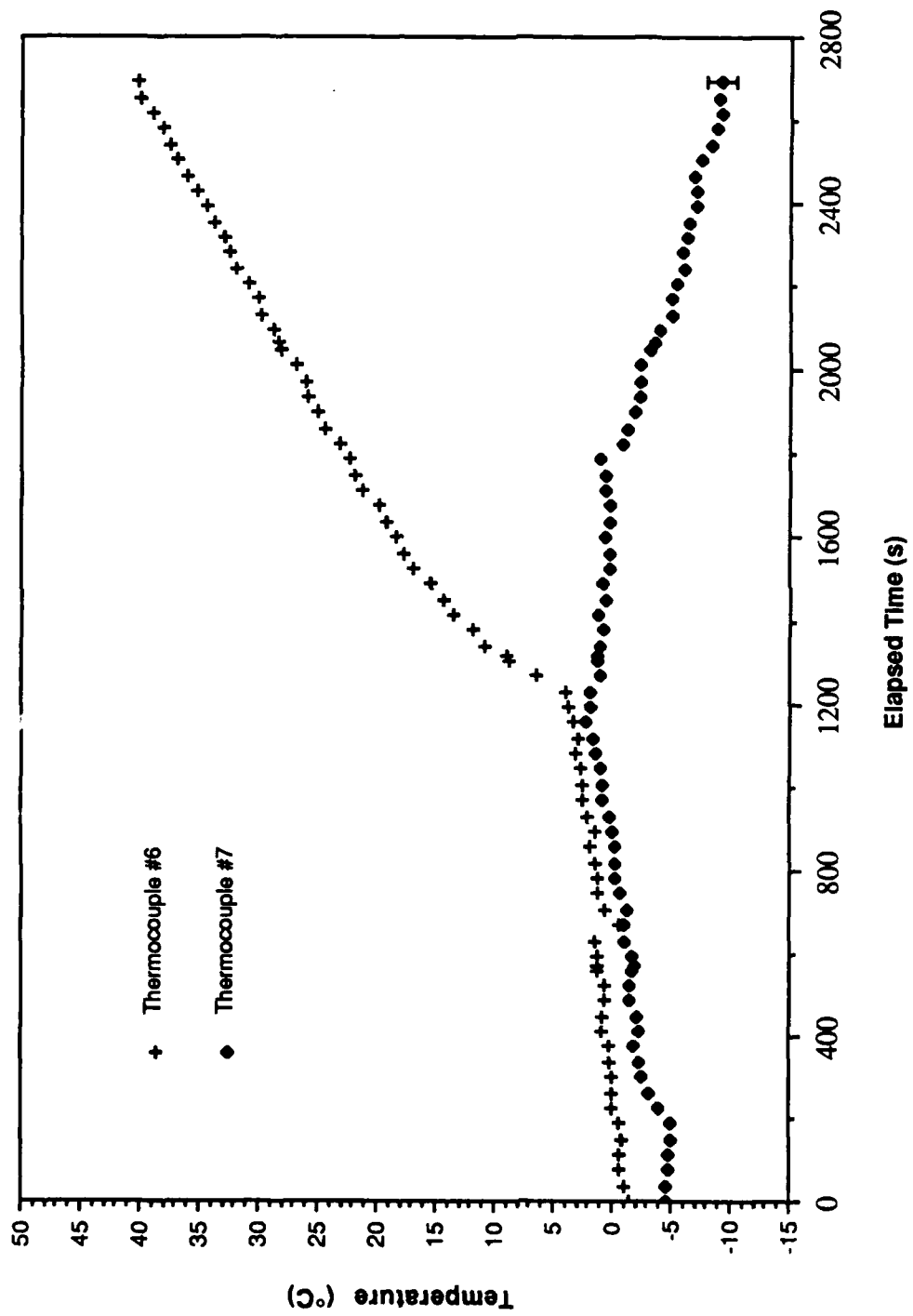


Figure 59. Liquid/Wick and Vapor Space Thermocouples for Frozen Start-up 1

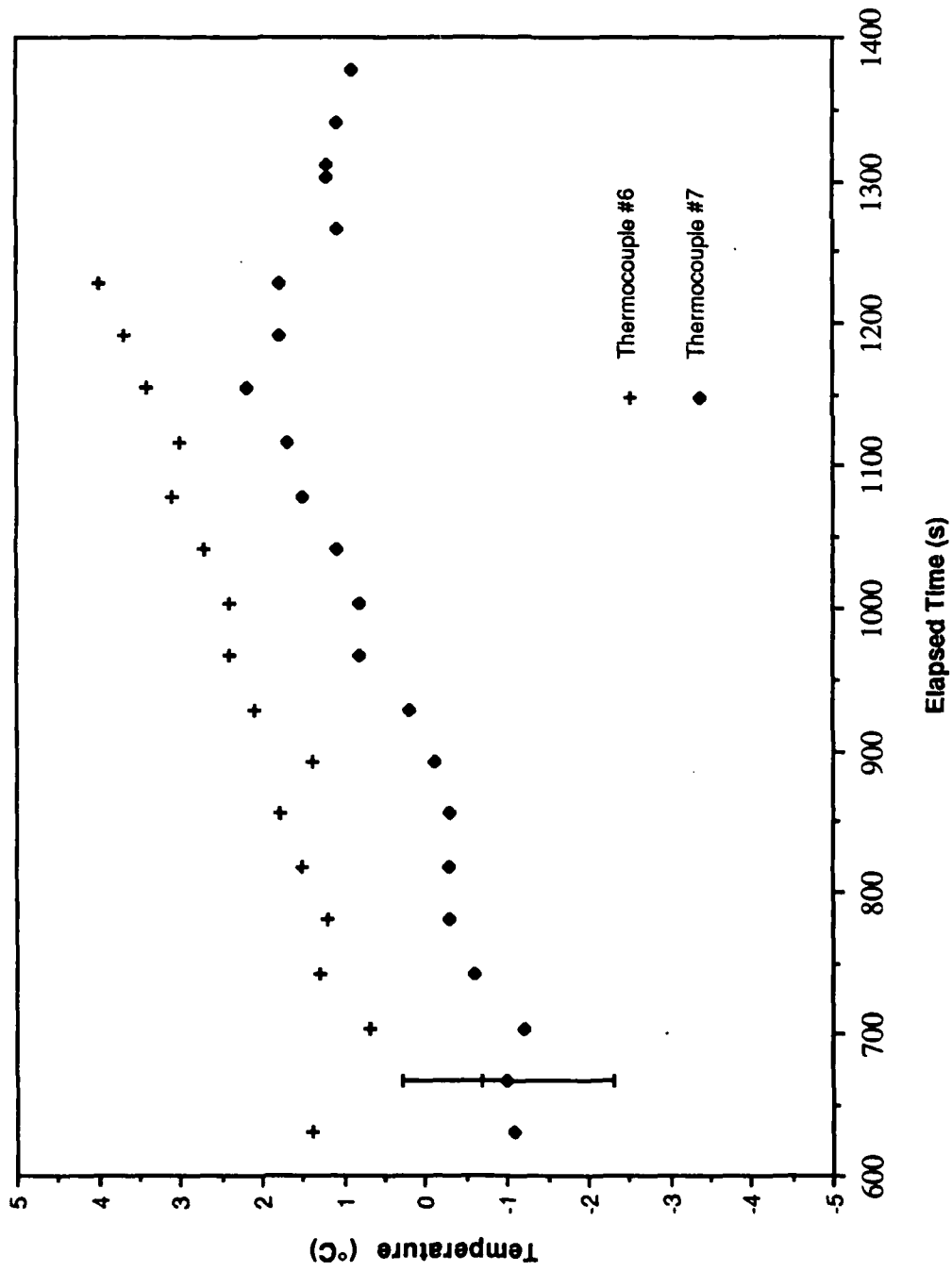


Figure 60. Enlargement of Figure 59

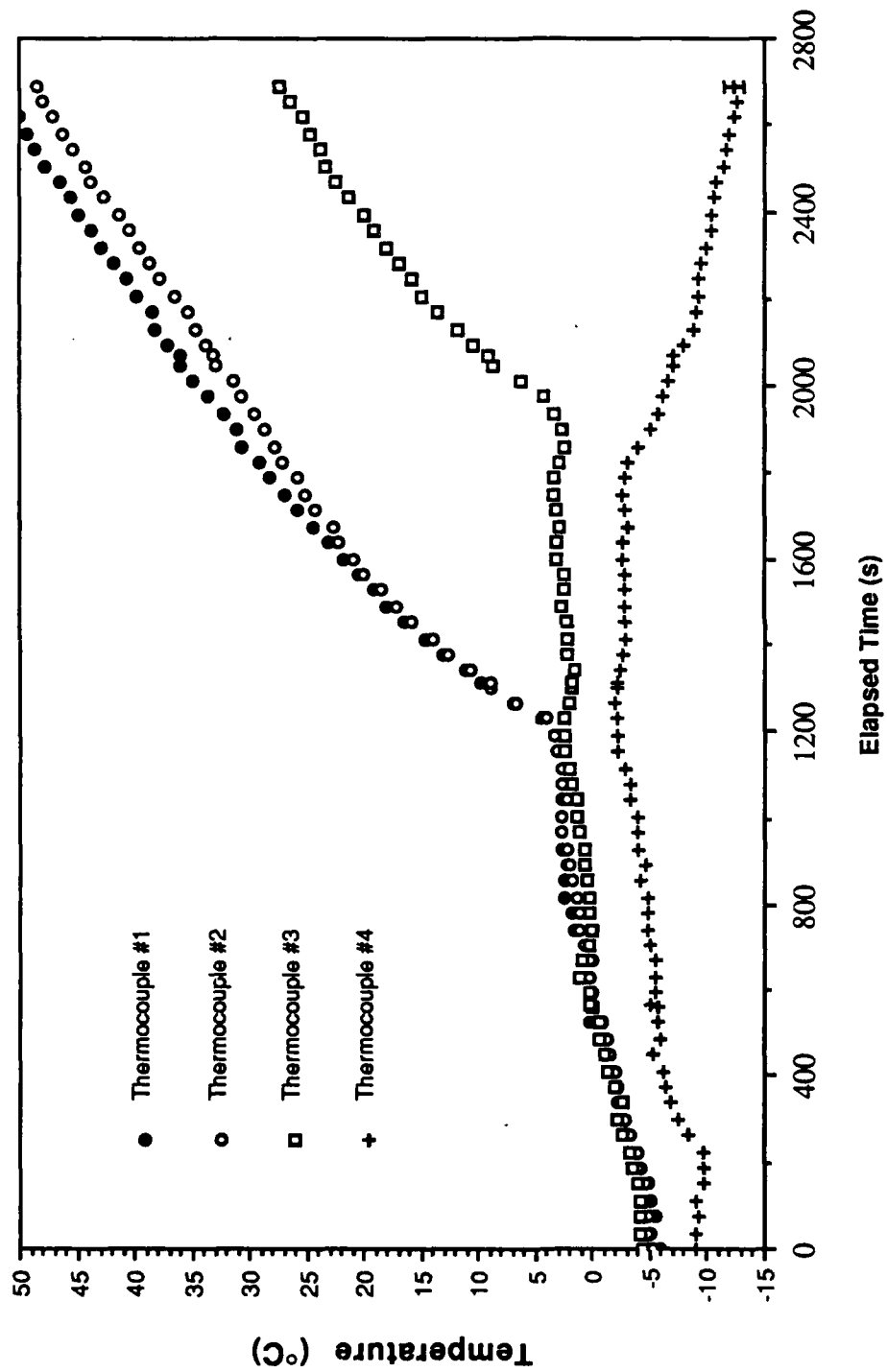


Figure 61. Outer Wall Measurements for Frozen Start-up 1

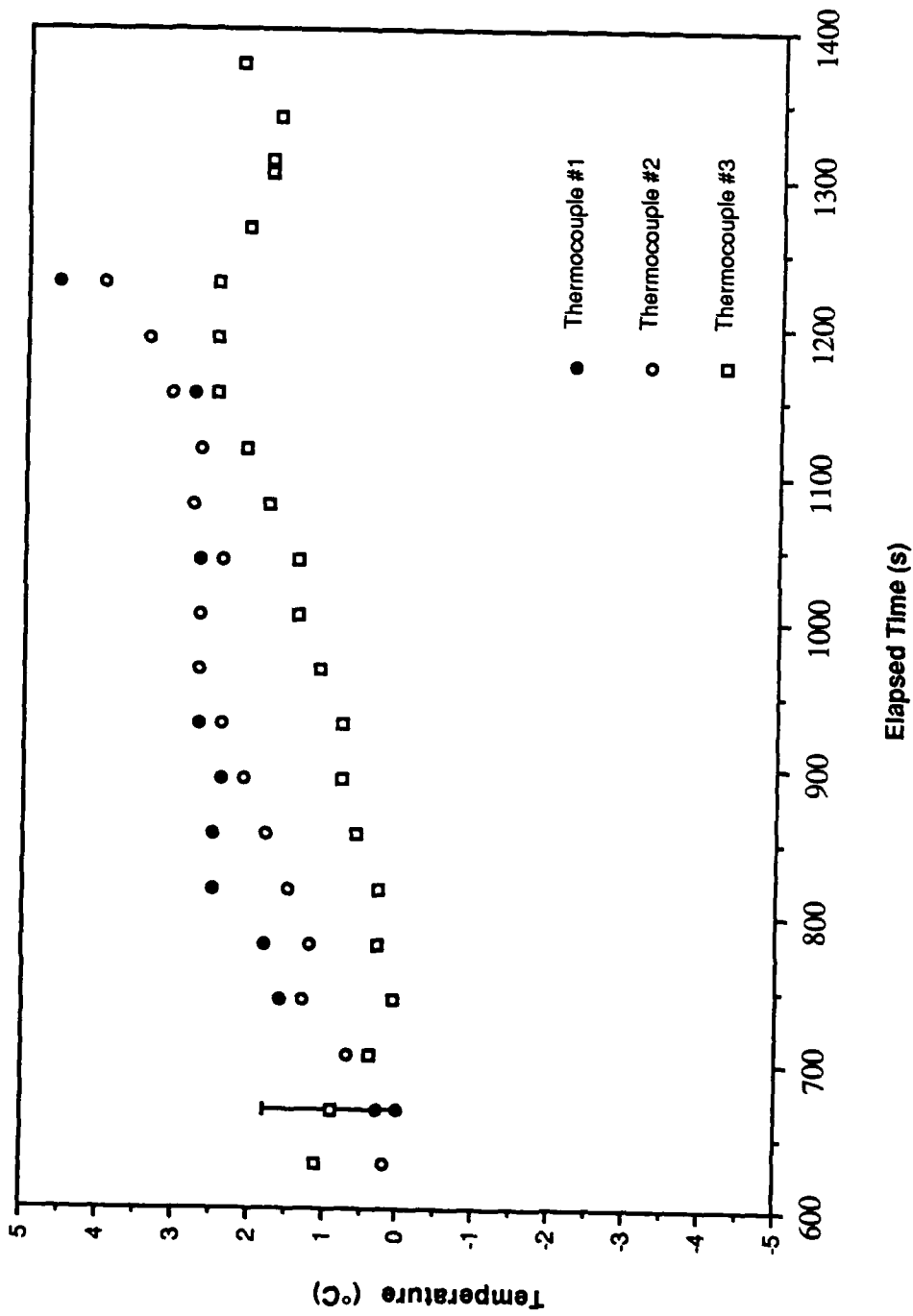


Figure 62. Enlargement of Outer Wall Thermocouples for Frozen Start-up 1

point on the major axis of the pipe as thermocouple 6; thermocouple 3 was at the adiabat/evaporator interface; and thermocouple 4 was at the condenser/ adiabat interface, at the same position on the major axis of the pipe as thermocouple 7. Thermocouples 1, 2, and 3 are shown on an enlarged time scale in Figure 62, which has the same time scale as Figure 60.

The input power from the strip heater was equal to 0.0 W at time zero, and was subjected to a step increase to 100 W at 90 s. Figure 59 shows that after the power was added the temperatures of the pipe at the location of thermocouples 6 and 7 slowly increased after 200 s until about 1200 s. Figure 60 further shows that thermocouple 6 was reading about 2°C higher than thermocouple 7 at 600 s, and that the temperature gap was reduced to 1°C at 1100 s. After 1150 s the gap started increasing again when the temperature of thermocouple 7 started decreasing, which it continues to do for the rest of the transient. After 1200 s, the temperature at thermocouple 6 begins to increase more rapidly than before and continues to do so for the rest of the transient.

Figure 61 shows that the temperatures of outer wall thermocouples 1 and 2 follow a path similar to that of thermocouple 6 for the entirety of the experiment, and thermocouple 4 follows a path similar to that of thermocouple 7 for the same time period. Thermocouple 3 shows that the outer wall temperature at the evaporator/adiabat interface rises with the other evaporator outer wall temperatures until about 1200 s, when the temperature of thermocouple 3 levels off to between 2 and 3°C until it starts increasing sharply at 1900 s. Figure 62 gives a better view of the reactions of thermocouples 1,2, and 3 immediately before and after the 1200-s mark.

At 1800 s and 2430 s the vacuum pump was briefly turned on to remove the small amount of noncondensable gases that had built up in the far end of the condenser away from the adiabat. Shortly after 1800 s, both thermocouples 7 and 4 showed an increased rate of temperature drop, while 6, 1, 2, and 3 showed no noticeable change in temperature trends. There was no noticeable change in temperature trends for any of the thermocouples after 2430 s. The power input to the evaporator from the heater was removed at 2580 s.

The ice in the evaporator began melting after 300 s, and appeared to have fully melted by 700 s. This could be seen through thermocouple 6 as the liquid/ice/wick temperature slowly increased but continued to stay near 0.0°C, the

freezing point of water, surpassing it around 300 s. Between 700 and 1200 s the liquid/wick temperature increased from 0.5°C to 3.5°C. These temperatures indicate that only liquid and vapor existed in the evaporator in this time frame. During this part of the transient, vapor was being produced in the evaporator and was flowing towards the condenser due to the pressure drop caused by the temperature difference between the frozen condenser and the newly melted evaporator.

The vapor space temperatures indicated by thermocouple 7 show that the working fluid in the adiabat was frozen and getting colder until 200 s. At this point the temperature started approaching the melting temperature of ice, which it reached at about 800 s. After 950 s, the adiabat seemed to be above 0°C, indicating that most or all of the water in the adiabat was either in the liquid or vapor state, while the working fluid in the condenser was observed to remain frozen. From 950 to 1150 s, the temperature of thermocouple 7 started approaching that of thermocouple 6, and just before 1200 s the temperature difference between these two thermocouples was less than 1°C. This indicates that the pipe was essentially isothermal in the inner channel of the pipe which includes the evaporator and adiabat. This can be most readily seen in the enlargement of the time scale for thermocouples 6 and 7 in Figure 60.

Shortly after 1200 s, two different but related things seemed to occur. First, the adiabat vapor temperature seemed to reach a peak and began declining. This suggests that the working fluid was cooling down. Throughout this experiment the adiabat was being influenced by two major factors: the conduction loss of energy to the coolant via the condenser, and the flow of warm vapor through the vapor channel as it was produced in the evaporator and flowed towards the cooler condenser. If the condenser were not frozen, the adiabat would have also been cooled by the flow of liquid through the wick from the condenser. For this transient, an increase in the vapor temperature of the adiabat (as occurred from about 200 s to 1200 s) means that the effect of the vapor flow was greater than the effect of the conduction from the coolant. However, shortly after 1200 s the temperature indicated by thermocouple 7 began to decrease.

Since the power input to the evaporator and the coolant temperature remained approximately constant, the only possible explanation for the decrease at thermocouple 7 is that the wick in the evaporator was drying out. This happens

if the amount of liquid being returned to the wick in the evaporator by gravity and capillary forces is less than the amount of liquid being turned into vapor in the evaporator due to the power input. If the condensed vapor is frozen in the condenser it cannot be returned to the evaporator by capillary pumping. If the condensed vapor is not frozen and appears in the wick as a liquid, it may not move back to the evaporator quickly enough to replenish the liquid being vaporized. This decreased velocity of the liquid is due to the increased viscosity of water near freezing temperatures. When this happens, eventually all of the liquid in the evaporator is turned into vapor and the wick dries out. The vapor in the evaporator is then superheated and evaporator temperatures rapidly increase. Shortly after 1200 s, this appears to happen in this transient.

Thermocouple 6 shows a rapid increase in the evaporator, and as the vapor was superheating there with no new vapor generation, it was no longer flowing across the evaporator and one would expect to see the adiabat temperature decrease due to the removal of the energy addition to it from vapor flow and the increased influence of conduction from the coolant. This is indeed what happened. In fact, the adiabat refroze from about 1500 s to 1800 s, at which point no more liquid remained anywhere in the pipe and only vapor and frozen water existed. The adiabat temperatures were then free to go below  $0.01^{\circ}\text{C}$ , the triple point of water, which happened after 1800 s. The solidification of liquid in the adiabat can be seen in Figure 59 as a near constant temperature slightly above  $0.0^{\circ}\text{C}$  shown by thermocouple 7.

Slightly before the temperature read by thermocouple 7 went below  $0.0^{\circ}\text{C}$  (around 1800 s), the heat pipe vacuum pump was briefly turned on to remove the small amount of noncondensable gases that had built up in the far end of the condenser from the adiabat. This also pulled some of the mass of vapor from the evaporator and adiabat sections into the condenser; and in the middle one-third of the condenser, some of the vapor brought down from the adiabat and evaporator froze rapidly. The ice formations caused by this rapid freezing are shown in Figure 63.

One effect of the removal of vapor mass from the adiabat is that the freezing process that was occurring now had a smaller amount of vapor mass to freeze, so the freezing process could now occur much more rapidly, as shown by the rapid drop-off of the adiabat vapor temperature after the heat pipe vacuum pump was

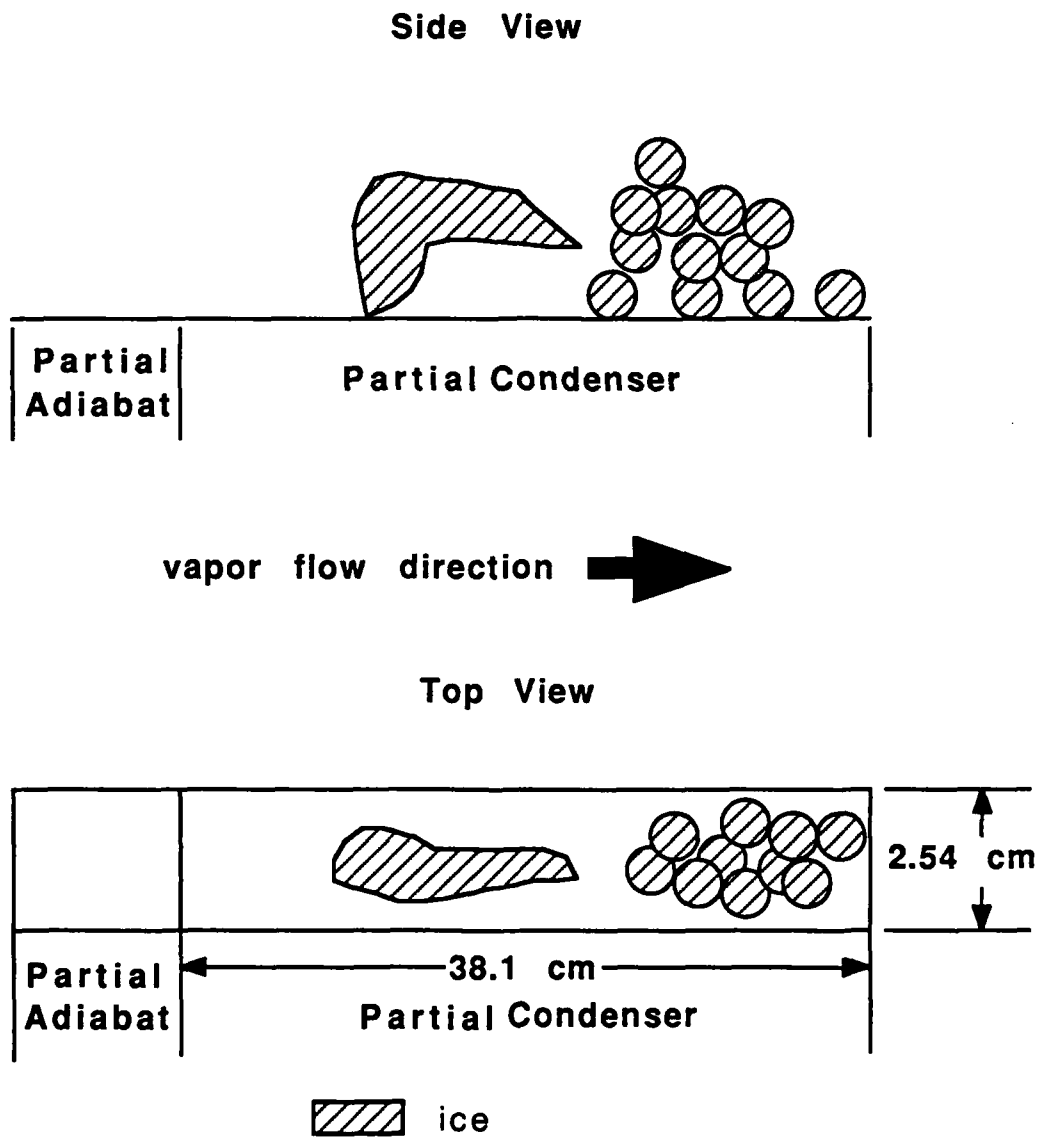


Figure 63. Diagram of Ice Formations

on. The temperature profile of thermocouple 6 indicates that the effect of this pumping on the evaporator was negligible. The vacuum pump was turned on again at 2430 s, but seemed to have little effect on either thermocouple shown in Figure 59. Thus the power was turned off at 2580 s. The internal measurements give a general idea of what is happening inside the pipe. The outer wall thermocouple measurements give further knowledge of what occurred during the phenomena listed above.

At zero time, all three outer wall thermocouples read temperatures similar to that of thermocouple 7 but were about 4°C lower than the wick temperature indicated by thermocouple 6, although all three are closer to thermocouple 6 than 7. This was because of the much higher thermal conductivity of aluminum than that of water. At this point, heat rejection to the coolant was the only significant influence on the pipe temperatures. After 200 s, the influence on temperature from the heater and the soon-to-melt ice became larger than that of the coolant and the evaporator outer wall thermocouples began approaching the temperature of thermocouple 6, reaching it at about 500 s.

The evaporator outer wall was essentially isothermal from time zero to 700 s. The melting of the ice was indicated by a constant temperature near 0.0°C in the outer wall from 500 s to just before 700 s. After 700 s, thermocouples 1 and 2 continued to track with thermocouple 6 until 1500 s, while thermocouple 3 hovered around 0.0°C until 850 s, suggesting that the evaporator working fluid was not fully melted until that time. Still, the shape of the temperature plot of thermocouple 3 remains essentially the same as that for thermocouples 1 and 2 from 700 to 950 s, actual values for thermocouple 3 reading about 1.5°C below those of 1 and 2. From 950 to 1150 s, the temperature indicated by thermocouple 3 followed the path of thermocouple 7, slowly catching up to the temperature of thermocouples 2 and 3 at 1175 s, for reasons similar to those given for the matchup between thermocouples 6 and 7. Figure 62 more clearly demonstrates this.

At 1200 s, thermocouple temperatures for 1 and 2 rose with those of thermocouple 6, suggesting that at least the half of the evaporator furthest from the condenser dried out instantaneously, but thermocouple 3 continued with a temperature rise so slow as to suggest that at least part of the other half of the evaporator was still operating. Shortly after 1800 s, however, the temperature of

thermocouple 3 made a sharp increase which implies that the evaporator was fully dried out at this point.

The temperature of thermocouple 1 rose slightly above that for thermocouple 2 after 1600 s, but the two temperature profiles show similar paths and are separated by a nearly constant temperature gap of 3°C.

The temperature profile of thermocouple 4 follows closely the shape of that for thermocouple 7, as expected. The temperature drop from thermocouple 7 to 4 ranged from 3 to 5°C.

The K thermocouples on the cover plate in the condenser conveyed no additional information except to show that the buildup of noncondensable gases during the transient was not significant. Therefore none of the K thermocouple data are shown here. The same is the case for the plot of power removed by the secondary coolant jacket.

#### 4.3.4 Transient 4 : Frozen Start-up Number 2

In the fourth experiment the heat pipe again had a positive tilt of 0.6° from the horizontal and the amount of working fluid added to the heat pipe was 100 ml, as in the previous experiment.

The experimental procedures leading up to the frozen start-up were as follows: the working fluid was added and then the wick was allowed to wet. The secondary coolant temperature was then lowered to 5°C over 15 min. This rapid lowering of the coolant temperature did not allow the pipe to decrease in temperature as isothermally as desired, and a large temperature difference between the evaporator and condenser occurred. This caused significant vapor flow from the evaporator to the condenser, where the vapor froze. Consequently, the evaporator dried out. The coolant temperature was raised so the ice could melt and rewet the wick in the evaporator. The working fluid of the heat pipe was then frozen over a period of 70 min, and frozen working fluid in all sections of the heat pipe was verified. 100 W was then added to the evaporator, and an unrecoverable dry out in the evaporator wick was instrumentally and visually verified. When the outer aluminum wall temperatures in the pipe reached 50°C, the power was turned off. The data presented for this run represent the time from 71 s before the power was turned on to 2200 s, the time when the power was

removed. Even though no data are presented from 2200 to 2800 s, the time scale on the plots will go from 0 to 2800 s so a comparison can be made with the plots of data for the other frozen start-up.

The placement of T thermocouples, the pressure transducer, the heat pipe vacuum attachment and the working fluid addition point are shown in Figure 64. The placement of the type K thermocouples is shown in Figure 65. Note that these K thermocouples are placed only on the outer surface of the cover plate in the condenser and adiabat.

Figure 66 displays the data for thermocouples 6, 7, 8, and 9 for this experiment. Figure 67 displays the data for thermocouples 1, 2, 3, and 4. Thermocouples 1, 2, 3, and 4 are in the shoulder of the aluminum wall and are in the same location as in the previous frozen start-up. Thermocouple 6 is in the wick/liquid region of the evaporator, 0.2921 m from the end of the evaporator away from the adiabat. Thermocouples 7, 8, and 9 all give vapor space temperatures. Thermocouple 7 is in the evaporator and is 0.4572 m from the far end of the evaporator from the adiabat. Thermocouple 8 is in the adiabat and is placed 0.0635 m from the condenser. Thermocouple 9 appears in the middle of the condenser.

Figure 66 shows that the wick/liquid temperature of the evaporator, represented by thermocouple 6, starts out the transient at the freezing point of water, and stays relatively constant until 300 s, when it starts slowly increasing in temperature. At 800 s, the temperature takes a short dip from 4 to 1°C and then back up to 4°C over a period of about 80 s. The temperature then starts a more rapid increase at the end of that 80-s period. The vapor space temperature represented by thermocouple 7 stays at a constant temperature of -5°C until 800 s, when it makes a small jump to -4°C. It stays there for approximately 120 s before making an increase to 4.5°C, which it reaches at 1200 s. The temperature remains there for about 80 s before making a rapid jump to 24°C over the next 200 s, until it reaches the temperature of thermocouple 6 at 1550 s. After that point, the temperatures of thermocouples 6 and 7 follow a similar path.

Thermocouples 8 and 9 follow similar paths throughout the transient, with the temperature of 8 staying approximately 5°C higher than that of 9. Both stay at an approximately constant temperature until 1200 s, when both experience a slight drop in temperature. Since thermocouple 8 is between thermocouples 7 and 9,

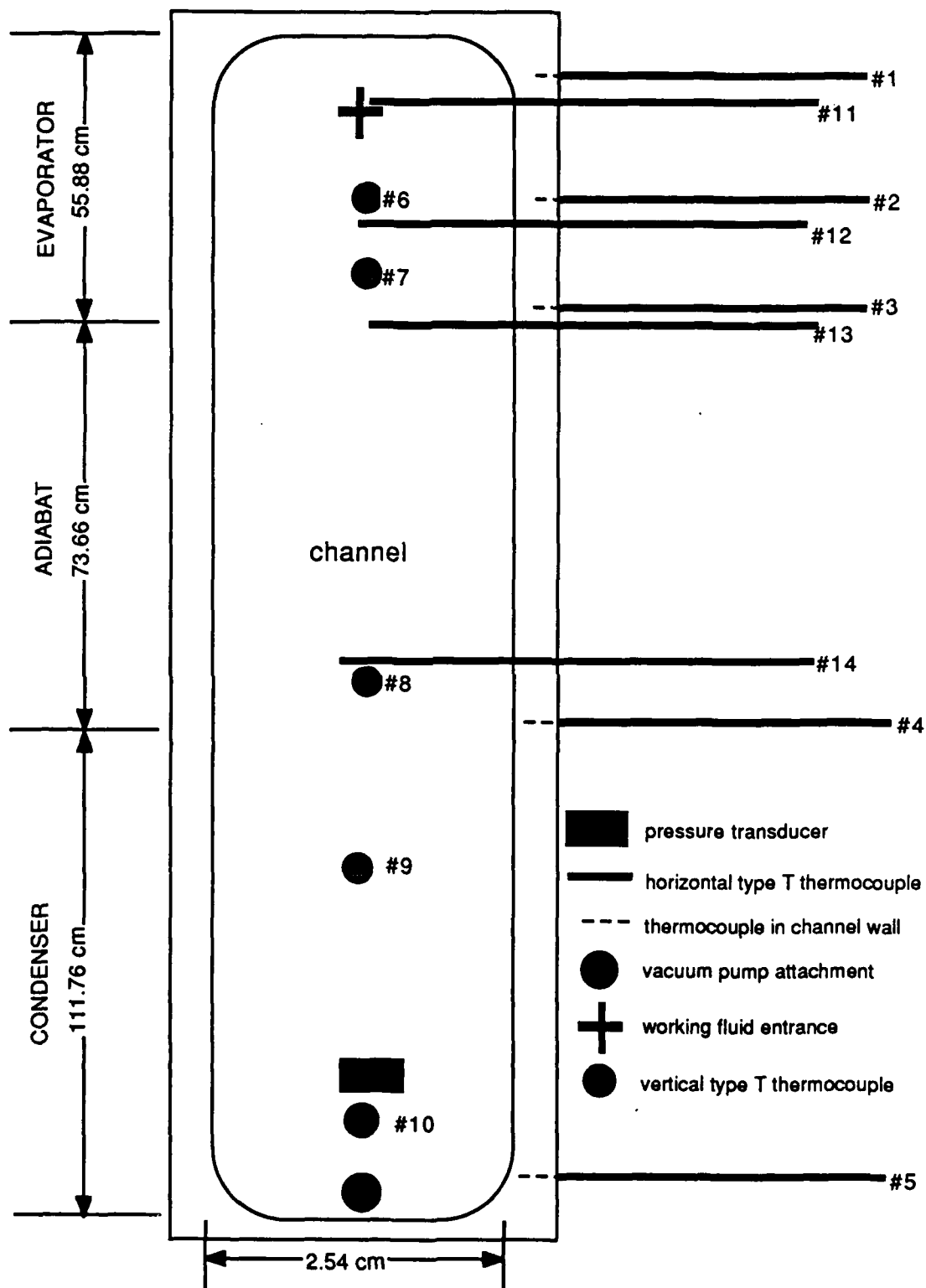


Figure 64. Location of Instrumentation (except K thermocouples) for Frozen 2

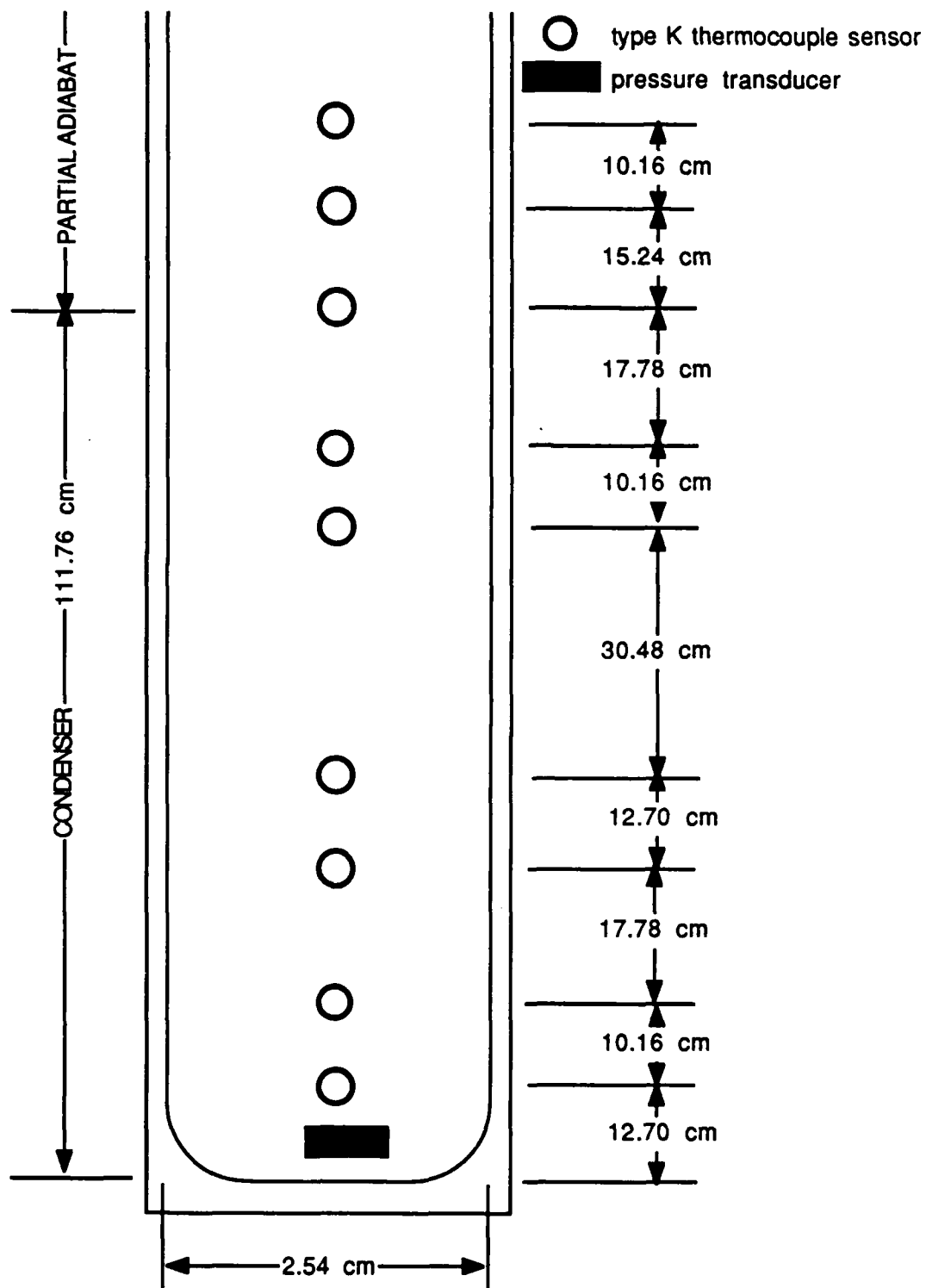


Figure 65. Location of K Thermocouples for Frozen 2

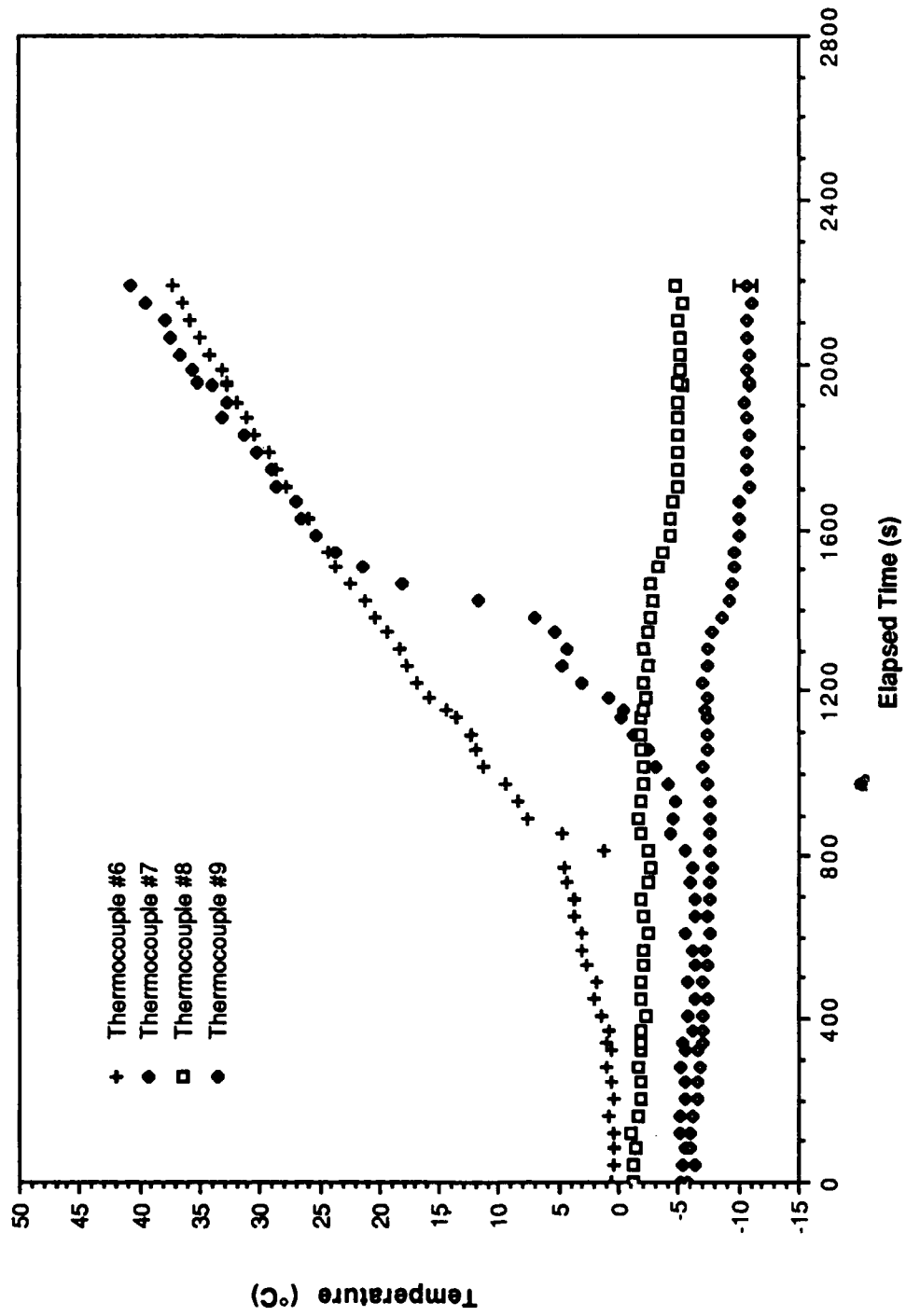


Figure 66. Wick/Liquid and Vapor Space Thermocouples for Frozen Start-up 2

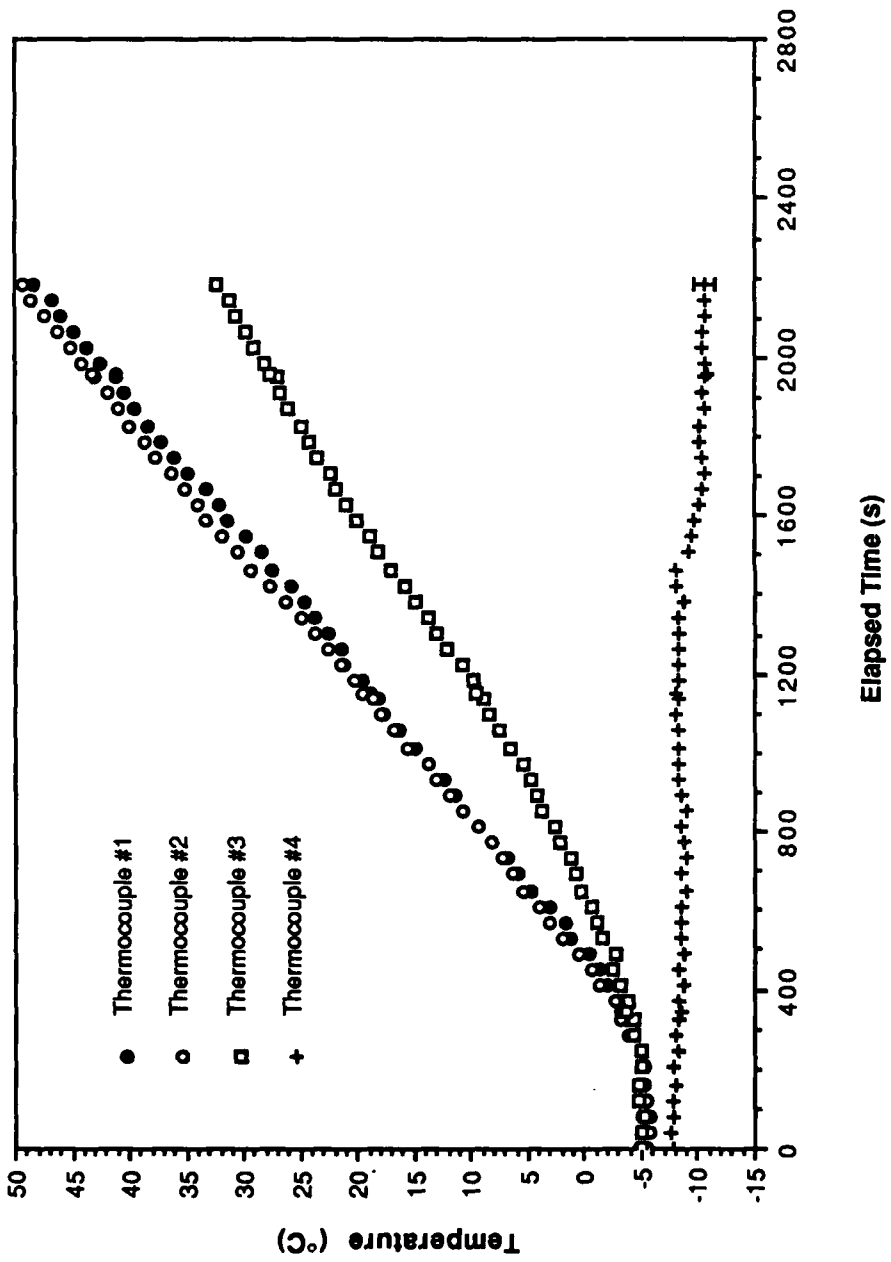


Figure 67. Outer Wall Measurements For Frozen Start-up 2

the corresponding temperature of 8 would be expected to lie below those of 7 and above those of 9, 7 being above the heater and 9 above the secondary coolant. However, the temperatures of thermocouple 8 are above those of thermocouple 7 until shortly after 1000 s. Since the path of the data of thermocouple 8 is similar to that of 9, it appears that there is some thermocouple error associated with 8, and that its actual temperatures are close to those of 9. This error is most likely due to conduction from the part of the thermocouple sheath that is not in the heat pipe channel but is in a room exposed to ambient conditions. The sheath of both thermocouples was placed in the heat pipe channel to reduce this error, as shown in Figure 38, but thermocouple 8 had 0.02 m less of its sheath in the channel than 9. While the thermocouple arrangement of 8 gives valid readings for most of the experiments presented in this section, where some vapor velocity is present, it seems that enough of the thermocouple sheath was not in the channel for the slow vapor velocities of this experiment.

In Figure 67 the outer aluminum wall temperature data can be seen. The thermocouples in the evaporator all read  $-5^{\circ}\text{C}$  until 300 s when all three start indicating increasing temperatures until they reach  $0.0^{\circ}\text{C}$ , where they stay constant for 40 s. The temperatures then start rising again, with those of thermocouples 1 and 2 rising at the same rate, slightly faster than those of 3. The condenser/adiabat interface outer aluminum wall temperature, represented by thermocouple 4, stays at an approximately constant temperature from 0 to 1450 s, when it undergoes a temperature drop of  $5^{\circ}\text{C}$  before holding at the new temperature,  $-10^{\circ}\text{C}$ , through the rest of the transient.

It appears that this transient goes through the same general steps of a frozen heat pipe transient as the first frozen start-up. Those processes are as follows: the melting of the ice in the evaporator; the slow increase in temperature of the evaporator as the liquid working fluid is turned to vapor; the eventual dry out of the evaporator as the vapor flow rate out of the evaporator is greater than the flow rate of returning liquid; and finally the superheating of the remaining vapor in the evaporator as the vapor no longer flows out of the evaporator and no new vapor generation is occurring in the evaporator. This last step is evidenced by a rapidly increasing temperature in the evaporator and a slower but still noticeable decrease of temperature in the rest of the pipe after the evaporator is completely void of liquid. There are some differences between the two frozen start-ups within

these steps, however.

In the second start-up, the evaporator was observed to be fully melted by 400 s, whereas the first frozen run did not reach that point until 700 s. Thermocouple 6 indicates further that the second transient experienced dry out at the location of the thermocouple at 800 s, and the first transient did not dry out at that location until 1200 s. The small dip in the temperature of thermocouple 6 of the second frozen start-up indicates that there was some cold liquid being returned to this evaporator, but not at a rate fast enough to offset the vaporization and prevent dry out. Thermocouple 7, which is near the evaporator/adiabat interface for the second frozen start-up, indicates that the evaporator was completely dried out at 1400 s, while that did not happen in the first transient until 2000 s. Slight dips in the temperatures of thermocouples 8 and 9 around the 1400-s mark support the proposal that the evaporator completely dried out at this point. It is also evident that during the second frozen start-up the adiabat never melted, whereas it did temporarily during the first start-up.

When considering the differences between the two frozen start-ups, it is important to analyze the amount of frozen working fluid in the evaporator wick section when the 100 W is added. The 100 ml of working fluid in the pipe is larger than the void area available in the wick, so the extra working fluid resides elsewhere in the pipe. During a normal, nonfrozen start-up, it would be held in the condenser. During the first frozen start-up most of the frozen working fluid was initially in the evaporator since this was where the working fluid initially entered the pipe. In the second frozen start-up, most of the extra working fluid rested was in the condenser, so while the wick in the evaporator was wetted, it contained no extra working fluid. This is most probably due to the pipe excursions that occurred before the frozen start-up was begun.

This is important when considering the time it takes the evaporator wick to dry out. The larger the mass of working fluid initially, the longer it takes for the pipe to vaporize the liquid working fluid, and the longer it will take for the evaporator to dry out. Also, with more mass, more vapor flows down the pipe due to the pressure drop until full dry out occurs. With more vapor coming down over the adiabat and condenser, it is possible that some of this vapor could actually melt the ice in the adiabat until dry out in the evaporator occurs. With a small amount of vapor flowing over the adiabat, it is possible that the vapor could be turned into

ice without ever melting any part of the adiabat. These different possible transients can be seen in the two frozen start-ups.

Thermocouple 4 in the outer aluminum wall at the condenser/adiabat interface in the second frozen start-up seems to react to this transient within the framework of the above explanation for the start-up. It stays at a relatively constant temperature of  $-7.5^{\circ}\text{C}$ , below the freezing point of water, until just after 1400 s, the time for full evaporator dry out, when the temperature makes a small dip to  $-10^{\circ}\text{C}$ . Thermocouples 1, 2, and 3 in the second transient seem to follow peculiar temperature excursions. It would be expected that thermocouple 2 would follow closely the path of thermocouple 6 and that 3 would closely follow the path of 7. It should be remembered, however, that outer wall thermocouples in the evaporator are being affected by conduction from the heat source below and conduction along the length of the pipe. When there is no large mass of working fluid above in the pipe near the section of the outer wall where the thermocouple is, it is possible that, even though that small mass may temporarily be at a colder temperature, the majority of the temperature effect on the outer wall is from the lengthwise path of conduction. In other words, thermocouples 2 and 3 could be more affected by what is happening at thermocouple 1 than what is happening at 6 or 7. This seems to have been the case.

Again, the K thermocouples on the cover plate in the condenser conveyed no additional information except to show that the buildup of noncondensable gases during the transient was not significant. Therefore none of the K thermocouple data are shown here. The same is the case for the plot of power removed by the secondary coolant jacket and for the plot of condenser vapor space pressure. The pressure tracked with the vapor space temperature of thermocouple 9 in the evaporator vapor space.

#### 4.3.5 Transient 5 : 25 W with Decreasing Secondary Coolant Temperature

In this run the heat pipe had a positive tilt of  $0.75^{\circ}$  from the horizontal. The amount of working fluid added to the pipe was 100 ml. As in the previous experiment, visual verification of a completely wetted wick was made prior to adding power to the pipe. The placement of type T thermocouples, the pressure transducer, the heat pipe vacuum attachment and the working fluid addition point

is shown in Figure 47. The placement of the type K thermocouples is shown in Figure 48. Note that this is the same instrumentation arrangement as for transient 2.

In this experiment, the heat pipe was subjected to a step power input from 0 to 25 W. The coolant temperature at the time power was added was  $5^{\circ}\text{C} \pm 0.5^{\circ}\text{C}$ . After steady-state conditions were reached, the secondary coolant temperature was reduced to  $0.0^{\circ}\text{C} \pm 0.5^{\circ}\text{C}$  and the pipe temperatures were allowed to come to equilibrium. The process was repeated at secondary coolant temperatures of  $-5.0$ ,  $-10.0$ ,  $-15.0$ , and  $-20.0^{\circ}\text{C}$ , with the pipe allowed to reach thermal equilibrium before the secondary coolant temperature was lowered again. The data presented show the transient from the time thermal equilibrium was reached with a secondary coolant temperature of  $0.0^{\circ}\text{C}$  to the time when it was apparent that thermal equilibrium would not be reached with a secondary coolant temperature of  $-20.0^{\circ}\text{C}$ . Figures 68 and 69 show the data for the secondary coolant temperature drops from  $0.0^{\circ}\text{C}$  to  $-5.0^{\circ}\text{C}$  and from  $-5.0^{\circ}\text{C}$  to  $-10.0^{\circ}\text{C}$ . Figures 70 and 71 show the data for the drops from  $-10.0^{\circ}\text{C}$  to  $-15.0^{\circ}\text{C}$  and from  $-15.0^{\circ}\text{C}$  to  $-20.0^{\circ}\text{C}$  and the results of the final drop. The data for vapor space thermocouples 7 and 9 are shown in Figures 68 and 70 and the data for thermocouples 1, 2, 3, and 4 are shown in Figures 69 and 71. The placement of these thermocouples is described in the description of transient 2.

At time zero seconds, the pipe was at thermal equilibrium with a power input of 25 W and a secondary coolant temperature of  $0.0^{\circ}\text{C}$ . At 390 s, the coolant temperature was reduced slowly until it reached  $-5.0^{\circ}\text{C}$  at 690 s. At 2180 s, the temperature was reduced again until it was  $-10^{\circ}\text{C}$  at 2480 s. Figures 68 and 69 show the data from 0 to 4300 s. At 4300 s the secondary coolant temperature was reduced until it reached  $-15.0^{\circ}\text{C}$  at 4600 s. At 6400 s this temperature was reduced until it reached  $-20.0^{\circ}\text{C}$  at 6700 s. The vacuum pump was turned on at 7280 for 60 s to remove some noncondensable gases that had built up in the far end of the condenser from the adiabat. The power input to the evaporator was stopped at 9500 s since an unrecoverable dry out in the evaporator occurred and ice had formed in the condenser. Figures 70 and 71 show the data from 4300 to 9500 s.

No unexpected temperature excursions are shown in Figures 68 and 69. After the drops in secondary coolant temperatures from  $0.0$  to  $-5.0^{\circ}\text{C}$  and from

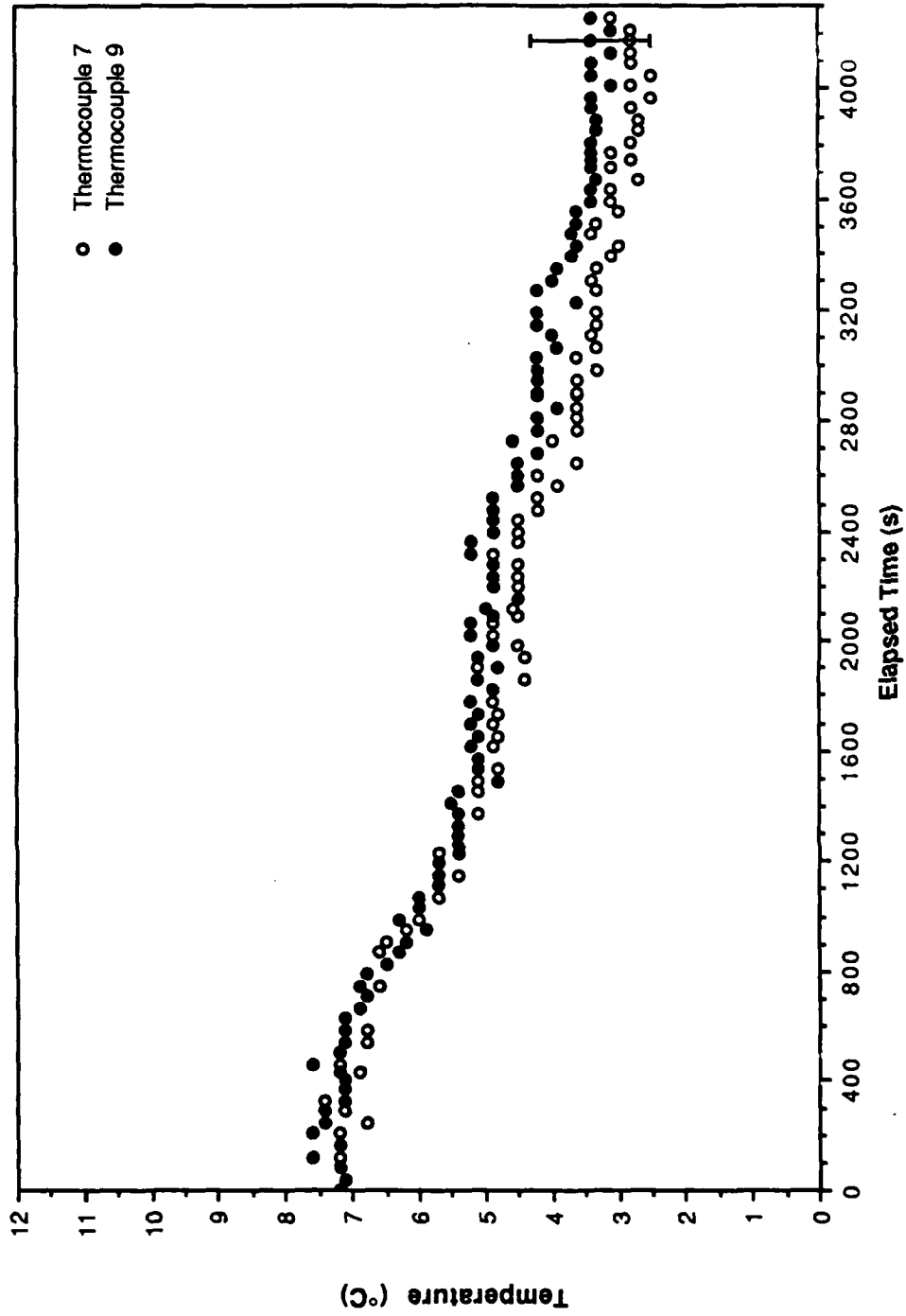


Figure 68. Vapor Space Temperatures for 25 W with Decreasing Secondary Coolant Temperature

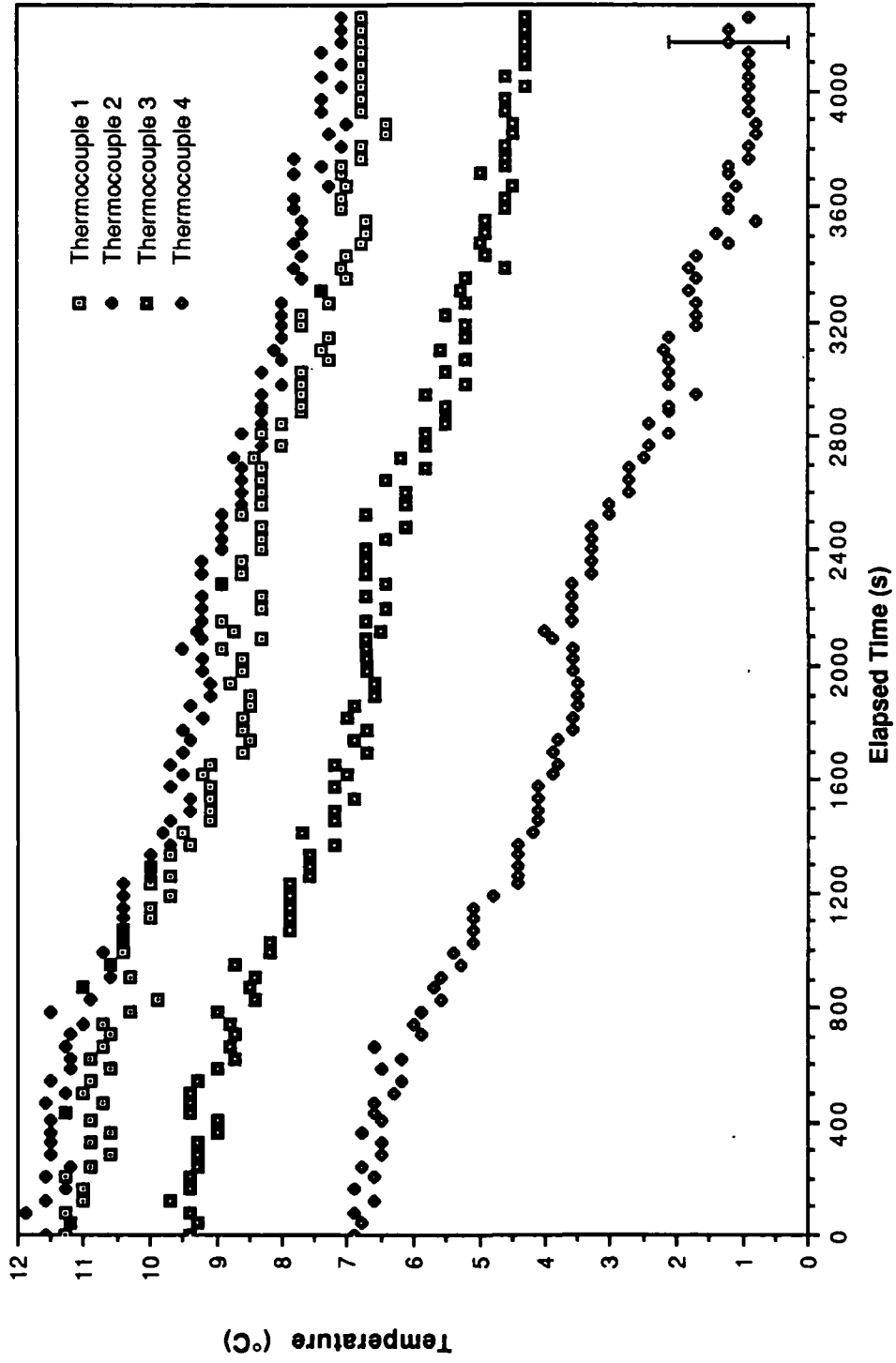


Figure 69. Outer Aluminum Wall Temperatures for 25 W with Decreasing Secondary Coolant Temperature

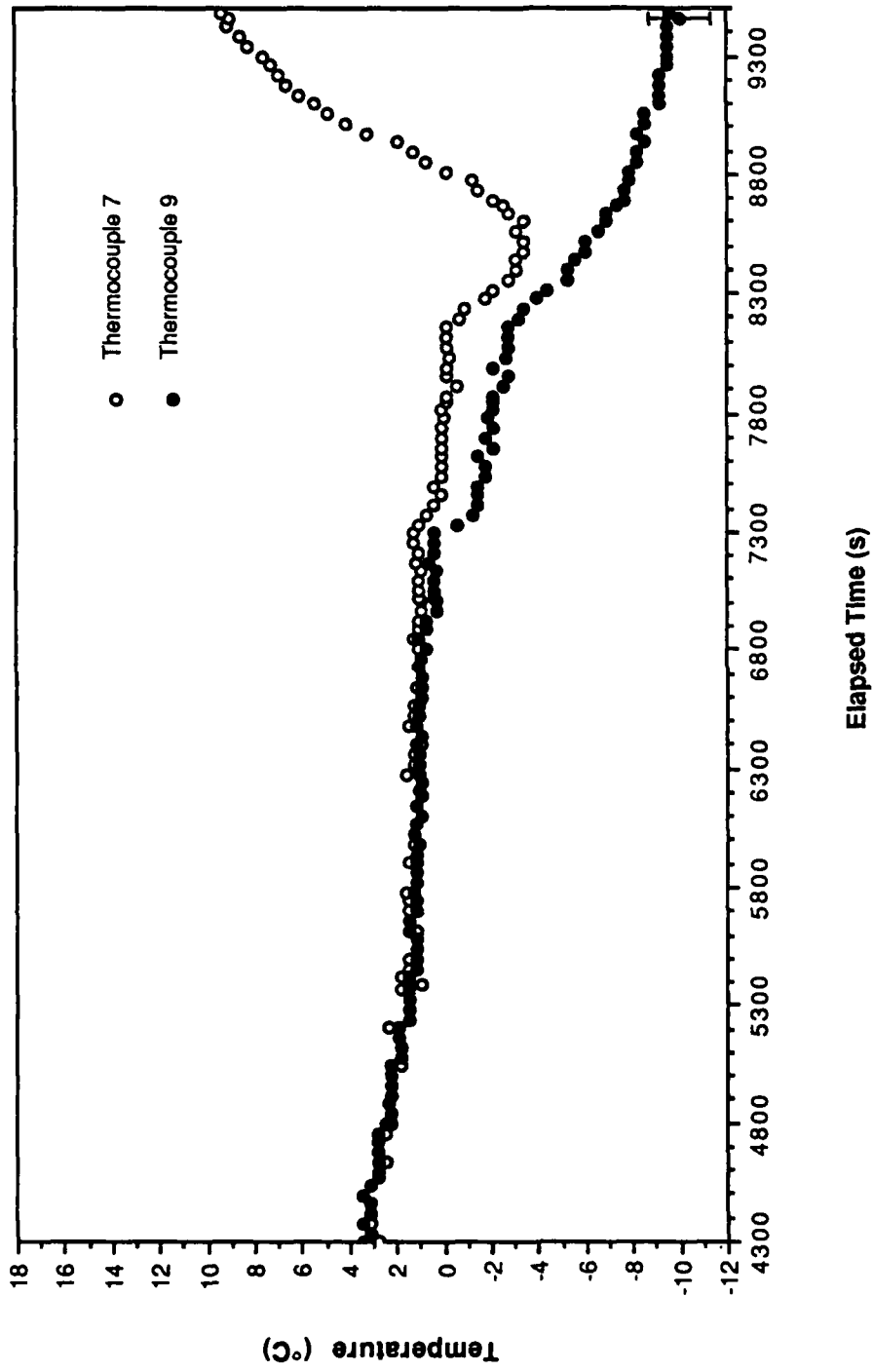


Figure 70. Vapor Space Temperatures for 25 W with Decreasing Secondary Coolant Temperature

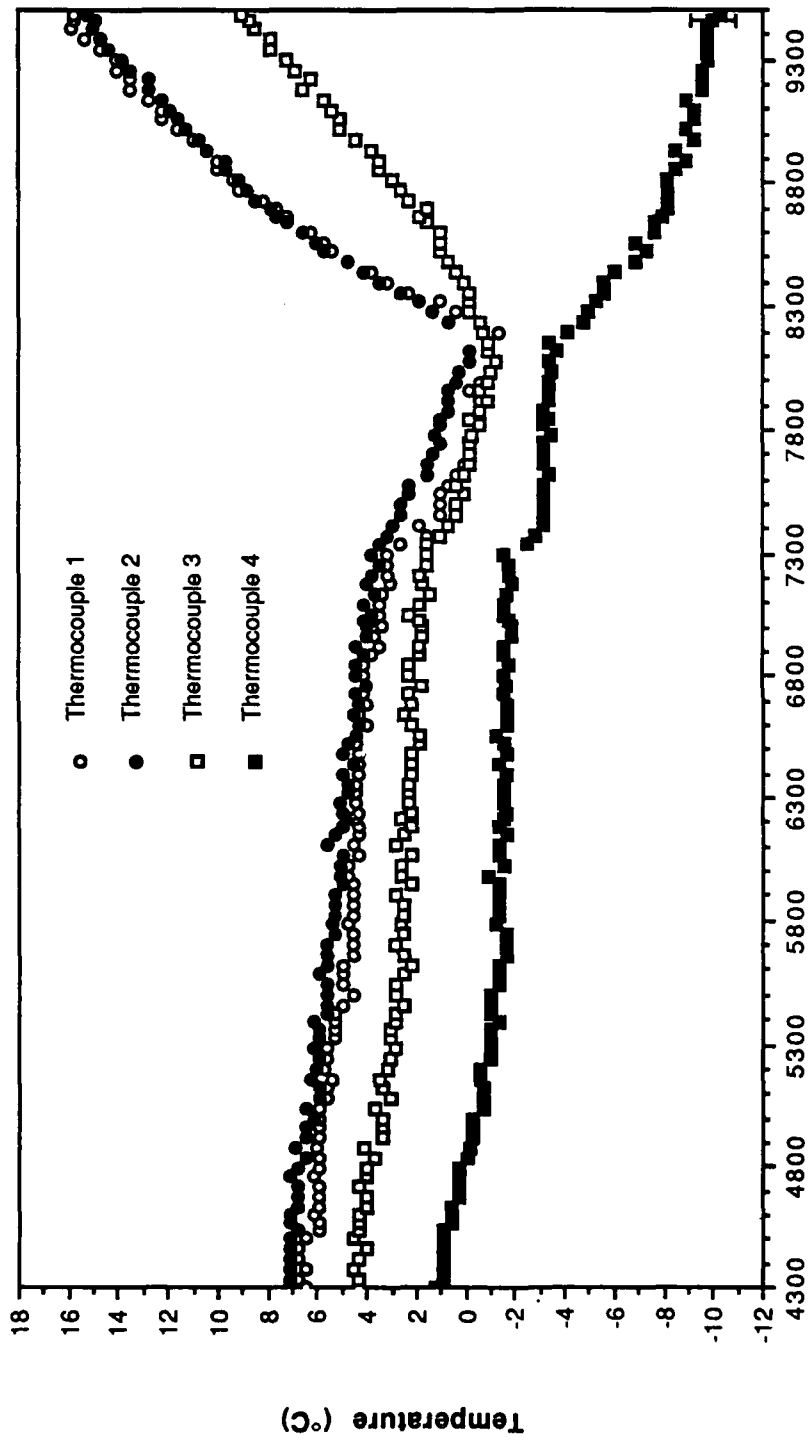


Figure 71. Outer Aluminum Wall Temperatures for 25 W  
with Decreasing Secondary Coolant Temperature

-5.0 to -10.0°C, the pipe comes to thermal equilibrium at 1500 s in the first case and at 3600 s in the second case. Nothing particularly unusual happens during the secondary coolant temperature drop from -10.0° to -15.0°C shown in Figures 70 and 71. The pipe reaches thermal equilibrium shortly after 5400 s for this drop. When the secondary coolant temperature drops from -15.0°C to -20.0°C after 6400 s, some different things occur.

First, there is no perceptible change in any of the temperatures displayed in the figures until 6800 s, when the temperature of thermocouple 9 makes a small drop from 1.0 to about 0.5°C. Then at 7300 s the rest of the thermocouples show perceptible drops in temperature and thermocouple 9 shows a more dramatic drop. Thermocouples 1, 2, and 3 continue to decrease in temperature until 8200 s, when they start increasing. The temperature of thermocouple 4 decreases slowly from 7300 to 8200 s and starts to drop off more dramatically at 8200 s. The temperature of thermocouple 7 decreases slowly from 7300 to 8200 s, drops off more dramatically at 8200 s, and begins a dramatic climb in temperature at 8500 s.

Between 6900 and 7300 s the temperature of thermocouple 9 stays at a constant just above 0.0°C. This suggests that freezing was occurring slowly in the condenser during this time period. This was also visually confirmed. Since the internal temperatures of the pipe were at or near the freezing point of water at this time it seems reasonable that these temperatures would remain essentially constant. Any further temperature decrease at any given position would indicate a complete lack of liquid in the wick at that position since the temperature would be below the value for which liquid could exist. This is what occurred near thermocouple 9 at 7300 s. At 7300 s the vacuum pump was also turned on to remove the noncondensable gases that had collected in the far end of the condenser from the adiabat. With the freezing beginning in the condenser and the vacuum pump on for 60 s, it seems that enough vapor was removed from the evaporator to allow for the inception of dry out in the evaporator at this point. This was not visually confirmed, but the drop in the temperature of the thermocouples at this time appears to be a result of this. The use of the vacuum pump at this point may have caused the inception of boiling to occur earlier than it may have done otherwise.

At 8200 s this freezing in the condenser caused more of the evaporator wick

to dry out, as seen by the increase in temperatures of thermocouples 1, 2, and 3. Also at 8000 s there is a drop in temperature for thermocouples 7, 9, and 4 that would be expected to be associated with the dry out in the evaporator. When the temperature of thermocouple 7, which is at the evaporator/adiabat interface, stops decreasing and starts increasing at 8500 s, it is clear that the entire evaporator is dried out. This dry out also keeps vapor from flowing to the adiabat and condenser, thus encouraging the freezing in those areas, especially in the condenser. This freezing in turn allows even less liquid to return to the evaporator, and the result is a fully dried out evaporator and a fully frozen condenser, with the adiabat being partially frozen near the condenser, partially dried out near the evaporator and containing all three phases of water somewhere in the middle.

#### 4.3.6 Transient 6 : Step Decrease in Power Input

This part analyzes what occurs when a a step decrease in the power input to the evaporator occurs. These data were taken from the time the power was removed from the experiment described in transient 2 and is shown in Figures 72, 73 and 74. The instrumentation for this set of data is the same as it was for the earlier experiment. The power input had been at 250 W in transient 2 before partial dry out had occurred in the evaporator wick. The time when this power was reduced to 0.0 W is represented by zero seconds in the data presented here. Liquid/wick thermocouple 6 and vapor space thermocouples 7 and 8 are represented in Figure 72. Outer aluminum wall thermocouples 1, 2, 3, and 4 are represented in Figure 73, and the power removed from the condenser of the heat pipe by the secondary coolant is shown in Figure 74. The coolant temperature during this transient was  $5^{\circ}\text{C} \pm 1.0^{\circ}\text{C}$ .

Figure 72 shows how the internal temperatures stayed close together while decreasing until they leveled between 12 and 13°C at 2900 s. The rewetting of the portion of the wick that had dried out in transient 2 can be seen in the rapid decrease in the temperature of thermocouple 1 in Figure 73. The wick appears to have been totally rewet at 1000 s when the temperature of thermocouple 1 joins those of 2 and 3. All temperatures represented in this figure level out between 12 and 14°C after 2800 s. The power removed through the

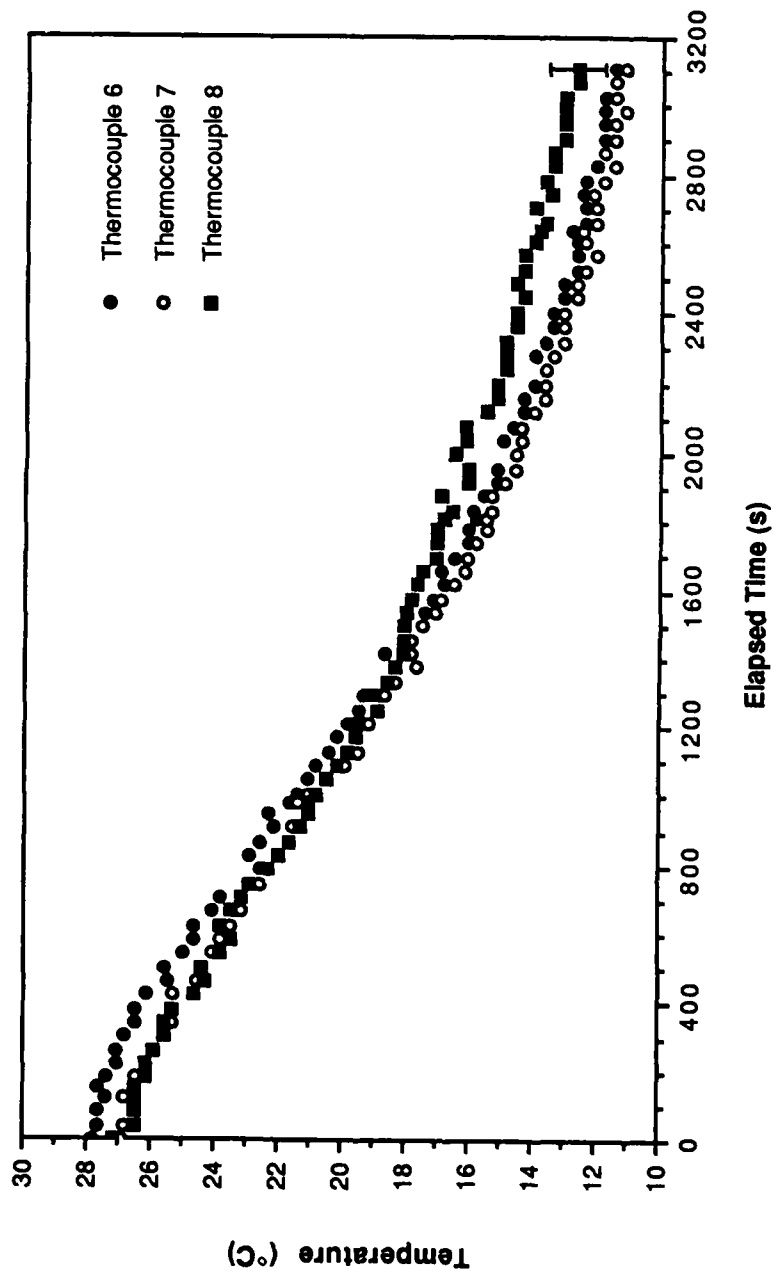


Figure 72. Vapor Space and Liquid Space For Downpower from 250 W

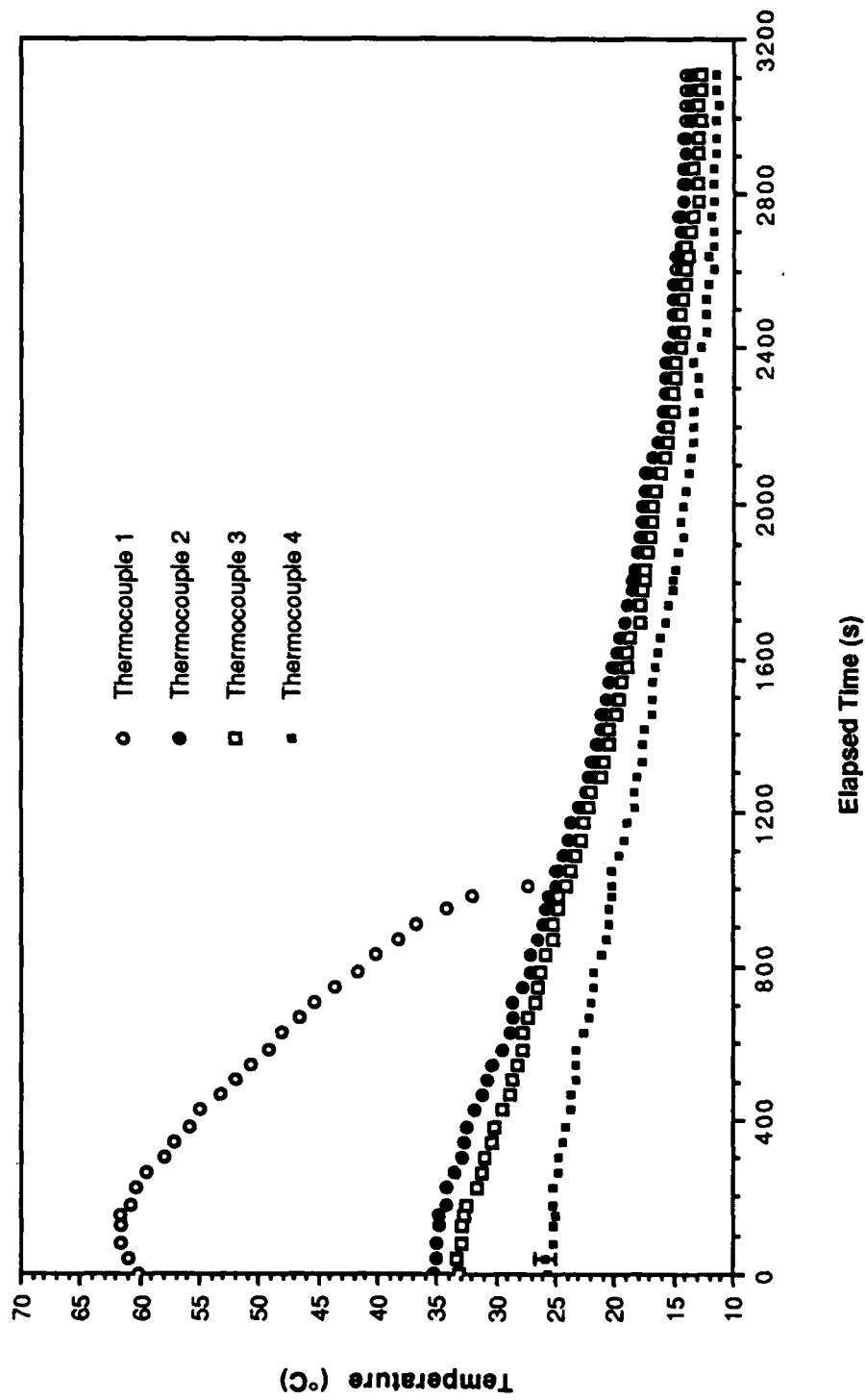


Figure 73. Outer Wall Temperatures For Downpower from 250 W

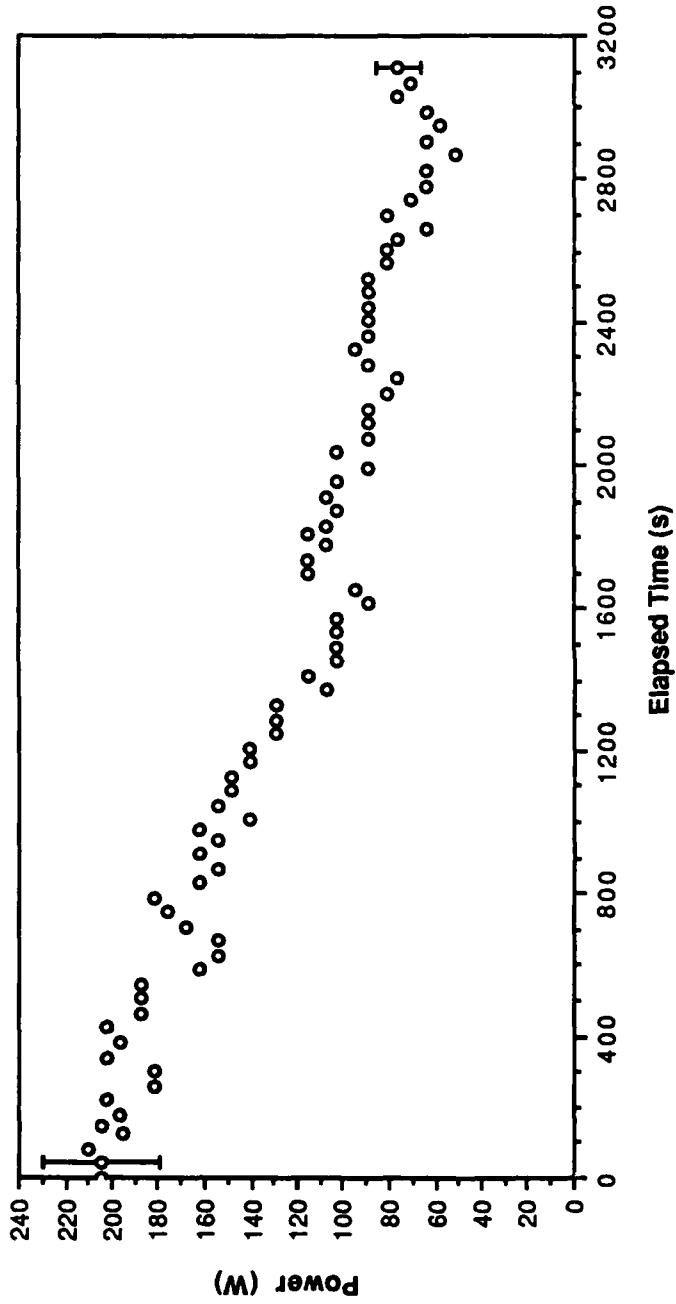


Figure 74. Power Removed By Secondary Coolant For Downpower from 250 W

condenser, shown in Figure 74, is just above 200 W at zero seconds and gradually decreases to a level near 60 W at 3200 s. This final value would be expected to be 0.0 W, but the higher value could be due to ambient gains since the internal pipe temperatures are well below room temperature, 24°C. Another possible explanation is that the pipe was still cooling down at this time, although at a very slow rate.

#### 4.4 Summary

The design for the heat pipe experiments presented in this section was very similar to that used for the experiments of the previous chapter, but there were some important improvements made. These improvements and the rest of the experimental apparatus design for the experiments in this section were discussed first. The experiments of Section 3 were essentially scoping runs for the experiments of this section, so the experimental design went into more detail in this section, for both those elements of the design that have changed and those that have not. Next, in Experimental Procedures, the methods of preparing the experimental apparatus for a heat pipe run were discussed. Finally, in Results and Discussion the data from six different runs were presented. The first analyzed a 0.0-100 W start-up and confirmed that the experiment was operating as a heat pipe. The second run was a 0.0-50-100-200-250 W transient. The next two runs were frozen start-ups. The fifth run was for a heat pipe that was operating at 25 W when the coolant temperature was reduced until the condenser of the pipe reached freezing conditions. Finally, the sixth run analyzed a 250.0 to 0.0 W shutdown of the heat pipe. For all of these runs, simultaneous measurements of vapor pressure, wick/liquid and vapor space temperatures, outer wall temperatures, and temperature drop across the secondary coolant jacket were incorporated with visual observations through the clear top to increase the knowledge of what was happening during these various transients. In the next section, attempts at modeling heat pipe transients with a computer code will be discussed.

## 5.0 MODELING WORK

Subsection 5.1 will describe the numerical model of a wicked heat pipe and the assumptions made in its development. A description of the physical heat pipe is also included. A complete derivation of the finite difference equations required for the numerical model will be described along with a discussion of the evaporation/condensation model used. In addition, the numerical solution technique will be presented.

In Subsection 5.2 the numerical model described in Subsection 5.1 will be applied to experimental data from the heat pipe in Section 3. Subsection 5.2 begins by comparing the experimental data with the numerical model results for different fluid charges. The fluid charge is defined as the amount of liquid in the wick prior to start-up. Since the charge cannot be directly measured in the operating pipe, sensitivity studies must be carried out to determine its value. Once the proper fluid charge is determined, the velocity and pressure profiles for both the liquid and vapor are compared. Finally, the transient temperature profiles for the outer wall, liquid and vapor regions are given.

The cases presented are:

1. A thermal power input of 250 W and a coolant water temperature of 293 K
2. A thermal power input of 100 W and a coolant water temperature of 293 K.

### 5.1 Heat Pipe Model Development

The heat pipe modeled in this study is the screen wick heat pipe described in Section 3. The design and dimensions of the heat pipe are shown in Figure 2. Unique to this heat pipe is its rectangular cross section and glass top. The glass top allows visual observations during heat pipe operation, and is well insulated when data are being taken. The working fluid is water. The walls and wick of the heat pipe are made of aluminum and stainless steel, respectively. The heat pipe is electrically heated and cooled convectively with a water jacket. The electric

heater has an output of 0 to 1500 W, while the cooling jacket can operate at temperatures from below freezing (260 K) to slightly below boiling (373 K). Operating temperatures are low enough and transient runs are short enough that the amount of noncondensable gases generated within the pipe is negligible.

### 5.1.1 Computational Model

A multinodal implicit finite difference model was developed to study the performance of wicked heat pipes experiencing rapid transients. In order to obtain velocity and pressure profiles, the mass and momentum conservation equations were approximated using a finite difference scheme with a 1-D nodal representation. A 2-D nodal scheme was used with a finite difference approximation of the energy conservation equation to generate temperature profiles for the heat pipe. Figure 75 illustrates the nodal scheme utilized to model the heat pipe displayed in Figure 2.

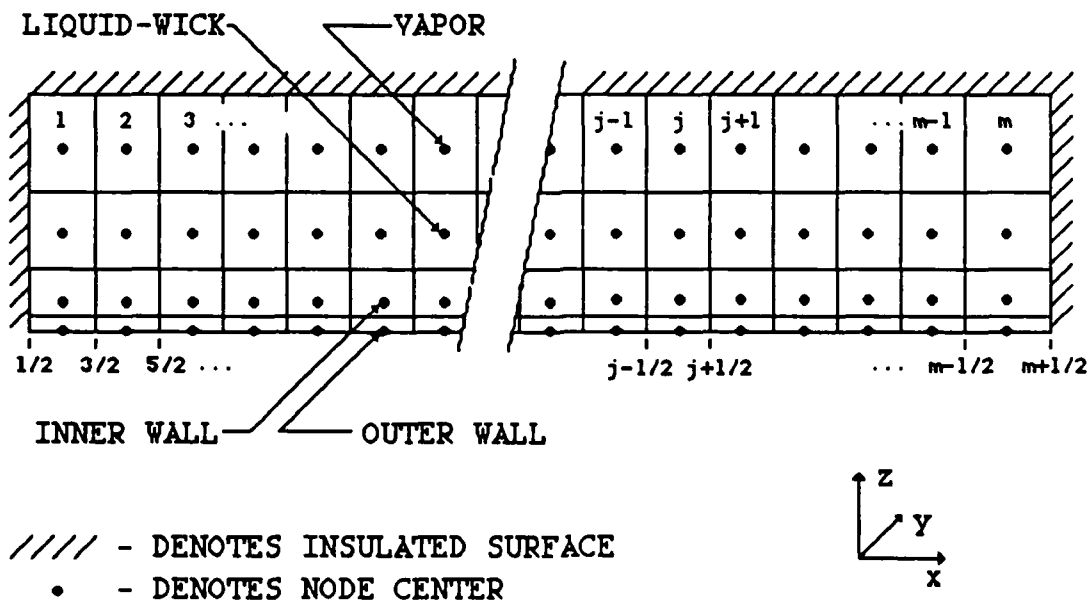


Figure 75. Nodal Scheme for the Heat Pipe Numerical Model

Several assumptions were made in the development of the overall heat pipe model. These are listed below:

- An electrical heater is the source of energy addition in the evaporator.
- A water cooling jacket is the method of energy removal in the condenser.
- Other than in the evaporator and the condenser the heat pipe is perfectly insulated.
- The heat pipe is in equilibrium with ambient conditions prior to start-up.
- The vapor and liquid are incompressible but thermally expandable fluids.
- Working fluid thermodynamic properties are computed explicitly as a function of temperature.
- The vapor phase is assumed to be at saturation conditions.

### 5.1.2 Development of the Mass Conservation Equation

The conservation of mass equation is used to solve for the velocities in the vapor and liquid regions. The conservation of mass equation is given in integral form as<sup>39</sup>

$$\frac{\partial}{\partial t} \int_V \rho \, dV = - \int_A \rho (\vec{v} \cdot \vec{n}) \, dA \quad (12)$$

where

- $\rho$  = density of the fluid
- $V$  = control volume
- $v$  = velocity vector
- $n$  = unit vector normal to the surface
- $A$  = surface area of the control volume
- $t$  = time.

### 5.1.2.1 Vapor Region

The vapor velocities can be determined by applying Equation 12 to the control volume shown in Figure 76. The evaporation and condensation mass flow rate is defined as  $S$ . In order to simplify Equation 12, the integrals are approximated with the following expressions:

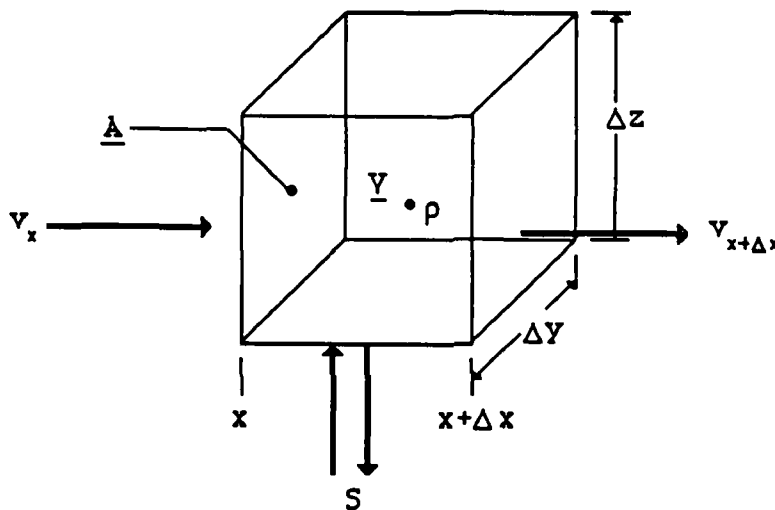


Figure 76. Vapor Control Volume for the Mass Conservation Equation

$$\int_V \rho \, dV = V \langle \rho \rangle \quad (13)$$

$$\int_A \rho (\vec{v} \cdot \vec{n}) \, dA = A \langle \rho v \rangle \quad (14)$$

where  $\langle \rho \rangle =$  volume averaged density

$\langle \rho v \rangle$  = area averaged mass flux

$V$  =  $\Delta x \Delta y \Delta z$

$A$  =  $\Delta y \Delta z$ .

Using the above approximations, Equation 12 is written for a 1-D nodal system in the evaporator section as

$$\frac{\partial}{\partial t} V \langle \rho \rangle = A_x \langle \rho v \rangle_x - A_{x+\Delta x} \langle \rho v \rangle_{x+\Delta x} + S \quad (15)$$

where  $S$  is the evaporation mass flow rate. Using this sign convention,  $S$  will be negative in the condenser. At this point, it is assumed that the area average is approximately constant over the control volume<sup>40</sup>. The averaging notation is dropped to simplify the notation. Dividing Equation 15 by  $V$  results in

$$\frac{\partial}{\partial t} \rho = \frac{(\rho v)_x}{\Delta x} - \frac{(\rho v)_{x+\Delta x}}{\Delta x} + S/V \quad (16)$$

Taking the limit as  $\Delta x$  approaches zero yields

$$\frac{\partial}{\partial t} \rho = -\frac{\partial}{\partial x} (\rho v) + S/V \quad (17)$$

A backwards difference approximation is applied to the spatial derivative, and an implicit formulation is used for the temporal derivative. Equation 17 may then be written as

$$\frac{\rho_j^{n+1} - \rho_j^n}{\Delta t} = \frac{\rho_{j-1}^{n+1} v_{j-1/2}^{n+1} - \rho_j^{n+1} v_{j+1/2}^{n+1}}{\Delta x_j} + \frac{S_j^{n+1}}{V_j} \quad (18)$$

It should be noted that Equation 18 has been written using a staggered grid. The velocities are located on the boundaries of the control cell and the density is positioned at the cell center. This has proven to be the most stable configuration

based on past research<sup>40</sup>. In addition, donor cell<sup>40</sup> notation is applied to the densities in the spatial derivative. This approximation assumes that the vapor entering the control cell is at the density in the cell from which it originates. Solving Equation 18 for  $v_{j+1/2}$  gives

$$v_{j+1/2}^{n+1} = \frac{\rho_{j-1}^{n+1} v_{j-1/2}^{n+1}}{\rho_j^{n+1}} + \frac{S_j^{n+1} \Delta x_j}{V_j \rho_j^{n+1}} - \frac{(\rho_j^{n+1} - \rho_j^n) \Delta x_j}{\Delta t \rho_j^{n+1}} \quad (19)$$

If the density is evaluated from the previous time step and held constant during the time step, Equation 19 can be simplified to give

$$v_{j+1/2}^{n+1} = \frac{\rho_{j-1}^n v_{j-1/2}^{n+1}}{\rho_j^n} + \frac{S_j^{n+1} \Delta x_j}{V_j \rho_j^n} \quad (20)$$

Equation 20, when applied to  $m$  vapor control cells, results in  $m$  coupled finite difference equations which can be solved directly once a boundary condition is defined. Two boundary conditions exist for the vapor velocity equations: the velocity is zero at the outer ends of the condenser and evaporator sections of the heat pipe. The velocity at the outer end of the evaporator is used as the boundary condition for the vapor equations because of the numeric scheme. This is equivalent to substituting  $v_{-1/2} = 0.0$  into Equation 20. The result is written as

$$v_{1/2}^{n+1} = \frac{S_1^{n+1} \Delta x_1}{V_1 \rho_1^n} \quad (21)$$

The remaining vapor velocities can be determined from Equation 20, once Equation 21 is solved.

### 5.1.2.2 Liquid Region

The development of the conservation of mass equation for the liquid region is similar to that for the vapor region. Differences arise since the liquid travels in the opposite direction to the vapor and the sign of the evaporation /condensation mass flow rate term changes. The liquid equations are developed by applying Equation 12 to the control volume shown in Figure 77. Beginning with Equation 21, the conservation of mass equation for the liquid region is written for the evaporator section as

$$\frac{\partial \rho}{\partial t} = - \frac{\partial}{\partial x} (\rho v) - s/v \quad (22)$$

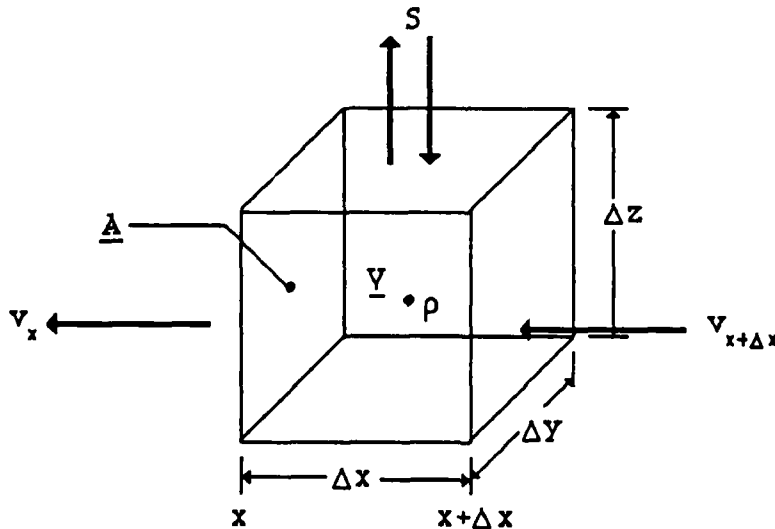


Figure 77. Liquid Control Volume for the Mass Conservation Equation

Equation 22 is simplified by applying a backwards difference approximation to the spatial derivative and using an implicit formulation for the temporal derivative as shown below

$$\frac{\rho_j^{n+1} - \rho_j^n}{\Delta t} = \frac{\rho_{j+1}^{n+1} v_{j+1/2}^{n+1} - \rho_j^{n+1} v_{j-1/2}^{n+1}}{\Delta x_j} - \frac{S_j^{n+1}}{V_j} \quad (23)$$

Solving for  $v_{j-1/2}^{n+1}$  yields

$$v_{j-1/2}^{n+1} = \frac{\rho_{j+1}^{n+1} v_{j+1/2}^{n+1}}{\rho_j^{n+1}} - \frac{S_j^{n+1} \Delta x_j}{V_j \rho_j^{n+1}} - \frac{(\rho_j^{n+1} - \rho_j^n) \Delta x_j}{\Delta t \rho_j^{n+1}} \quad (24)$$

If the density is evaluated explicitly and then held constant during the time step, Equation 24 simplifies to

$$v_{j-1/2}^{n+1} = \frac{\rho_{j+1}^n v_{j+1/2}^{n+1}}{\rho_j^n} - \frac{S_j^{n+1} \Delta x_j}{V_j \rho_j^n} \quad (25)$$

Boundary conditions are conceptually similar for the liquid and vapor regions. For the liquid region, however, the condenser outer wall velocity is used as the boundary condition,  $v_{m+1/2} = 0.0$ , because of the numeric scheme. Applying this boundary condition to Equation 25 yields

$$v_{m-1/2}^{n+1} = - \frac{S_m^{n+1} \Delta x_j}{V_m \rho_m^n} \quad (26)$$

Equations 26 and 25 form a set of  $m$  equations that can be solved directly for the cell boundary velocities.

### 5.1.3 Evaporation / Condensation Mass Flow Rate Model

A term that has not been fully defined thus far in the development of the conservation of mass equations is the evaporation and condensation mass flow

rate,  $S$ . This quantity has presented many problems for transient heat pipe models. Chang<sup>25</sup>, in his transient model, used the steady-state value of  $S$ , given as

$$S = \frac{Q}{h_{fg}} \quad (27)$$

where  $Q$  = heat source  
 $h_{fg}$  = latent heat of evaporation.

This approximation is subject to error during most transients since part of the externally applied energy will go into stored energy in the wall, liquid-wick section, and vapor region of a heat pipe. Other models of evaporation and condensation are based on kinetic theory<sup>41,42</sup>. One of these is based on simple kinetic theory<sup>42</sup>,

$$S = A \sqrt{\frac{M}{2\pi RT_v}} \left( P_l(T_{sat}) - P_v \right) \quad (28)$$

where  $A$  = cross-sectional area for mass transfer  
 $M$  = molecular weight of the working fluid  
 $R$  = universal gas constant  
 $T_v$  = vapor temperature  
 $P_l(T_{sat})$  = saturation pressure of the liquid for its given temperature  
 $P_v$  = vapor pressure.

This equation requires tight coupling with the conservation equations in order to achieve convergence, primarily due to the tremendous impact a small change in the pressure difference has on the mass flow rate. Additional problems can occur with the amount of pressure recovery allowed in the condenser. To date, no transient modeling results which reach steady-state have been published using this type of model.

The coupling problems associated with the kinetic theory model and the inaccuracy of the steady-state model led, in the present work, to the model developed below. This model assumes that the evaporation and condensation mass flow rates can be calculated by subtracting the stored thermal flux from the input thermal flux to obtain the net energy available for evaporation and condensation. This relationship is expressed as

$$S = \frac{Q - Q_{\text{store}}}{h_{fg}} \quad (29)$$

A drawback to this model is the necessity to determine the exact value of  $Q_{\text{store}}$  at any instant in time. It is herein hypothesized that  $Q_{\text{store}}$  can be given as a function of time in the form

$$Q_{\text{store}}(t) = Q e^{-\lambda t} \quad (30)$$

where  $\lambda$  is defined as the stored energy time constant. The value of  $\lambda$  depends upon the geometry of the heat pipe, the physical properties of the heat pipe, and the particular transient. The calculation of  $\lambda$  and the basis for Equation 30 will be discussed in Subsection 5.3.

#### 5.1.4 Development Of The Momentum Conservation Equation

A one-dimensional treatment is employed in developing the conservation of momentum equation for both the liquid and vapor regions in a heat pipe. In both of these regions, the momentum equation is solved in order to generate the pressure profiles. The momentum equation is given in integral form as<sup>39</sup>

$$\frac{\partial}{\partial t} \int_V \rho \vec{v} \, dV + \int_A \rho \vec{v} (\vec{v} \cdot \vec{n}) \, dA = \int_V \rho \vec{F} \, dV + \int_A (\vec{T} \cdot \vec{n}) \, dA \quad (31)$$

where  $\underline{F}$  = sum of all body forces per unit mass on the fluid  
 $\underline{T}$  = tensor of all surface stresses exerted on the fluid<sup>40</sup>

and all other variables are as previously defined. The area integrals in Equation 31 can be broken into two integrals: an integral over the wall area,  $\underline{W}$ , and an integral over the fluid area,  $\underline{L}$ .

$$\int_{\underline{A}} (\underline{T} \underline{n}) \, d\underline{A} = \int_{\underline{L}} (\underline{T} \underline{n}) \, d\underline{L} + \int_{\underline{W}} (\underline{T} \underline{n}) \, d\underline{W} \quad (32)$$

The only body force considered in this study is that due to the local acceleration,  $\underline{g}$ . The stress tensor in Equation 32 can be expanded in terms of the pressure and shear components for the two areas to give<sup>40</sup>

$$\int_{\underline{L}} (\underline{T} \underline{n}) \, d\underline{L} = - \int_{\underline{L}} P \underline{n} \, d\underline{L} + \int_{\underline{L}} (\underline{\pi} \underline{n}) \, d\underline{L} \quad (33a)$$

$$\int_{\underline{W}} (\underline{T} \underline{n}) \, d\underline{W} = - \int_{\underline{W}} P \underline{n} \, d\underline{W} + \int_{\underline{W}} (\underline{\pi} \underline{n}) \, d\underline{W} \quad (33b)$$

where  $P$  = pressure component  
 $\pi$  = shear component.

These expansions allow simplifications to be made. The shear component of Equation 33a and the pressure component of Equation 33b are zero for a 1-D development. In addition, the inertial term of Equation 31 is zero for the wall area integral, since the velocity of the fluid is zero over this area. Substituting the remaining terms of Equations 32, 33a, and 33b into Equation 31 yields

$$\frac{\partial}{\partial t} \int_V \rho \vec{v} \, dV + \int_L \rho \vec{v} (\vec{v} \cdot \vec{n}) \, dL = - \int_V \rho g \, dV - \int_L P \vec{n} \, dL + \int_W (\vec{\pi} \cdot \vec{n}) \, dW \quad (34)$$

The volume and area integrals of the momentum equation are defined in a manner similar to the mass conservation equation development. These are given as

$$\int_V \rho \vec{v} \, dV = V \langle \langle \rho v \rangle \rangle \quad (35)$$

and

$$\int_A \rho \vec{v} (\vec{v} \cdot \vec{n}) \, dA = A \langle \rho v^2 \rangle \quad (36)$$

Furthermore, the wall shear force integral can be reduced to an algebraic equation. The axial wall shear force is assumed to be proportional to the axial momentum flux through the usual friction factor relationship and is defined as<sup>40</sup>

$$\int_W (\vec{\pi} \cdot \vec{n}) \, dW = - \frac{f \Delta x P_w \langle \rho v^2 \rangle}{2} \quad (37)$$

where  $P_w$  is defined as the wall perimeter and  $f$  is given as the friction factor. Using the above area and volume integral approximations and Equation 37, Equation 34 can be written as

$$\begin{aligned}
v \frac{\partial \langle \rho v \rangle}{\partial t} + \langle \rho v^2 \rangle_{x+\Delta x} A_{x+\Delta x} - \langle \rho v^2 \rangle_{A_x} = -Vg \langle \rho \rangle \sin \theta \\
-PA_{x+\Delta x} + PA_x - \frac{f \Delta x P_w \langle \rho v^2 \rangle}{2}
\end{aligned} \tag{38}$$

where  $\theta$  is defined as the angle measured from the heat pipe to the horizontal axis (counterclockwise negative). It is assumed that the area average remains constant over the control volume and thus the averaging notation is dropped. Equation 38 can be written in differential form by dividing through by the volume,  $V$ , and taking the limit as  $\Delta x$  goes to zero. Equation 38 is then given as

$$\frac{\partial \rho v}{\partial t} + \frac{\partial (\rho v^2)}{\partial x} = -\rho g \sin \theta - \frac{\partial P}{\partial x} - \frac{f \Delta x P_w \rho v^2}{2V} \tag{39}$$

#### 5.1.4.1 Vapor Region

To change Equation 39 from a partial differential equation to an algebraic equation, a finite difference scheme is employed. Using the same procedure as in the mass equation development, a backwards difference scheme is employed for the spatial derivative, while an implicit formulation is used on the temporal derivative. Moreover, a staggered grid is used for the fluid velocities along with donor cell notation for the densities. This requires that the velocities be evaluated at the cell boundaries and the density and pressure at the cell center. The unit cell is illustrated in Figure 78.

With these approximations, Equation 39 is written for the vapor control volume illustrated in Figure 78 as

$$\begin{aligned}
\frac{\rho_j^{n+1} v_j^{n+1} - \rho_j^n v_j^n}{\Delta t} + \frac{\rho_j^{n+1} (v_{j+1/2}^{n+1})^2 - \rho_{j-1}^{n+1} (v_{j-1/2}^{n+1})^2}{\Delta x} = \\
-\rho_j^{n+1} g \sin \theta - \frac{P_j^{n+1} - P_{j-1}^{n+1}}{\Delta x} - \frac{f \Delta x P_w \rho_j^{n+1} (v_j^{n+1})^2}{2V}
\end{aligned} \tag{40}$$

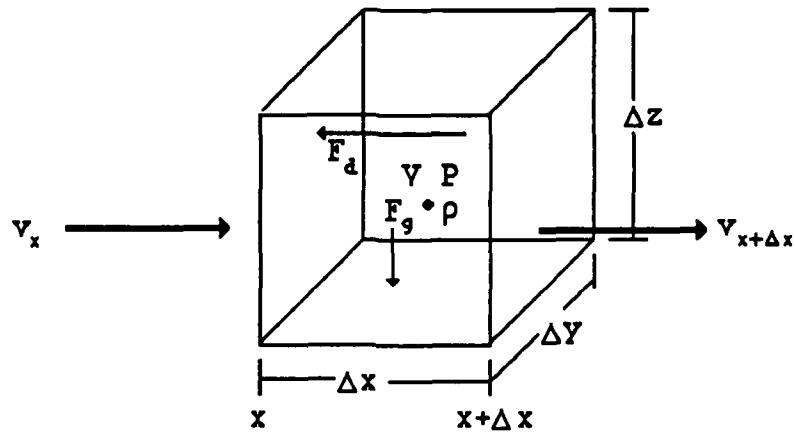


Figure 78. Vapor Control Volume for Axial Momentum

The pressure,  $P_j^{n+1}$ , can readily be solved for in Equation 40 to give

$$P_j^{n+1} = P_{j-1}^{n+1} - \Delta x \left[ \frac{\rho_j^{n+1} v_j^{n+1} - \rho_j^n v_j^n}{\Delta t} + \frac{\rho_j^{n+1} (v_{j+1/2}^{n+1})^2}{\Delta x} - \frac{\rho_{j-1}^{n+1} (v_{j-1/2}^{n+1})^2}{\Delta x} - \rho_j^{n+1} g \sin \theta - \frac{f \Delta x P_w \rho_j^{n+1} (v_j^{n+1})^2}{2V} \right] \quad (41)$$

where

$$v_j^{n+1} = \frac{v_{j+1/2}^{n+1} + v_{j-1/2}^{n+1}}{2}$$

Evaluating the density from the previous time step, Equation 39 reduces to

$$P_j^{n+1} = P_{j-1}^{n+1} - \Delta x \left[ \frac{\rho_j^n v_j^{n+1} - \rho_j^n v_j^n}{\Delta t} + \frac{\rho_j^n (v_{j+1/2}^{n+1})^2}{\Delta x} - \frac{\rho_{j-1}^n (v_{j-1/2}^{n+1})^2}{\Delta x} - \rho_j^n g \sin \theta - \frac{f \Delta x P_w \rho_j^n (v_j^{n+1})^2}{2V} \right] \quad (42)$$

To evaluate the vapor friction factor in Equation 42, it is assumed that the friction drag forces on the liquid-wick area are equivalent to those occurring on a smooth wall area. Therefore, the friction factor for turbulent flow is given by the Blasius equation<sup>43</sup>

$$f = 0.079 R_e^{-1/4} \quad (43)$$

where  $R_e$  is the Reynolds number. If the vapor flow is laminar, the friction factor is given by<sup>44</sup>

$$f = \frac{64}{R_e} \quad (44)$$

When Equation 42 is applied to the nodal scheme of Figure 75, a set of  $m$  coupled finite difference equations results with  $m+1$  unknowns. A boundary condition is needed to reduce the number of unknowns to  $m$ . Since the pressure at  $P_0$  is not available, it is assumed that the pressure,  $P_{1/2}$  can be defined as the saturation pressure for the temperature of node 1. This pressure is denoted by  $P_{bcv}$ . Applying the vapor velocity boundary condition at  $j=1/2$  and inserting  $P_{bcv}$  into Equation 42 gives

$$P_1^{n+1} = P_{bcv} - \frac{\Delta x}{2} \left[ \frac{\rho_1^n v_1^{n+1} - \rho_1^n v_1^n}{\Delta t} + \frac{\rho_1^n (v_{1/2}^{n+1})^2}{\Delta x} - \rho_1^n g \sin \theta - \frac{f \Delta x P_w \rho_1^n (v_1^{n+1})^2}{2V} \right] \quad (45)$$

Once the temperature at node 1 is known, Equation 45 and the set of  $m-1$  equations determined by Equation 42 can be solved directly.

### 5.1.4.2 Liquid Region

The development of the liquid momentum equation begins by applying Equation 39 to the control volume shown in Figure 79. As with the vapor momentum equation, a backwards difference scheme is used for the spatial derivatives and an implicit formulation is employed for the temporal derivative.

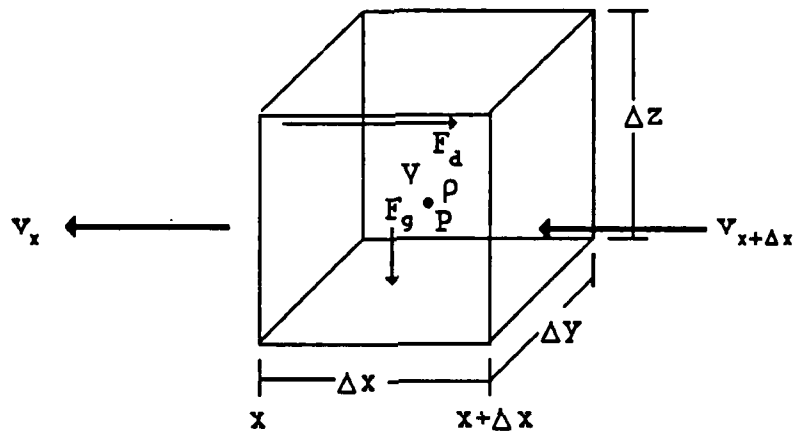


Figure 79. Liquid Control Volume for Axial Momentum

The resulting finite difference equation is given as

$$\frac{\rho_j^{n+1} v_j^{n+1} - \rho_j^n v_j^n}{\Delta t} + \frac{\rho_j^{n+1} (v_{j-1/2}^{n+1})^2 - \rho_{j+1}^{n+1} (v_{j+1/2}^{n+1})^2}{\Delta x} = -\rho_j^{n+1} g \sin \theta - \frac{P_j^{n+1} - P_{j+1}^{n+1}}{\Delta x} - \frac{f \Delta x P_w \rho_j^{n+1} (v_j^{n+1})^2}{2V} \quad (46)$$

The solution to this equation is readily found for  $P_j^{n+1}$  as

$$P_j^{n+1} = P_{j+1}^{n+1} - \Delta x \left[ \frac{\rho_j^{n+1} v_j^{n+1} - \rho_j^n v_j^n}{\Delta t} + \frac{\rho_j^{n+1} (v_{j-1/2}^{n+1})^2}{\Delta x} - \frac{\rho_{j+1}^{n+1} (v_{j+1/2}^{n+1})^2}{\Delta x} - \rho_j^{n+1} g \sin \theta - \frac{f \Delta x P_w \rho_j^{n+1} (v_j^{n+1})^2}{2V} \right] \quad (47)$$

Assuming the density can be evaluated from the previous time step, Equation 47 reduces to

$$P_j^{n+1} = P_{j+1}^{n+1} - \Delta x \left[ \frac{\rho_j^n v_j^{n+1} - \rho_j^n v_j^n}{\Delta t} + \frac{\rho_j^n (v_{j-1/2}^{n+1})^2}{\Delta x} - \frac{\rho_{j+1}^n (v_{j+1/2}^{n+1})^2}{\Delta x} - \rho_j^n g \sin \theta - \frac{f \Delta x P_w \rho_j^n (v_j^{n+1})^2}{2V} \right] \quad (48)$$

The friction pressure drop term in Equation 48 is written as the standard Fanning equation; however, depending upon the wick geometry, this term can be evaluated using a variety of forms<sup>11</sup>. The form of the Fanning equation that is most appropriate to the heat pipe in this study is Darcy's equation and is given as<sup>11</sup>

$$\Delta P_1 = \frac{\mu l_{\text{eff}} \dot{m}}{\rho K A} \quad (49)$$

where  $\mu$  = liquid viscosity  
 $l_{\text{eff}}$  = effective length  
 $\dot{m}$  = liquid mass flow rate  
 $K$  = wick permeability  
 $A$  = liquid flow cross-sectional area

The effective length is defined for a control volume by Dunn and Reay<sup>11</sup> as

$$l_{\text{eff}} = \frac{\Delta x}{2} \quad (50)$$

in the evaporator and condenser sections, and

$$l_{\text{eff}} = \Delta x \quad (51)$$

in the adiabatic section. The permeability, K, for a loosely wrapped wick can be approximated as a series of parallel annular passages<sup>34</sup> such that

$$K = \frac{2\epsilon r_{h,1}^2}{f(f_1, R_{e1})} \quad (52)$$

where

$$r_{h,1}^2 = \frac{2w\delta}{w+2\delta} \quad (53)$$

- $\epsilon$  = liquid volume fraction
- $w$  = width of flow channel
- $\delta$  = height of flow channel

The denominator of Equation 52 is a function of the flow channel width and height. Values for this function are given by Chi<sup>38</sup>. Substituting Equation 49 into Equation 48 yields,

$$P_j^{n+1} = P_{j+1}^{n+1} - \Delta x \left[ \frac{\rho_j^n v_j^{n+1} - \rho_j^n v_j^n}{\Delta t} + \frac{\rho_j^n (v_{j-1/2}^{n+1})^2}{\Delta x} - \frac{\rho_{j+1}^n (v_{j+1/2}^{n+1})^2}{\Delta x} - \rho_j^n g \sin\theta - \frac{\mu l_{\text{eff}} m_j^{n+1}}{\rho_j^n K A \Delta x} \right] \quad (54)$$

A unique boundary condition is employed to solve the set of m equations generated by Equation 54. The extreme end of the condenser section,  $j=m+1/2$ , is assumed to be flooded (i.e., the radius of curvature is infinite). From Equation 1, the pressure of the liquid must then be equal to the pressure of the vapor at this location. Equation 42 can be written for the vapor pressure at the condenser wall as

$$P_{m+1/2}^{n+1} = P_m^{n+1} - \frac{\Delta x}{2} \left[ \frac{\rho_m^n v_m^{n+1} - \rho_m^n v_m^n}{\Delta t} - \frac{\rho_{m-1}^n (v_{m-1/2}^{n+1})^2}{\Delta x} - \rho_m^n g \sin \theta - \frac{f \Delta x P_w \rho_m^n (v_m^{n+1})^2}{2V} \right] \quad (55)$$

To apply the boundary condition, the liquid and vapor equations are equated at  $m+1/2$  such that

$$(P_{m+1/2}^{n+1})_{\text{liquid}} = (P_{m+1/2}^{n+1})_{\text{vapor}} = P_{\text{bcl}} \quad (56)$$

This boundary condition is inserted into Equation 54 to give

$$P_m^{n+1} = P_{\text{bcl}} - \frac{\Delta x}{2} \left[ \frac{\rho_m^n v_m^{n+1} - \rho_m^n v_m^n}{\Delta t} + \frac{\rho_m^n (v_{m-1/2}^{n+1})^2}{\Delta x} - \rho_m^n g \sin \theta - \frac{\mu l_{\text{eff}}^m v_m^{n+1}}{\rho_m^n K A \Delta x} \right] \quad (57)$$

Equation 57 together with the set of  $m-1$  equations formed by Equation 54 can be solved directly to generate the liquid axial pressure profile in the heat pipe.

### 5.1.5 Development of the Energy Conservation Equation

A 2-D development of the energy equation is used to model the axial and radial temperature profiles of a heat pipe. A 2-D energy equation is used in order to account for axial and radial conduction/convection effects. The nodal scheme is comprised of four radial nodes; an outer wall region, an inner wall region, a liquid-wick region, and a vapor region (as depicted in Figure 75) each with  $m$  axial nodes. Separate energy equations which are generic to that region are written for each radial node.

### 5.1.5.1 General Development

The conservation of energy equation is given in integral form as<sup>39</sup>

$$\frac{\partial}{\partial t} \int_V \rho e \, dV + \int_A \rho e (\vec{v} \cdot \vec{n}) \, dA = \int_V \rho (\vec{F} \cdot \vec{v}) \, dV + \int_A [(\vec{T} \cdot \vec{v}) - \vec{q}'' \cdot \vec{n}] \, dA \quad (58)$$

where  $e$  = total energy  
 $q''$  = energy flux.

It is assumed that the potential and kinetic energy terms are small relative to the internal energy. This is justified by the relatively low speeds expected in a water heat pipe and the absence of hydrostatic effects in the heat pipe of Section 3. It is further assumed that the work done by shear stresses and body forces is negligible. The total energy is given as<sup>40</sup>

$$e = i + \frac{v^2}{2} + gz \quad (59)$$

$$e \cong i \quad (60)$$

$$e \cong h - Pv \quad (61)$$

where  $i$  = internal energy  
 $h$  = enthalpy  
 $v$  = specific volume.

Substituting Equation 61 into Equation 58 yields

$$\frac{\partial}{\partial t} \int_V (\rho h - P) dV + \int_A (\rho h - P) (\vec{v} \cdot \vec{n}) dA = \int_A P (\vec{v} \cdot \vec{n}) dA - \int_A (\vec{q}'' \cdot \vec{n}) dA \quad (62)$$

Cancelling terms gives

$$\frac{\partial}{\partial t} \int_V (\rho h - P) dV + \int_A \rho h (\vec{v} \cdot \vec{n}) dA = - \int_A (\vec{q}'' \cdot \vec{n}) dA \quad (63)$$

In accordance with the development of the mass and momentum conservation equations, the volume and surface integrals are defined as

$$\int_V (\rho h - P) dV = V \langle\langle \rho h - P \rangle\rangle \quad (64)$$

$$\int_A \rho h (\vec{v} \cdot \vec{n}) dA = A \langle \rho h v \rangle \quad (65)$$

$$\int_A (\vec{q}'' \cdot \vec{n}) dA = A \langle q'' \rangle \quad (66)$$

The above definitions for the volume and area averages allow the energy equation to be simplified to

$$V \frac{\partial}{\partial t} \langle\langle \rho h - P \rangle\rangle + \langle \rho h v \rangle_{A_{x+\Delta x}} - \langle \rho h v \rangle_{A_x} = - \langle q'' \rangle_{A_{x+\Delta x}} - \langle q'' \rangle_{A_x} - \langle q'' \rangle_{A_{z+\Delta z}} - \langle q'' \rangle_{A_z} \quad (67)$$

where  $A_z = \Delta x \Delta y$ .

Equation 67 can be written in differential form by dividing by  $V$  and taking the limit as  $\Delta x$  and  $\Delta z$  go to zero. This gives

$$\frac{\partial}{\partial \tau} \langle \rho h - P \rangle + \frac{\partial}{\partial x} \langle \rho h v \rangle = - \frac{\partial}{\partial x} \langle q'' \rangle - \frac{\partial}{\partial z} \langle q'' \rangle \quad (68)$$

The above equation represents the general energy equation for a heat pipe control volume in this study.

#### 5.1.5.2 Outer Wall Region

Many simplifications can be made to Equation 68 when it is applied to a wall region. The change in internal energy for solids can be written as

$$di = C_p dT \quad (69)$$

Moreover, the convective energy transport is zero since the velocity is zero in the wall. Furthermore, it is assumed that the area average is constant over the control volume and thus the averaging notation is dropped. Using the above definitions and assumptions, the energy balance for a wall region can be written as

$$\frac{\partial}{\partial \tau} \rho C_p T = - \frac{\partial}{\partial x} q'' - \frac{\partial}{\partial z} q'' \quad (70)$$

To simplify Equation 70, the modes of energy transport through the wall control volume must be identified.

The available energy transport modes for an outer wall control volume are shown in Figure 80. In every outer wall node there exists axial conduction to neighboring outer wall nodes and radial conduction to the inner wall node. The evaporator and condenser sections are characterized by radial energy transport from the electric heater and to the water cooling jacket. The adiabatic

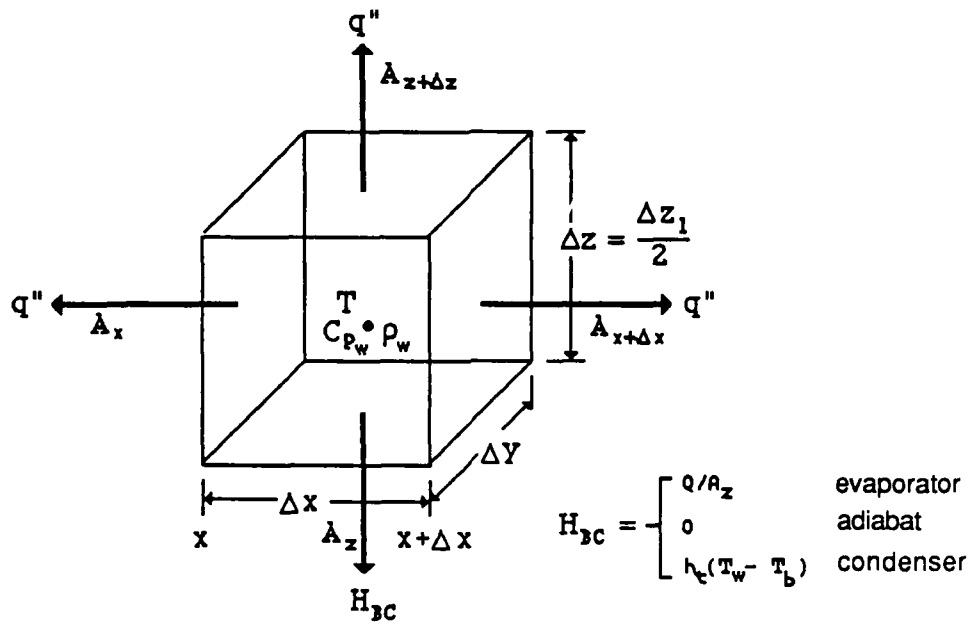


Figure 80. Outer Wall Region Control Volume for the Energy Equation

section is assumed to be perfectly insulated and thus no external energy transport exists. As with the mass and momentum equations, a backwards differencing scheme is employed for the spatial derivative, while an implicit formulation is used for the temporal derivative. Referring to Figure 80, Equation 70 can be expanded as

$$\frac{\rho C_p (T_{1,j}^{n+1} - T_{1,j}^n)}{\Delta t} = - \frac{K_w}{\Delta x_{j-1}^2} (T_{1,j}^{n+1} - T_{1,j-1}^{n+1}) - H_{BC} - \frac{K_w}{\Delta x_{j+1}^2} (T_{1,j}^{n+1} - T_{1,j+1}^{n+1}) - \frac{2K_w}{\Delta z_1^2} (T_{1,j}^{n+1} - T_{2,j}^{n+1}) \quad (71)$$

$$\begin{aligned}
H_{BC} &= \frac{Q}{V} && \text{(evaporator)} \\
&= 0 && \text{(adiabatic)} \\
&= \frac{2h_t}{\Delta z_1} (T_{1,j}^{n+1} - T_b) && \text{(condenser)}
\end{aligned}$$

$$\Delta x_{j-1}^2 = \Delta x_j \frac{\Delta x_{j-1} + \Delta x_j}{2}$$

$$\Delta x_{j+1}^2 = \Delta x_j \frac{\Delta x_{j+1} + \Delta x_j}{2}$$

- and
- $\Delta z_1$  = distance from the outer wall to the inner wall
  - $K_w$  = wall conductivity
  - $V$  =  $\Delta x \Delta y \Delta z_1 / 2$
  - $h_t$  = convective heat transfer coefficient
  - $T_b$  = bulk coolant temperature.

Equation 71 can be rearranged to give

$$\begin{aligned}
& - \frac{K_w}{\Delta x_{j-1}^2} T_{1,j-1}^{n+1} + \left( \frac{\rho_w C_{p_w}}{\Delta t} + \frac{K_w}{\Delta x_{j-1}^2} + \frac{K_w}{\Delta x_{j+1}^2} + \frac{2K_w}{\Delta z_1^2} \right) T_{1,j}^{n+1} \\
& - \frac{K_w}{\Delta x_{j+1}^2} T_{1,j+1}^{n+1} - \frac{2K_w}{\Delta z_1^2} T_{2,j}^{n+1} = \frac{\rho_w C_{p_w}}{\Delta t} T_{1,j}^n - H_{BC} \quad (72)
\end{aligned}$$

or

$$- aT_{1,j-1}^{n+1} + cT_{1,j}^{n+1} - dT_{2,j}^{n+1} - eT_{1,j+1}^{n+1} = f \quad (73)$$

The terms, a, c, d, e, and f, in Equation 73, are defined in Appendix F. In the solution of the wall region energy equation, the thermal properties are held constant throughout the transient. The convective heat transfer coefficient is

determined by assuming flow through a rectangular passage with the upper surface heated. This can be approximated by the Dittus-Boelter equation<sup>45</sup>:

$$h_t = \frac{0.023 R_e^{4/5} P_r^{0.4} K_c}{D_h} \quad (74)$$

where  $P_r$  = Prandlt number  
 $K_c$  = coolant conductivity  
 $D_h$  = hydraulic diameter.

As shown in Figure 75, the ends of the heat pipe are assumed to be well insulated. This translates into two boundary conditions that can be used for each radial region:

$$K_w \frac{dT}{dx} \Big|_{j=1/2} = 0 \quad (75)$$

$$K_w \frac{dT}{dx} \Big|_{-1/2} = 0 \quad (76)$$

Applying Equations 75 and 76 at the ends of the heat pipe gives

$$\left( \frac{\rho_w C_{p_w}}{\Delta t} + \frac{K_w}{\Delta x_2^2} + \frac{2K_w}{\Delta z_1^2} \right) T_{1,1}^{n+1} - \frac{K_w}{\Delta x_2^2} T_{1,2}^{n+1} - \frac{2K_w}{\Delta z_1^2} T_{2,1}^{n+1} = \frac{\rho_w C_{p_w}}{\Delta t} T_{1,1}^n - H_{BC} \quad (77)$$

$$\begin{aligned}
 & - \frac{K_w}{\Delta x_{m-1}^2} T_{1,m-1}^{n+1} + \left( \frac{\rho_w C_{p_w}}{\Delta t} + \frac{K_w}{\Delta x_{m-1}^2} + \frac{2K_w}{\Delta z_1^2} \right) T_{1,m}^{n+1} \\
 & - \frac{2K_w}{\Delta z_1^2} T_{2,m}^{n+1} = \frac{\rho_w C_{p_w}}{\Delta t} T_{1,m}^n - H_{BC} \quad (78)
 \end{aligned}$$

### 5.1.5.3 Inner Wall Region

The development of the inner wall region energy equation begins by applying Equation 70 to the control volume illustrated in Figure 81. As depicted in Figure 81, the modes of energy transport involve axial and radial conduction to the neighboring nodes. Using the same differencing pattern as described for the outer wall region, Equation 68 can be written as

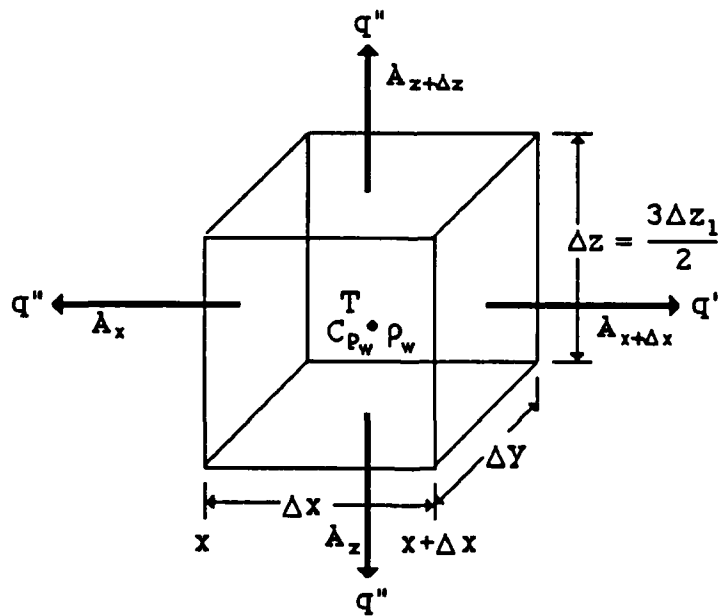


Figure 81. Inner Wall Region Control Volume for the Energy Equation

$$\frac{\rho_w C_{p_w} (T_{2,j}^{n+1} - T_{2,j}^n)}{\Delta t} = - \frac{K_w}{\Delta x_{j-1}^2} (T_{2,j}^{n+1} - T_{2,j-1}^{n+1}) - \frac{K_w}{\Delta x_{j+1}^2} (T_{2,j}^{n+1} - T_{2,j+1}^{n+1}) - \frac{2K_w}{3\Delta z_1^2} (T_{2,j}^{n+1} - T_{1,j}^{n+1}) - \frac{2R}{3\Delta z_1} (T_{2,j}^{n+1} - T_{3,j}^{n+1}) \quad (79)$$

where

$$R = \left( \frac{\Delta z_1}{K_w} + \frac{\Delta z_2}{2K_w L_j^n} \right)^{-1} \quad (80)$$

$$K_w L_j^n = \epsilon K_L^n + (1-\epsilon) K_{wick} \quad (81)$$

and

$K_L^n$  = liquid conductivity

$K_{wick}$  = wick material conductivity

$\epsilon$  = liquid volume fraction

$\Delta z_2$  = liquid-wick thickness

$\frac{3\Delta z_1}{2}$  = inner wall region thickness

The conductivity of the liquid-wick region given in Equation 81 is determined by assuming that the wick and working fluid are effectively in parallel<sup>11</sup>. Collecting terms, Equation 79 can be written as

$$- \frac{2K_w}{3\Delta z_1^2} T_{1,j}^{n+1} - \frac{K_w}{\Delta x_{j-1}^2} T_{2,j-1}^{n+1} + \left( \frac{\rho_w C_{p_w}}{\Delta t} + \frac{2K_w}{3\Delta z_1^2} + \frac{K_w}{\Delta x_{j-1}^2} + \frac{K_w}{\Delta x_{j+1}^2} + \frac{2R}{3\Delta z_1} \right) T_{2,j}^{n+1} - \frac{K_w}{\Delta x_{j+1}^2} T_{2,j+1}^{n+1} - \frac{2R}{3\Delta z_1} T_{3,j}^{n+1} = \frac{\rho_w C_{p_w}}{\Delta t} T_{2,j}^n \quad (82)$$

or

$$- aT_{2,j-1}^{n+1} - bT_{1,j}^{n+1} + cT_{2,j}^{n+1} - dT_{3,j}^{n+1} - eT_{2,j+1}^{n+1} = f \quad (83)$$

The terms, a, b, c, d, e, and f, in Equation 83 are defined in Appendix F. Applying

the boundary conditions given by Equations 75 and 76 yields the following two equations:

$$\begin{aligned}
 - \frac{2K_w}{3\Delta z_1^2} T_{1,1}^{n+1} + \left( \frac{\rho_w C_{p_w}}{\Delta t} + \frac{2K_w}{3\Delta z_1^2} + \frac{K_w}{\Delta x_2^2} + \frac{2R}{3\Delta z_1} \right) T_{2,1}^{n+1} \\
 - \frac{K_w}{\Delta x_2^2} T_{2,2}^{n+1} - \frac{2R}{3\Delta z_1} T_{3,1}^{n+1} = \frac{\rho_w C_{p_w}}{\Delta t} T_{2,1}^n \quad (84)
 \end{aligned}$$

$$\begin{aligned}
 - \frac{2K_w}{3\Delta z_1^2} T_{1,m}^{n+1} - \frac{K_w}{\Delta x_{m-1}^2} T_{2,m-1}^{n+1} + \left( \frac{\rho_w C_{p_w}}{\Delta t} + \frac{2K_w}{3\Delta z_1^2} + \frac{K_w}{\Delta x_{m-1}^2} \right. \\
 \left. + \frac{2R}{3\Delta z_1} \right) T_{2,m}^{n+1} - \frac{2R}{3\Delta z_1} T_{3,m}^{n+1} = \frac{\rho_w C_{p_w}}{\Delta t} T_{2,m}^n \quad (85)
 \end{aligned}$$

#### 5.1.5.4 Liquid-Wick Node

The liquid-wick energy equation is developed based on a simplification of Equation 68, the general energy equation. The energy equation for the liquid-wick node is broken into a liquid volume and a wick volume. In the liquid volume, it is assumed that the liquid is at constant pressure over a time step. This allows the change in internal energy to be approximated as

$$di \equiv C_{p_L} dT \quad (86)$$

This equation is used only for the temporal derivative term. In the wick volume, the internal energy is given by Equation 69. It is further assumed that the value of the enthalpy convected into and out of the control volume is constant during the transient. These assumptions allow Equation 62 to be written as

$$\frac{\partial}{\partial t} \langle \rho C_p T \rangle_{\text{liquid}} + \frac{V_{\text{wick}}}{V_L} \frac{\partial}{\partial t} \langle \rho C_p T \rangle_{\text{wick}} + \frac{\partial}{\partial x} \langle \rho_L h_L v \rangle =$$

$$- \frac{1}{\varepsilon} \frac{\partial}{\partial x} \langle q'' \rangle - \frac{1}{\varepsilon} \frac{\partial}{\partial z} \langle q'' \rangle \quad (87)$$

The liquid-wick region has several energy transport modes: axial and radial conduction to its neighboring nodes, axial convection through the node, and evaporation/condensation. Using the differencing techniques discussed in the wall energy equation development and the control volume illustrated in Figure 82, Equation 87 can be written as

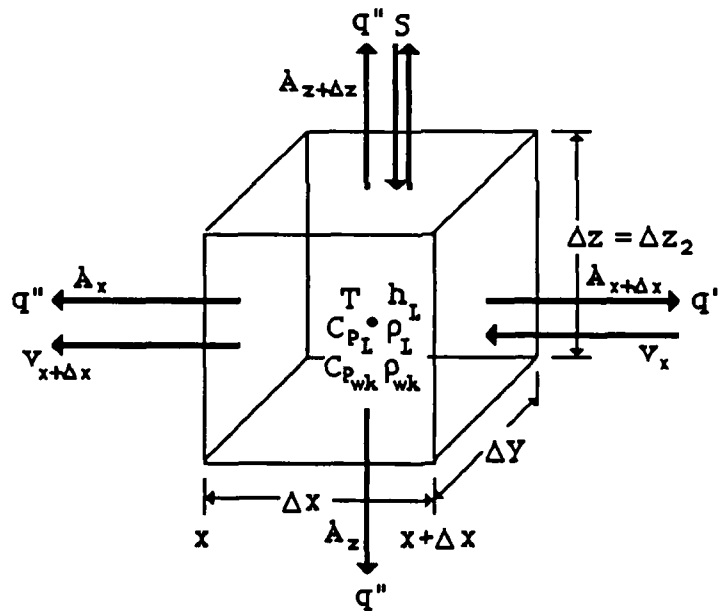


Figure 82. Liquid-Wick Region Control Volume for the Energy equation

$$\begin{aligned}
& \frac{1-\epsilon}{\epsilon} \left( \frac{\rho_{wk} C_{p_{wk}} T_{3,j}^{n+1} - \rho_{wk} C_{p_{wk}} T_{3,j}^n}{\Delta t} \right) + \frac{\rho_{Lj}^n C_{p_{Lj}}^n T_{3,j}^{n+1} - \rho_{Lj}^n C_{p_{Lj}}^n T_{3,j}^n}{\Delta t} + \\
& \frac{\rho_{Lj}^n h_L v_{j-1/2}^{n+1} - \rho_{Lj+1}^n h_L v_{j+1/2}^{n+1}}{\Delta x} = - \frac{K_{wL_{j-1}}^n}{\epsilon \Delta x_{j-1}^2} (T_{3,j}^{n+1} - T_{3,j-1}^{n+1}) - \\
& \frac{K_{wL_{j+1}}^n}{\epsilon \Delta x_{j+1}^2} (T_{3,j}^{n+1} - T_{3,j+1}^{n+1}) - \frac{R}{\epsilon \Delta z_2} (T_{3,j}^{n+1} - T_{2,j}^{n+1}) - \\
& \frac{R_v}{\epsilon \Delta z_2} (T_{3,j}^{n+1} - T_{4,j}^{n+1}) - \frac{S_j^{n+1} h_v}{V_L} \quad (88)
\end{aligned}$$

where

$$R_v = \left( \frac{\Delta z_2}{2K_{wL_j}^n} + \frac{\Delta z_3}{2K_v} \right)^{-1} \quad (89)$$

$$K_{wL_{j-1}}^n = \left( \frac{K_{wL_j}^n + K_{wL_{j-1}}^n}{2} \right)$$

$$K_{wL_{j+1}}^n = \left( \frac{K_{wL_{j+1}}^n + K_{wL_j}^n}{2} \right)$$

and  $h_L$  = liquid enthalpy  
 $h_v$  = vapor enthalpy  
 $V_L$  = liquid volume =  $eDxDy\Delta z_2$   
 $\Delta z_3$  = vapor thickness.

Collecting terms in Equation 88 yields

$$\begin{aligned}
& - \frac{R}{\epsilon \Delta z_2} T_{2,j}^{n+1} - \frac{K_{wL_{j-1}}^n}{\epsilon \Delta x_{j-1}^2} T_{3,j-1}^{n+1} + \left( \frac{\rho_{Lj}^n C_{p_{Lj}}^n}{\Delta t} + \left( \frac{1-\epsilon}{\epsilon} \right) \frac{\rho_{wk} C_{p_{wk}}}{\Delta t} + \frac{R}{\epsilon \Delta z_2} + \right. \\
& \left. \frac{K_{wL_{j-1}}^n}{\epsilon \Delta x_{j-1}^2} + \frac{K_{wL_{j+1}}^n}{\epsilon \Delta x_{j+1}^2} + \frac{R_v}{\epsilon \Delta z_2} \right) T_{3,j}^{n+1} - \frac{K_{wL_{j+1}}^n}{\epsilon \Delta x_{j+1}^2} T_{3,j+1}^{n+1} - \frac{R_v}{\epsilon \Delta z_2} T_{4,j}^{n+1} =
\end{aligned}$$

$$\left( \frac{1-\epsilon}{\epsilon} \frac{\rho_{wk} C_{p_{wk}}}{\Delta t} + \frac{\rho_{Lj}^n C_{p_{Lj}}^n}{\Delta t} \right) T_{3,j}^n + \frac{\rho_{Lj+1}^n h_L v_{j+1/2}^{n+1} - \rho_{Lj}^n h_L v_{j-1/2}^{n+1}}{\Delta x} - \frac{S_j^{n+1} h_v}{V_L} \quad (90)$$

or

$$- aT_{3,j-1}^{n+1} - bT_{2,j}^{n+1} + cT_{3,j}^{n+1} - dT_{4,j}^{n+1} - eT_{3,j+1}^{n+1} = f \quad (91)$$

The terms, a, b, c, d, e, and f, in Equation 91 are defined in Appendix F. Applying both the boundary conditions given by Equations 75 and 76 and the velocity boundary conditions for the heat pipe ends ( $v_{j=1/2} = 0$  and  $v_{j=m+1/2} = 0$ ) to Equation 90 results in the following two equations:

$$\begin{aligned} & - \frac{R}{\epsilon \Delta z_2} T_{2,1}^{n+1} + \left( \frac{\rho_{L1}^n C_{p_{L1}}^n}{\Delta t} + \frac{1-\epsilon}{\epsilon} \frac{\rho_{wk} C_{p_{wk}}}{\Delta t} + \frac{R}{\epsilon \Delta z_2} + \right. \\ & \left. + \frac{K_{wL2}^n}{\epsilon \Delta x_2^2} + \frac{R_v}{\epsilon \Delta z_2} \right) T_{3,1}^{n+1} - \frac{K_{wL2}^n}{\epsilon \Delta x_2^2} T_{3,2}^{n+1} - \frac{R_v}{\epsilon \Delta z_2} T_{4,1}^{n+1} = \\ & \left( \frac{1-\epsilon}{\epsilon} \frac{\rho_{wk} C_{p_{wk}}}{\Delta t} + \frac{\rho_{L1}^n C_{p_{L1}}^n}{\Delta t} \right) T_{3,1}^n + \frac{\rho_{L2}^n h_L v_{3/2}^{n+1}}{\Delta x} \\ & - \frac{S_1^{n+1} h_v}{V_L} \quad (92) \end{aligned}$$

$$\begin{aligned}
& - \frac{R}{\epsilon \Delta z_2} T_{2,m}^{n+1} - \frac{K_{wL}^n}{\epsilon \Delta x_{j-1}^2} T_{3,m-1}^{n+1} + \left( \frac{\rho_{Lm}^n C_{pLm}^n}{\Delta t} + \left( \frac{1-\epsilon}{\epsilon} \right) \frac{\rho_{wk} C_{p_{wk}}}{\Delta t} + \right. \\
& \left. \frac{R}{\epsilon \Delta z_2} + \frac{K_{wL}^n}{\epsilon \Delta x_{m-1}^2} + \frac{R_v}{\epsilon \Delta z_2} \right) T_{3,m}^{n+1} - \frac{R_v}{\epsilon \Delta z_2} T_{4,m}^{n+1} = \\
& \left( \left( \frac{1-\epsilon}{\epsilon} \right) \frac{\rho_{wk} C_{p_{wk}}}{\Delta t} + \frac{\rho_{Lm}^n C_{pLm}^n}{\Delta t} \right) T_{3,m}^n - \frac{\rho_{Lm}^n h_L v_{m-1/2}^{n+1}}{\Delta x} \\
& - \frac{S_m^{n+1} h_v}{V_L} \tag{93}
\end{aligned}$$

### 5.1.5.5 Vapor Region

Similar to the previous developments, the vapor energy equation formulation begins with Equation 68. The possible energy transport mechanisms are illustrated in Figure 83: axial conduction and convection to adjacent vapor nodes, conduction to the liquid-wick node, and evaporation/condensation. As depicted in Figure 75, the top of the heat pipe is well insulated. It is assumed that no energy transport through the top of the heat pipe occurs. It is also assumed that the water vapor can be treated as an ideal gas and thus the temporal change in pressure will be included. This allows the internal energy to be expressed as<sup>45</sup>

$$\begin{aligned}
di &= dh - d(Pv) \\
&= C_{p_v} dT - R dT \\
&= (C_{p_v} - R) dT \\
&= C_{v_v} dT \tag{94}
\end{aligned}$$

where  $C_v$  = specific heat at constant volume.

Applying the differencing techniques, as discussed in the development of the wall region energy equation, to Equation 68, gives

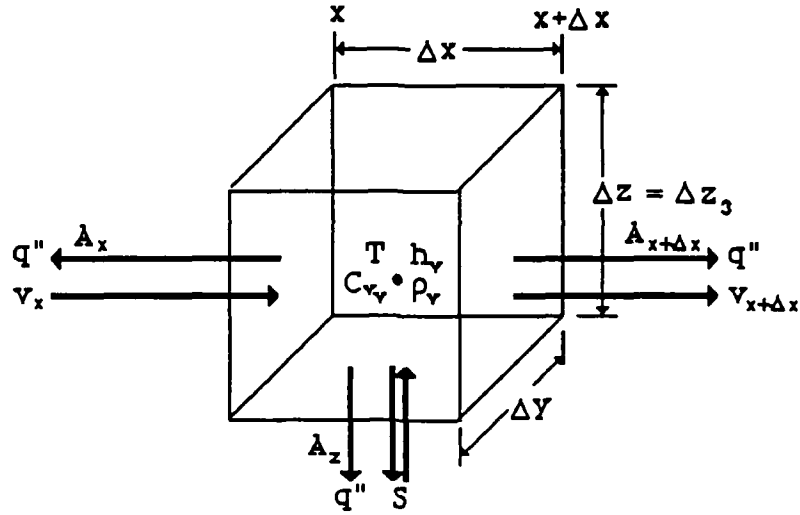


Figure 83. Vapor Region Control Volume for the Energy Equation

$$\begin{aligned}
 & \frac{\rho_{vj}^n C_{vj}^n T_{4,j}^{n+1} - \rho_{vj}^n C_{vj}^n T_{4,j}^n}{\Delta t} + \frac{\rho_{vj}^n h_v v_{j+1/2}^{n+1} - \rho_{vj-1}^n h_v v_{j-1/2}^{n+1}}{\Delta x} = \\
 & \frac{K_{vj-1}^2}{\Delta x_{j-1}^2} (T_{4,j}^{n+1} - T_{4,j-1}^{n+1}) - \frac{K_{vj+1}^2}{\Delta x_{j+1}^2} (T_{4,j}^{n+1} - T_{4,j+1}^{n+1}) - \\
 & \frac{R_v}{\Delta z_j} (T_{4,j}^{n+1} - T_{3,j}^{n+1}) + \frac{S_j^{n+1} h_v}{V_v} \quad (95)
 \end{aligned}$$

Collecting terms yields

$$\begin{aligned}
 & - \frac{R_v}{\Delta z_j} T_{3,j}^{n+1} - \frac{K_{vj-1}^n}{\Delta x_{j-1}^2} T_{4,j-1}^{n+1} + \left( \frac{\rho_{vj}^n C_{vj}^n}{\Delta t} + \frac{R_v}{\Delta z_j} + \frac{K_{vj-1}^n}{\Delta x_{j-1}^2} + \right. \\
 & \left. \frac{K_{vj+1}^n}{\Delta x_{j+1}^2} \right) T_{4,j}^{n+1} - \frac{K_{vj+1}^n}{\Delta x_{j+1}^2} T_{4,j+1}^{n+1} = \frac{\rho_{vj}^n C_{vj}^n}{\Delta t} T_{4,j}^n + \frac{S_j^{n+1} h_v}{V_v} +
 \end{aligned}$$

$$\frac{\rho_{vj-1}^n h_v v_{j-1/2}^{n+1} - \rho_{vj}^n h_v v_{j+1/2}^{n+1}}{\Delta x} \quad (96)$$

or

$$- aT_{4,j-1}^{n+1} - bT_{3,j}^{n+1} + cT_{4,j}^{n+1} - eT_{4,j+1}^{n+1} = f \quad (97)$$

The terms, a, b, c, e, and f, in Equation 97 are defined in Appendix F. Applying both the vapor velocity boundary conditions at the heat pipe ends ( $v_{j=1/2} = 0$  and  $v_{j=m+1/2} = 0$ ) and the energy equation boundary conditions given by Equations 75 and 76 to Equation 96 yields the following two equations:

$$\begin{aligned} - \frac{R_v}{\Delta z_3} T_{3,1}^{n+1} + \left( \frac{\rho_{v1}^n C_{v1}^n}{\Delta t} + \frac{R_v}{\Delta z_3} + \frac{K_{v2}^n}{\Delta x_2^2} \right) T_{4,1}^{n+1} \\ \frac{K_{v2}^n}{\Delta x_2^2} T_{4,2}^{n+1} = \frac{\rho_{v1}^n C_{v1}^n}{\Delta t} T_{4,1}^n + \frac{S_1^{n+1} h_v}{V_v} + \\ - \frac{\rho_{v1}^n h_v v_{3/2}^{n+1}}{\Delta x} \end{aligned} \quad (98)$$

$$\begin{aligned} - \frac{R_v}{\Delta z_3} T_{3,m}^{n+1} - \frac{K_{vm-1}^n}{\Delta x_{m-1}^2} T_{4,m-1}^{n+1} + \left( \frac{\rho_{vm}^n C_{vm}^n}{\Delta t} + \frac{R_v}{\Delta z_3} + \right. \\ \left. \frac{K_{vm-1}^n}{\Delta x_{m-1}^2} \right) T_{4,m}^{n+1} = \frac{\rho_{vm}^n C_{vm}^n}{\Delta t} T_{4,m}^n + \frac{S_m^{n+1} h_v}{V_v} + \\ \frac{\rho_{vm-1}^n h_v v_{m-1/2}^{n+1}}{\Delta x} \end{aligned} \quad (99)$$

### 5.1.6 Solution Procedure

The velocity, pressure and temperature profiles are obtained through the solution of the conservation equations. The equations required for the solution

are given in Table 6. From the boundary conditions, a direct solution can be obtained for the mass and momentum equations. The energy equation, however, requires the solution of a  $4m \times 4m+1$  matrix formed by Equations 70, 73, 81 and 87. The matrix is shown in Figure 84. Several techniques are available for matrix solutions; Gaussian Elimination, Gauss-Siedel, Successive Displacements, Successive Overrelaxation, and Simultaneous Displacements<sup>46</sup> to name a few. The solution technique used in this study is Gauss-Siedel. Gauss-Siedel involves an iterative technique for matrix solution. To use Gauss-Siedel, a set of  $4m$  equations given in a general form as

$$\sum_{j=1}^{4m} b_j T_j = f_j \quad (100)$$

must be rearranged into

$$T_i^{k+1} = \frac{f_i}{b_i} - \sum_{j=1}^{i-1} \frac{b_j}{b_i} T_j^{k+1} - \sum_{j=i+1}^{4m} \frac{b_j}{b_i} T_j^k \quad i=1, 2, \dots, 4m \quad (101)$$

where  $k$  is the iteration index. The solution of the  $4m$  coupled finite difference equations begins by supplying a guess vector,  $T^k$ . The solution scheme then marches through the set of  $4m$  equations solving for the vector,  $T^{k+1}$ . As each equation is solved, the guess vector is updated. This iteration process continues until convergence is reached. The most common convergence criteria is given as<sup>46</sup>

$$\left| \frac{T_i^{k+1} - T_i^k}{T_i^{k+1}} \right| < \xi \quad i=1, 2, \dots, m \quad (102)$$

where  $\xi$  usually ranges from  $10^{-4}$  to  $10^{-6}$ . The initial guess vector for a time step is the solution vector from the previous time step.

The flow chart of the solution scheme is shown in Figure 85. After the initial conditions are read in, the time constant, given in Equation 29, is evaluated from a simplified form of the energy equation. The simplified energy equation treats the entire heat pipe as one axial node and assumes the vapor region is

Table 6. Summary of the Equations used in the Heat Pipe Model Solution

Equation	Description	Boundary Equations
$v_{j-1/2}^{n+1} = \frac{\rho_{j-1}^n v_{j-1/2}^{n+1}}{\rho_j^n} + \frac{S_j^{n+1} \Delta x_j}{v_j \rho_j^n} \quad (20)$	Vapor Velocity	(21)
$v_{j-1/2}^{n+1} = \frac{\rho_{j+1}^n v_{j+1/2}^{n+1}}{\rho_j^n} - \frac{S_j^{n+1} \Delta x_j}{v_j \rho_j^n} \quad (25)$	Liquid Velocity	(26)
$P_j^{n+1} = P_{j-1}^{n+1} - \Delta x \left[ \frac{\rho_j^{n+1} v_j^{n+1} - \rho_j^n v_j^n}{\Delta t} + \frac{\rho_j^{n+1} (v_{j+1/2}^{n+1})^2}{\Delta x} - \frac{\rho_{j-1}^n (v_{j-1/2}^{n+1})^2}{\Delta x} - \rho_j^n g \sin \theta - \frac{f \Delta x P_w \rho_j^n (v_j^{n+1})^2}{2V} \right] \quad (42)$	Vapor Pressure	(45)

Table 6. Continued

Equation	Description	Boundary Equations
$P_j^{n+1} = P_{j+1}^{n+1} - \Delta x \left[ \frac{\rho_j^n v_j^{n+1} - \rho_j^n v_j^n}{\Delta t} + \frac{\rho_j^n (v_{j-1/2}^{n+1})^2}{\Delta x} - \frac{\rho_{j+1}^n (v_{j+1/2}^{n+1})^2}{\Delta x} - \rho_j^n g \sin \theta - \frac{\mu_{eff}^{n+1}}{\rho_j^n K A \Delta x} \right] \quad (54)$	Liquid Pressure	(57)
$-\frac{K_w}{\Delta x_{j-1}^2} T_{1,j-1}^{n+1} + \left( \frac{\rho_w C_p w}{\Delta t} + \frac{K_w}{\Delta x_{j-1}^2} + \frac{K_w}{\Delta z_1^2} + \frac{2K_w}{\Delta z_1} \right) T_{1,j}^{n+1} - \frac{K_w}{\Delta x_{j+1}^2} T_{1,j+1}^{n+1} - \frac{2K_w}{\Delta z_1^2} T_{2,j}^{n+1} = \frac{\rho_w C_p w}{\Delta t} T_{1,j}^n - H_{bc} \quad (72)$	Outer Wall Temperature	(75, 76)
$-\frac{2K_w}{3\Delta z_1^2} T_{1,j}^{n+1} - \frac{K_w}{\Delta x_{j-1}^2} T_{2,j-1}^{n+1} + \left( \frac{\rho_w C_p w}{\Delta t} + \frac{2K_w}{3\Delta z_1^2} + \frac{K_w}{\Delta x_{j-1}^2} + \frac{K_w}{\Delta x_{j+1}^2} \right) T_{2,j}^{n+1} + \frac{2R}{3\Delta z_1} T_{2,j}^{n+1} - \frac{K_w}{\Delta x_{j+1}^2} T_{2,j+1}^{n+1} - \frac{2R}{3\Delta z_1} T_{3,j}^{n+1} = \frac{\rho_w C_p w}{\Delta t} T_{2,j}^n \quad (82)$	Inner Wall Temperature	(84, 85)

Table 6. Concluded

Equation	Description	Boundary Equations
$  \begin{aligned}  & - \frac{R}{\epsilon \Delta z_2} T_{2,j}^{n+1} - \frac{Kw_{j-1}^n}{\epsilon \Delta x_{j-1}} T_{3,j-1}^{n+1} + \left( \frac{\rho_{Lj}^n Cp_{Lj}^n}{\Delta t} + \frac{1-\epsilon}{\epsilon} \rho_{wk} Cp_{wk} \right) \frac{R}{\Delta t} + \frac{R}{\epsilon \Delta z_2} \\  & \frac{Kw_{j-1}^n}{\epsilon \Delta x_{j-1}^2} + \frac{Kw_{j+1}^n}{\epsilon \Delta x_{j+1}} + \frac{R_v}{\epsilon \Delta z_2} T_{3,j}^{n+1} - \frac{Kw_{j+1}^{n+1}}{\epsilon \Delta x_{j+1}^2} T_{3,j+1}^{n+1} - \frac{R_v}{\epsilon \Delta z_2} T_{4,j}^{n+1} = \\  & \left( \frac{1-\epsilon}{\epsilon} \rho_{wk} Cp_{wk} \right) \frac{\rho_{Lj}^n Cp_{Lj}^n}{\Delta t} T_{3,j}^n + \frac{\rho_{Lj+1}^{n+1} h_{v,j+1/2} - \rho_{Lj}^{n+1} h_{v,j-1/2}}{\Delta x}  \end{aligned}  $	<p>Liquid Temperature</p>	<p>(92, 93)</p>
$  \begin{aligned}  & - \frac{R_v}{\Delta z_3} T_{3,j}^{n+1} - \frac{Kv_{j-1}^n}{\Delta x_{j-1}} T_{4,j-1}^{n+1} + \left( \frac{\rho_{vj}^n Cv_{vj}^n}{\Delta t} + \frac{R_v}{\Delta z_3} + \frac{Kv_{j-1}^n}{\Delta x_{j-1}^2} + \right. \\  & \left. \frac{Kv_{j+1}^n}{\Delta x_{j+1}} \right) T_{4,j}^{n+1} - \frac{Kv_{j+1}^{n+1}}{\Delta x_{j+1}^2} T_{4,j+1}^{n+1} = \frac{\rho_{vj}^n Cv_{vj}^n}{\Delta t} T_{4,j}^n + \frac{S_j^{n+1} h_v}{V_v} + \\  & \frac{\rho_{vj-1}^n h_{v,j-1/2} - \rho_{vj}^n h_{v,j+1/2}}{\Delta x}  \end{aligned}  $	<p>Vapor Temperature</p>	<p>(98, 99)</p>
$  - \frac{S_j^{n+1} h_v}{V_L} \quad (90)  $		



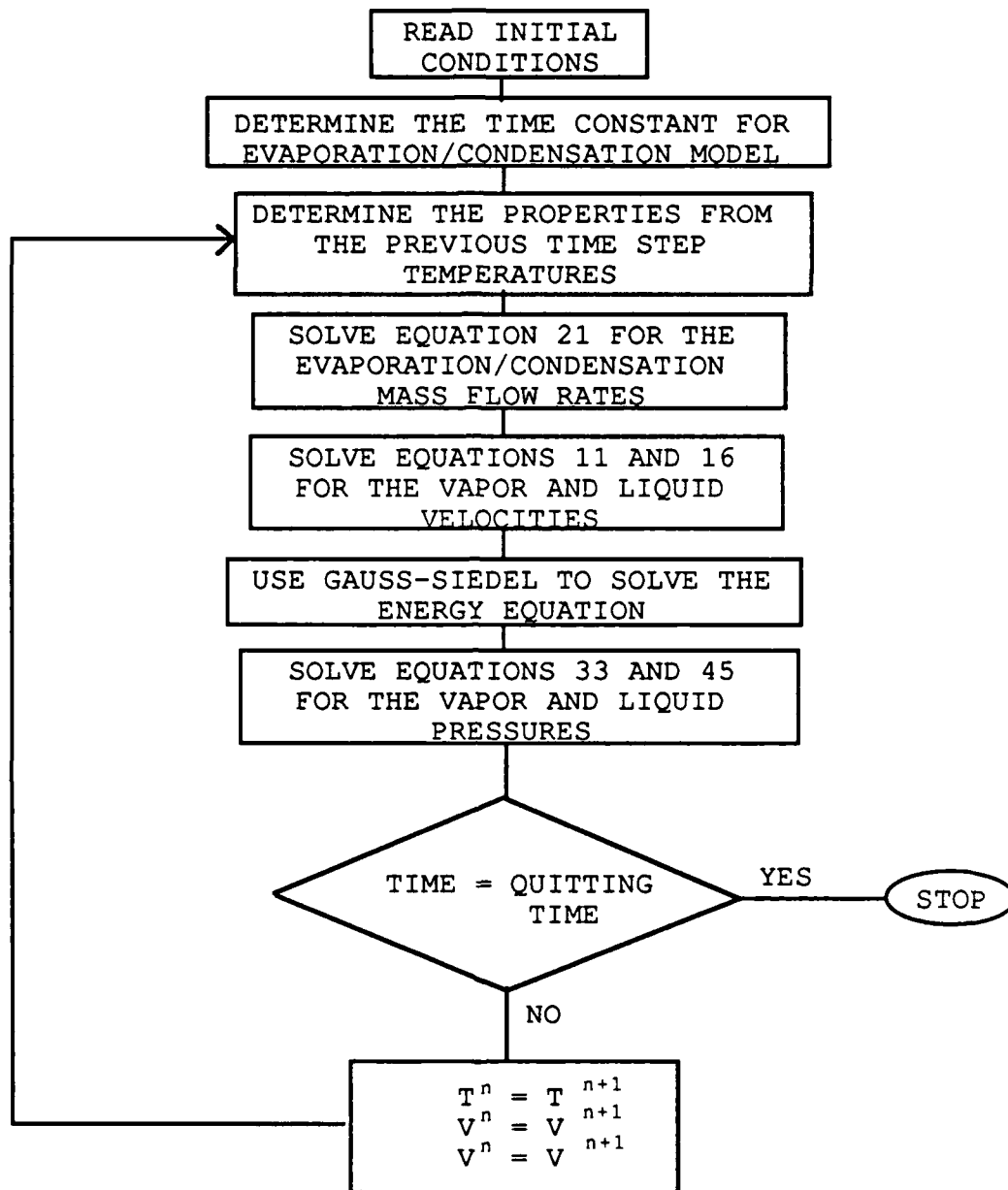


Figure 85. Flow Chart Illustrating the Solution Scheme

isothermal. The vapor region and adiabatic section are excluded since it is assumed that no temperature drops occur in these areas. The simplified model employs five nodes: the outer wall region in the evaporator section, inner wall region in the evaporator section, liquid-wick region of the evaporator and condenser sections, inner wall region of the condenser section, and outer wall region of the condenser section. The energy flux from the heater and the temperature of the coolant water serve as boundary conditions for the model. When energy conservation equations are written for each node, a five by five tridiagonal matrix is generated, which is easily solved by Gaussian-Elimination to obtain the temperature at each node. The simplified model is run through the given transient until steady-state is reached. At each time step, the stored energy that existed during that time step is saved in an array. Using values from this array at specified times in the transient, the stored energy constant,  $\lambda$ , in Equation 30 is evaluated.

The transient model begins by first calculating the thermal properties from the heat pipe initial temperature. Second, the evaporation /condensation mass flow rates are calculated for each axial location from the stored energy relationship (Equation 29). The liquid and vapor velocities are determined from the continuity equations (Equations 25 and 20). The energy equation is then solved. The solution of the energy equation provides the boundary condition,  $P_{bcv}$ , needed to solve the vapor momentum equation. The liquid and vapor pressure profiles are determined from Equations 54 and 42. At this point, if the transient has not been terminated, the previous time step's velocity, pressure, and temperature are updated with the new values and the thermal properties are evaluated for the next time step.

## 5.2 Application of the Model

Prior to discussing the results, it is important to briefly describe the steps involved in the start-up of the experimental heat pipe; for a detailed description see Section 3. First, the disassembled heat pipe is thoroughly cleaned with acetone. The wick screen is cut for the width and length of the heat pipe (0.0245 m by 2.39 m), and the wick layers are laid at the bottom of the heat pipe. It is very difficult but necessary that the screen layers be flat, since any objects or wrinkles

in the wick down will alter the vapor flow. At this point, the glass top and O-ring seal are placed on the top of the heat pipe and the vacuum pump is turned on. An O-ring is used between the glass and the heat pipe wall to ensure a good seal. Once the heat pipe is evacuated to 1.0-0.5 mtorr, the working fluid is introduced through a buret. The heat pipe is then allowed to come to thermodynamic equilibrium with ambient conditions. During this process, boiling occurs in the wick. It has been observed that part of the working fluid condenses on the glass top during this process. With this start-up procedure, it is difficult to determine exactly how much liquid remains in the wick. Once equilibrium is established, the heater is quickly brought to power and the coolant water pump is started.

The use of water as the working fluid in an aluminum heat pipe produces hydrogen. Prior to the start of a transient run, the hydrogen and other noncondensable gases are removed from the heat pipe by the vacuum pump. The amount of water vapor removed during this process is not well known. However, the amount of hydrogen evolved during the transient run has been found to be small and is not felt to significantly impact transient results.

### 5.2.1 Initial Conditions

Knowledge of the exact initial conditions of the TAMU heat pipe prior to start-up is crucial. For both transient cases, the initial conditions of the heat pipe and thermal properties of the heat pipe materials are given in Table 7. An initial fluid charge of 250 mL of water was injected into the heat pipe. As previously mentioned, the amount of fluid that remained in the wick was not directly determined. The wick structure consisted of four layers of 18 by 18 stainless steel mesh. The height of the wick structure and the distance between mesh layers are calculated and not measured for the present report. The mesh has a pore opening of  $9.906 \times 10^{-4}$  m and a wire diameter of  $4.318 \times 10^{-4}$  m. From Equation 1, these values give a maximum capillary pumping head of  $186 \text{ N/m}^2$  with the surface tension evaluated at 323 K ( $s = 67.93 \times 10^{-3} \text{ N/m}$ )<sup>22</sup>. As shown in Figure 2, the heat pipe sections have the following lengths: evaporator = 0.60 m, adiabatic = 0.15 m, and condenser = 1.64 m. The width of the heat pipe vapor space is 0.0254 m and the aluminum walls are 0.003175 m thick. The heat pipe has no

Table 7. Initial Conditions and Thermal Constants

Initial Conditions	
Working Fluid	Water
Initial Charge	250 mL
Number of Mesh Layers	4
Stainless Steel Mesh Size	18 x 18
Width of Mesh Pore Opening	0.0009906 m
Mesh Wire Diameter	0.0004318 m
Coolant Temperature	293 K
Initial Heat Pipe Temperature	293 K
Coolant Mass Flow Rate	0.126 kg/s
Evaporator Length	0.6 m
Adiabatic Length	0.15 m
Condenser Length	1.64 m
Heat Pipe Vapor Space Width	0.0254 m
Heat Pipe Wall Thickness	0.003175 m
Angle of Tilt	0.0 radians

Table 7. Concluded

Thermal Constants	
Stainless Steel Conductivity	17.3 w/m-K
Stainless Steel Density	8000 kg/m <sup>3</sup>
Stainless Steel Specific Heat	447 J/kg-K
Wall Conductivity	205 w/m-K
Wall Density	875 J/kg-K
Wall Specific Heat	2770 kg/m <sup>3</sup>
Coolant Conductivity	0.603 w/m-K
Coolant Prandtl Number	6.95
Coolant Viscosity	0.001002 N-s/m <sup>2</sup>

angle of tilt measured from the horizontal axis for the transients described herein. The coolant water pump produces a mass flow rate of 0.126 kg/s. It should be noted that the electric heater and water coolant jacket cover the length of the evaporator and condenser sections, respectively.

### 5.2.2 Results at Two Hours Into the Transient

The experimental heat pipe was run through a transient of two hours for both power input cases. At two hours there seemed to be no change with time in the heat pipe temperatures which were being measured at 12 axial locations via thermocouples. The experimenter believed that the heat pipe had reached steady-state and turned the heater off.

To compare the numerical model to the experimental data, the computer code, HPTAC (Heat Pipe Transient Analysis Code), was run for identical conditions for both transients. The number of nodes used and important calculated parameters for both cases are presented in Table 8. Since the amount of liquid in the wick during the start-up was not determined experimentally, the code was run with various fluid charges. These results are illustrated for the two cases in Figures 86 and 87. In both figures, there are plots of an experimental heat pipe run (EXP. DATA) and an experimental conduction run (EXP. CDCT.). The experimental "conduction run" is an experiment in which no fluid is used in the heat pipe. This was done to illustrate the greater efficiency of the heat pipe in transporting energy as opposed to a metal rod. The numerical results are illustrated by the dashed lines for various fluid charges. As seen in both figures, there are significant differences between the experiment and numerically generated results.

A complete description of the experimental heat pipe performance is in Section 3. The following is a preliminary discussion.

First consider the solid line with circles in Figure 86. This line represents the outer wall temperature data taken at steady-state with a 250-W power input, a cooling water temperature of 293 K, the heat pipe glass cover in place and sealed, a vacuum of 1.0-0.5 mtorr in the pipe, and no working fluid in the pipe. Under these conditions, the presumption is that all power input to the evaporator is conducted through the pipe outer wall to the heat sink (condenser). Power is

Table 8. Important Parameters Used or Calculated in the Numerical Model

	Case I	Case II
Power Input	250 W	100 W
Number of Axial Evaporator Nodes	8	8
Number of Axial Adiabatic Nodes	2	2
Number of Axial Condenser Nodes	10	10
Fluid Charge Used for the Reference Curves	100 ml	180 ml
Coolant Heat Transfer Coefficient	$543.9 \text{ W/m}^2\text{-K}$	$543.9 \text{ W/m}^2\text{-K}$
Wick Permeability	$9.08 \times 10^{-9} \text{ m}^2$	$9.68 \times 10^{-8} \text{ m}^2$
Stored Energy Time Constant	$0.01332 \text{ 1/s}$	$0.007323 \text{ 1/s}$
Time Step	1.0 s	1.0 s

**LEGEND**  
 --- 76 ML  
 - - - 80 ML  
 - - - 85 ML  
 - - - 90 ML  
 - - - 100 ML  
 - - - EXP. DATA  
 - - - EXP. CDCT.

Q = 250 WATTS  
 TC = 293.00 K  
 TIME = 2 HOURS  
 EVAP. = 0.00-0.60 M  
 ADIA. = 0.60-0.76 M  
 COND. = 0.76-2.39 M

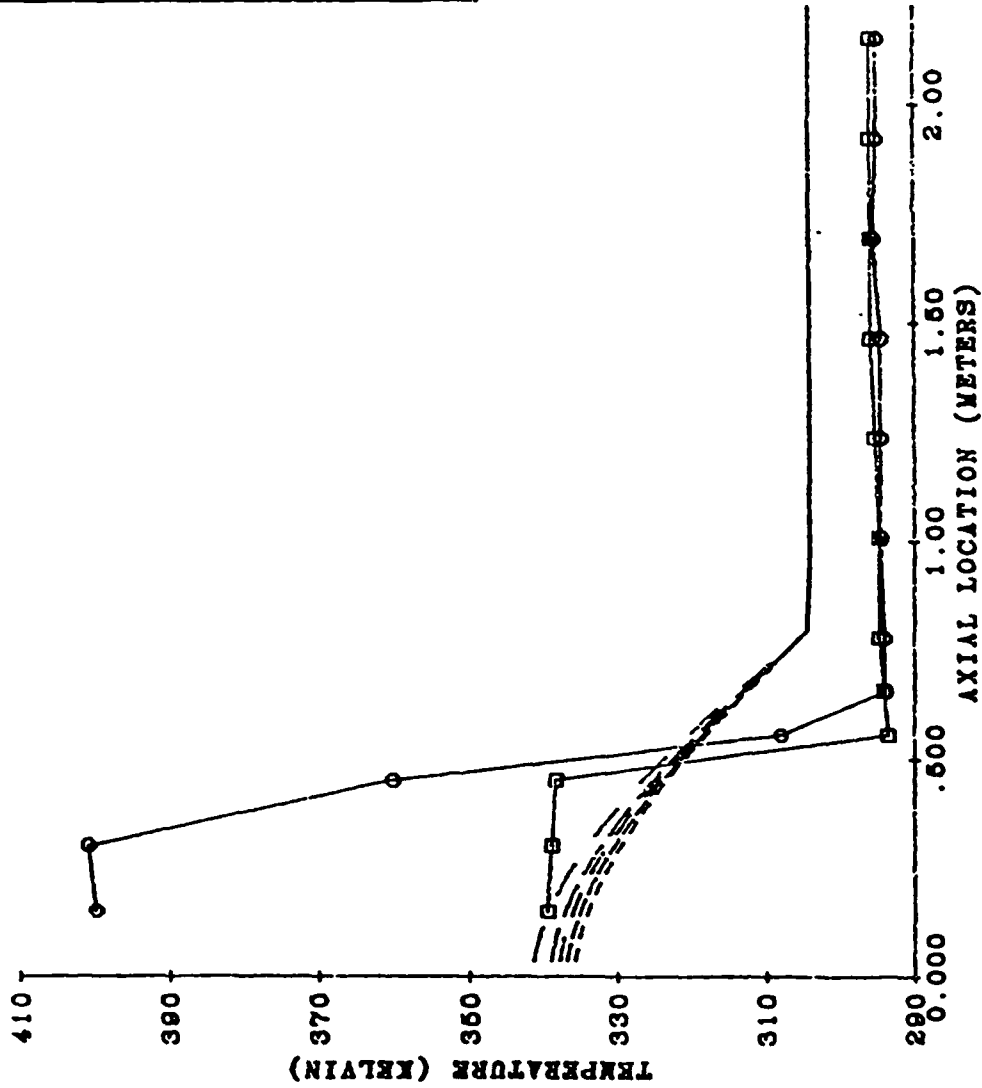


Figure 86. Computed Outer Wall Temperature Profiles for Various Fluid Charges Compared with Experimental Data for a Power Input of 250 W

**LEGEND**

- - - - - 100 ML  
 - - - - - 120 ML  
 - - - - - 140 ML  
 - - - - - 160 ML  
 - - - - - 180 ML  
 - - - - - EXP. DATA  
 - - - - - EXP. CDCT.

Q = 100 WATTS  
 TC = 293.00 K  
 TIME = 2 HOURS  
 EVAP. = 0.00-0.60 M  
 ADIA. = 0.60-0.76 M  
 COND. = 0.76-2.39 M

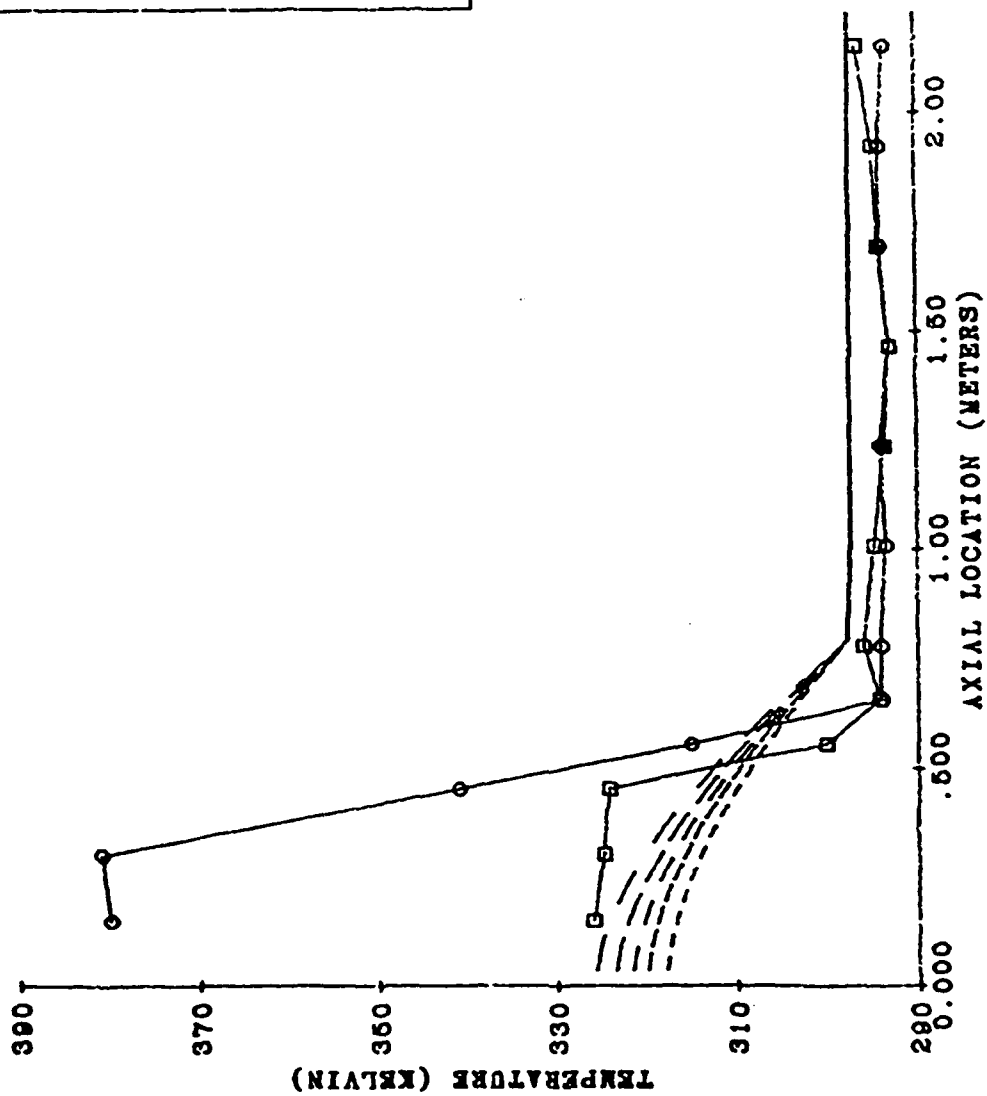


Figure 87. Computed Outer Wall Temperature Profiles for Various Fluid Charges Compared with Experimental Data for a Power Input of 100 W

input uniformly to the evaporator. The temperature distribution in the evaporator should therefore be roughly parabolic with the peak temperature occurring at the outer end of the evaporator and a zero slope of the temperature profile at that point. The temperature profile should be linear through the adiabatic region since the pipe is well insulated, and should slope very sharply in the condenser region which is designed to be an infinite heat sink at 293 K.

The actual data show that the condenser does seem to be uniform in temperature, but at 293 K! If this is exactly true, it means that there is no convective energy transport to the coolant. Thus, if conduction is occurring in the condenser wall, very little energy seems to be going to the coolant.

Considering the adiabatic region, we see a sharp temperature decrease at the evaporator end, but a flat temperature profile in the condenser half-side of the adiabatic region. This may indicate that the energy being conducted from the evaporator is being carried to the condenser cooling jacket via the rather thick support side walls of the heat pipe rather than through what is called the "outer" wall.

Considering the temperatures in the evaporator region, we see that the profile is roughly parabolic; however, the peak temperature seems to occur at about the midpoint of the evaporator. This means that as much energy is being conducted to the outer end of the evaporator as is being conducted to the condenser end, the presumed sole heat sink for the heat pipe! There thus seems to be significant energy loss out the evaporator end of the pipe. We now shift our attention to the solid line with squares, the presumed operating heat pipe condition.

The condenser is again seen to be at a uniform 293 K throughout. This suggests that condensation is not occurring in this region, as in fact there is no difference in the condenser temperature between the "operating" and "conduction only" modes. The adiabatic region temperature does change in the operating compared with the "conduction only" mode. The temperature at the evaporator end of the adiabatic region drops to the condenser temperature and the adiabatic region is at a uniform temperature throughout. This may mean that there is some heat pipe action in the adiabatic region. Similarly, the evaporator region is seen to be at a uniform temperature about 40 deg hotter than the adiabatic region. Nonetheless, the temperature in the evaporator region is uniform and about 60

deg cooler than it was when "conduction only" was the presumed energy transfer mechanism. The fact that the evaporator is at a uniform temperature and cooler than the "conduction only" case indicates that the heat pipe action is occurring. The evaporator portion of the pipe is very likely operating in a thermosiphon mode, rejecting energy through the vertical walls and end of the heat pipe. There seems to be little axial energy transport by vapor or liquid motion in the pipe.

As previously mentioned, problems arise in identifying the amount of liquid in the wick. Since it is not apparent whether the heat pipe was operating under the conditions for which it was designed, the amount of liquid present is uncertain. It should be remembered, however, that the purpose of the numerical model is to gain a better understanding of the thermal hydraulic performance of a heat pipe. With this in mind, fluid charges of 100 ml and 180 ml are used as the reference charges for the 250- and 100-W cases, respectively, to generate the temperature, velocity, and pressure profiles. These values were selected since they produce temperatures which correspond closely with the first thermocouple's temperature in the evaporator, as shown in Figures 86 and 87. It should be noted that the capillary limit, given by Equation 1, would be exceeded for charges less than 80 ml in the 250-W case.

The actual fluid charge is very important in determining the temperature, pressure, and velocity profiles. Since the distance between wick layers is not known, it is assumed that they are equally spaced by a distance dependent on the fluid charge. This distance and the fluid charge greatly affect the permeability value, as shown by Equation 43. A larger pressure drop in the liquid region will result from a smaller permeability value. In addition, the fluid charge affects the pressure drop through the volume fraction. Smaller liquid volume fractions cause higher liquid velocities, which in turn cause larger pressure drops. For the assumed wick-liquid model, the pressure drop in the liquid phase will increase as the fluid charge decreases through the effects of permeability and volume fraction. Moreover, as fluid charge increases, the stored energy constant decreases due to the larger thermal capacitance.

The temperature profiles for the 250- and 100-W runs are illustrated in Figures 88 and 89, respectively. It can be seen that there are very small temperature drops between the outer wall and inner wall regions and between the liquid and vapor regions. The small temperature drop between the liquid and

**LEGEND**

 OUTER WALL  
 INNER WALL  
 LIQUID  
 VAPOR

Q = 250 WATTS  
 TC = 293.00 K  
 TIME = 2 HOURS  
 EVAP. = 0.00-0.60 M  
 ADIA. = 0.60-0.75 M  
 COND. = 0.75-2.39 M

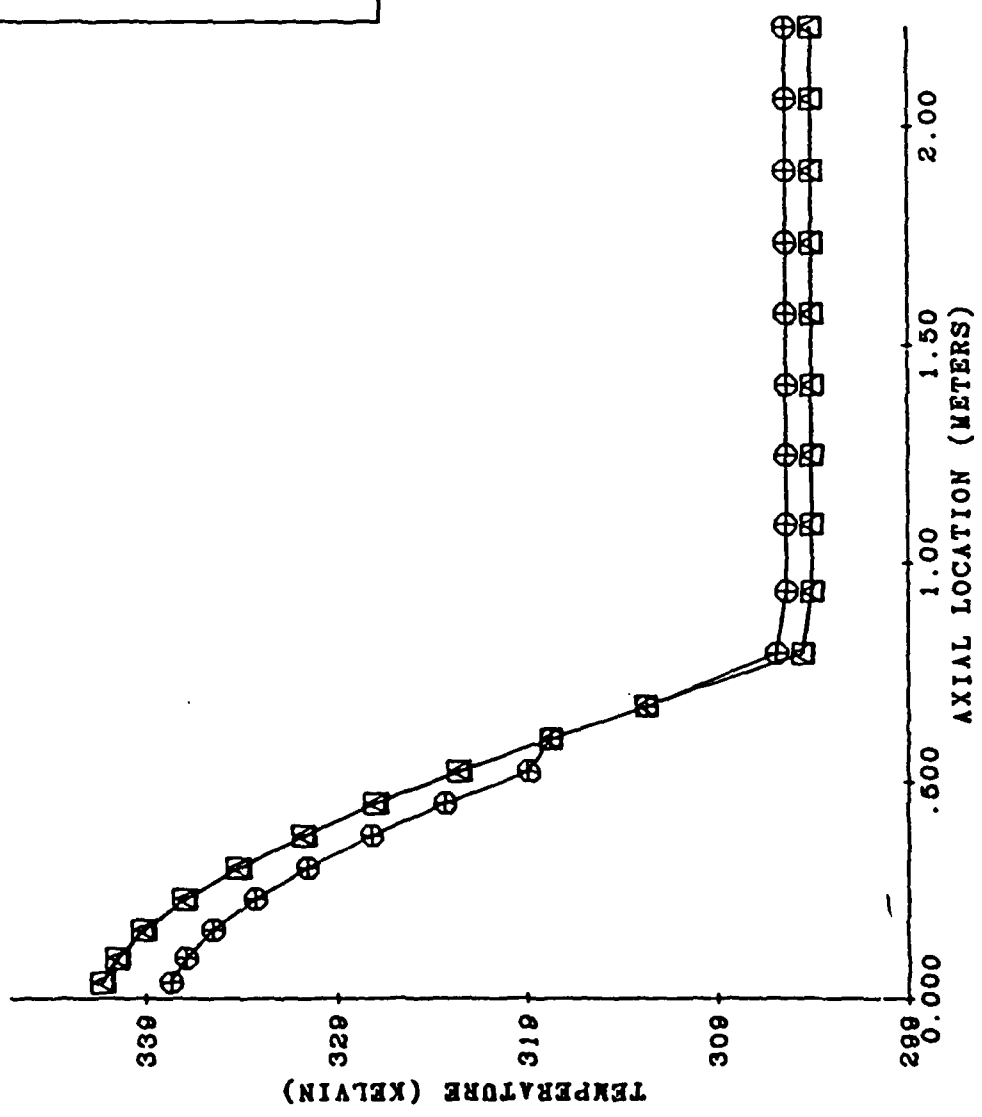


Figure 88. Heat Pipe Temperatures at Different Radial Locations for a Power Input of 250 W and a Fluid Charge of 100 ml

**LEGEND**

- OUTER WALL
- △ INNER WALL
- LIQUID
- ⊕ VAPOR

Q = 100 WATTS  
 TC = 293.00 K  
 TIME = 2 HOURS  
 EVAP. = 0.00-0.60 M  
 ADIA. = 0.60-0.75 M  
 COND. = 0.75-2.39 M

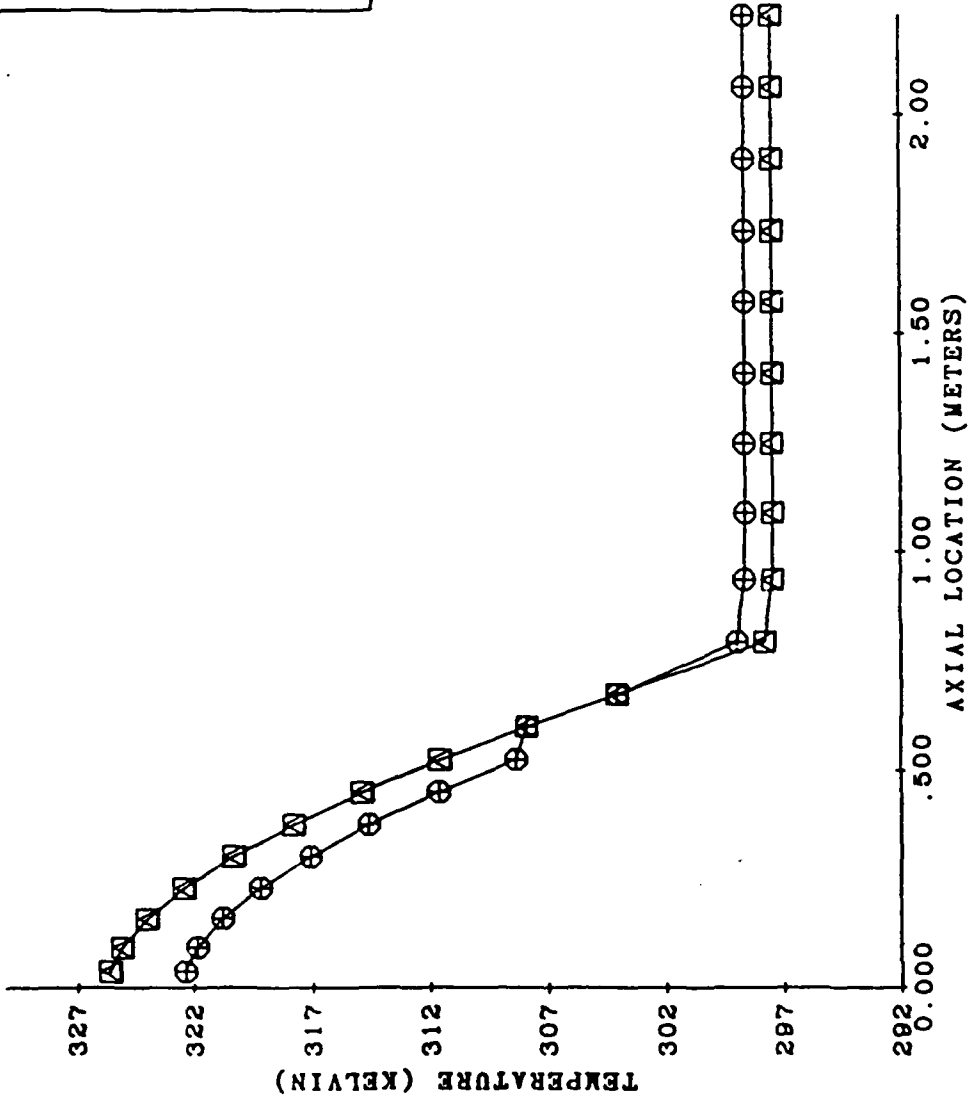


Figure 89. Heat Pipe Temperatures at Different Radial Locations for a Power Input of 100 W and a Fluid Charge of 180 ml

vapor regions is as predicted by theory<sup>11</sup>. The small temperature drop between the outer and inner wall regions is due to the extremely small distance between the nodes ( 0.0016 m) and the high thermal conductivity of aluminum (Table 7). Investigation of Figures 88 and 89 shows a change in the liquid and vapor temperature gradients in the evaporator section compared with the adiabatic section. This is due to neglecting radial energy transport in the adiabatic region. Since there is no energy gain or loss in the adiabatic region, the temperature differences between radial nodes become negligible as steady-state is reached. This phenomenon requires the slopes to change as indicated by the dog-leg at 0.5 m.

The pressure profiles are illustrated for the 250- and 100-W cases in Figures 90 and 91. The liquid and vapor profiles in Figure 90 are similar to the profiles shown in Figure 4. The vapor pressure decreases through the evaporator due to acceleration and friction forces. It continues to drop in the adiabatic section due to frictional forces and then increases in the condenser due to acceleration pressure gains. The liquid pressure drop is primarily due to friction forces. The effect of the change in velocity can be seen in these profiles since the curves are nonlinear. In Figure 91, however, the vapor pressure falls below the liquid pressure. This phenomenon has been noted by Ernst<sup>47</sup>, and would require the meniscus in the wick to be convex. Although this is possible in principle, it is unlikely to occur in reality since there is an excess of liquid in the condenser region under normal heat pipe operating conditions<sup>11</sup>. If this phenomenon occurs in simulations, the practice has been to set the vapor pressure equal to the liquid pressure, thus disregarding any pressure recovery.

The vapor and liquid velocity profiles for both the 250- and 100-W cases are shown in Figures 92 through 95. These profiles are characteristic of those predicted by theory<sup>11</sup>. No measured velocity profiles are available for comparison. It should be noted that if the steady state maximum velocity (0.0025 m/s) is used to calculate the velocity front and the front is assumed to begin at the adiabatic-condenser interface, the front would have traveled only 18 m in the 2-h transient for the 250-W run. The liquid would travel 4 m in the 100-W transient. The distances and velocities are not proportional due to the charge-permeability model.

Three-dimensional plots of temperature versus time versus distance for the

**LEGEND**

--- VAPOR  
 - - - LIQUID

Q = 250 WATTS  
 TC = 293.00 K  
 FL. CHARGE = 100 mL  
 TIME = 2 HOURS  
 EVAP. = 0.00-0.60 M  
 ADIA. = 0.60-0.75 M  
 COND. = 0.76-2.38 M

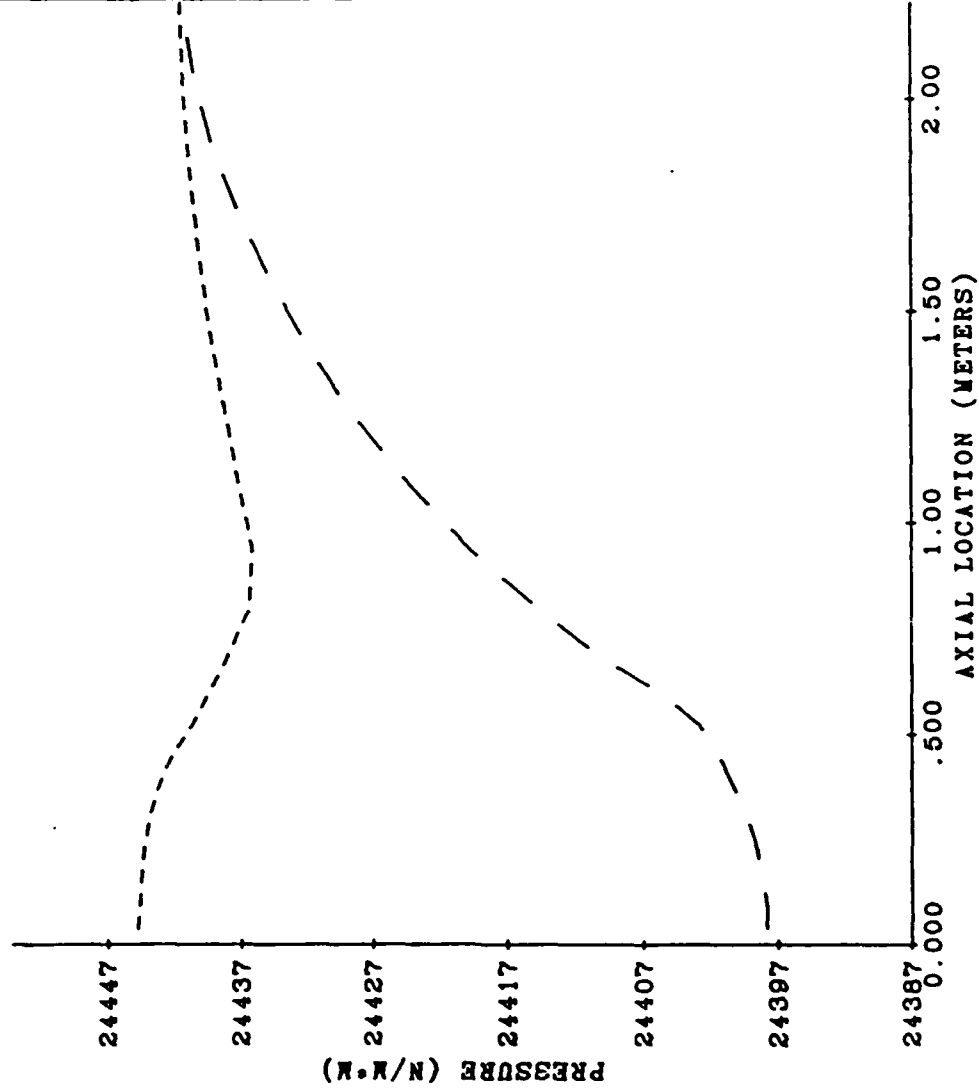


Figure 90. Liquid and Vapor Pressure Profiles for a Power Input of 250 W and a fluid charge of 100 ml

**LEGEND**  
 - - - - VAPOR  
 - - - - LIQUID

Q = 100 WATTS  
 TC = 293.00 K  
 FL. CHARGE = 180 mL  
 TIME = 2 HOURS  
 EVAP. = 0.00-0.60 M  
 ADIA. = 0.60-0.75 M  
 COND. = 0.76-2.39 M

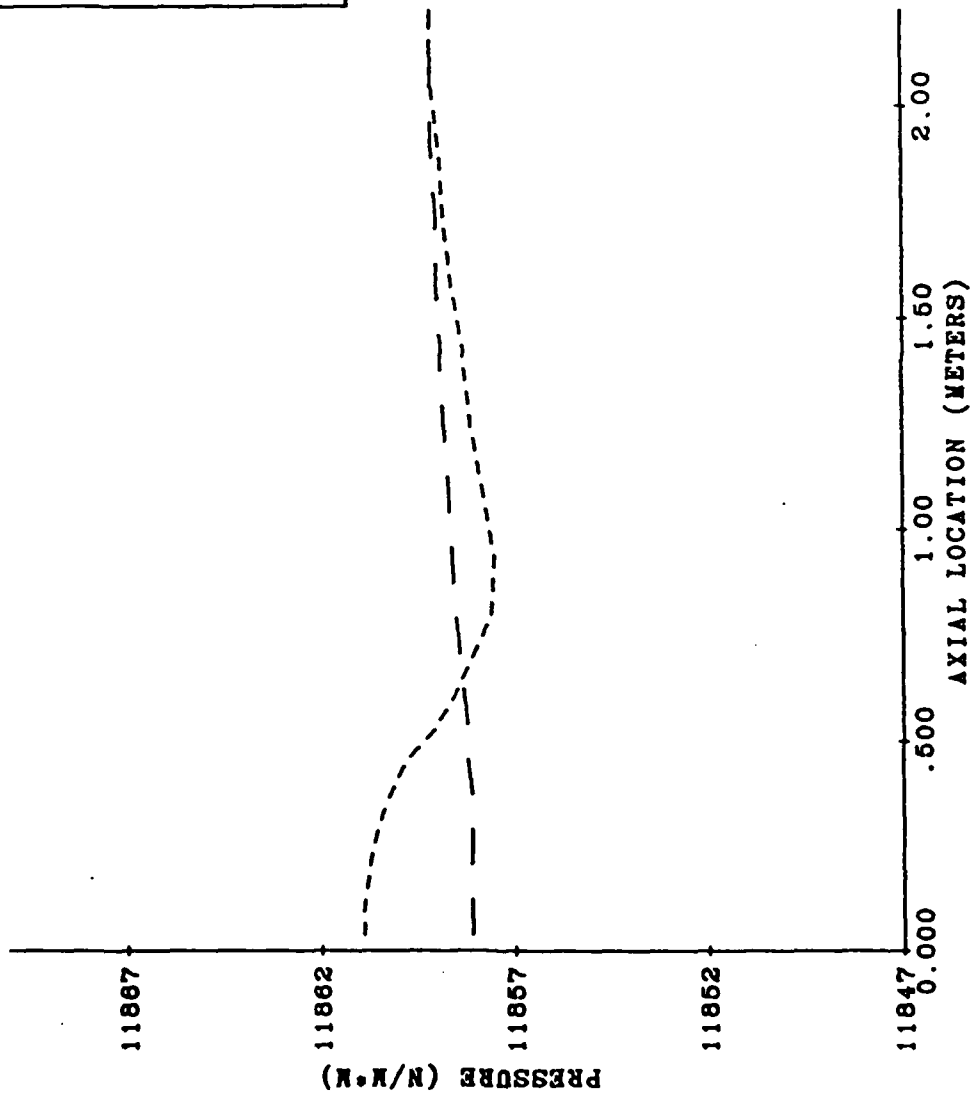


Figure 91. Liquid and Vapor Pressure Profiles for a Power Input of 100 W and a fluid charge of 180 ml

**LEGEND**  
 --- VAPOR  
 Q = 250 WATTS  
 TC = 293.00 K  
 FL. CHARGE = 100 mL  
 TIME = 2 HOURS  
 EVAP. = 0.00-0.60 M  
 ADIA. = 0.60-0.75 M  
 COND. = 0.75-2.39 M

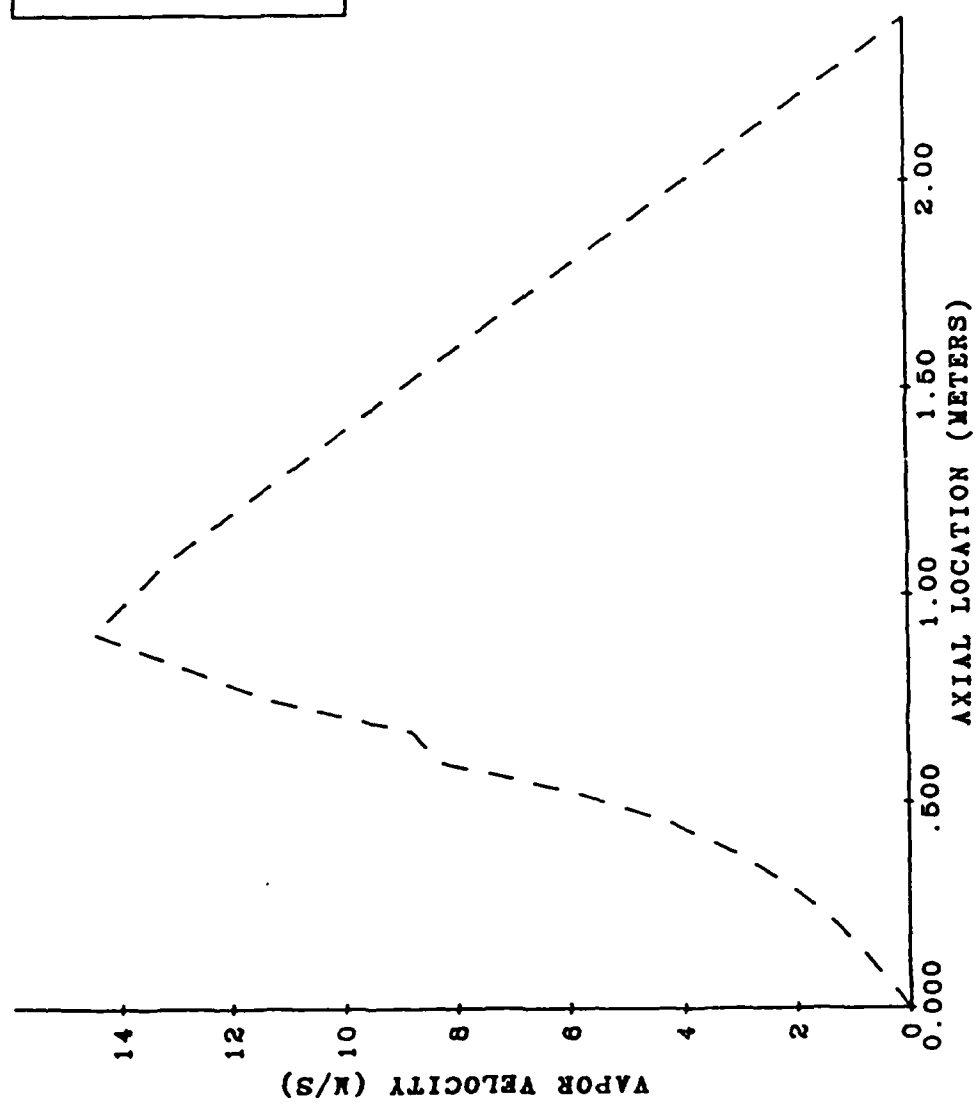


Figure 92. Vapor Velocity Profile for a Power Input of 250 W and a Fluid Charge of 100 ml

**LEGEND**

--- LIQUID

Q = 250 WATTS  
 TC = 293.00 K  
 FL. CHARGE = 100 mL  
 TIME = 2 HOURS  
 EVAP. = 0.00-0.60 M  
 ADIA. = 0.60-0.75 M  
 COND. = 0.75-2.39 M

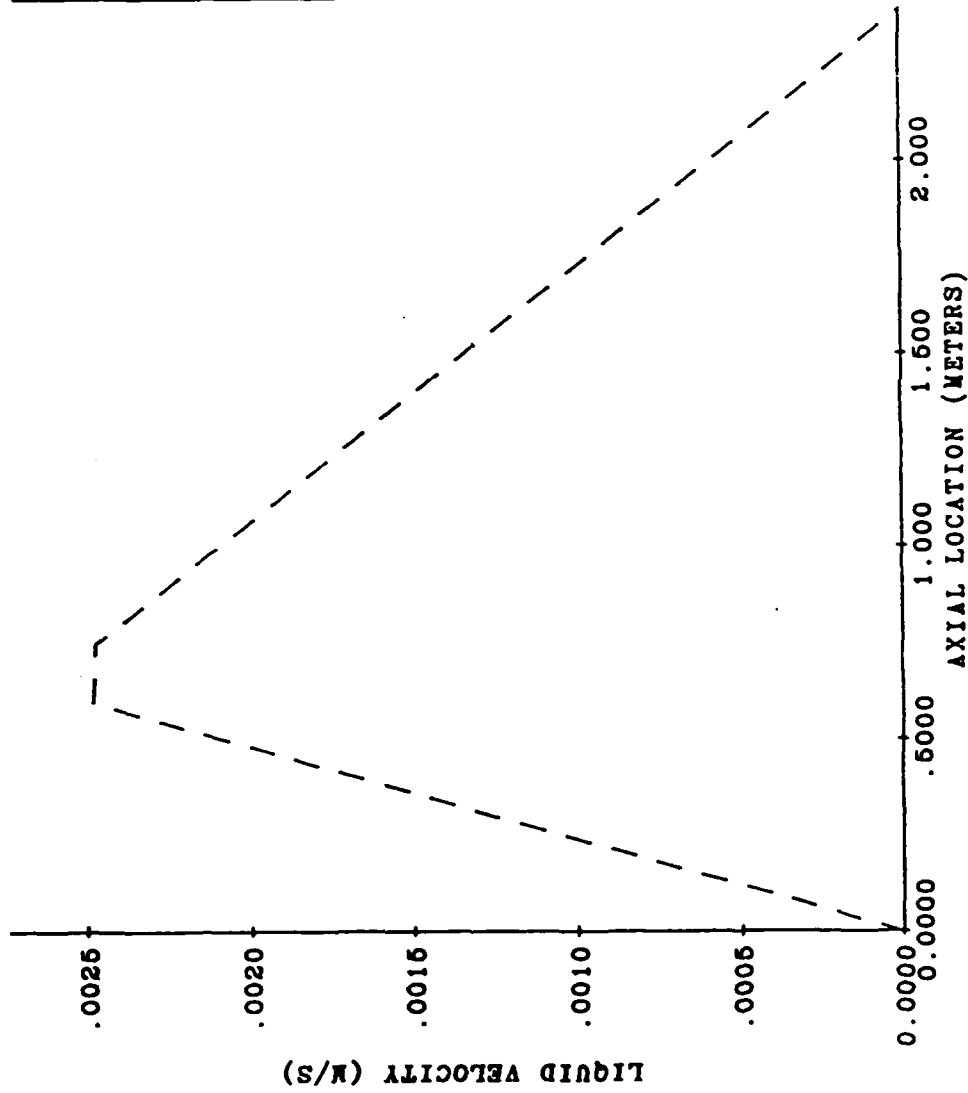


Figure 93. Liquid Velocity Profile for a Power Input of 250 W and a Fluid Charge of 100 ml

**LEGEND**  
 --- VAPOR  
 Q = 100 WATTS  
 TC = 293.00 K  
 FL. CHARGE = 180 ML  
 TIME = 2 HOURS  
 EVAP. = 0.00-0.60 M  
 ADIA. = 0.60-0.75 M  
 COND. = 0.75-2.39 M

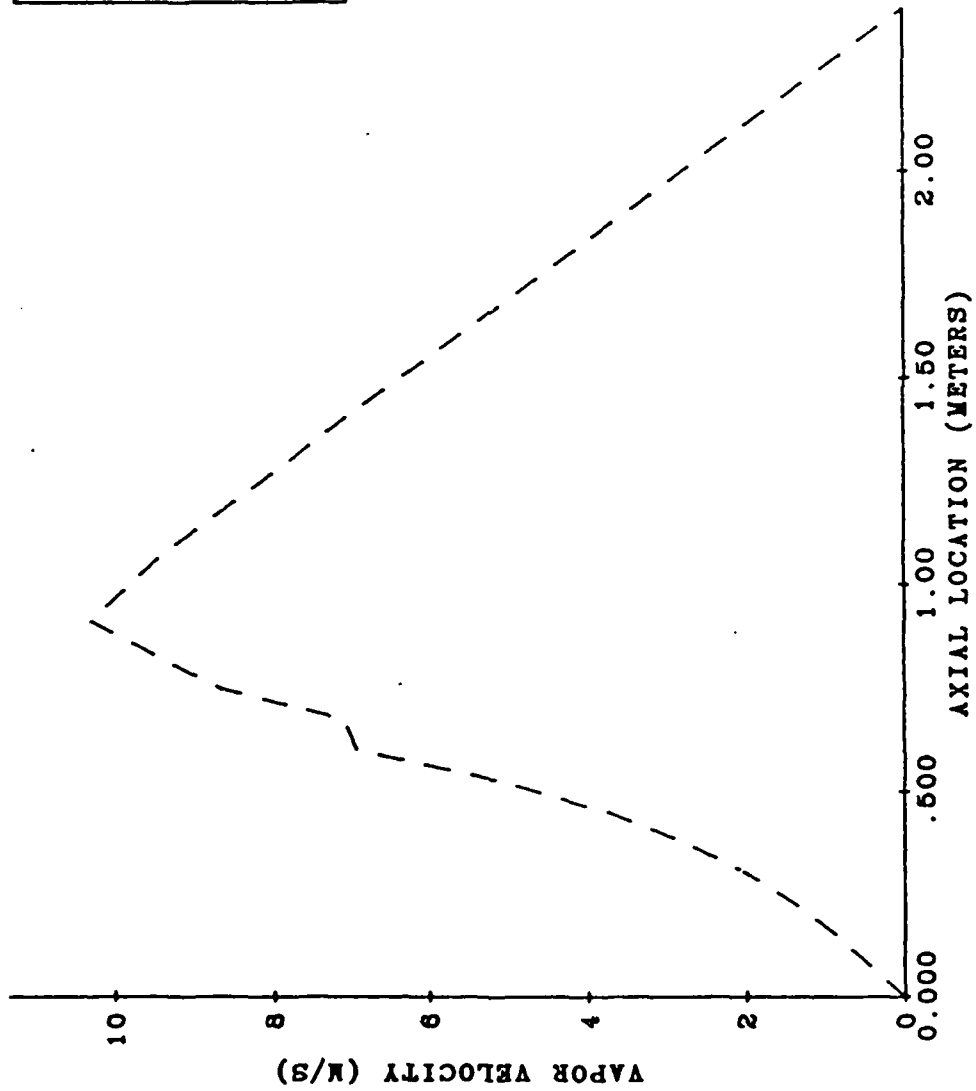


Figure 94. Vapor Velocity Profile for a Power Input of 100 W and a Fluid Charge of 180 ml

**LEGEND**  
 --- LIQUID  
 Q = 100 WATTS  
 TC = 293.00 K  
 FL. CHARGE = 180 mL  
 TIME = 2 HOURS  
 EVAP. = 0.00-0.60 M  
 ADIA. = 0.60-0.75 M  
 COND. = 0.75-2.39 M

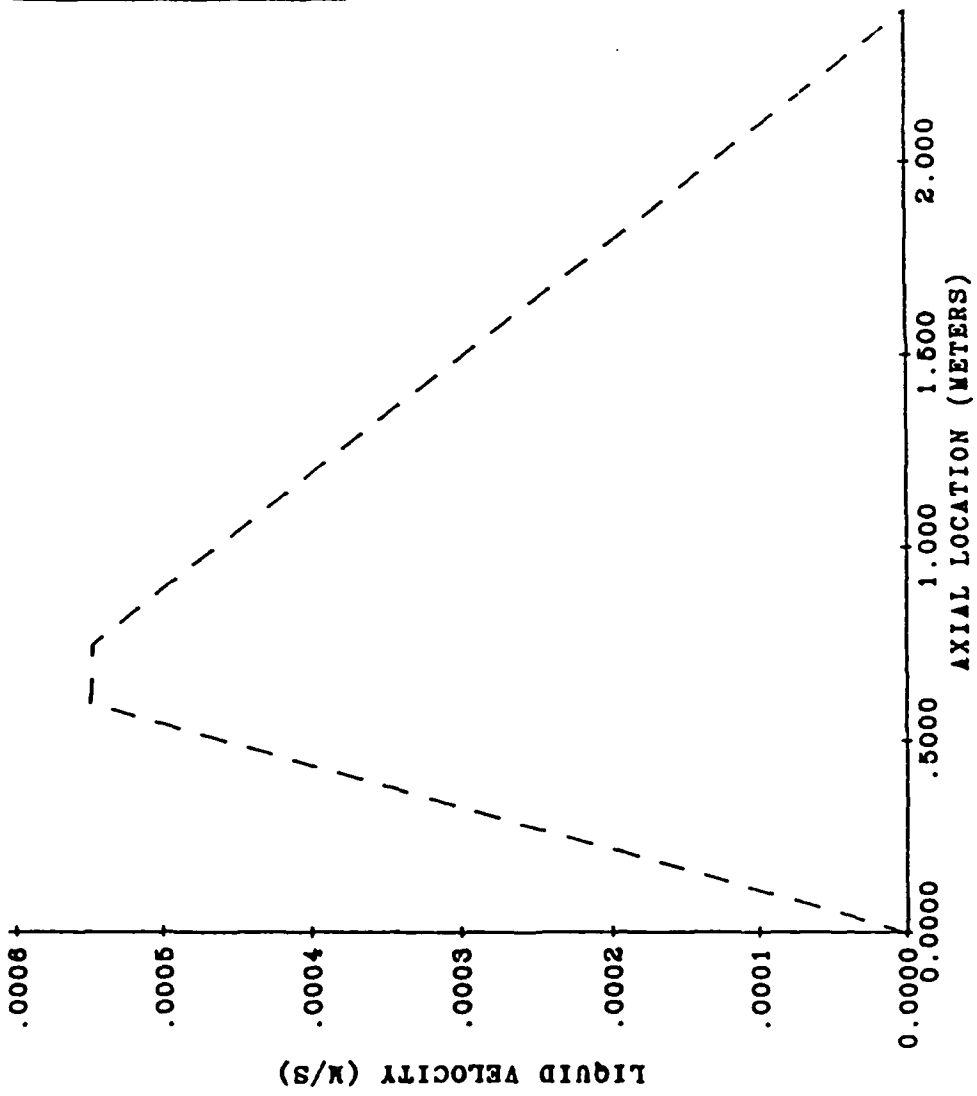


Figure 95. Liquid Velocity Profile for a Power Input of 100 W and a Fluid Charge of 180 ml

outer wall, liquid, and vapor regions are shown in Figures 96 through 101. The temperature plots illustrate the heat pipe response using an exponential stored energy model. In each case, the temperature initially rises quickly since there is little evaporation and all the input energy goes into sensible temperature increases. As time increases, the evaporation/condensation mass flow rate increases and approaches the steady-state value. This causes the temperature in the evaporator to drop. In addition, the cooler liquid from the condenser begins to return to the evaporator. The figures show that the evaporator section continues to drop in temperature even at the 2-h point, although the rate at which the temperature drops is decreasing. If this model were run to steady-state, the temperatures in the evaporator and adiabatic sections will drop until the vapor region becomes almost isothermal at the temperature of the condenser.

### 5.3 Summary

Subsection 5.1 presented the development of a transient heat pipe computational model. The development included the application and simplification of the continuity, momentum, and energy equations for a wicked water heat pipe. A simplified stored energy model was used to calculate the transient evaporation and condensation rates.

The analysis presented in Subsection 5.2 contains many uncertainties. The two principal uncertainties are: the mode in which the experimental heat pipe operated and the amount of liquid in the wick prior to the transient. These uncertainties would have to be resolved in order to accurately compare the numerical model with the experimental data. Although these uncertainties exist, pressure and velocity profiles have been generated which agree qualitatively with theory. The temperature overshoot seen in the evaporator is thought to be due to the use of an exponential model for stored energy. This phenomena has not been demonstrated experimentally.

The next section will present conclusions for the results of this report and will summarize the overall report. Furthermore, suggestions for future work will be made.

**LEGEND**

Q = 250 WATTS  
 TC = 293.00 K  
 FL. CHARGE = 100 mL  
 EVAP. = 0.00-0.60 M  
 ADIA. = 0.60-0.75 M  
 COND.. = 0.75-2.39 M

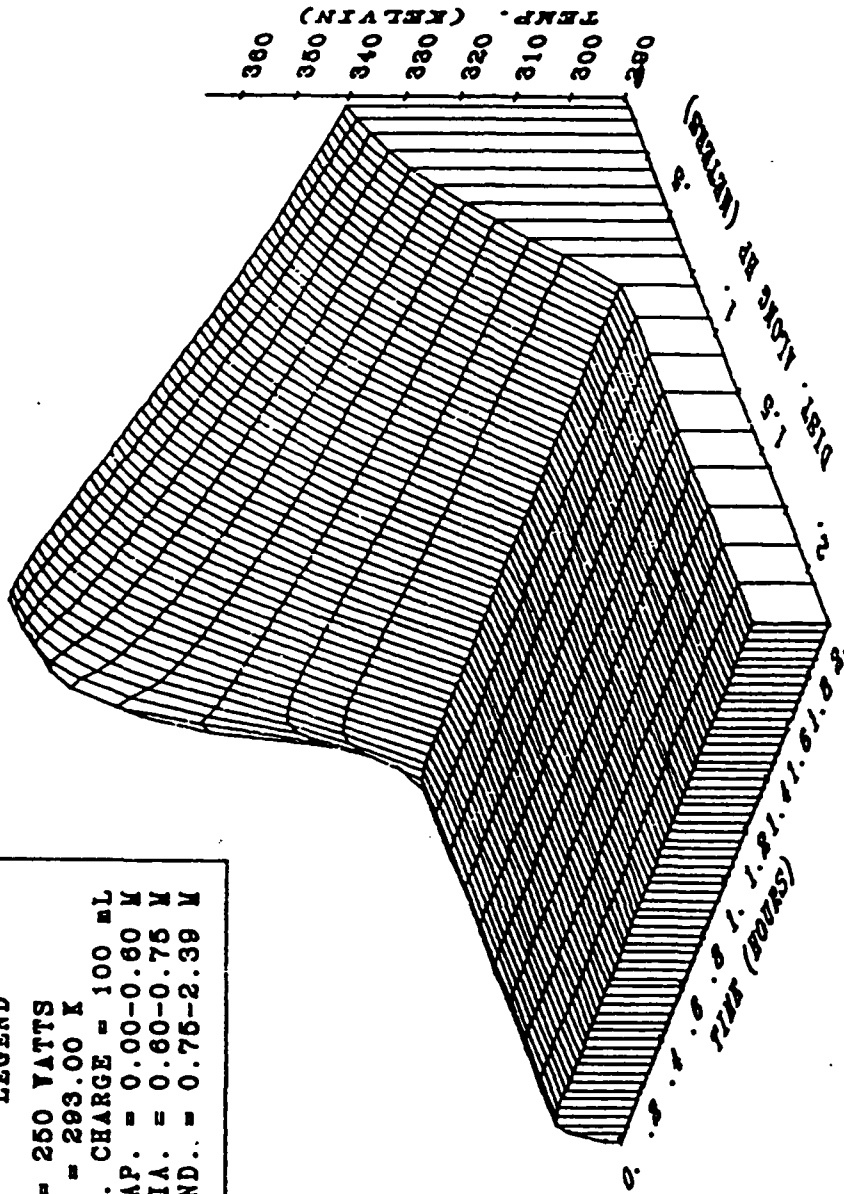


Figure 96. Outer Wall Temperature Profiles for a Power Input of 250 W and a Fluid Charge of 100 ml

**LEGEND**

Q = 100 WATTS  
 TC = 293.00 K  
 FL. CHARGE = 180 mL  
 EVAP. = 0.00-0.60 M  
 ADIA. = 0.60-0.75 M  
 COND. = 0.75-2.39 M

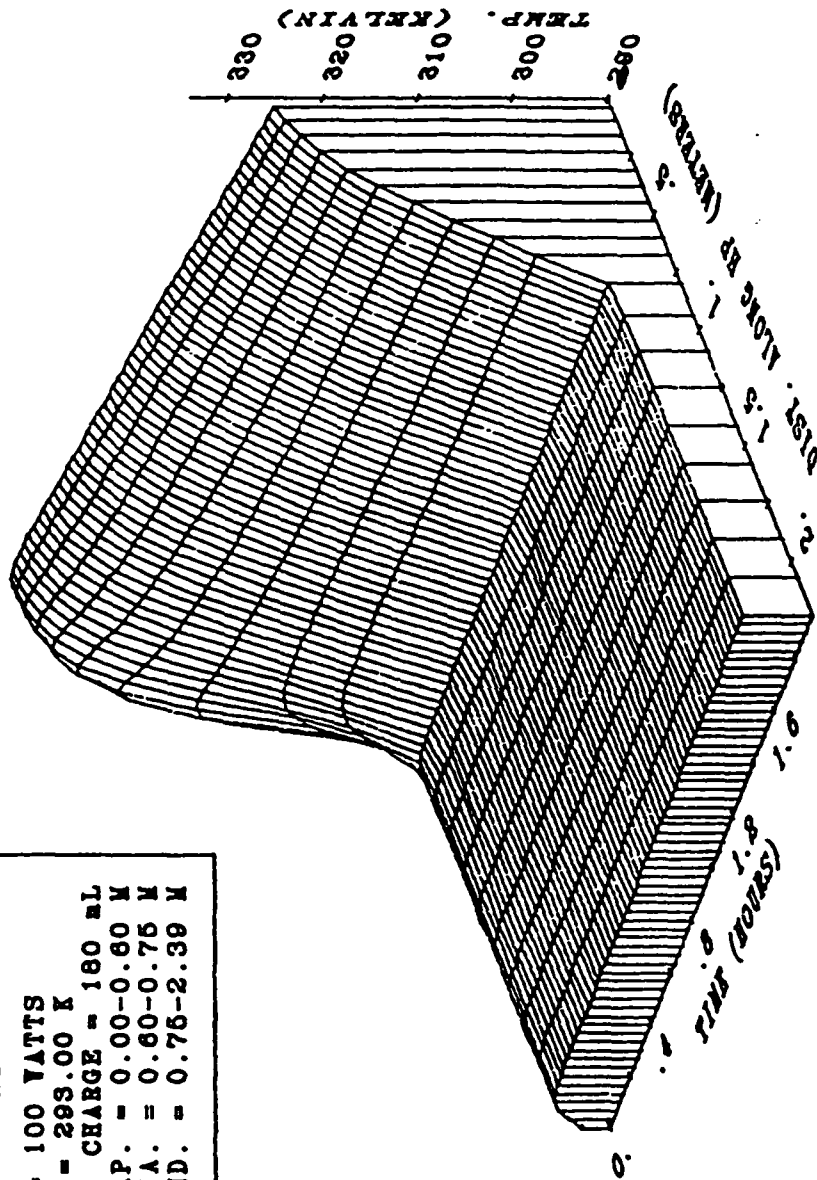


Figure 97. Outer Wall Temperature Profiles for a Power Input of 250 W and a Fluid Charge of 180 ml

**LEGEND**  
 Q = 250 WATTS  
 TC = 293.00 K  
 FL. CHARGE = 100 mL  
 EVAP. = 0.00-0.60 M  
 ADIA. = 0.60-0.75 M  
 COND. = 0.75-2.39 M

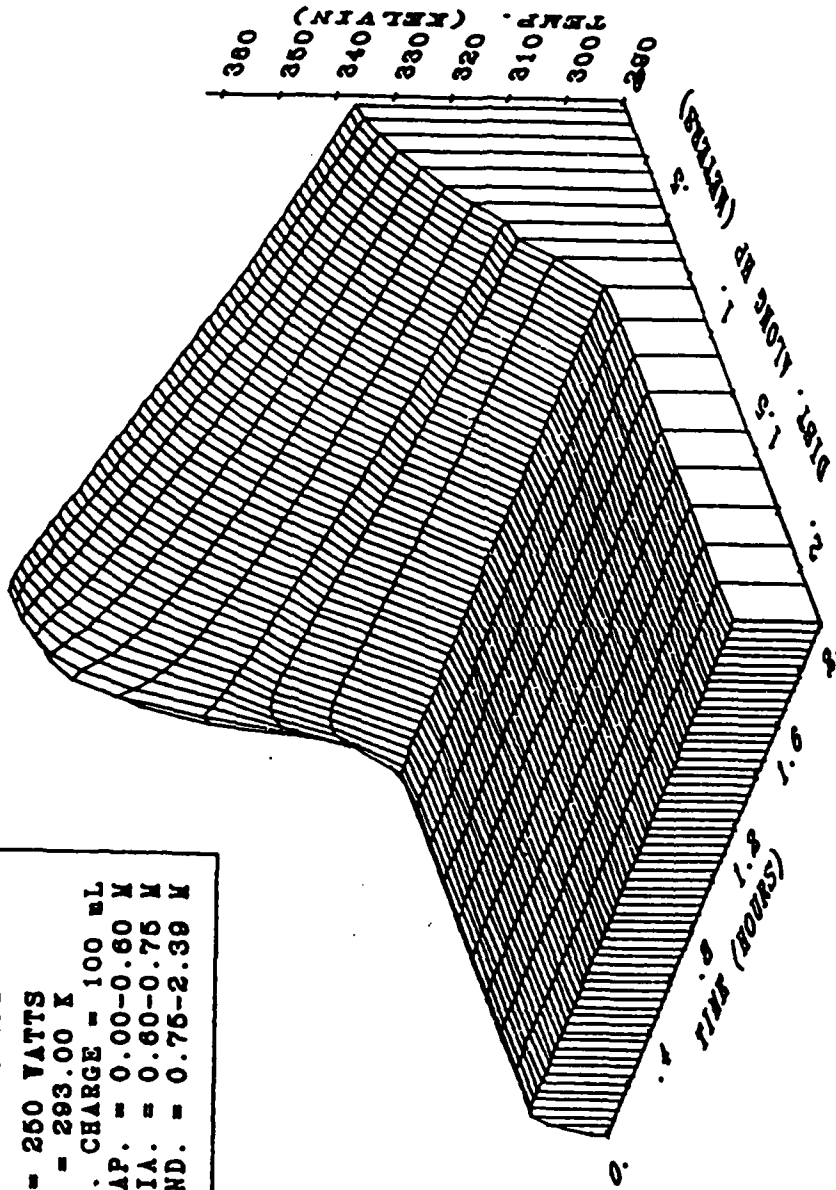


Figure 98. Liquid Temperature Profiles for a Power Input of 250 W and a Fluid Charge of 100 ml

**LEGEND**

Q = 100 WATTS  
 TC = 293.00 K  
 FL. CHARGE = 180 mL  
 EVAP. = 0.00-0.60 M  
 ADIA. = 0.60-0.75 M  
 COND. = 0.75-2.39 M

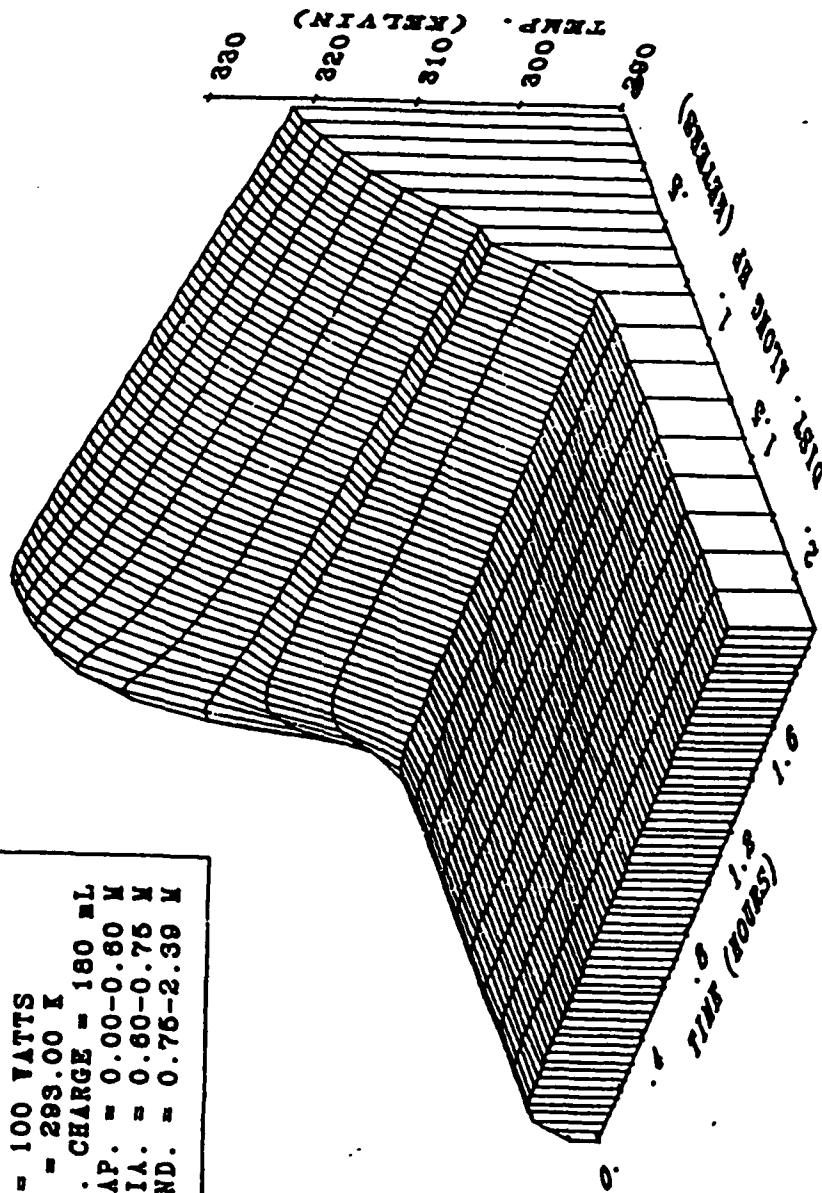


Figure 99. Liquid Temperature Profiles for a Power Input of 250 W and a Fluid Charge of 180 ml

**LEGEND**  
 Q - 250 WATTS  
 TC - 293.00 K  
 FL. CHARGE - 100 mL  
 EVAP. - 0.00-0.60 M  
 ADIA. - 0.60-0.75 M  
 COND. - 0.75-2.39 M

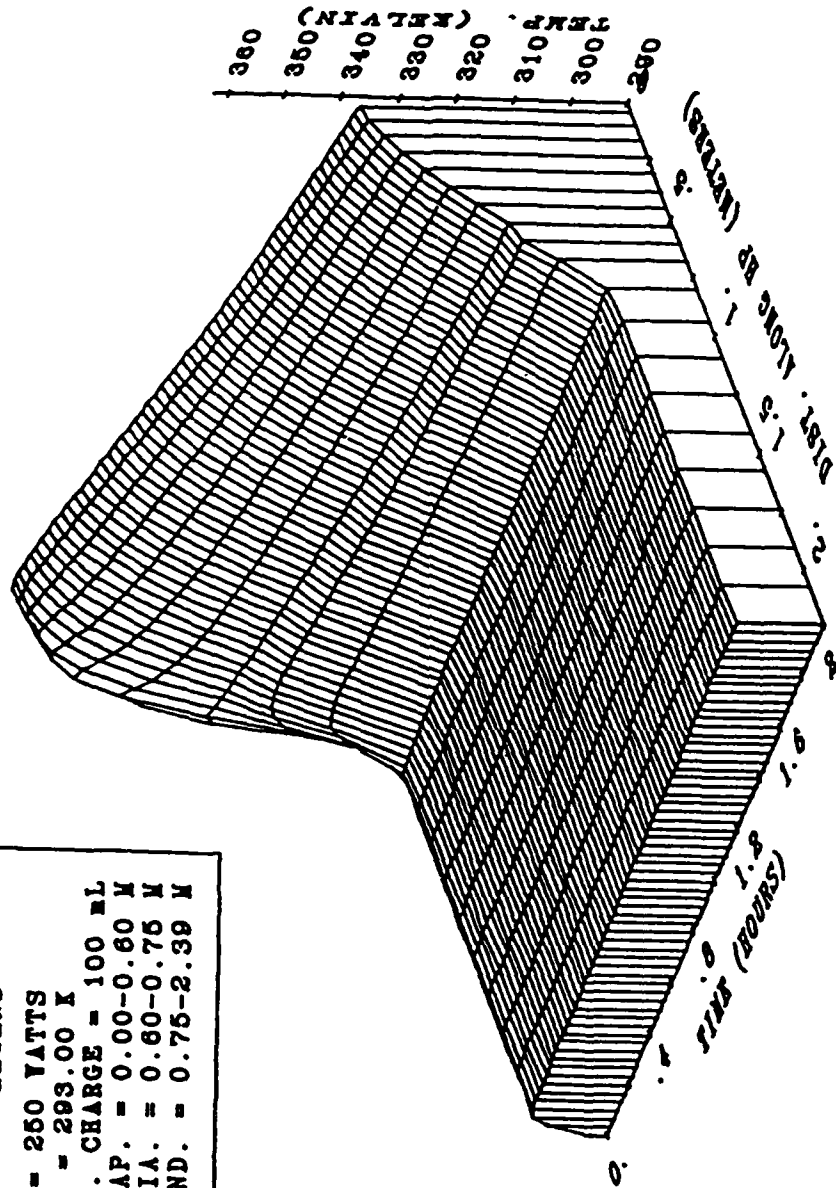


Figure 100. Vapor Temperature Profiles for a Power Input of 250 W and a Fluid Charge of 100 ml

**LEGEND**  
 Q = 100 WATTS  
 TC = 293.00 K  
 FL. CHARGE = 180 mL  
 EVAP. = 0.00-0.60 M  
 ADIA. = 0.60-0.75 M  
 COND. = 0.75-2.39 M

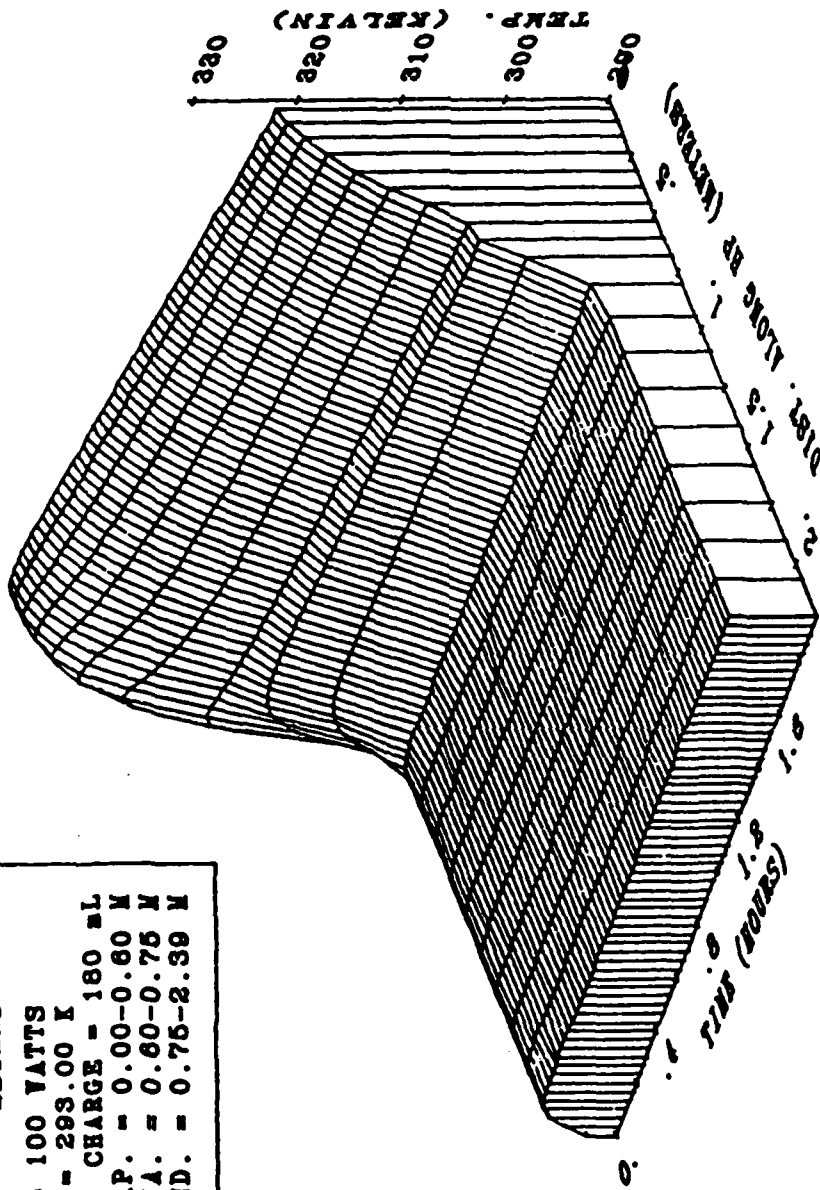


Figure 101. Vapor Temperature Profiles for a Power Input of 250 W and a Fluid Charge of 180 ml

## 6.0 CONCLUSIONS AND RECOMMENDATIONS

Three different sets of experiments have been performed to investigate the transient nature of heat pipes and failures that may occur in those transients. The first set, described in Section 2, studied the entrainment phenomena. In a glass-walled heat pipe air was blown over wetted wick material in order to determine the onset of entrainment. The experimental results presented indicate that the Weber number can be used to predict the point at which the liquid in a wick becomes unstable, but not necessarily when liquid is physically removed from the wick. Also, it is possible that the reversal of flow in the wick without removal of liquid from the wick could be the actual inception of the entrainment limit, and previous measurements of entrainment carried out by listening for the sounds of drops impinging on the end of the condenser would overestimate this limit.

The second set of experiments described in Section 3 used a specially designed heat pipe with a rectangular cross section, flat mesh-type wick and a clear top through which internal mechanisms of heat pipe operation could be observed. The transient conditions observed were start-up and load change. Thermocouples on the outside of the pipe and inside the vapor space were used to measure temperature profiles during operation and a data acquisition system was used to concurrently display and record all measurements as the experiments ran.

A series of runs was performed to verify proper operation as a heat pipe. Several start-ups were then performed from zero power and ambient conditions to power levels of 100 and 250 W. Three start-ups to 100 W confirmed expected phenomena; in each case a time delay was seen due to stored energy effects before any response was noted, followed by an exponential temperature increase to equilibrium at the new power level with an equilibrium temperature distribution inside and outside the pipe. In addition, it was shown that the temperature along the instrumented length of the vapor channel remained uniform throughout the start-up. Startup to 250 W showed no departure from the behavior established by 100-W start-ups, with the exception of higher equilibrium temperature distributions corresponding to the higher power level.

Finally, one run was performed by taking the heat pipe from one operating power level to another. The heat pipe was started up with a 100-W energy input and allowed to come to equilibrium. This start-up behaved exactly as would be expected based on the prior start-ups to the same power level. In this case, however, the input power was then increased to 250 W, and the heat pipe was allowed to reestablish equilibrium at this new power level. Following the power increase, a short lived transient was observed in the vapor channel, resulting in a sharp temperature increase in the evaporator and a drop in temperature in the condenser, both of which returned shortly thereafter to their previous states. Analysis of the vapor temperature and pressure data in the heat pipe leads to the hypothesis of a temporary wick dryout, followed by a rewetting of the wick and resumption of normal operation as a possible explanation of the observed behavior. Boiling was not seen in the evaporator wick.

In the third set of transient experiments presented in Section 4, vapor space and wick/liquid temperatures and internal pressure were measured. A normal start-up experiment was performed, as was an experiment with step changes in input power levels. Two frozen start-ups were then performed. In another experimental series, the pipe was brought to steady-state conditions with a power input of 25 W, and the secondary coolant temperature was lowered until the heat pipe working fluid froze and the evaporator wick dried out. Finally, data were obtained on a step decrease in power input to the evaporator.

The start-up from zero power to 100 W behaved normally and as predicted by theory. In the start-up from zero to 50 W the wick in the evaporator dried out but was rewetted and the pipe continued to behave as predicted by theory after the rewet. The dry out and rewetting of the wick was not predicted by theory, however. This is similar to the temporary dry out observed in Section 3, but the duration of the temporary dry out was much longer here. The reason for the dry out is not confirmed, but it is suspected that the wick in the evaporator was not fully wetted when the transient began. Still, this is of interest for heat pipe start-up operation because of the potential for failure during the start-up. When the power input was increased from 50 W to 100 W the heat pipe reacted normally, with an initial increase in temperatures, and eventually reached steady-state conditions. This is also what happened when the power was increased from 100 to 200 W. When the power level was increased again from 200 to 250 W, there was a

partial but unrecoverable dry out in the wick of the evaporator.

The two frozen start-ups were performed with water as the initially frozen working fluid and with a step increase of 0 to 100 W. In both cases the working fluid in the evaporator wick melted and evaporated, and eventually the wick in the evaporator dried out. The working fluid in the condenser remained frozen for the entire transient, and the adiabat working fluid partially melted until the evaporator was completely dried out. At this point the working fluid in the adiabat that had melted refroze. When the evaporator wick was completely dry, there was a simultaneous drop in the condenser and adiabat temperatures. The first frozen start-up took longer to dry out than the second, and the suspected reason is that there was more frozen working fluid in the evaporator wick in the first than in the second frozen start-up.

When the thawed pipe was brought to steady-state conditions with a power input of 25 W, the pipe behaved as predicted by theory as it was cooled down by a decreasing secondary coolant temperature; that is, decreasing accordingly in temperature until the internal temperature of the pipe neared freezing. The pipe stayed at a uniform temperature near the freezing point of the working fluid, water, until the condenser working fluid started freezing. This freezing was accompanied by the beginning of dry out in the evaporator wick. Eventually the entire evaporator dried out and the entire condenser froze. The adiabat working fluid was partially frozen and partially liquid before the evaporator was completely dry. After this dry out, except for the portion of the adiabat nearest the evaporator, the adiabat working fluid was completely frozen. These unique data on frozen heat pipes show there are many parameters to be considered in frozen start-ups of a heat pipe, including the power input, secondary coolant temperature and amount of working fluid in the wick.

Finally, in the step power decrease from 250 to 0 W, the pipe behaved as would be expected by theory.

In addition to the experimental work, a multinodal, implicit, finite difference model, Heat Pipe Transient Analysis Code (HPTAC), has been developed to simulate heat pipe rapid transients and was presented in Section 5. The mass, momentum and energy conservation equations are employed to generate the velocity, pressure and temperature profiles in a heat pipe. A lumped capacitance exponential model for stored energy is used in order to achieve a solution for the

thermal hydraulic phenomena associated with a heat pipe.

The numerical model is unique in that it accounts for the fraction of input energy that goes into stored energy through the use of a simplified transient energy storage model which drives a spatial complex convection/conduction model. This approach was developed in order to correct the errors of previous steady-state models and to avoid the tight coupling required by kinetic theory models. Since this model is a function of time only, the 1-D mass and momentum conservation equations are solved directly, while the 2-D energy conservation equation is solved using a Gauss-Siedel scheme.

The HPTAC code was developed to solve the finite difference equations describing a heat pipe. This model was applied to the heat pipe of Section 3 in order to compare calculated results with the experimental data. The temperature drops expected in transient heat pipe operation were predicted by the numerical model. Since the amount of liquid in the actual wick was poorly known, velocity and pressure profiles for both the liquid and vapor regions were generated using best fit values for the fluid charge. These profiles agreed with existing theory. The pressure profiles illustrate the effect of friction and acceleration forces on the vapor and liquid phases. These profiles were used to eliminate some fluid charges for which the capillary limit would be exceeded. In addition, comparison of the two reference transient cases demonstrates that a larger pressure drop results from a smaller fluid charge for the liquid-wick model used. The velocity profiles illustrate the effects of uniform evaporation and condensation fluxes.

The exponential energy storage model generated transient temperature profiles that have not been experimentally confirmed. In the calculated profiles, temperature rises quickly after the start of the transient until evaporation and condensation begin to reach steady-state values. At this point, the temperature begins to drop and will continue to decrease until the entire vapor region becomes almost isothermal. This behavior is inherent in using an exponential function to model the rate at which evaporation/condensation vary with time. The value of the stored energy time constant greatly affects the temperature overshoot. This report hypothesized that an estimate for this parameter could be determined from a transient calculation using a simplified energy storage equation. However, since this approach produces the overshoot just described, it appears that the model underpredicts the value of the stored energy time

constant,  $\lambda$ . A larger value of  $\lambda$  would cause the evaporation/condensation mass flow rate to increase at a faster rate. This would result in a much smaller temperature overshoot, if any. The magnitude of  $\lambda$  could be made large enough so that the stored energy term goes to zero. Effectively, this would be equivalent to using steady-state theory. This would eliminate the temperature overshoot, but would greatly underestimate the transient response of the heat pipe. In conclusion, the value of the stored energy time constant has a large effect on the heat pipe transient. Until more accurate predictions of  $\lambda$  can be made, this model of evaporation/condensation is useful only as a tool with which to gain a better understanding of the thermal hydraulic behavior of a heat pipe.

The phenomena controlling heat pipe operation discussed in Sections 3 and 4 could not have been identified without the simultaneous observation of outer wall and vapor temperatures, vapor pressure and visual checks utilized in this experiment. It is vital that researchers consider the implications of internal transients, initially undetected by external means, in modeling heat pipe performance.

In the analysis of frozen start-ups, it is felt that the most immediate concern should be in determining the relative roles that the secondary coolant temperature, power input, and amount of working fluid in the wick play in the transient.

## REFERENCES

1. F. R. Best and R. Wick, "Measurement and Analysis of Mission Required Rapid Heat Pipe Transients Using Internal Optical Observations," Unsolicited Proposal to the Air Force from Texas A&M University Nuclear Engineering Dept., College Station, Texas (1984).
2. C. J. Camarda, "Analysis and Radiant Heating Tests of a Heat-Pipe-Cooled Leading Edge," NASA TN D-8468, Langley Research Center, Hampton, Virginia (1977).
3. J. E. Deverall, E. S. Keddy, J. E. Kemme, and J. R. Phillips, "Gravity-Assist Heat Pipes for Thermal Control Systems," LA-5985-MS, Los Alamos National Laboratory, Los Alamos, New Mexico (1975).
4. G. T. Colwell, "Prediction of Cryogenic Heat Pipe Performance," Final Report, NASA Grant NSG-2054, Georgia Institute of Technology, Atlanta, Georgia (1977).
5. J. E. Deverall and J. E. Kemme, "Satellite Heat Pipe," LA-3278, Los Alamos National Laboratory, Los Alamos, New Mexico (Sept. 1970).
6. J. E. Deverall, E. W. Salmi, and R. J. Knapp, "Orbital Heat Pipe Experiment," LA-3714, Los Alamos National Laboratory, Los Alamos, New Mexico (1967).
7. R. S. Gaugler, General Motors Corp., Dayton, Ohio, US Patent Application, Dec. 21, 1942, Published US Patent No. 2350348, (June 6, 1944).
8. G. M. Grover, US Atomic Energy Commission, Los Alamos, New Mexico, "Evaporation-Condensation Heat Transfer Device," United States Patent No. 3229759, (Jan. 18, 1966).
9. G. M. Grover, T. P. Cotter, and G. F. Erikson, "Structure of Very High Thermal Conductance," J. Appl. Phys., 35 (6), pp 1990-1991, (1964).

10. T. P. Cotter, "Theory of Heat Pipes," LA-3246-MS, Los Alamos National Laboratory, Los Alamos, New Mexico (1965).
11. P. Dunn and D. A. Reay, Heat Pipes, Pergamon Press, Oxford, (1978).
12. C. A. Busse, "Heat Pipe Research in Europe", 2nd Int. Conf. on Thermionic Elec. Power Generation, Stresa, Italy, Report EUR 4210, f, e: 1969, pp 461 - 475, (May 1968).
13. D. Chisholm, The Heat Pipe, Mills and Boon Ltd., London (1971).
14. W. Bienert and P. J. Brennan, "Transient Performance of Electrical Feedback-Controlled Variable Conductance Heat Pipes," Dynatherm Corporation, Cockeysville, Maryland, ASME paper 71-Av-27 (1971).
15. C. C. Roberts and K. T. Feldman Jr., "Predicting Performance of Heat Pipes with Partially Saturated Wicks," Bell Telephone Laboratories, Naperville, Illinois, 72-WA/HT-38 (1972).
16. Y. Kamotani, "User's Manual for Thermal Analysis Program of Axially Grooved Heat Pipe (HTGAP)," NASA Johnson Space Center, Clear Lake, Texas, NAS 1.26:170563 (1978).
17. S. Drouilhet and J. Buchlin, "An Experimental and Numerical Study of an Air-To-Air Heat Exchanger Using Liquid Reservoir Variable Conductance Heat Pipes," von Karman Institute for Fluid Dynamics, Rhode St. Genèse, Belgium, AD-A113 354/5(1982).
18. F. C. Prenger Jr., "Heat Pipe Computer Program (HTPIPE) User's Manual," Los Alamos National Laboratory, Los Alamos, New Mexico, LA-8101-M (1979).
19. D. C. Kane, Analytical Treatment of Gravity Effects on Gas Loaded Variable Conductance Heat Pipes, Master's Thesis, Naval Postgraduate School, Monterey, Ca. (1980).

20. W. A. Davis Jr., Optimization of an Internally Finned Rotating Heat Pipe, Master's Thesis, Naval Postgraduate School, Monterey, Ca. (1980).
21. H. J. Su, "Heat Transfer in Porous Media with Fluid Phase Changes," Lawrence Berkeley Laboratory, Berkeley California, LBL-13187 (1981).
22. A. F. Kleinholz, Analysis of Smooth and Axially Finned Rotating Heat Pipe Condensers, Master's Thesis, Naval Postgraduate School, Monterey, Ca. (1983).
23. G. A. McLennan, "A Computer Code for the Simulation of Heat Pipe Operation," Argonne National Laboratories, Argonne, Illinois, ANL-83-108 (1983).
24. K. N. Shukla, "Transient Response of a Gas-Controlled Heat Pipe," AIAA Progress in Astronautics and Aeronautics Series (1980).
25. W. S. Chang, Heat Pipe Startup from the Supercritical State, Ph. D. Thesis, Georgia Institute of Technology, Atlanta, Georgia (1981).
26. V. I. Tolubinski, E.N. Shevchuk and V. D. Stambrovski, "Study of Liquid-Metal Heat Pipe Characteristics at Start-Up and Operation Under Gravitation," 3rd International Heat Pipe Conference, Palo Alto, California (1978).
27. L. L. Vasliev and S. V. Konev, "Heat Pipes," Heat Transfer-Soviet Research, Vol. 6, No. 1 (1974).
28. A. A. Cenkner, B. E. Nelson, and J.T. Chuvala, "Dynamic Testing of a Cryogenic Heat Pipe/Radiator," Proceedings of the International Heat Transfer Conference, Toronto, Canada, (1978).
29. J. E. Beam, Unsteady Heat Transfer in Heat Pipes, Ph. D. Dissertation, University of Dayton, Dayton, Ohio, (1985).

30. D. Tilton, J. Johnson, J. Glottschlich, and S. Iden, "Transient Response of A Liquid Metal Heat Pipe," University of Kentucky, Lexington, Kentucky, AFWAL-TR-86-2037 (Aug. 1986).
31. G. T. Colwell, "Modeling of Transient Heat Pipe Operation," Georgia Institute of Technology, Atlanta, Georgia, NASA Grant NAG-1-392 ( July 1987).
32. G. A. Asselman and D. B. Green, "Heat Pipes," Philips Tech. Rev., Vol 33, pg. 104-113, No. 4, (1973).
33. C. L. Tien, "Fluid Mechanics of Heat Pipes," Annual Review Fluid Mech., Am. Inst. Physics, Vol. 7, pg. 167-185, (1975).
34. S. W. Chi, Heat Pipe Theory and Practice A Source Book, McGraw-Hill Book Company, New York, (1976).
35. J. E. Kemme, "Vapor Flow Considerations in Conventional Gravity-Assist Heat Pipes," Proceedings of the 2nd International Heat Pipe Conference, Vol. I, pp. 11-22, (1972).
36. M. N. Ivanovskii, V.P. Sorokin, and I. V. Yagodkin, The Physical Principles of Heat Pipes, translated by R. Berman and G. Rice, Clarendon Press, Oxford, 1982.
37. E. Schmic, Properties of Water and Steam in SI-Units, 2nd ed., Springer-Verlag, Munich (1981).
38. C. L. Tien, "Fluid Mechanics of Heat Pipes," Annual Review Fluid Mech., Am. Inst. Physics, Vol. 7, pg. 167-185, (1975).
39. J. C. Slattery, Momentum, Energy, and Mass Transfer in Continua, McGraw-Hill Book Co., New York, (1972).
40. C. W. Stewart, VIPRE-01: A Thermal-Hydraulic Analysis Code for Reactor Cores Volume I, Research Reports Center, Palo Alto, Ca., (1983).
41. V. I. Subbotin, D. N. Sorokin, D. M. Ovechkin, and A. P. Kudryavtsev, "Heat Exchange on Boiling of Metals under Natural Convective Conditions", Nauka, Moscow, (1969).

42. J. G. Collier, Convective Boiling and Condensation, McGraw-Hill Book Co., New York, (1981).
43. R. B. Bird, W. E. Stewart, and E. N. Lightfoot, Transport Phenomena, John Wiley & Sons, New York, pg. 410, (1960).
44. R. W. Fox and A. T. McDonald, Introduction to Fluid Mechanics, John Wiley & Sons, New York, pg. 363, (1978).
45. F. P. Incropera and D. P. Dewitt, Fundamentals of Heat Transfer, John Wiley & Sons, New York, (1981).
46. B. Carnahan, H. A. Luther, and J. O. Wilkes, Applied Numerical Methods, John Wiley & Sons, New York, (1969).
47. D. M. Ernst, "Evaluation of Theoretical Heat Pipe Performance", Thermionic Specialist Conference, Palo Alto, Calif., (1967).

## APPENDIX A

### HAHL COMPUTER CODE LISTING

```
10 REM*****
20 REM
30 REM VS=SPECIFIC VOLUME OF LIQUID WATER(M3/KG)
40 REM
50 REM SV=SPECIFIC VOLUME OF WATER VAPOR(M3/KG)
60 REM
70 REM VY=DYNAMIC VISCOSITY OF LIQUID WATER(KG/S-M)
80 REM
90 REM VV=DYNAMIC VISCOSITY OF WATER VAPOR(KG/S-M)
100 REM
110 REM
120 REM SIG=SURFACE TENSION OF WATER (N/M)
130 REM
140 REM LH=LATENT HEAT OF VAPORIZATION (J/KG)
150 REM
160 REM KW=PERMIABILITY OF WICK MATER- IAL(M2)
170 REM
180 REM TW=WICK THICKNESS(CM)
190 REM
200 REM WW=WICK WIDTH(CM)
210 REM
220 REM EL=EVAPORATOR LENGTH(CM)
230 REM
240 REM AL=ADIABATIC LENGTH(CM)
250 REM
260 REM CL=CONDENSER LENGTH(CM)
270 REM
280 REM LC=CRITICAL LENGTH(MM)
290 REM
300 REM LE=EFFECTIIVE LENGTH OF HEAT PIPE(CM)
310 REM
320 REM LT=TOTAL LENGTH OF HEAT PIPE(CM)
330 REM
340 REM AW=WICK CROSS-SECTIONAL AREA(CM2)
350 REM
360 REM AV=CROSS-SECTIONAL AREA OF VAPOR CHANNEL(M2)
370 REM
380 REM WS=WIRE OR MESH SPACING OF WICK MATERIAL(INCHES)
390 REM
400 REM WD=WIRE DIAMETER IN WICK MATERIAL(INCHES)
410 REM
420 REM RC=EFFECTIVE CAPILLARY RADIUS(M)
430 REM
```

```

440 REM AC=CHANNEL AREA (VAPOR AREA + WICK AREA) (CM^2)
450 REM
460 REM RE=EFFECTIVE (HYDRAULIC) RADIUS OF HEAT PIPE (CM)
470 REM
480 REM RV=EFFECTIVE RADIUS OF VAPOR CHANNEL(M^2)
490 REM QE=LIMITING HEAT FLUX FOR ENTRAINMENT LIMIT(W/CM^2)
500 REM QS=LIMITING HEAT FLUX FOR SONIC LIMIT(W/CM^2)
510 REM QC=LIMITING HEAT FLUX FOR CAPILLARY LIMIT(W/CM^2)
520 REM T=TEMPERATURE (C) [INTERNALLY CONVERTED TO KELVIN]
530 REM
540 REM*****
550 PRINT"[CLR]"
560 V=53248
570 POKE V+40,7
580 POKEV+21,2
590 POKE2041,13
600 FORN=0TO62
610 READQ
620 POKE832+N,Q
630 NEXT N
640 POKEV+2,255
650 POKEV+3,55
660 DATA255,255,255,255,255,255,255
670 DATA224,56,7,224,56,7
680 DATA224,56,7
690 DATA0,56,0,0,57,131
700 DATA24,57,131,24,57,199
710 DATA60,57,199,60,57,239
720 DATA102,57,239,102,57,187
730 DATA255,57,187,195,57,147
740 DATA195,57,131,0,56,0
750 DATA0,56,0,0,56,0
760 DATA3,255,192,3,255,192
770 DIM K(9),A(23),LA(12),B(9,6),LB(8,2),P(5,4)
780 PRINT"[CLR]LIST CALCULATED PROPERTIES?"
790 INPUT"[C/RT]{C/RT}(Y/N)";Y$
800 PRINT"NEW DIMENSIONS?"
810 INPUT"[C/RT]{C/RT}(Y/N)";N$
820 IFN$="N"THEN3660
835 IFES="R"THENGOTO3250
840 INPUT"ENTER DATA OR READ CARDS";E$
850 IFES="R"THENGOTO4280
860 IFES<>"E"THENGOTO840
870 GOTO3250
880 PRINT"[C/DN]{C/DN}{C/RT}TEMPERATURE, {C/UP}O{C/DN}C"
890 INPUT"[C/DN]{C/RT}T=";T
900 PRINT"[CLR]{C/DN}{C/DN}PLEASE STAND BY..."
910 K(1)=-7.691234564
920 K(2)=-26.08023696
930 K(3)=-168.1706546

```

940 K(4) = 64.23285504  
950 K(5) = -118.9646225  
960 K(6) = 4.167117320  
970 K(7) = 20.97506760  
980 K(8) = 1E9  
990 K(9) = 6  
1010 A(0) = 6.824687741E3  
1020 A(1) = -5.422063673E2  
1030 A(2) = -2.096666205E4  
1040 A(3) = 3.941286787E4  
1050 A(4) = -6.733277739E4  
1060 A(5) = 9.902381028E4  
1070 A(6) = -1.093911774E5  
1080 A(7) = 8.590841667E4  
1090 A(8) = -4.511168742E4  
1100 A(9) = 1.418138926E4  
1110 A(10) = -2.017271113E3  
1120 A(11) = 7.982692717  
1130 A(12) = -2.616571843E-2  
1140 A(13) = 1.522411790E-3  
1150 A(14) = 2.284279054E-2  
1160 A(15) = 2.421647003E2  
1170 A(16) = 1.269716088E-10  
1180 A(17) = 2.074839328E-7  
1190 A(18) = 2.174020350E-8  
1200 A(19) = 1.105710498E-9  
1210 A(20) = 12.93441934  
1220 A(21) = 1.308119072E-5  
1230 A(22) = 6.047626338E-14  
1240 LA(1) = 8.438375405E-1  
1250 LA(2) = 5.362162162E-4  
1260 LA(3) = 1.72  
1270 LA(4) = 7.342278489E-2  
1280 LA(5) = 4.975858870E-2  
1290 LA(6) = 6.5371543E-1  
1300 LA(7) = 1.15E-6  
1310 LA(8) = 1.5108E-5; LA(9) = 1.4188E-1  
1320 LA(10) = 7.002753165  
1330 LA(11) = 2.995284926E-4  
1340 LA(12) = 2.04E-1  
1350 B(0,0) = 1.683599274E1  
1360 B(0,1) = 2.856067796E1  
1370 B(0,2) = -5.438923329E-1  
1380 B(0,3) = 4.330662834E-1  
1390 B(0,4) = -6.547711697E-1  
1400 B(0,5) = 8.565182058E-2  
1410 B(1,1) = 6.670375918E-2  
1420 B(1,2) = 1.388983801  
1430 B(2,1) = 8.390104328E-2

1440 B(2,2)=2.614670893E-2  
1450 B(2,3)=-3.373439453E-2  
1460 B(3,1)=4.520918904E-1  
1470 B(3,2)=1.069036614E-1  
1480 B(4,1)=-5.975336707E-1  
1490 B(4,2)=-8.847535804E-2  
1500 B(5,1)=5.958051609E-1  
1510 B(5,2)=-5.159303373E-1  
1520 B(5,3)=2.075021122E-1  
1530 B(6,1)=1.190610271E-1  
1540 B(6,2)=-9.876174132E-2  
1550 B(7,1)=1.683998803E-1  
1560 B(7,2)=-5.809438001E-2  
1570 B(8,1)=6.552390126E-3  
1580 B(8,2)=5.710218649E-4  
1590 B(9,0)=1.936587558E2  
1600 B(9,1)=-1.388522425E3  
1610 B(9,2)=4.126607219E3  
1620 B(9,3)=-6.508211677E3  
1630 B(9,5)=-2.693088365E3  
1640 B(9,6)= 5.235718623E2  
1650 LB(0,0)=7.633333333E-1  
1660 LB(6,1)=4.006073948E-1  
1670 LB(7,1)=8.636081627E-2  
1680 LB(8,1)=-8.532322921E-1  
1690 LB(8,2)= 3.460208861E-1  
1700 L0=15.74373327  
1710 L1=-34.17061978  
1720 L2=19.31380707  
1730 I1=4.260321148  
1740 O(0)=.0181583  
1750 O(1)=.0177624  
1760 O(2)=.0105287  
1770 O(3)=-.0036744  
1780 P(0,0)=0.501938  
1790 P(0,1)=0.235622  
1800 P(0,2)=-0.274637  
1810 P(0,3)= 0.145831  
1820 P(0,4)=-0.0270448  
1830 P(1,0)= 0.162888  
1840 P(1,1)= 0.789393  
1850 P(1,2)=-0.743539  
1860 P(1,3)= 0.263129  
1870 P(1,4)=-0.0253093  
1880 P(2,0)=-0.1303560  
1890 P(2,1)= 0.6736650  
1900 P(2,2)=-0.9594560  
1910 P(2,3)= 0.3472470  
1920 P(2,4)=-0.0267758  
1930 P(3,0)= 0.9079190

```

1940 P(3,1)= 1.2075520
1950 P(3,2)=-0.687343
1960 P(3,3)= 0.213486
1970 P(3,4)=-0.0822904
1980 P(4,0)=-0.5511190
1990 P(4,1)= 0.0670665
2000 P(4,2)=-0.497089
2010 P(4,3)= 0.100754
2020 P(4,4)= 0.0602253
2030 P(5,0)= 0.1465430
2040 P(5,1)=-0.0843370
2050 P(5,2)= 0.1952860
2060 P(5,3)=-0.0329320
2070 P(5,4)=-0.0202595
2080 TP=647.15
2090 BB=235.8E-3
2100 B6=-.625
2110 EX=1.256
2120 T=T+273.15
2130 TR=T/647.3:TT=1-TR
2140 X1=0
2150 FOR N=1 TO 5
2160 X1=X1+K(N)*TT^N
2170 NEXT N
2180 X2=X1/TR/(1+K(6)*TT+K(7)*TT*TT)
2190 X3=TT/(K(8)*TT*TT+K(9))
2200 BETA=EXP(X2-X3)
2210 PS=22120000*BETA
2220 REM PS IS THE SATURATION PRESSURE
2230 Y=1-LA(1)*TR*TR-LA(2)*TR^-6
2240 Z=Y+(LA(3)*Y*Y-2*LA(4)*TR+2*LA(5)*BETA)^.5
2250 X1=A(11)*LA(5)*Z^(-5/17)
2260 X2=A(12)+A(13)*TR+A(14)*TR*TR+A(15)*(LA(6)-TR)^10
2270 X2=X2+A(16)/(LA(7)+TR^19)
2280 X3=(A(17)+2*A(18)*BETA+3*A(19)*BETA^2)
2290 X3=X3/(LA(8)+TR^11)
2300 X4=A(20)*TR^18*(LA(9)+TR*TR)
2310 X4=X4*(-3*(LA(10)+BETA)^-4+LA(11))
2320 X5=3*A(21)*(LA(12)-TR)*BETA*BETA
2330 X6=4*A(22)*TR^-20*BETA^3
2340 VR=X1+X2-X3-X4+X5+X6
2350 VS=VR*.00317
2360 BL=L0+L1*TR+L2*TR*TR
2370 X=EXP(LB(0,0)*TT)
2380 X1=I1*TR/BETA
2390 X2=0
2400 FORMU=1TO5
2410 GOSUB2890
2420 X3=0
2430 FORNU=1TONN

```

```

2440 GOSUB2940
2450 X3=X3+B(MU,NU)*X^Z
2460 NEXTNU
2470 X2=X2+MU*BETA^(MU-1)*X3
2480 NEXTMU
2490 X3=0
2500 FORMU=6TO8
2510 GOSUB2890
2520 X4=0
2530 FOR LM=1TO LL
2540 GOSUB3130
2550 X4=X4+LB(MU,LM)*X^XX
2560 NEXTLM
2570 X5=0
2580 FORNU=1 TO NN
2590 GOSUB2940
2600 X5=X5+B(MU,NU)*X^Z
2610 NEXTNU
2620 X3=X3+(((MU-2)*BETA^(1-MU)*X5)/1E20)
2621 X3=X3/((BETA^(2-MU)+X4)/1E10)^2
2630 NEXT MU
2640 X4=0
2650 FORNU=0TO6
2660 X4=X4+B(9,NU)*X^NU
2670 NEXT NU
2680 X4=X4*11*(BETA/BL)^10
2690 SV=(X1-X2-X3+X4)*.00317
2700 X1=0
2710 TM=647.27/T
2720 FORK=0TO3
2730 X1=X1+O(K)*TM^K
2740 NEXTK
2750 V0=1/TM^.5/X1*1E-6
2760 X1=0
2770 FORI=0TO5
2780 X2=0
2790 FORJ=0TO4
2800 X2=X2+P(I,J)*(TM-1)^I*(3.147E-3/VS-1)^J
2810 NEXTJ
2820 X1=X1+X2
2830 NEXTI
2840 VY=V0*EXP(3.147E-3/VS*X1)
2850 X1=((TP-T)/TP)^EX*BB
2860 X2=1+B6*((TP-T)/TP)
2870 SIG=X1*X2
2880 RETURN
2890 IFMU=2 OR MU=5 THEN NN=3:GOTO2910
2900 NN=2
2910 IFMU=8THENLL=2:GOTO2930
2920 LL=1
2930 RETURN

```

```

2940 IFMU=1 AND NU=1THENZ=13
2950 IFMU=1 AND NU=2THENZ=3
2960 IFMU=2 AND NU=1THENZ=18
2970 IFMU=2 AND NU=2THENZ=2
2980 IFMU=2 AND NU=3THENZ=1
2990 IFMU=3 AND NU=1THENZ=18
3000 IFMU=3 AND NU=2THENZ=10
3010 IFMU=4 AND NU=1THENZ=25
3020 IFMU=4 AND NU=2THENZ=14
3030 IFMU=5 AND NU=1THENZ=32
3040 IFMU=5 AND NU=2THENZ=28
3050 IFMU=5 AND NU=3THENZ=24
3060 IFMU=6 AND NU=1THENZ=12
3070 IFMU=6 AND NU=2THENZ=11
3080 IFMU=7 AND NU=1THENZ=24
3090 IFMU=7 AND NU=2THENZ=18
3100 IFMU=8 AND NU=1THENZ=24
3110 IFMU=8 AND NU=2THENZ=14
3120 RETURN
3130 IFMU=6 AND LA=1THENXX=14
3140 IFMU=7 AND LA=1THENXX=19
3150 IFMU=8 AND LA=1THENXX=54
3160 IFMU=8 AND LA=2THENXX=27
3170 RETURN
3180 LH=2497.1-2.365*(T-273.15):LH=LH*1000
3190 TC=T-273.15
3200 VV=-9.9242744E-14*TC^3+4.56012051E-11*TC^2
3201 VV = VV+3.17986594E-8*TC+8.84863492E-6
3210 QC=.0001
3220 ER=.01
3230 INC=10000
3240 RETURN
3250 PRINT"{C/RT}CRITICAL LENGTH (MM)"
3260 INPUT"{C/RT}LC=";LC
3270 PRINT"{C/DN}{C/DN}{C/DN}{C/DN}WICK PERMIABILITY, M^2"
3280 PRINT"(IF NOT KNOWN, ENTER 0.)"
3290 INPUT"PERMIABILITY";KW
3300 PRINT"{C/DN}{C/RT}WICK THICKNESS (CM)"
3310 INPUT"{C/RT}T=";TW
3320 PRINT"{C/DN}{C/RT}WICK WIDTH (CM)"
3330 INPUT"{C/RT}W=";WW
3340 PRINT"{C/DN}{C/RT}EVAPORATOR LENGTH (CM)"
3350 INPUT"{C/RT}L{C/DN}E{C/UP}=";EL
3360 PRINT
3370 PRINT"{C/DN}{C/RT}ADIABATIC LENGTH (CM)"
3380 INPUT"{C/RT}L{C/DN}A{C/UP}=";AL
3390 PRINT
3400 PRINT"{C/DN}{C/RT}CONDENSER LENGTH (CM)"
3410 INPUT"{C/RT}L{C/DN}C{C/UP}=";CL
3420 PRINT"{C/DN}{C/RT}WIRE (MESH) SPACING (INCHES)"
3430 INPUT"{C/RT}WS=";WS

```

```

3440 PRINT"[C/DN]{C/RT}WIRE DIAMETER (INCHES) "
3450 INPUT"[C/RT]WD=";WD
3460 PRINT"[C/DN]{C/RT}CHANNEL AREA W/O WICK (CM^2) "
3470 INPUT"[C/RT]A=";AC
3480 REM COMPUTE EFFECTIVE RADIUS OF
3490 REM HEAT PIPE
3500 RE=2*AC/WW
3510 REM CALCULATE EFFECTIVE AREA (CM^2) BASED ON
3511 REM EFFECTIVE RADIUS
3520 AE=^*RE*RE
3530 AW=TW*WW*AE/AC
3540 LC=LC/1000
3550 IFKW=0THENKW=1E-10
3560 RC=(WD+WS)/2*2.54/100
3570 LE=(EL+CL)/2+AL
3580 LT=EL+AL+CL
3590 REM COMPUTE WICK X-SECTIONAL AREA
3600 REM COMPUTE VAPOR CHANNEL CROSS-SECTIONAL AREA (M^2)
3610 AV=(AE-AW)/10000
3620 REM RADIUS OF VAPOUR CHANNEL EQUALS
3630 REM RADIUS OF HEAT PIPE MINUS THE
3640 REM THICKNESS OF THE WICK
3650 RV=(RE-TW)/100
3660 GOSUB880
3670 GOSUB3180
3680 GOSUB4000
3690 IFYS<>"Y"THEN GOTO3850
3700 PRINT"SPECIFIC VOLUME OF WATER (M^3/KG) "
3710 PRINT"[C/RT]{C/RT}{C/RT}{C/RT}{C/RT}";VS
3720 PRINT"[C/DN]{C/RT}SPECIFIC VOLUME OF VAPOR (M^3/KG) "
3730 PRINT"[C/RT]{C/RT}{C/RT}{C/RT}{C/RT}";SV
3740 PRINT"[C/DN]{C/RT}SURFACE TENSION (N/M) "
3750 PRINT"[C/RT]{C/RT}{C/RT}{C/RT}{C/RT}";SIG
3760 PRINT"[C/DN]{C/RT}LATENT HEAT OF VAPORIZATION (J/KG) "
3770 PRINT"[C/RT]{C/RT}{C/RT}{C/RT}{C/RT}";LH
3780 PRINT"[C/DN]{C/RT}DYNAMIC VISCOSITY OF WATER (KG/M-S) "
3790 PRINT"[C/RT]{C/RT}{C/RT}{C/RT}{C/RT}";VY
3800 PRINT"[C/DN]{C/RT}DYNAMIC VISCOSITY OF VAPOR (KG/M-S) "
3810 PRINT"[C/RT]{C/RT}{C/RT}{C/RT}{C/RT}";VV
3820 PRINT"HIT ANY KEY TO CONTINUE"
3830 GETA$:IFA$=""THEN3830
3840 PRINT"[C/UP] "
3850 QE=SQR(2*^*LH*LH*SIG/LC/SV)
3855 IFYS="N"THENPRINT"{CLR}"
3860 PRINT"ENTRAINMENT LIMIT, W/CM^2:";QE/10000
3870 QV=RV*RV*LH*PS/16/SV/VV/(LE/100)
3880 PRINT"[C/DN]{C/RT}VISCOUS LIMIT, W/CM^2:";QV/10000
3890 QS=1.159*LH*(PS/SV)^.5
3900 PRINT"[C/DN]{C/RT}SONIC LIMIT, W/CM^2:";QS/10000
3910 MS=QS*SV/LH/(613.7*T)^.5
3920 PRINT"[C/RT]{C/RT}{C/RT}{C/RT}M=";MS
3930 PRINT"[C/DN]{C/RT}CAPILLARY LIMIT, W/CM^2:";QC/AE

```

```

3935 PRINT"[C/RT]{C/RT}{C/RT}{C/RT}METHOD";MT
3940 PRINT"[C/RT]{C/RT}{C/RT}{C/RT}M=";MV
3950 PRINT"[C/RT]{C/RT}{C/RT}{C/RT}R[C/DN]E[C/UP]=";RN
3960 PRINT"HIT ANY KEY TO CONTINUE"
3970 GETAS:IFAS=" "THEN3970
3980 PRINT"[C/UP]                                {C/DN}"
3990 GOTO780
4000 RN=2*RV*QC/AV/VV/LH
4010 FF=0.038/RN^0.25
4020 FT=(.019*VV/AV/RE^2*SV/LH)*(2*RE*QC/AV/LH/VV)^.75
4030 MV=QC/AV*SV/LH/(613.7*T)^.5
4040 FV=FT/(1+.165*MV*MV)^.75
4050 FL=VY*VS/KW/(AW/10000)/LH
4060 DEL=QC-(2*SIG/RC-9.8*2*RV/VS)/(LE/100)/(FL+FV)
4070 IFABS(DEL)<ERTHEN4130
4080 IF DEL<0 THEN QC=QC+INC:GOTO4000
4090 QC=QC-INC
4100 INC=INC/10
4110 QC=QC+INC
4120 GOTO4000
4130 IFRN>2300ANDMV>.2THEN MT=1: RETURN
4135 MT=2
4140 QC=.001
4150 INC=10000
4160 RN=2*RV*QC/AV/VV/LH
4170 FF=0.038/RN^0.25
4180 MV=QC/AV*SV/LH/(613.7*T)^.5
4190 FV=(.019*VV/AV/RE^2*SV/LH)*(2*RE*QC/AV/LH/VV)^.75
4200 DEL=QC-(2*SIG/RC-9.8*2*RV/VS)/(LE/100)/(FL+FV)
4210 IFABS(DEL)<ERTHEN4270
4220 IF DEL<0 THEN QC=QC+INC:GOTO4160
4230 QC=QC-INC
4240 INC=INC/10
4250 QC=QC+INC
4260 GOTO4160
4270 RETURN
4280 READ LC
4285 READ KW
4290 READ TW
4300 READ WW
4310 READ EL
4320 READ AL
4330 READ CL
4340 READ WS
4350 READ WD
4360 READ AC
4370 GOTO 3500
4380 END
4390 DATA 0.1154
4400 DATA 4.0E-08
4410 DATA 0.1

```

4420 DATA 2.54  
4430 DATA 60  
4440 DATA 15  
4450 DATA 164  
4460 DATA 0.0060  
4470 DATA 0.0045  
4480 DATA 0.9525

READY.

## APPENDIX B

### HTPIPE COMPUTER CODE LISTING

```
10 SCREEN 0,0,0: KEY OFF : CLS : WIDTH 80
20 CLEAR, 49152!
30 DIM LT%(2),TJ(260),TK(310),X(55),Y(55),F(55),G(55),H(55),AT(15,20),
   AP(10),T(32),TT(32)
40 OPEN "C:OUTDATA" FOR OUTPUT AS #2
50 ON ERROR GOTO 3900
60 LOCATE 25,1:COLOR 0,7:PRINT"-PLEASE WAIT-":COLOR 7,0:
   PRINT" Loading DASH-8 I/O address and thermocouple lookup table
   data":LOCATE 1,1
70 DEF SEG = 0
80 SG = 256 * PEEK(&H511) + PEEK(&H510)
90 SG = SG + 49152!/16
100 DEF SEG = SG
110 BLOAD "DASH8.BIN", 0
120 OPEN "DASH8.ADR" FOR INPUT AS #1
130 INPUT #1, BASADR%
140 CLOSE #1
150 DASH8 = 0
160 FLAG% = 0
170 MD% = 0 'Mode 0 = initialization
180 DTS = "ON "
190 VHT=1
200 CALL DASH8 (MD%, BASADR%, FLAG%)
210 IF FLAG% <> 0 THEN PRINT"INSTALLATION ERROR"
220 'Load thermocouple linearizing look up data
230 GOSUB 1470
240 COSUB 2090 'Load data for spline fit for pressure calculation
250 COSUB 2860
260 'Set gain (AV) at 100 for type J T/C's, 0.5 for pressure meter,
   and 50 for type K T/C's
270 AV0=100
280 AV1=.5
290 AV2=50
300 CLS
310 '---- STEP 2: Initialize an integer array DE(15) to receive data
320 DIM D%(2,15) '16 elements, one for each EXP-16 channel
330 'Also initialize a corresponding real array to receive
   temperature data
340 '
350 '----- STEP 3: Get cold junction compensation temperature
360 'Output of CJC channel is scaled at 24.4mV/deg.C. This
   corresponds to
370 '0.1 deg.C./bit. Dividing output in bits by 10 yields degrees C.
380 '
```

```

390 'Lock DASH-8 to channel #7 (CJC channel selected) using mode 1
400 MD%=1 : LT%(0)=7 : LT%(1) = 7
410 CALL DASH8 (MD%, LT%(0), FLAG%)
420 IF FLAG% <> 0 THEN PRINT "ERROR IN SETTING CJC CHANNEL" : END
430 'Next get CJC data from this channel using Mode 4
440 MD% = 4 : CJ% = 0
450 CALL DASH8 (MD%, CJ%, FLAG%)
460 'Change output in bits to real temperature
470 CJC = CJ%/10
480 '
490 C%=C%+1:OLDTM$=DATIME$: DATIME%=TIME$
500 '----- STEP 4: Get the thermocouple data
510 FOR CH% = 0 TO 2
520 GOSUB 1250
550 ' CH% - specifies DASH-8 channel that EXP-16 is connected to (0-7).
560 ' D%(15) - integer data array to receive data from channels.
570 '
580 '----- STEP 5: Convert data to volts and linearize
590 IF CH%=0 THEN GOSUB 620:GOTO 740
600 IF CH%=2 THEN GOSUB 680:GOTO 740
610 IF CH%=1 THEN GOTO 950
620 FOR I = 0 TO 14
630 V = (D%(0,I)*5)/(AV0*2048)
640 GOSUB 1820
650 T(I)=TC           'degrees Centigrade
660 NEXT I
670 RETURN
680 FOR I = 0 TO 14
690 V = (D%(2,I)*5)/(AV2*2048)
700 GOSUB 3260
710 T(I+15)=TC       'degrees Centigrade
720 NEXT I
730 RETURN
740 FOR K = 0 TO 20
750 FOR L = 10 TO 2 STEP -1
750 AT(L,K)=AT(L-1,K)
770 NEXT L
780 AT(1,K)=T(K)
790 AT(0,K)=0
800 FOR L = 1 TO 10
810 AT(0,K)=AT(0,K)+AT(L,K)/10
820 NEXT L
830 NEXT K
840 GOTO 950
950 V=D%(1,0)*5/(AV1*2048)
860 GOSUB 1990
870 FOR K =10 TO 2 STEP -1
880 AP(K)=AP(K-1)
890 NEXT K
900 AP(1)=PR

```

```

910 AP(0)=0
920 FOR K = 1 TO 10
930 AP(0)=AP(0)+ AP(K)/10
940 NEXT K
941 TIME1=VAL(RIGHT$(DATIME$,2))
942 TIME2=VAL(RIGHT$(OLDTM$,2))
943 IF TIME2 > TIME1 THEN TIME1=TIME1+60
945 PRATE = (AP(1)-AP(2))/(TIME1-TIME2)
950 NEXT CH%
960 '----- STEP 6: Display temperature data
970 LOCATE 1,1
930 AA$ = INKEY$
990 IF (AA$="S") OR (AA$="s") THEN CLOSE#2:CLS:END
1000 IF (AA$="I") OR (AA$="i") THEN GOSUB 2790
1010 IF (AA$="D") OR (AA$="d") THEN GOTO 1030 'Toggle to turn
      on/off write to disk function
1020 GOTO 1050
1030 IF DT$ = "ON " THEN DT$ = "OFF": GOTO 1070
1040 DT$ = "ON "
1050 IF PC% < VW% THEN PC% = PC% + 1:GOTO 1220
1060 PC% = 0
1065 T(20)=T(14):AT(0,20)=AT(0,14)
1070 PRINT "CHANNEL #:"TAB(25)"1      2      3      4
      5      6      7"
1080 PRINT USING "Temperature (C):   ###.##  ##.##  ##.##
      ##.##  ##.##  ##.##  ##.##";T(0),T(1),T(2),T(3),T(4),T(5),T(6)
1090 PRINT USING "Average Temp.(C)   ##.##  ##.##  ##.##
      ##.##  ##.##  ##.##  ##.##";AT(0,0),AT(0,1),AT(0,2),AT(0,3),
      AT(0,4),AT(0,5),AT(0,6)
1100 LOCATE 6,1
1110 PRINT "CHANNEL #:"TAB(25)"8      9      10     11
      12     13     14"
1120 PRINT USING "Temperature (C):   ##.##  ##.##  ##.##
      ##.##  ##.##  ##.##  ##.##";T(7),T(8),T(9),T(10),T(11),T(12),
      T(13)
1130 PRINT USING "Average Temp.(C)   ##.##  ##.##  ##.##
      ##.##  ##.##  ##.##  ##.##";AT(0,7),AT(0,8),AT(0,9),AT(0,10),
      AT(0,11),AT(0,12),AT(0,13)
1140 LOCATE 11,1
1150 PRINT "CHANNEL #:"TAB(24)"G1      G2      G3      G4      G5
      COOLANT"
1160 PRINT USING "Temperature (C):   ##.##  ##.##  ##.##  ##.##
      ##.##  ##.##  ##.##";T(19),T(18),T(17),T(16),T(15),T(20)
1170 PRINT USING "Average Temp.(C)   ##.##  ##.##  ##.##  ##.##
      ##.##  ##.##  ##.##";AT(0,19),AT(0,18),AT(0,17),AT(0,16),
      AT(0,15),AT(0,20)
1180 LOCATE 20,1
1190 PRINT USING "CJC = ##.## deg. C.   P = #####.### Torr
      (Ave = #####.###) PRESSURIZATION RATE = #####.### Torr/sec";
      CJC;PR;AP(0);PRATE

```

```

1200 PRINT "Reading was taken at ";DATIME$;" on ";DATE$
1210 LOCATE 23,50:PRINT USING "DISK WRITE IS &";DT$
1220 IF DT$ = "ON " THEN GOSUB 2680
1230 GOTO 350 'repeat scan of channels
1240 '
1250 '---- Subroutine to convert EXP-16 channels to number of bits
1260 'First lock DASH-8 on the one channel that EXP-16 is
connected to.
1270 LT%(0) = CH% : LT%(1) = CH% : MD% = 1
1280 CALL DASH8 (MD%, LT%(0), FLAG%)
1290 IF FLAG% <> 0 THEN PRINT "ERROR IN SETTING CHANNEL" : END
1300 'Next select each EXP-16 channel in turn and convert it.
1310 'Digital outputs OP1-4 drive the EXP-16 sub-multiplexer address,
so use
1320 'mode 14 to set up the sub-multiplexer channel.
1330 FOR SI = 0 TO 14 'note use of integer index SI
1340 SID%=SI
1350 MD% = 14
1360 CALL DASH8 (MD%, SID%, FLAG%) 'address set
1370 IF FLAG% <> 0 THEN PRINT "ERROR IN EXP-16 CHANNEL NUMBER" : END

1380 'Now that channel is selected, perform A/D conversion using
mode 4.
1390 'Transfer data to corresponding array element D%(SID%)
1400 MD% = 4 'do 1 A/D conversion
1410 CALL DASH8 (MD%, D%(CH%,SID%), FLAG%)
1420 IF FLAG% <> 0 THEN PRINT "ERROR IN PERFORMING A/D CONVERSION":
PRINT FLAG%
1430 'Now repeat sequence for all other EXP-16 channels
1440 NEXT SI
1450 'All done - return from subroutine
1460 RETURN
1470 '----- Table lookup data for J type thermocouple
Run this subroutine only in the initialization section of your
program
1490 'Number of points, voltage step interval (mV), starting
voltage (mV)
1500 DATA 257 , .2 , -8.2
1510 READ NJ, SIJ, SVJ
1520 'Temperature at -8.2mv, -8.0mv, -7.8mv etc.
1530 DATA -215.0,-205.3,-196.1,-187.7,-179.9,-172.8,-165.9,-159.3,-
153.1,-147.1
1540 DATA -141.2,-135.6,-130.0,-124.6,-119.3,-114.2,-109.1,-104.2, -
99.2, -94.4
1550 DATA -89.7, -85.0, -80.3, -75.8, -71.3, -66.8, -62.4, -58.0, -
53.7, -49.3
1560 DATA -45.1, -40.8, -36.7, -32.5, -28.3, -24.2, -20.1, -16.1, -
12.0, -8.0
1570 DATA -4.0, -0.0, 3.9, 7.9, 11.8, 15.7, 19.6, 23.5,
27.4, 31.2

```

```

1580 DATA 35.1, 38.9, 42.7, 46.5, 50.3, 54.1, 57.8, 61.6,
      65.3, 69.1
1590 DATA 72.8, 76.5, 80.3, 84.0, 87.7, 91.4, 95.1, 99.7,
      102.4, 106.1
1600 DATA 109.8, 113.4, 117.1, 120.7, 124.4, 128.0, 131.7, 135.3,
      139.0, 142.6
1610 DATA 146.2, 149.9, 153.5, 157.1, 160.7, 164.3, 168.0, 171.6,
      175.2, 178.8
1620 DATA 182.4, 186.0, 189.6, 193.2, 196.8, 200.4, 204.0, 207.6,
      211.2, 214.8
1630 DATA 218.4, 222.0, 225.6, 229.2, 232.8, 236.4, 240.0, 243.6,
      247.2, 250.8
1640 DATA 254.5, 258.1, 261.7, 265.3, 268.9, 272.5, 276.1, 279.7,
      283.3, 286.9
1650 DATA 290.5, 294.1, 297.7, 301.4, 305.0, 308.6, 312.2, 315.8,
      319.4, 323.0
1660 DATA 326.7, 330.3, 333.9, 337.5, 341.1, 344.8, 348.4, 352.0,
      355.6, 359.3
1670 DATA 362.9, 366.5, 370.1, 373.8, 377.4, 381.0, 384.7, 388.3,
      391.9, 395.5
1680 DATA 399.2, 402.8, 406.4, 410.1, 413.7, 417.3, 420.9, 424.5,
      428.2, 431.8
1690 DATA 435.4, 439.0, 442.6, 446.3, 449.9, 453.5, 457.1, 460.7,
      464.3, 467.9
1700 DATA 471.5, 475.1, 478.7, 482.3, 485.9, 489.5, 493.1, 496.7,
      500.2, 503.8
1710 DATA 507.3, 510.9, 514.5, 518.0, 521.6, 525.1, 528.7, 532.2,
      535.7, 539.3
1720 DATA 542.8, 546.3, 549.8, 553.3, 556.8, 560.3, 563.8, 567.3,
      570.8, 574.2
1730 DATA 577.7, 581.2, 584.6, 588.1, 591.5, 594.9, 598.4, 601.8,
      605.2, 608.6
1740 DATA 612.0, 615.4, 618.8, 622.1, 625.5, 628.9, 632.2, 635.6,
      638.9, 642.3
1750 DATA 645.6, 648.9, 652.2, 655.5, 658.8, 662.1, 665.4, 668.7,
      672.0, 675.2
1760 DATA 678.5, 681.7, 685.0, 688.2, 691.5, 694.7, 697.9, 701.1,
      704.3, 707.5
1770 DATA 710.7, 713.9, 717.1, 720.3, 723.5, 726.6, 729.8, 733.0,
      736.1, 739.3
1780 DATA 742.4, 745.6, 748.7, 751.8, 755.0, 758.1, 761.2
1790 FOR I = 0 TO NJ-1:READ TJ(I):NEXT I
1800 RETURN
1810 '
1820 '----- Interpolation routine to find J thermocouple temperature
1830 'Entry variables:-
1840 '   CJC = cold junction compensator temperature in deg. C.
1850 '   V = thermocouple voltage in volts
1860 'Exit variables:-
1870 '   TC = temperature in degrees Centigrade

```

```

1880 'Execution time on std. IBM P.C. = 46 milliseconds
1890 'Perform CJC compensation for J type
1900 VJ = 1000*V + 1.277 + (CJC-25)*.05155 'VJ in mV (corrected
      4/5/85)
1910 '
1920 'Find look up element
1930 EJ = INT((VJ-SVJ)/SIJ)
1940 IF EJ<0 THEN TC=TJ(0):GOTO 1980 'Out of bounds, round to
      lower limit
1950 IF EJ>NJ-2 THEN TC=TJ(NJ-1):GOTO 1980 'Out of bounds,round
      to upper limit
1960 'Do interpolation
1970 TC = TJ(EJ) + (TJ(EJ+1) - TJ(EJ))*(VJ-EJ*SIJ-SVJ)/SIJ 'Centigrade
1980 RETURN
1990 ' Subroutine to calculate pressure from voltage
2000 IF V <= X(1) THEN PR = .001:RETURN
2010 IF V = > X(55) THEN PR = 1000:RETURN
2020 FOR K = 2 TO 55
2030 IF V < X(K) THEN 2050
2040 NEXT K
2050 K=K-1
2060 W = (V-X(K))/(X(K+1)-X(K))
2070 PR = Y(K) + F(K)*W + G(K)*W^2 + H(K)*W^3
2080 RETURN
2090 FOR I = 1 TO 55
2100 READ X(I), Y(I), F(I), G(I), H(I)
2110 NEXT I
2120 RETURN
2130 DATA 0.0216,0.001,1.152039E-0,-1.520389E-4,1.164153E-10
2140 DATA 0.0278,0.002,1.436064E-3,-7.236689E-4,2.87605E-4
2150 DATA 0.0383,0.003,1.403014E-3,-9.641326E-4,5.611184E-4
2160 DATA 0.0556,0.004,9.037234E-4,3.07868E-4,-2.115917E-4
2170 DATA 0.0691,0.005,1.218899E-3,-6.566939E-4,4.377999E-4
2180 DATA 0.0877,0.006,8.84685E-4,2.084242E-5,9.447272E-5
2190 DATA 0.1012,0.007,8.871799E-04,3.151444E-4,-2.023241E-4
2200 DATA 0.1111,0.008,1.140417E-3,-2.84916E-4,1.444985E-4
2210 DATA 0.1235,0.009,9.959343E-4,-6.89365E-6,1.090951E-5
2220 DATA 0.1358,0.010,8.86203E-3,1.668209E-3,-5.302392E-4
2230 DATA 0.2432,0.020,.0095114,3.732406E-4,1.153592E-4
2240 DATA 0.3395,0.030,9.513834E-3,2.941843E-4,1.919819E-4
2250 DATA 0.4259,0.040,9.466967E-3,1.481336E-3,-9.483006E-4
2260 DATA 0.5025,0.050,1.049817E-2,-2.03906E-3,1.540884E-3
2270 DATA 0.5864,0.060,9.265861E-3,1.551393E-3,-8.172523E-4
2280 DATA 0.6568,0.070,1.008595E-2,-1.033772E-3,9.4782E-4
2290 DATA 0.7284,0.080,9.360003E-3,2.040306E-3,-1.400304E-3
2300 DATA 0.7901,0.090,1.109663E-2,-3.744628E-3,2.648002E-3
2310 DATA 0.8642,0.100,5.922229E-2,7.571723E-2,-3.743951E-2
2320 DATA 1.2441,0.200,9.745134E-2,-9.405315E-4,3.489196E-3
2330 DATA 1.6041,0.300,9.513949E-2,-8.894235E-3,1.375474E-2
2340 DATA 1.9271,0.400,8.942052E-2,2.003414E-2,-9.454668E-3

```

```

2350 DATA 2.1706,0.500,9.392368E-2,-9.695515E-3,1.077186E-2
2360 DATA 2.4088,0.600,9.198612E-2,1.308775E-2,-5.073905E-3
2370 DATA 2.6047,0.700,9.736969E-2,9.049624E-3,-6.419296E-3
2380 DATA 2.7900,0.800,0.1044669,-1.178993E-2,7.323034E-3
2390 DATA 2.9912,0.900,9.743704E-2,-8.271963E-3,1.083495E-2
2400 DATA 3.1818,1.000,.6110165,.4423876,-.0534041
2410 DATA 4.2088,2.000,.8606494,3.194034E-2,.1074103
2420 DATA 4.8706,3.000,.8777054,-3.307223E-2,.1553668
2430 DATA 5.3365,4.000,.8709702,-.269639,.3986688
2440 DATA 5.6541,5.000,.8403325,.4507399,-.2910724
2450 DATA 5.8238,6.000,1.289714,-1.214498,.9247843
2460 DATA 6.0382,7.000,.834555,.3305124,-.1650674
2470 DATA 6.2206,8.000,.999622,-7.136273E-2,7.174075E-2
2480 DATA 6.3529,9.000,.9440796,-6.374979E-2,.1196702
2490 DATA 6.4694,10.00,5.769986,-.5861635,4.816178
2500 DATA 7.0412,20.00,8.287316,-.828743,2.541428
2510 DATA 7.2900,30.00,8.490602,-2.623325,4.132723
2520 DATA 7.4382,40.00,8.380468,2.423147,-.8036146
2530 DATA 7.5176,50.00,9.385612,-4.380738,4.995125
2540 DATA 7.5865,60.00,8.382393,.9266091,.6910076
2550 DATA 7.6235,70.00,8.815776,2.368357,-1.184133
2560 DATA 7.6500,80.00,9.999909,1.438902,-1.438311
2570 DATA 7.6765,90.00,13.66595,-14.34004,10.6741
2580 DATA 7.7188,100.0,46.84252,119.0398,-65.85234
2590 DATA 7.8353,200.0,126.9047,-47.53644,20.63171
2600 DATA 8.0047,300.0,108.3893,-35.10249,26.7324
2610 DATA 8.2006,400.0,89.51311,26.81351,-16.32662
2620 DATA 8.3488,500.0,107.63,-30.9457,23.31565
2630 DATA 8.5182,600.0,90.41804,5.260346,4.32161
2640 DATA 8.6506,700.0,91.10517,25.3441,-16.44927
2650 DATA 8.7565,800.0,110.8648,-66.81552,55.95073
2660 DATA 8.8835,900.0,84.65207,15.34747,4.577637E-4
2670 DATA 8.9576,1000.,0,0,0
2680 FOR I=0 TO 20
2690 IF I=14 THEN 2710
2700 PRINT#2, T(I);
2710 NEXT I
2720 PRINT#2, CJC;PR;AP(0);DATIME$
2730 RETURN
2740 IF ERR=61 THEN 2770
2750 PRINT "ERROR NUMBER";ERR
2760 STOP
2770 BEEP:BEEP
2780 END
2790 CLS
2800 LOCATE 10,10
2810 PRINT"INPUT NUMBER OF READINGS/SCREEN PRINT (CURRENTLY";VW";)":
2820 INPUT VW
2830 CLS
2840 RETURN

```

2850  $V = (D\% (O, I) * 5) / (AVO * 2048)$   
 2860 '----- Table lookup data for K type thermocouple  
 2880 'Number of points, voltage step interval (mV), starting voltage  
 (mV)  
 2890 DATA 309 , .2 , -6.6  
 2900 READ NK, SIK, SVK  
 2910 'Temperature at -6.6mv, -6.4mV, -6.2mV etc.  
 2920 DATA -353.5, -249.3, -224.0, -207.6, -194.3, -182.8, -172.3, -162.8, -  
 153.8, -145.4  
 2930 DATA -137.3, -129.6, -122.3, -115.2, -108.3, -101.6, -95.1, -88.7, -  
 82.5, -76.4  
 2940 DATA -70.4, -64.6, -58.8, -53.1, -47.5, -42.0, -36.6, -31.2, -  
 25.9, -20.6  
 2950 DATA -15.4, -10.2, -5.1, -0.0, 5.0, 10.1, 15.1, 20.0, 25.0, 29.9  
 2960 DATA 34.8, 39.7, 44.6, 49.5, 54.3, 59.1, 64.0, 68.8, 73.6, 78.4  
 2970 DATA 83.2, 88.0, 92.9, 97.7, 102.5, 107.4, 112.2, 117.1, 122.0, 126.9  
 2980 DATA 131.8, 136.7, 141.7, 146.6, 151.6, 156.5, 161.5, 166.5, 171.5, 176.5  
 2990 DATA 181.6, 186.6, 191.6, 196.6, 201.6, 206.6, 211.6, 216.6, 221.5, 226.5  
 3000 DATA 231.5, 236.4, 241.4, 246.3, 251.2, 256.1, 261.0, 265.9, 270.8, 275.6  
 3010 DATA 280.5, 285.3, 290.2, 295.0, 299.8, 304.6, 309.4, 314.3, 319.1, 323.9  
 3020 DATA 328.7, 333.4, 338.2, 343.0, 347.8, 352.6, 357.3, 362.1, 366.9, 371.6  
 3030 DATA 376.4, 381.1, 385.9, 390.6, 395.4, 400.1, 404.8, 409.6, 414.3, 419.0  
 3040 DATA 423.8, 428.5, 433.2, 437.9, 442.6, 447.3, 452.0, 456.8, 461.5, 466.2  
 3050 DATA 470.9, 475.6, 480.3, 485.0, 489.7, 494.4, 499.1, 503.8, 508.5, 513.1  
 3060 DATA 517.8, 522.5, 527.2, 531.9, 536.6, 541.3, 546.0, 550.7, 555.4, 560.0  
 3070 DATA 564.7, 569.4, 574.1, 578.8, 583.5, 588.2, 592.9, 597.6, 602.3, 607.0  
 3080 DATA 611.7, 616.4, 621.2, 625.9, 630.6, 635.3, 640.0, 644.8, 649.5, 654.2  
 3090 DATA 658.9, 663.7, 668.4, 673.2, 677.9, 682.7, 687.4, 692.2, 696.9, 701.7  
 3100 DATA 706.5, 711.3, 716.1, 720.8, 725.6, 730.4, 735.2, 740.0, 744.8, 749.7  
 3110 DATA 754.5, 759.3, 764.1, 769.0, 773.8, 778.7, 783.5, 788.4, 793.3, 798.1  
 3120 DATA 803.0, 807.9, 812.8, 817.7, 822.6, 827.5, 832.4, 837.3, 842.2, 847.2  
 3130 DATA 852.1, 857.1, 862.0, 867.0, 872.0, 876.9, 881.9, 886.9,

```

891.9, 896.9
3140 DATA 901.9, 906.9, 911.9, 916.9, 922.0, 927.0, 932.0, 937.1,
942.2, 947.2
3150 DATA 952.3, 957.4, 962.5, 967.6, 972.7, 977.8, 982.9, 988.0,
993.1, 998.2
3160 DATA 1003.4, 1008.5, 1013.7, 1018.8, 1024.0, 1029.2, 1034.4, 1039.6,
1044.8, 1050.0
3170 DATA 1055.2, 1060.4, 1065.6, 1070.8, 1076.1, 1081.3, 1086.6, 1091.9,
1097.2, 1102.4
3180 DATA 1107.7, 1113.0, 1118.3, 1123.7, 1129.0, 1134.3, 1139.7, 1145.0,
1150.4, 1155.8
3190 DATA 1161.2, 1166.6, 1172.0, 1177.4, 1182.9, 1188.3, 1193.8, 1199.2,
1204.7, 1210.2
3200 DATA 1215.7, 1221.2, 1226.8, 1232.3, 1237.9, 1243.5, 1249.1, 1254.7,
1260.3, 1265.9
3210 DATA 1271.6, 1277.3, 1282.9, 1288.6, 1294.3, 1300.1, 1305.8, 1311.5,
1317.3, 1323.1
3220 DATA 1328.9, 1334.7, 1340.5, 1346.4, 1352.2, 1358.1, 1363.9, 1369.8,
1375.7
3230 FOR I = 0 TO NK-1:READ TK(I):NEXT I
3240 RETURN
3250 '
3260 '----- Interpolation routine to find K thermocouple
temperature
3270 'Entry variables:-
3280 '   CJC = cold junction compensator temperature in deg. C.
3290 '   V = thermocouple voltage in volts
3300 'Exit variables:-
3310 '   TC = temperature in degrees Centigrade
3320 'Execution time on std. IBM P.C. = 46 milliseconds
3330 'Perform CJC compensation for K type
3340 VK = 1000*V + 1! + (CJC-25)*.0405      'VK in mV
3350 '
3360 'Find look up element
3370 EK = INT((VK-SVK)/SIK)
3380 IF EK<0 THEN TC=TK(0):GOTO 3420 'Out of bounds, round to
lower limit
3390 IF EK>NK-2 THEN TC=TK(NK-1):GOTO 3420 'Out of bounds,round
to upper limit
3400 'Do interpolation
3410 TC = TK(EK) + (TK(EK+1) - TK(EK))*(VK-EK*SIK-SVK)/SIK
'Centigrade
3420 RETURN
3800 END

```

## APPENDIX C

### HP-TK1 BASIC File Listing

```
10 SCREEN 0,0,0: KEY OFF : CLS : WIDTH 80
20 CLEAR, 49152!
30 DIM
LT%(2),TJ(260),X(55),Y(55),F(55),G(55),H(55),AT(15,20),AP(10),T(32),PRS(3),XDVL(
3),T3(8)
35 ON ERROR GOTO 2740
40 OPEN "C:OUTDATA" FOR OUTPUT AS #2
60 LOCATE 25,1:COLOR 0,7:PRINT"-PLEASE WAIT-";:COLOR 7,0:PRINT" Loading
DASH-8 I/O address and thermocouple lookup table data":LOCATE 1,1
70 DEF SEG = 0
80 SG = 256 * PEEK(&H511) + PEEK(&H510)
90 SG = SG + 49152!/16
100 DEF SEG = SG
110 BLOAD "DASH8.BIN", 0
120 OPEN "DASH8.ADR" FOR INPUT AS #1
130 INPUT #1, BASADR%
140 CLOSE #1
150 DASH8 = 0
160 FLAG% = 0
170 MD% = 0      'Mode 0 = initialization
180 DT$ = "ON "
190 VW%=1
200 CALL DASH8 (MD%, BASADR%, FLAG%)
210 IF FLAG% <>0 THEN PRINT"INSTALLATION ERROR"
220 'Load thermocouple linearizing look up data
230 GOSUB 1470
240 GOSUB 2090 'Load data for spline fit for pressure calculation
250 GOSUB 50000
251 GOSUB 53000
260 'Set gain (AV) at 100 for type J T/C's, 0.5 for pressure meter, and 500 for      type T
T/C's
270 AV0=200
280 AV1=.5
290 AV2=1000
291 AV3=200
300 CLS
310 '---- STEP 2: Initialize an integer array D%(15) to receive data -----
320 DIM D%(3,15) '16 elements, one for each EXP-16 channel
```

```

330 'Also initialize a corresponding real array to receive temperature data
340 '
350 '----- STEP 3: Get cold junction compensation temperature -----
360 'Output of CJC channel is scaled at 24.4mV/deg.C. This corresponds to
370 '0.1 deg.C./bit. Dividing output in bits by 10 yields degrees C.
380 '
390 'Lock DASH-8 to channel #7 (CJC channel selected) using mode 1
400 MD%=1 : LT%(0)=7 : LT%(1) = 7
410 CALL DASH8 (MD%, LT%(0), FLAG%)
420 IF FLAG% <> 0 THEN PRINT "ERROR IN SETTING CJC CHANNEL" : END
430 'Next get CJC data from this channel using Mode 4
440 MD% = 4 : CJ% = 0
450 CALL DASH8 (MD%, CJ%, FLAG%)
460 'Change output in bits to real temperature
470 CJC = CJ%/10
480 '
490 C%=C%+1:OLDTM$=DATIME$: DATIME$=TIME$
500 '----- STEP 4: Get the thermocouple data -----
510 FOR CH% = 0 TO 3
520 GOSUB 1250
530 'This step is written as a subroutine so you can use it in your own
540 'programs by editing it out. Entry parameters are:-
550 ' CH% - specifies DASH-8 channel that EXP-16 is connected to (0-7).
560 ' D%(15) - integer data array to receive data from channels.
570 '
580 '----- STEP 5: Convert data to volts and linearize -----
590 IF CH%=0 THEN GOSUB 620:GOTO 740
600 IF CH%=2 THEN GOSUB 690:GOTO 950
610 IF CH%=1 THEN GOTO 845
611 IF CH%=3 THEN GOTO 612
612 FOR I=0 TO 8
613 V=(D%(3,I)*5)/(AV3*2048)
614 GOSUB 54000
615 T3(I)=TC
616 NEXT I
617 GOTO 950
620 FOR I = 0 TO 14
630 V = (D%(0,I)*5)/(AV0*2048)
640 GOSUB 51000
650 T(I)=TC      'degrees Centigrade
660 NEXT I
670 RETURN
690 V = (D%(2,0)*5)/(AV2*2048)
695 TDIFV = V

```

```

696 RETURN
740 FOR K = 0 TO 15
750 FOR L = 10 TO 2 STEP -1
760 AT(L,K)=AT(L-1,K)
770 NEXT L
780 AT(1,K)=T(K)
790 AT(0,K)=0
800 FOR L = 1 TO 10
810 AT(0,K)=AT(0,K)+AT(L,K)/10
820 NEXT L
830 NEXT K
840 GOTO 950
845 FOR M = 0 TO 1
850 V=D%(1,M)*5/(AV1*2048)
860 GOSUB 1990
862 PRS(M) = PR
863 XDVL(M) = XDV
865 NEXT M
870 FOR K =10 TO 2 STEP -1
880 AP(K)=AP(K-1)
890 NEXT K
900 AP(1)=PR
910 AP(0)=0
920 FOR K = 1 TO 10
930 AP(0)=AP(0)+ AP(K)/10
940 NEXT K
941 TIME1=VAL(RIGHT$(DATIME$,2))
942 TIME2=VAL(RIGHT$(OLDTM$,2))
943 IF TIME2 > TIME1 THEN TIME1=TIME1+60
945 PRATE = (AP(1)-AP(2))/(TIME1-TIME2)
946 IF ABS(PRATE) >= .03 THEN LET VW% = 10
947 IF ABS(PRATE) < .03 THEN LET VW% = 1
950 NEXT CH%
960 '----- STEP 6: Display temperature data -----
970 LOCATE 1,1
980 AA$ = INKEY$
990 IF (AA$="S") OR (AA$="s") THEN CLOSE#2:CLS:END
1000 IF (AA$="I") OR (AA$="i") THEN GOSUB 2790
1010 IF (AA$="D") OR (AA$="d") THEN GOTO 1030 'Toggle to turn on/off write to disk
function
1020 GOTO 1050
1030 IF DT$ = "ON " THEN DT$ = "OFF": GOTO 1070
1040 DT$ = "ON "
1050 IF PC% < VW% THEN PC% = PC% + 1:GOTO 1220

```

```

1060 PC% = 0
1070 PRINT "CHANNEL #:"TAB(25)" 1    2    3    4    5 "
1080 PRINT USING "Temperature (C): ###.# ###.# ###.# ###.#
###.#";T(0),T(1),T(2),T(3),T(4)
1090 PRINT "CHANNEL #:"TAB(25)" 6    7    8    9    10 "
1091 PRINT USING "Temperature (C): ###.# ###.# ###.# ###.# ###.#
";T(5),T(6),T(7),T(8),T(9)
1092 PRINT "CHANNEL #:"TAB(25)"11   12   13   "
1093 PRINT USING "Temperature (C): ###.# ###.# ###.# ";T(10),T(11),T(12)
1100 LOCATE 8,1
1110 PRINT "CHANNEL #:"TAB(25)"1    2    3    4    5   "
1120 PRINT USING "coverplate temp (c) ###.# ###.# ###.# ###.# ###.#
";T3(0),T3(1),T3(2),T3(3),T3(4)
1125 PRINT "CHANNEL #:"TAB(25)"6    7    8    9   "
1130 PRINT USING "coverplate temp (C) ###.# ###.# ###.#
###.#";T3(5),T3(6),T3(7),T3(8)
1162 LOCATE 15,1
1164 PRINT "Total Voltage Differential of Coolant"
1166 PRINT USING "   ###.##### Volts";TDIFV
1180 LOCATE 20,1
1190 PRINT USING "CJC = ###.# deg. C.   P-cond = #####.### Torr   P-evap =
#####.### Torr           ";CJC;PRS(0);PRS(1)
1200 PRINT "Reading was taken at ";DATIME$;" on ";DATE$
1210 LOCATE 23,50:PRINT USING "DISK WRITE IS &";DT$
1220 IF DT$ = "ON " THEN GOSUB 2680
1230 GOTO 350 'repeat scan of channels
1240 '
1250 '---- Subroutine to convert EXP-16 channels to number of bits -----
1260 'First lock DASH-8 on the one channel that EXP-16 is connected to.
1270 LT%(0) = CH% : LT%(1) = CH% : MD% = 1
1280 CALL DASH8 (MD%, LT%(0), FLAG%)
1290 IF FLAG% <> 0 THEN PRINT "ERROR IN SETTING CHANNEL" : END
1300 'Next select each EXP-16 channel in turn and convert it.
1310 'Digital outputs OP1-4 drive the EXP-16 sub-multiplexer address, so use
1320 'mode 14 to set up the sub-multiplexer channel.
1321 IF CH%=0 THEN M=14
1322 IF CH%=1 THEN M=1
1323 IF CH%=2 THEN M=0
1324 IF CH%=3 THEN M=8
1330 FOR SI = 0 TO M 'note use of integer index Si
1340 SID%=SI
1350 MD% = 14
1360 CALL DASH8 (MD%, SID%, FLAG%) 'address set
1370 IF FLAG% <> 0 THEN PRINT "ERROR IN EXP-16 CHANNEL NUMBER" : END

```

```

1380 'Now that channel is selected, perform A/D conversion using mode 4.
1390 'Transfer data to corresponding array element D%(SID%)
1400 MD% = 4 'do 1 A/D conversion
1410 CALL DASH8 (MD%, D%(CH%,SID%), FLAG%)
1420 IF FLAG% <> 0 THEN PRINT "ERROR IN PERFORMING A/D
CONVERSION":PRINT FLAG%
1430 'Now repeat sequence for all other EXP-16 channels
1440 NEXT SI
1450 'All done - return from subroutine
1460 RETURN
1470 '----- Table lookup data for J type thermocouple -----
1480 'Run this subroutine only in the initialization section of your program
1490 'Number of points, voltage step interval (mV), starting voltage (mV)
1500 DATA 257 , .2 , -8.2
1510 READ NJ, SIJ, SVJ
1520 'Temperature at -8.2mv, -8.0mV, -7.8mV etc.
1530 DATA -215.0,-205.3,-196.1,-187.7,-179.9,-172.8,-165.9,-159.3,-153.1,-147.1
1540 DATA -141.2,-135.6,-130.0,-124.6,-119.3,-114.2,-109.1,-104.2, -99.2, -94.4
1550 DATA -89.7, -85.0, -80.3, -75.8, -71.3, -66.8, -62.4, -58.0, -53.7, -49.3
1560 DATA -45.1, -40.8, -36.7, -32.5, -28.3, -24.2, -20.1, -16.1, -12.0, -8.0
1570 DATA -4.0, -0.0, 3.9, 7.9, 11.8, 15.7, 19.6, 23.5, 27.4, 31.2
1580 DATA 35.1, 38.9, 42.7, 46.5, 50.3, 54.1, 57.8, 61.6, 65.3, 69.1
1590 DATA 72.8, 76.5, 80.3, 84.0, 87.7, 91.4, 95.1, 98.7, 102.4, 106.1
1600 DATA 109.8, 113.4, 117.1, 120.7, 124.4, 128.0, 131.7, 135.3, 139.0, 142.6
1610 DATA 146.2, 149.9, 153.5, 157.1, 160.7, 164.3, 168.0, 171.6, 175.2, 178.8
1620 DATA 182.4, 186.0, 189.6, 193.2, 196.8, 200.4, 204.0, 207.6, 211.2, 214.8
1630 DATA 218.4, 222.0, 225.6, 229.2, 232.8, 236.4, 240.0, 243.6, 247.2, 250.8
1640 DATA 254.5, 258.1, 261.7, 265.3, 268.9, 272.5, 276.1, 279.7, 283.3, 286.9
1650 DATA 290.5, 294.1, 297.7, 301.4, 305.0, 308.6, 312.2, 315.8, 319.4, 323.0
1660 DATA 326.7, 330.3, 333.9, 337.5, 341.1, 344.8, 348.4, 352.0, 355.6, 359.3
1670 DATA 362.9, 366.5, 370.1, 373.8, 377.4, 381.0, 384.7, 388.3, 391.9, 395.5
1680 DATA 399.2, 402.8, 406.4, 410.1, 413.7, 417.3, 420.9, 424.5, 428.2, 431.8
1690 DATA 435.4, 439.0, 442.6, 446.3, 449.9, 453.5, 457.1, 460.7, 464.3, 467.9
1700 DATA 471.5, 475.1, 478.7, 482.3, 485.9, 489.5, 493.1, 496.6, 500.2, 503.8
1710 DATA 507.3, 510.9, 514.5, 518.0, 521.6, 525.1, 528.7, 532.2, 535.7, 539.3
1720 DATA 542.8, 546.3, 549.8, 553.3, 556.8, 560.3, 563.8, 567.3, 570.8, 574.2
1730 DATA 577.7, 581.2, 584.6, 588.1, 591.5, 594.9, 598.4, 601.8, 605.2, 608.6
1740 DATA 612.0, 615.4, 618.8, 622.1, 625.5, 628.9, 632.2, 635.6, 638.9, 642.3
1750 DATA 645.6, 648.9, 652.2, 655.5, 658.8, 662.1, 665.4, 668.7, 672.0, 675.2
1760 DATA 678.5, 681.7, 685.0, 688.2, 691.5, 694.7, 697.9, 701.1, 704.3, 707.5
1770 DATA 710.7, 713.9, 717.1, 720.3, 723.5, 726.6, 729.8, 733.0, 736.1, 739.3
1780 DATA 742.4, 745.6, 748.7, 751.8, 755.0, 758.1, 761.2
1790 FOR I = 0 TO NJ-1:READ TJ(I):NEXT I
1800 RETURN

```

```

1810 '
1990 ' Subroutine to calculate pressure from voltage
2000 IF V <= X(1) THEN PR = .001:RETURN
2010 IF V => X(55) THEN PR = 1000:RETURN
2020 FOR K = 2 TO 55
2030 IF V < X(K) THEN 2050
2040 NEXT K
2050 K=K-1
2055 XDV = V
2060 W = (V-X(K))/(X(K+1)-X(K))
2070 PR = (V-X(K))/(X(K+1)-X(K))*(Y(K+1)-Y(K))+Y(K)
2080 RETURN
2090 FOR I = 1 TO 55
2100 READ X(I), Y(I), F(I), G(I), H(I)
2110 NEXT I
2130 DATA 0.0216,0.001,1.152039E-0,-1.520389E-4,1.164153E-10
2140 DATA 0.0278,0.002,1.436064E-3,-7.236689E-4,2.87605E-4
2150 DATA 0.0383,0.003,1.403014E-3,-9.641326E-4,5.611184E-4
2160 DATA 0.0556,0.004,9.037234E-4,3.07868E-4,-2.115917E-4
2170 DATA 0.0691,0.005,1.218899E-3,-6.566989E-4,4.377999E-4
2180 DATA 0.0877,0.006,8.84685E-4,2.084242E-5,9.447272E-5
2190 DATA 0.1012,0.007,8.871799E-04,3.151444E-4,-2.023241E-4
2200 DATA 0.1111,0.008,1.140417E-3,-2.84916E-4,1.444985E-4
2210 DATA 0.1235,0.009,9.959843E-4,-6.89365E-6,1.090951E-5
2220 DATA 0.1358,0.010,8.86203E-3,1.668209E-3,-5.302392E-4
2230 DATA 0.2432,0.020,.0095114,3.732406E-4,1.153592E-4
2240 DATA 0.3395,0.030,9.513834E-3,2.941843E-4,1.919819E-4
2250 DATA 0.4259,0.040,9.466967E-3,1.481336E-3,-9.483006E-4
2260 DATA 0.5025,0.050,1.049817E-2,-2.03906E-3,1.540884E-3
2270 DATA 0.5864,0.060,9.265861E-3,1.551393E-3,-8.172523E-4
2280 DATA 0.6568,0.070,1.008595E-2,-1.033772E-3,9.4782E-4
2290 DATA 0.7284,0.080,9.360003E-3,2.040306E-3,-1.400304E-3
2300 DATA 0.7901,0.090,1.109663E-2,-3.744628E-3,2.648002E-3
2310 DATA 0.8642,0.100,5.922229E-2,7.871723E-2,-3.793951E-2
2320 DATA 1.2441,0.200,9.745134E-2,-9.405315E-4,3.489196E-3
2330 DATA 1.6041,0.300,9.513949E-2,-8.894235E-3,1.375474E-2
2340 DATA 1.9271,0.400,8.942052E-2,2.003414E-2,-9.454668E-3
2350 DATA 2.1706,0.500,9.892368E-2,-9.695515E-3,1.077186E-2
2360 DATA 2.4088,0.600,9.198612E-2,1.308775E-2,-5.073905E-3
2370 DATA 2.6047,0.700,9.736969E-2,9.049624E-3,-6.419286E-3
2380 DATA 2.7900,0.800,0.1044669,-1.178993E-2,7.323034E-3
2390 DATA 2.9912,0.900,9.743704E-2,-8.271963E-3,1.083495E-2
2400 DATA 3.1818,1.000,.6110165,.4423876,-.0534041
2410 DATA 4.2088,2.000,.8606494,3.194034E-2,.1074103

```

```

2420 DATA 4.8706,3.000,.8777054,-3.307223E-2,.1553668
2430 DATA 5.3365,4.000,.8709702,-.269639,.3986688
2440 DATA 5.6541,5.000,.8403325,.4507399,-.2910724
2450 DATA 5.8288,6.000,1.289714,-1.214498,.9247843
2460 DATA 6.0882,7.000,.834555,.3305124,-.1650674
2470 DATA 6.2206,8.000,.999622,-7.136273E-2,7.174075E-2
2480 DATA 6.3529,9.000,.9440796,-6.374979E-2,.1196702
2490 DATA 6.4694,10.00,5.769986,-.5861635,4.816178
2500 DATA 7.0412,20.00,8.287316,-.828743,2.541428
2510 DATA 7.2900,30.00,8.490602,-2.623325,4.132723
2520 DATA 7.4382,40.00,8.380468,2.423147,-.8036146
2530 DATA 7.5176,50.00,9.385612,-4.380738,4.995125
2540 DATA 7.5865,60.00,8.382383,.9266091,.6910076
2550 DATA 7.6235,70.00,8.815776,2.368357,-1.184133
2560 DATA 7.6500,80.00,9.999909,1.438902,-1.438811
2570 DATA 7.6765,90.00,13.66595,-14.34004,10.6741
2580 DATA 7.7188,100.0,46.84252,119.0398,-65.88234
2590 DATA 7.8353,200.0,126.9047,-47.53644,20.63171
2600 DATA 8.0047,300.0,108.3893,-35.10249,26.71324
2610 DATA 8.2006,400.0,89.51311,26.81351,-16.32662
2620 DATA 8.3488,500.0,107.63,-30.9457,23.31568
2630 DATA 8.5182,600.0,90.41804,5.260346,4.32161
2640 DATA 8.6506,700.0,91.10517,25.3441,-16.44927
2650 DATA 8.7565,800.0,110.8648,-66.81552,55.95073
2660 DATA 8.8835,900.0,84.65207,15.34747,4.577637E-4
2670 DATA 8.9576,1000.,0,0,0
2675 RETURN
2680 FOR I=0 TO 12
2700 PRINT#2,USING"###.# ";T(I);
2710 NEXT I
2711 FOR I=0 TO 8
2712 PRINT#2,USING"###.# ";T3(I);
2713 NEXT I
2720 PRINT#2,USING"###.# ";CJC;
2721 PRINT#2,USING"###.## ";PRS(0);
2722 PRINT#2,USING"#.### ";XDVL(0);
2723 PRINT#2,USING"##### ";TDIFV;
2724 PRINT#2,USING"##### ";TIMER
2730 RETURN
2740 IF ERR=61 THEN 2770
2750 PRINT "ERROR NUMBER";ERR
2760 STOP
2770 BEEP:BEEP
2780 END

```

```

2790 CLS
2800 LOCATE 10,10
2810 PRINT"INPUT NUMBER OF READINGS/SCREEN PRINT
(CURRENTLY";VW%;"");
2820 INPUT VW%
2830 CLS
2840 RETURN
50000 '----- Table lookup data for T type thermocouples-----
50010 'Run this subroutine only in the initialization section of your program
50020 'Number of points, voltage step interval (mV), starting voltage (mV)
50030 DATA 138 , .2 , -6.4
50040 READ NT, SIT, SVT
50050 'Temperature at -6.4mV, -6.2mV, -6.0mV etc.
50060 DATA -324.6,-253.7,-229.4,-213.5,-199.8,-187.8,-176.8,-166.6,-157.0,-147.9
50070 DATA -139.2,-131.0,-123.0,-115.4,-108.0,-100.8, -93.8, -87.0, -80.4, -74.0
50080 DATA -67.7, -61.5, -55.4, -49.4, -43.6, -37.9, -32.2, -26.7, -21.2, -15.8
50090 DATA -10.5, -5.2, -0.0, 5.1, 10.2, 15.3, 20.3, 25.2, 30.1, 34.9
50100 DATA 39.7, 44.5, 49.2, 53.8, 58.4, 63.0, 67.6, 72.0, 76.5, 80.9
50110 DATA 85.3, 89.7, 94.0, 98.3, 102.6, 106.8, 111.1, 115.3, 119.4, 123.6
50120 DATA 127.7, 131.8, 135.9, 139.9, 143.9, 148.0, 151.9, 155.9, 159.9, 163.8
50130 DATA 167.7, 171.6, 175.5, 179.3, 183.2, 187.0, 190.8, 194.6, 198.4, 202.1
50140 DATA 205.9, 209.6, 213.3, 217.0, 220.7, 224.4, 228.1, 231.7, 235.4, 239.0
50150 DATA 242.6, 246.2, 249.8, 253.4, 256.9, 260.5, 264.0, 267.6, 271.1, 274.6
50160 DATA 278.1, 281.6, 285.1, 288.6, 292.1, 295.5, 299.0, 302.4, 305.8, 309.3
50170 DATA 312.7, 316.1, 319.5, 322.9, 326.3, 329.6, 333.0, 336.4, 339.7, 343.1
50180 DATA 346.4, 349.7, 353.0, 356.4, 359.7, 363.0, 366.3, 369.6, 372.8, 376.1
50190 DATA 379.4, 382.6, 385.9, 389.2, 392.4, 395.6, 398.9, 402.1
50200 DIM TT(NT-1)
50210 FOR I = 0 TO NT-1:READ TT(I):NEXT I
50220 RETURN
50230 '
51000 '-----Interpolation routine to find T thermocouple temperature-----
51010 'Entry variables:-
51020 ' CJC = cold junction compensator temperature in deg. C.
51030 ' V = thermocouple voltage in volts
51040 'Exit variables:-
51050 ' TC = temperature in degrees Centigrade
51060 ' TF = temperature in degrees Fahrenheit
51070 'Execution time on std. IBM P.C. = 46 milliseconds
51080 'Perform CJC compensation for T type
51090 VT = 1000*V + .992 + (CJC-25)*.040667 'VT in mV
51100 '
51110 'Find look up element
51120 ET = INT((VT-SVT)/SIT)

```

```

51130 IF ET<0 THEN TC=TT(0):GOTO 51170 'Out of bounds, round to lower limit
51140 IF ET>NT-2 THEN TC=TT(NT-1):GOTO 51170 'Out of bounds,round to upper
limit
51150 'Do interpolation
51160 TC = (TT(ET+1) - TT(ET))*(VT-ET*SIT-SVT)/SIT + TT(ET)
51170 TF = TC*9/5 + 32 'Fahrenheit
51180 RETURN
53000 '----- Table lookup data for K type thermocouple -----
53010 'Run this subroutine only in the initialization section of your program
53020 'Number of points, voltage step interval (mV), starting voltage (mV)
53030 DATA 309 , .2 , -6.6
53040 READ NK, SIK, SVK
53050 'Temperature at -6.6mv, -6.4mV, -6.2mV etc.
53060 DATA -353.5,-249.3,-224.0,-207.6,-194.3,-182.8,-172.3,-162.8,-153.8,-145.4
53070 DATA -137.3,-129.6,-122.3,-115.2,-108.3,-101.6, -95.1, -88.7, -82.5, -76.4
53080 DATA -70.4, -64.6, -58.8, -53.1, -47.5, -42.0, -36.6, -31.2, -25.9, -20.6
53090 DATA -15.4, -10.2, -5.1, -0.0, 5.0, 10.1, 15.1, 20.0, 25.0, 29.9
53100 DATA 34.8, 39.7, 44.6, 49.5, 54.3, 59.1, 64.0, 68.8, 73.6, 78.4
53110 DATA 83.2, 88.0, 92.9, 97.7, 102.5, 107.4, 112.2, 117.1, 122.0, 126.9
53120 DATA 131.8, 136.7, 141.7, 146.6, 151.6, 156.5, 161.5, 166.5, 171.5, 176.5
53130 DATA 181.6, 186.6, 191.6, 196.6, 201.6, 206.6, 211.6, 216.6, 221.5, 226.5
53140 DATA 231.5, 236.4, 241.4, 246.3, 251.2, 256.1, 261.0, 265.9, 270.8, 275.6
53150 DATA 280.5, 285.3, 290.2, 295.0, 299.8, 304.6, 309.4, 314.3, 319.1, 323.9
53160 DATA 328.7, 333.4, 338.2, 343.0, 347.8, 352.6, 357.3, 362.1, 366.9, 371.6
53170 DATA 376.4, 381.1, 385.9, 390.6, 395.4, 400.1, 404.8, 409.6, 414.3, 419.0
53180 DATA 423.8, 428.5, 433.2, 437.9, 442.6, 447.3, 452.0, 456.8, 461.5, 466.2
53190 DATA 470.9, 475.6, 480.3, 485.0, 489.7, 494.4, 499.1, 503.8, 508.5, 513.1
53200 DATA 517.8, 522.5, 527.2, 531.9, 536.6, 541.3, 546.0, 550.7, 555.4, 560.0
53210 DATA 564.7, 569.4, 574.1, 578.8, 583.5, 588.2, 592.9, 597.6, 602.3, 607.0
53220 DATA 611.7, 616.4, 621.2, 625.9, 630.6, 635.3, 640.0, 644.8, 649.5, 654.2
53230 DATA 658.9, 663.7, 668.4, 673.2, 677.9, 682.7, 687.4, 692.2, 696.9, 701.7
53240 DATA 706.5, 711.3, 716.1, 720.8, 725.6, 730.4, 735.2, 740.0, 744.8, 749.7
53250 DATA 754.5, 759.3, 764.1, 769.0, 773.8, 778.7, 783.5, 788.4, 793.3, 798.1
53260 DATA 803.0, 807.9, 812.8, 817.7, 822.6, 827.5, 832.4, 837.3, 842.2, 847.2
53270 DATA 852.1, 857.1, 862.0, 867.0, 872.0, 876.9, 881.9, 886.9, 891.9, 896.9
53280 DATA 901.9, 906.9, 911.9, 916.9, 922.0, 927.0, 932.0, 937.1, 942.2, 947.2
53290 DATA 952.3, 957.4, 962.5, 967.6, 972.7, 977.8, 982.9, 988.0, 993.1, 998.2
53300 DATA
1003.4,1008.5,1013.7,1018.8,1024.0,1029.2,1034.4,1039.6,1044.8,1050.0
53310 DATA
1055.2,1060.4,1065.6,1070.8,1076.1,1081.3,1086.6,1091.9,1097.2,1102.4
53320 DATA
1107.7,1113.0,1118.3,1123.7,1129.0,1134.3,1139.7,1145.0,1150.4,1155.8
53330 DATA

```

```

1161.2,1166.6,1172.0,1177.4,1182.9,1188.3,1193.8,1199.2,1204.7,1210.2
53340 DATA
1215.7,1221.2,1226.8,1232.3,1237.9,1243.5,1249.1,1254.7,1260.3,1265.9
53350 DATA
1271.6,1277.3,1282.9,1288.6,1294.3,1300.1,1305.8,1311.5,1317.3,1323.1
53360 DATA 1328.9,1334.7,1340.5,1346.4,1352.2,1358.1,1363.9,1369.8,1375.7
53370 DIM TK(NK-1)
53380 FOR I = 0 TO NK-1:READ TK(I):NEXT I
53390 RETURN
53400 '
54000 '----- Interpolation routine to find K thermocouple temperature -----
54010 'Entry variables:-
54020 ' CJC = cold junction compensator temperature in deg. C.
54030 ' V = thermocouple voltage in volts
54040 'Exit variables:-
54050 ' TC = temperature in degrees Centigrade
54060 ' TF = temperature in degrees Fahrenheit
54070 'Execution time on std. IBM P.C. = 46 milliseconds
54080 'Perform CJC compensation for K type
54090 VK = 1000*V + 1! + (CJC-25)*.0405 'VK in mV
54100 '
54110 'Find look up element
54120 EK = INT((VK-SVK)/SIK)
54130 IF EK<0 THEN TC=TK(0):GOTO 51170 'Out of bounds, round to lower limit
54140 IF EK>NK-2 THEN TC=TK(NK-1):GOTO 51170 'Out of bounds,round to upper
limit
54150 'Do interpolation
54160 TC = (TK(EK+1) - TK(EK))*(VK-EK*SIK-SVK)/SIK +TK(EK) 'Centigrad
54170 TF = TC*9/5 + 32 'Fahrenheit
54180 RETURN
55000 END

```

## Appendix D

### Data Collection Batch File

A:  
HP-Tk1  
COPY C:OUTDATA B:apr17.1  
HP-Tk1  
COPY C:OUTDATA B:apr17.2  
HP-Tk1  
COPY C:OUTDATA B:apr17.3  
HP-tk1  
COPY C:OUTDATA B:apr17.4  
HP-Tk1  
COPY C:OUTDATA B:apr17.5  
PAUSE \*\*\* OUTPUT DISK IN DRIVE B IS FULL. PLEASE REPLACE DISK 1 \*\*\*  
HP-Tk1  
COPY C:OUTDATA B:apr17.6  
HP-Tk1  
COPY C:OUTDATA B:apr17.7  
HP-Tk1  
COPY C:OUTDATA B:apr17.8  
HP-Tk1  
COPY C:OUTDATA B:apr17.9  
HP-Tk1  
COPY C:OUTDATA B:apr17.10  
PAUSE CHANGE DISKETTE IN DRIVE B:USE DISKETTE #3  
HP-Tk1  
COPY C:OUTDATA B:apr17.11  
HP-Tk1  
COPY C:OUTDATA B:apr17.12  
HP-Tk1  
COPY C:OUTDATA B:apr17.13  
HP-Tk1  
COPY C:OUTDATA B:apr17.14  
HP-Tk1  
COPY C:OUTDATA B:apr17.15  
PAUSE PLEASE PLACE EMPTY DISKETTE IN DRIVE B:USE DISK 4  
HP-Tk1  
COPY C:OUTDATA B:apr17.16  
HP-Tk1  
COPY C:OUTDATA B:apr17.17

HP-Tk1  
COPY C:OUTDATA B:apr17.18  
HP-Tk1  
COPY C:OUTDATA B:apr17.19  
HP-tk1  
COPY C:OUTDATA B:apr17.20  
PAUSE \*\*\*PLEASE PLACE DISK 5 IN DRIVE B  
HP-Tk1  
COPY C:OUTDATA B:apr17.21  
HP-Tk1  
COPY C:OUTDATA B:apr17.22  
HP-Tk1  
COPY C:OUTDATA B:apr17.23  
HP-tk1  
COPY C:OUTDATA B:apr17.24  
HP-tk1  
COPY C:OUTDATA B:apr17.25  
PAUSE \*\*\*PLEASE PLACE DISK 6 IN DRIVE B  
HP-Tk1  
COPY C:OUTDATA B:apr17.26  
HP-tk1  
COPY C:OUTDATA B:apr17.27  
HP-Tk1  
COPY C:OUTDATA B:apr17.28  
HP-Tk1  
COPY C:OUTDATA B:apr17.29  
HP-Tk1  
COPY C:OUTDATA B:apr17.30  
PAUSE \*\*\*DATA DISK FULL...PLEASE PLACE DATA DISK 7 IN DRIVE B  
HP-tk1  
COPY C:OUTDATA B:apr17.31  
HP-tk1  
COPY C:OUTDATA B:apr17.32  
HP-Tk1  
COPY C:OUTDATA B:apr17.33  
HP-tk1  
COPY C:OUTDATA B:apr17.34  
HP-Tk1  
COPY C:OUTDATA B:apr17.35  
PAUSE \*\*\*\*DATA DISK FULL...PLEASE PLACE DATA DISK 8 IN DRIVE B  
HP-Tk1  
COPY C:OUTDATA B:apr17.36  
HP-Tk1  
COPY C:OUTDATA B:apr17.37

HP-Tk1  
COPY C:OUTDATA B:apr17.38  
HP-Tk1  
COPY C:OUTDATA B:apr17.39  
HP-Tk1  
COPY C:OUTDATA B:apr17.40  
pause \*\*\*\*data disk full...disk 9 please  
hp-tk1  
copy c:outdata b:apr17.41  
hp-tk1  
copy c:outdata b:apr17.42  
hp-tk1  
copy c:outdata b:apr17.43  
hp-tk1  
copy c:outdata b:apr17.44  
hp-tk1  
copy c:outdata b:apr17.45  
pause \*\*\*\*\*data disk full...disk 10 please  
hp-tk1  
copy c:outdata b:apr17.46  
hp-tk1  
copy c:outdata b:apr17.47  
hp-tk1  
copy c:outdata b:apr17.48  
hp-tk1  
copy c:outdata b:apr17.49  
hp-tk1  
copy c:outdata b:apr17.50  
pause \*\*\*\*\*data disk full...disk 11 s'il vous plait  
hp-tk1  
copy c:outdata b:apr17.51  
hp-tk1  
copy c:outdata b:apr17.52  
hp-tk1  
copy c:outdata b:apr17.53  
hp-tk1  
copy c:outdata b:apr17.54  
hp-tk1  
copy c:outdata b:apr17.55

APPENDIX E

COMPUTER CODE LISTING

PROGRAM HPTAC

```

C*****
C*****
C**** PROGRAM HPTAC ****
C*****
C*           THIS PROGRAM WAS WRITTEN BY JAMES S. PEERY TO
C* ANALYZE THE RESPONSE OF A WATER HEAT PIPE DUE TO RAPID ENERGY
C* INPUTS. IT IS ASSUMED THAT THE HEAT PIPE IS IN EQUILLIBRIUM
C* WITH ITS SURROUNDINGS. THE CODE SOLVES THE CONTINUITY, MOMENTUM,
C* AND ENERGY EQUATIONS TO OBTAIN THE VELOCITY, PRESSURE, AND
C* TEMPERATURE PROFILES IN THE PIPE. IT IS ALSO ASSUMED THAT THE
C* HEAT PIPE IS AT A SATURATED STATE THROUGHOUT THE TRANSIENT.
C*
C*****
C*****
C-
C- -----
C- DEFINITION OF ARRAYS:                               UNITS
C- -----
C-
C- DENL1- DENSITY OF LIQUID AT TIME=T                   KG/M3
C- DENL2- DENSITY OF LIQUID AT TIME=T+1                 KG/M3
C- SPELC1- VELOCITY OF LIQUID AT TIME=T AT NODE INTERFACE M/S
C- SPELC2- VELOCITY OF LIQUID AT TIME=T+1 AT NODE INTERFACE M/S
C- PRESL1- PRESSURE OF LIQUID AT TIME=T                 N/M2
C- PRESL2- PRESSURE OF LIQUID AT TIME=T+1              N/M2
C- TEMPL1- TEMPERATURE OF LIQUID AT TIME=T             KELVIN
C- TEMPL2- TEMPERATURE OF LIQUID AT TIME=T+1          KELVIN
C- SHLIQ1- SPECIFIC HEAT OF LIQUID AT TIME=T           J/(KG-K)
C- SHLIQ2- INTERNAL ENERGY OF LIQUID AT TIME=T+1     J/(KG-K)
C- VISCOL- VISCOSITY OF LIQUID                        (N-S)/M2
C- CONL- CONDUCTIVITY OF LIQUID                       W/(M-K)
C- DENV1- DENSITY OF VAPOR AT TIME=T                   KG/M3
C- DENV2- DENSITY OF VAPOR AT TIME=T+1                 KG/M3
C- SPEVC1- VELOCITY OF VAPOR AT TIME=T AT NODE INTERFACE M/S
C- SPEVC2- VELOCITY OF VAPOR AT TIME=T+1 AT NODE INTERFACE M/S
C- PRESV1- PRESSURE OF VAPOR AT TIME=T                 N/M2
C- PRESV2- PRESSURE OF VAPOR AT TIME=T+1              N/M2
C- TEMPV1- TEMPERATURE OF VAPOR AT TIME=T             KELVIN
C- TEMPV2- TEMPERATURE OF VAPOR AT TIME=T+1          KELVIN
C- SHVAP1- INTERNAL ENERGY OF VAPOR AT TIME=T       J/(KG-K)
C- SHVAP2- INTERNAL ENERGY OF VAPOR AT TIME=T+1     J/(KG-K)
C- VISCOV- VISCOSITY OF VAPOR                        (N-S)/M2

```

C-	CONV-	CONDUCTIVITY OF VAPOR	W/(M-K)
C-	SOURCE-	MASS FLOW RATE OF EVAPORATION/CONDENSATION	KG/S
C-	HETIN-	HEAT INPUT	W
C-	HETOUT-	HEAT OUTPUT	W
C-	DELX-	WIDTH OF A NODE	M
C-	SIGMA-	SURFACE TENSION IN EACH L-V NODE	N/M
C-	DPVAP-	PRESSURE DIFFERENCE BETWEEN NODES IN THE VAPOR	N/M2
C-	DPLIQ-	PRESSURE DROP FROM NODE TO NODE IN THE LIQUID	N/M2
C-	TEMPIN-	ALL TEMPERATURES AT ITERATION J	KELVIN
C-	TEMPOUT-	ALL TEMPERATURES AT ITERATION J+1	KELVIN
C-	REYNV-	REYNOLDS NUMBER FOR THE VAPOR REGION	---
C-	HDB-	HEAT TRANSFER COEFFICIENT BETWEEN VAPOR AND LIQUID	W/M2-K
C-	PRV-	PRANDLT NUMBER OF THE VAPOR	---
C-	SOURCE-	EVAPORATION/CONDENSATION RATE	KG/S
C-	XSAVE-	EXTRA ARRAY	---
C-	FSAVE-	EXTRA ARRAY	---
C-	RR1-	COEFFICIENTS FOR R->P,E RELATIONSHIP	---
C-	CF1-	COEFFICIENTS FOR P->H RELATIONSHIP FOR LIQUID	---
C-	CF2-	COEFFICIENTS FOR P->H RELATIONSHIP FOR LIQUID	---
C-	CF3-	COEFFICIENTS FOR P->H RELATIONSHIP FOR LIQUID	---
C-	CG1-	COEFFICIENTS FOR P->H RELATIONSHIP FOR VAPOR	---
C-	CG2-	COEFFICIENTS FOR P->H RELATIONSHIP FOR VAPOR	---
C-	CG3-	COEFFICIENTS FOR P->H RELATIONSHIP FOR VAPOR	---
C-	CT1-	COEFFICIENTS FOR P->T RELATIONSHIP FOR LIQUID	---
C-	CT2-	COEFFICIENTS FOR P->T RELATIONSHIP FOR LIQUID	---
C-	CT3-	COEFFICIENTS FOR P->T RELATIONSHIP FOR VAPOR	---
C-	CT4-	COEFFICIENTS FOR P->T RELATIONSHIP FOR VAPOR	---
C-	CN1-	COEFFICIENTS FOR P->V RELATIONSHIP FOR LIQUID	---
C-	CN2-	COEFFICIENTS FOR P->V RELATIONSHIP FOR VAPOR	---
C-	AA1-	COEFFICIENTS FOR T->@ RELATIONSHIP FOR INTERFACE	---
C-	AA2-	COEFFICIENTS FOR T->VISCOSITY FOR LIQUID	---
C-	AA3-	COEFFICIENTS FOR T->VISCOSITY FOR VAPOR	---
C-	AK-	COEFFICIENT FOR T->PRESSURE FOR SATURATION	---
C-	AL-	COEFFICIENT FOR T->PRESSURE FOR SATURATION	---
C-	CLSH-	COEFFICIENT FOR T->SPECIFIC HEAT FOR LIQUID	---
C-	CVSH-	COEFFICIENT FOR T->SPECIFIC HEAT FOR LIQUID	---
C-	CLTC-	COEFFICIENT FOR T->CONDUCTIVITY FOR LIQUID	---
C-	AZ-	COEFFICIENT FOR T->DENSITY FOR LIQUID	---
C-	BBZ-	COEFFICIENT FOR T->DENSITY FOR LIQUID	---
C-	NYZ-	EXPONENTS FOR T->DENSITY FOR LIQUID	---
C-	LYZ-	EXPONENTS FOR T->DENSITY FOR LIQUID	---
C-	NZZ-	EXPONENTS FOR T->DENSITY FOR VAPOR	---
C-	LUZ-	EXPONENTS FOR T->DENSITY FOR VAPOR	---
C-	BL-	COEFFICIENT FOR T->DENSITY FOR VAPOR	---
C-	TT1-	TEMPERATURES FROM SIMPLIFIED ENERGY EQUATION	KELVIN
C-	D1-	USED BY ENERI TO BE SENT TO ELIM FOR SOLUTION	---
C-	A1-	USED BY ENERI AS NODE (I-1) AND (I+1)	---
C-	B1-	USED BY ENERI AS NODE (I)	---
C-	CC1-	USED BY ENERI AS RHS OF ENERGY EQUATION	---
C-	TS-	INITIAL HEAT PIPE TEMPERATURES FOR ENERI	KELVIN
C-	STORE-	STORED ENERGY CALCULATED FROM ENERI	WATTS
C-			

C- -----	
C- DEFINITION OF VARIABLES:	
C- -----	
C-	
C- PCRIT- CRITICAL PRESSURE	N/M2
C- TEMPK- CRITICAL TEMPERATURE	KELVIN
C- BETA1- INPUT PARAMETER FOR SUBROUTINE SURTEN	---
C- AMOLE- MOLECULAR WIEGHT OF WORKING FLUID	KG/ (KG-MOLE)
C- GASC- ABSOLUTE GAS CONSTANT	J/ (KG-MOLE-@K)
C- FLUDK- CONDUCTIVITY OF LIQUID	W/M-K
C- SHFLUD- SPECIFIC HEAT OF LIQUID	J/KG-K
C- DFLUD- DENSITY OF LIQUID	KG/M3
C- VOLF- POROSITY OF THE WICK-LIQUID STRUCTURE	---
C- WICKP- PERMABILITY OF THE WICK	M2
C- WICKK- CONDUCTIVITY OF WICK	W/M-K
C- SHWICK- SPECIFIC HEAT OF WICK	J/KG-K
C- DWICK- DENSITY OF WICK	KG/M3
C- RAD11- RADIUS OF CURVATURE OF NODE 1	M
C- RADIN- RADIUS OF CURVATURE OF NODE N	M
C- RADBN- RADIUS OF CURVATURE OF NODE N AT TIME T	M
C- WALLK- CONDUCTIVITY OF WALL	W/M-K
C- SHWALL- SPECIFIC HEAT OF WALL	J/KG-K
C- DWALL- DENSITY OF WALL	KG/M3
C- COOLK- CONDUCTIVITY OF COOLANT	W/M-K
C- PRCUL- PRANLT NUMBER OF COLLANT	---
C- VISCUL- VISCOSITY OF COOLANT	N-S/M
C- TEMPC- TEMPERATURE OF COOLANT	KELVIN
C- CMFR- COOLANT MASS FLOW RATE	KG/S
C- FDNUN- FULLY DEVELOPED NUSSELT NUMBER	---
C- GRAV- FORCE DUE TO GRAVITY	M/S2
C- THETA- ANGLE BETWEEN HORIZONTAL AND GRAV	RADIANS
C- SHREFV- SPECIFIC HEAT OF VAPOR AT 273.15 K	J/ (KG-K)
C- SHREFL- SPECIFIC HEAT OF LIQUID AT 273.15 K	J/ (KG-K)
C- ENREF- VAPOR ENTHALPY AT 273.15 K	J/KG
C- HDBCO- HEAT TRANSFER COEFFICIENT OF COOLANT	W/M2-K
C- TTOL- RELATIVE CONVERGENCE CRITERIA FOR ENERGY EQ.	---
C- DELT- DIFFERENTIAL TIME STEP	S
C- PI- VALUE OF PI	---
C- NE- NUMBER OF EVAPORATOR NODES	---
C- NA- NUMBER OF ADIABATIC NODES	---
C- NC- NUMBER OF CONDENSOR NODES	---
C- EVAPL- LENGTH OF EVAPORATOR SECTION	M
C- ADIAL- LENGTH OF ADIABATIC SECTION	M
C- CONDL- LENGTH OF CONDENSOR SECTION	M
C- DELZL- Z WIDTH OF LIQUID-WICK REGION	M
C- DELZV- Z WIDTH OF VAPOR REGION	M
C- DELZ- Z WIDTH OF LIQUID AND VAPOR REGIONS	M
C- DELY- Y WIDTH OF HEAT PIPE	M
C- VOLL- VOLUME OF INITIAL HEAT PIPE CHARGE	LITER
C- AREAL- CROSS SECTIONAL AREA OF LIQUID-WICK REGION	M2
C- AREAV- CROSS SECTIONAL AREA OF VAPOR REGION	M2
C- AREAC- CROSS SECTIONAL AREA FOR COOLANT FLOW	M2



C- IP6 =1 NOT USED  
C- IP7 =1 NOT USED  
C- IP8 =0 NOT USED  
C- IP9 =0 NOT USED  
C- IP10 =0 NOT USED  
C- IP11 =0 NOT USED  
C- IP12 =0 NOT USED

C-  
C-  
C-  
C-

-----  
C-  
IMPLICIT REAL (A-H,O-Z)  
COMMON /TEMP/TEMPO1(100),TEMPO2(100),TEMPW1(100),TEMPW2(100),  
+           TEMPL1(100),TEMPL2(100),TEMPV1(100),TEMPV2(100),  
+           TEMPIN(1000),TEMPOUT(1000),NX  
COMMON /PRES/PRESL1(100),PRESL2(100),PRESV1(100),PRESV2(100),  
+           DPLIQ(100),DPVAP(100)  
COMMON /DENS/DENL1(100),DENL2(100),DENV1(100),DENV2(100)  
COMMON /SPEED/SPELC1(100),SPELC2(100),SPELB1(100),SPELB2(100),  
+           SPEVC1(100),SPEVC2(100),SPEVB1(100),SPEVB2(100)  
COMMON /SPHEAT/SHLIQ1(100),SHLIQ2(100),SHVAP1(100),SHVAP2(100)  
COMMON /PROP/CONL(100),CONV(100),VISCOL(100),  
+           VISCOV(100),REYNV(100),HDB(100),PRV(100)  
COMMON /SETUP/DELX(100),HETIN(100),HETOUT(100),SOURCE(100),  
+           SIGMA(100),XSAVE(100),FSAVE(100)  
COMMON /COEFF/RR1(25),CF1(9),CF2(9),CF3(9),CG1(12),  
+           CG2(9),CG3(7),CT1(2,4),CT2(5,5),CT3(5,5),  
+           CT4(5,5),CN1(3,5),CN2(4,3),AA1(5),AA2(7),  
+           AA3(7),AK(9),AL(12),CLSH(6),CVSH(6),CLTC(6),  
+           AZ(12),BBZ(9,6),BL(4),PCRIT,TEMPK,BETA1,  
+           NYZ(8),LYZ(8),NZZ(8,3),LUZ(8,2)  
COMMON /EZENG/TT1(5),D1(5,6),A1(5),B1(5),CC1(5),TS(5),STORE(1000)  
COMMON /OUTPU/RTIME,ERRMAX,NRE,ITER,ITIME,IREAD  
COMMON /INITIL/AMOLE,GASC,FLUDK,SHFLUD,DFLUD,VOLF,WICKP,WICKK,  
+           SHWICK,DWICK,RADI1,RADIN,RADBN,WALLK,SHWALL,DWALL,  
+           COOLK,PRCUL,VISCU,TEMPC,CMFR,FDNUN,GRAV,THETA,  
+           SHREFV,SHREFL,ENREF,HDBCO,  
+           TTOL,DELT,PI,QSTC  
COMMON /GEOMHP/EVAPL,ADIAL,CONDL,DELZL,DELZV,DELZ,DELY,VOLL,  
+           AREAL,AREAV,AREAC,WALLT,PWETV,PWETL,PWETC,  
+           POPEN,WDIA,FWAR,DELPV,DELPL,N,NE,NA,NC,LAYERS,  
+           NFAKE  
COMMON /FLAGS/IF1,IF2,IF3,IF4,IF5,IF6,IF7,IF8,IF9,IF10,IF11,IF12  
COMMON /PFLAGS/IP1,IP2,IP3,IP4,IP5,IP6,IP7,IP8,IP9,IP10,IP11,IP12

C-  
C- ZERO OUT ALL VARIABLES  
C-

DATA RTIME,ERRMAX,NRE,ITER,ITIME,IREAD/0.0,0.0,4\*0/  
DATA AMOLE,GASC,FLUDK,SHFLUD,DFLUD,VOLF,WICKP,WICKK,  
+           SHWICK,DWICK,RADI1,RADIN,RADBN,WALLK,SHWALL,DWALL,  
+           COOLK,PRCUL,VISCU,TEMPC,CMFR,FDNUN,GRAV,THETA,  
+           SHREFV,SHREFL,ENREF,HDBCO,TTOL,DELT,PI,QSTC/32\*0.0/  
DATA EVAPL,ADIAL,CONDL,DELZL,DELZV,DELZ,DELY,VOLL,

```

+ AREAL, AREAV, AREAC, WALLT, PWETV, PWETL, PWETC,
+ POPEN, WDIA, FWAR, DELPV, DELPL, N, NE, NA, NC, LAYERS,
+ NFAKE, NX/20*0.0, 7*0/
DATA IF1, IF2, IF3, IF4, IF5, IF6, IF7, IF8, IF9, IF10, IF11, IF12/12*0/
DATA IP1, IP2, IP3, IP4, IP5, IP6, IP7, IP8, IP9, IP10, IP11, IP12/12*0/
C-
C- CREATE FILES FOR INPUT AND OUTPUT OF DATA
C-
OPEN (UNIT=2, FILE='INHOPE', STATUS='OLD')
OPEN (UNIT=4, FILE='WATCOF', STATUS='OLD')
OPEN (UNIT=5, FILE='RESTART', STATUS='OLD')
OPEN (UNIT=8, FILE='OUT1', STATUS='UNKNOWN')
OPEN (UNIT=9, FILE='OUTIT', STATUS='UNKNOWN')
C-
C- READ IN NUMBER OF NODES IN EACH REGION
C-
READ (2, 1001) NE, NA, NC, N, NY, IREAD
NX=N*NY
C-
C- ZERO OUT ARRAYS
C-
DO 100 I=1, 100
DENL1 (I)=0.0
DENL2 (I)=0.0
SPELC1 (I)=0.0
SPELC2 (I)=0.0
SPELB1 (I)=0.0
SPELB2 (I)=0.0
PRESL1 (I)=0.0
PRESL2 (I)=0.0
TEMPL1 (I)=0.0
TEMPL2 (I)=0.0
SHLIQ1 (I)=0.0
SHLIQ2 (I)=0.0
CONL (I)=0.0
VISCOL (I)=0.0
DPLIQ (I)=0.0
DENV1 (I)=0.0
DENV2 (I)=0.0
SPEVC1 (I)=0.0
SPEVC2 (I)=0.0
SPEVB1 (I)=0.0
SPEVB2 (I)=0.0
PRESV1 (I)=0.0
PRESV2 (I)=0.0
TEMPV1 (I)=0.0
TEMPV2 (I)=0.0
SHVAP1 (I)=0.0
SHVAP2 (I)=0.0
CONV (I)=0.0
VISCOV (I)=0.0
DPVAP (I)=0.0

```

```

        TEMPO1 (I) =0.0
        TEMPO2 (I) =0.0
        TEMPW1 (I) =0.0
        TEMPW2 (I) =0.0
        DELX (I) =0.0
        REYNV (I) =0.0
        PRV (I) =0.0
        HDB (I) =0.0
        SOURCE (I) =0.0
        HETIN (I) =0.0
        HETOUT (I) =0.0
        SIGMA (I) =0.0
        XSAVE (I) =0.0
        FSAVE (I) =0.0
100  CONTINUE
      DO 200 I=1,1000
        TEMPIN (I) =0.0
        TEMPOUT (I) =0.0
        STORE (I) =0.0
200  CONTINUE
C-
C- CALL PROGRAM BODY
C-
      CALL BEGIN
1001 FORMAT (12 (I6))
C-
C- CLOSE FILES FOR INPUT AND OUTPUT
C-
      CLOSE (2)
      CLOSE (4)
      CLOSE (5)
      CLOSE (8)
      CLOSE (9)
      STOP
      END
      SUBROUTINE BEGIN
C-
C- -----
C-
C- SUBROUTINE BEGIN:
C-
C-           THIS SUBROUTINE IS THE HEART OF THE PROGRAM.
C- IT MAKES ALL OF THE SUBROUTINE CALLS. IT IS THE STRUCTURE OF THE
C- FLOW CHART TO FOR THE SOLUTION TO THE PROBLEM AT HAND.
C-
C- -----
C-
      IMPLICIT REAL (A-H,O-Z)
      COMMON /TEMP/TEMPO1 (100), TEMPO2 (100), TEMPW1 (100), TEMPW2 (100),
+           TEMPL1 (100), TEMPL2 (100), TEMPV1 (100), TEMPV2 (100),
+           TEMPIN (1000), TEMPOUT (1000), NX
      COMMON /PRES/PRESL1 (100), PRESL2 (100), PRESV1 (100), PRESV2 (100),

```

```

+           DPLIQ(100),DPVAP(100)
COMMON /DENS/DENL1(100),DENL2(100),DENV1(100),DENV2(100)
COMMON /SPEED/SPELC1(100),SPELC2(100),SPELB1(100),SPELB2(100),
+           SPEVC1(100),SPEVC2(100),SPEVB1(100),SPEVB2(100)
COMMON /SPHEAT/SHLIQ1(100),SHLIQ2(100),SHVAP1(100),SHVAP2(100)
COMMON /PROP/CONL(100),CONV(100),VISCOL(100),
+           VISCOV(100),REYNV(100),HDB(100),PRV(100)
COMMON /SETUP/DELX(100),HETIN(100),HETOUT(100),SOURCE(100),
+           SIGMA(100),XSAVE(100),FSAVE(100)
COMMON /COEFF/RR1(25),CF1(9),CF2(9),CF3(9),CG1(12),
+           CG2(9),CG3(7),CT1(2,4),CT2(5,5),CT3(5,5),
+           CT4(5,5),CN1(3,5),CN2(4,3),AA1(5),AA2(7),
+           AA3(7),AK(9),AL(12),CLSH(6),CVSH(6),CLTC(6),
+           AZ(12),BBZ(9,6),BL(4),PCRIT,TEMPK,BETA1,
+           NYZ(8),LYZ(8),NZZ(8,3),LUZ(8,2)
COMMON /EZENG/TT1(5),D1(5,6),A1(5),B1(5),CC1(5),TS(5),STORE(1000)
COMMON /OUTPU/RTIME,ERRMAX,NRE,ITER,ITIME,IREAD
COMMON /INITIL/AMOLE,GASC,FLUDK,SHFLUD,DFLUD,VOLF,WICKP,WICKK,
+           SHWICK,DWICK,RADI1,RADIN,RADBN,WALLK,SHWALL,DWALL,
+           COOLK,PRCUL,VISCU,TEMPC,CMFR,FDNUN,GRAV,THETA,
+           SHREFV,SHREFL,ENREF,HDBCO,
+           TTOL,DELT,PI,QSTC
COMMON /GEOMHP/EVAPL,ADIAL,CONDL,DELZL,DELZV,DELZ,DELY,VOLL,
+           AREAL,AREAV,AREAC,WALLT,PWETV,PWETL,PWETC,
+           POPEN,WDIA,FWAR,DELPV,DELPL,N,NE,NA,NC,LAYERS,
+           NFAKE
COMMON /FLAGS/IF1,IF2,IF3,IF4,IF5,IF6,IF7,IF8,IF9,IF10,IF11,IF12
COMMON /PFLAGS/IP1,IP2,IP3,IP4,IP5,IP6,IP7,IP8,IP9,IP10,IP11,IP12

```

```

C-
C- CALL SUBROUTINE TO READ IN INPUTS AND SET ARRAYS TO CONSTANTS
C- IF NEEDED.
C-
C-     CALL INPUT
C-
C- CALL SUBROUTINE TO READ THE COEFFICIENTS NEEDED FOR THE PROPRTY
C- RELATIONSHIPS.
C-
C-     CALL INCOF
C-
C- FIND PRESSURE IN EACH NODE FROM TEMPERATURE
C-
C-     CALL TTP
C-
C- DETERMINE DENSITY AND SPECIFIC HEATS OF LIQUID AND VAPOR AT EACH
C- NODE FROM TEMPERATURE FOR INITIAL CONDITIONS
C-
C-     CALL GETPROP
C-
C- CALL SUBROUTINE TO FIND WICK PERMABILITY AND VOLUME FRACTION
C-
C-     CALL GEO
C-

```

```

C- WRITE OUT INITIAL CONDITIONS
C-
    CALL OUTPUTE
C-
C- DETERMINE THE TIME CONSTANT ON THE STORED ENERGY
C-
    IF(IREAD.EQ.5) GO TO 134
    IF(IF10.EQ.1) GO TO 133
    CALL TIMCON
C-
C- DETERMINE CONDUCTIVITIES OF THE LIQUID FROM TEMPERATURE
C-
    133 CALL CONLIQ
C-
C- DETERMINE CONDUCTIVITIES OF THE VAPOR FROM TEMPERATURE
C-
    CALL CONVAP
C-
C- FIND VISCOSITIES FROM TEMPERATURES
C-
    CALL VISFT
C-
C- DETERMINE SPECIFIC HEATS FROM TEMPERATURE
C-
    CALL SPECHT
C-
C- DETERMINE THE PRANDLT NUMBER OF THE VAPOR FOR EACH NODE
C-
    CALL PRANDLT
C-
C- USE SIMPLIFIED ENERGY EQUATION TO GET A GUESS ON THE TEMPERATURES
C- FOR THE NEXT ITME STEP
C-
    CALL ENERI
C-
C- SET RESULTS FROM ENERI TO NEXT TIME STEP TEMPERATURES
C-
    134 CALL TGUESS
C-
C- INITIALIZE OTHER DEPENDENT VARIABLES
C-
    CALL INITIAL
C-
C- WRITE OUT CONDITIONS FOR INITIAL ITERATION
C-
    CALL OUTPUTI
C-
C- SET UP LOOP TO SOLVE TRANSIENT CAUSE (IT8=NUMBER OF TIME STEPS)
C-
    DO 500 ITIME=1,IF8
C-
C- DETERMINE THE TIME OF THE TRANSIENT

```

```

C-          RTIME=RTIME+DELT
C-
C- SET UP A LOOP TO SOLVE THE MATRIX BY GAUSS-SIEDEL ITERATION
C-
C-          DO 300 ITER=1,IF9
C-
C- DETERMINE THE EVAPORATION/CONDENSATION RATE
C-
C-          CALL EVAP
C-
C- DETERMINE THE LIQUID VELOCITIES
C-
C-          CALL CONMASL
C-
C- DETERMINE THE VAPOR VELOCITIES
C-
C-          CALL CONMASV
C-
C- DETERMINE THE REYNOLDS NUMBER OF THE VAPOR FOR EACH NODE
C-
C-          CALL REYN
C-
C- DETERMINE THE HEAT TRANSFER COEFFICIENT BETWEEN THE LIQUID AND VAPOR
C-
C-          CALL HTCF
C-
C- CALL SUBROUTINE TO SOLVE FULL ENERGY EQUATION
C-
C-          CALL ENERGY
C-
C- USE GAUSS-SIEDEL TO SOLVE THE MATRIX
C-
C-          CALL SIEDEL
C-
C- END TIME STEP IF ALL TEMPERATURES HAVE CONVERGED
C-
C-          IF (ERRMAX.LE.TTOL) GO TO 400
C-
C- WRITE OUT CONDITIONS FOR ITERATION STEP
C-
C-          CALL OUTPUTI
300    CONTINUE
C-
C- DETERMINE THE PRESSURE DROPS FOR THE LIQUID
C-
C-          400    CALL MOMTUML
C-
C- DETERMINE THE PRESSURE DROPS FOR THE VAPOR
C-
C-          CALL MOMTUMV
C-

```

```

C- FIND THE PRESSURE IN LAST NODE FROM THE SATURATION TEMPERATURE
C-
      CALL PRESFT
C-
C- DETERMINE PRESURE PROFILES
C-
      CALL PREGES
C-
C- WRITE OUT CONDITIONS FOR TIME STEP
C-
      CALL OUTPUTE
C-
C- SET ALL VALUES OF TIME STEP TO PREVIOUS TIME STEP
C-
      CALL DENSE
C-
C- DETERMINE CONDUCTIVITIES OF THE LIQUID FROM TEMPERATURE
C-
      CALL CONLIQ
C-
C- DETERMINE CONDUCTIVITIES OF THE VAPOR FROM TEMPERATURE
C-
      CALL CONVAP
C-
C- FIND VISCOSITIES FROM TEMPERATURES
C-
      CALL VISFT
C-
C- DETERMINE SPECIFIC HEATS FROM TEMPERATURE
C-
      CALL SPECHT
C-
C- DETERMINE THE PRANDLT NUMBER OF THE VAPOR FOR EACH NODE
C-
      CALL PRANDLT
      CALL NEXTTS
500 CONTINUE
C-
C- REWIND UNIT 5
C-
      REWIND (5)
C-
C- WRITE FINAL VALUES OUT TO FILE RESTART
C-
      CALL FINISH
C-
C- PRINT OUT ALL CONSTANTS OF IMPORTANCE TO THE SOLUTION
C-
      CALL OUTCONT
      RETURN
      END
      SUBROUTINE CONLIQ

```

```

C-
C-----
C-
C-   SUBROUTINE CONLIQ:
C-
C-           THIS SUBROUTINE CALCULATES THE THERMAL
C-   CONDUCTIVITY OF THE LIQUID AS A FUNCTION OF TEMPERATURE.
C-   A FIFTH DEGREE LEAST SQUARES FIT IS DONE TO PROPERTY DATA FOUND
C-   IN COLLIER.
C-----
C-
C-   IMPLICIT REAL (A-H,O-Z)
C-   COMMON /TEMP/TEMPO1(100),TEMPO2(100),TEMPW1(100),TEMPW2(100),
+       TEMPL1(100),TEMPL2(100),TEMPV1(100),TEMPV2(100),
+       TEMPIN(1000),TEMPOUT(1000),NX
C-   COMMON /PROP/CONL(100),CONV(100),VISCOL(100),
+       VISCOV(100),REYNV(100),HDB(100),PRV(100)
C-   COMMON /COEFF/RR1(25),CF1(9),CF2(9),CF3(9),CG1(12),
+       CG2(9),CG3(7),CT1(2,4),CT2(5,5),CT3(5,5),
+       CT4(5,5),CN1(3,5),CN2(4,3),AA1(5),AA2(7),
+       AA3(7),AK(9),AL(12),CLSH(6),CVSH(6),CLTC(6),
+       AZ(12),BBZ(9,6),BL(4),PCRIT,TEMPK,BETA1,
+       NYZ(8),LYZ(8),NZZ(8,3),LUZ(8,2)
C-   COMMON /GEOMHP/EVAPL,ADIAL,CONDL,DELZL,DELZV,DELZ,DELY,VOLL,
+       AREAL,AREAV,AREAC,WALLT,PWETV,PWETL,PWETC,
+       POPEN,WDIA,FWAR,DELPV,DELPL,N,NE,NA,NC,LAYERS,
+       NFAKE
C-   COMMON /PFLAGS/IP1,IP2,IP3,IP4,IP5,IP6,IP7,IP8,IP9,IP10,IP11,IP12
C-
C- SET UP LOOP TO CALCULATE THE CONDUCTIVITIES AT EACH NODE
C-
C-   DO 200 I=1,N
C-       SUM=0.0
C-
C- APPLY COEFFICIENTS FROM LEAST SQUARES FIT
C-
C-   DO 100 J=1,6
C-       SUM=SUM+CLTC(J)*TEMPL2(I)**(J-1)
100   CONTINUE
C-       CONL(I)=SUM
200   CONTINUE
C-   RETURN
C-   END
C-   SUBROUTINE CONMASL
C-----
C-
C-   SUBROUTINE CONMASL:
C-
C-           THIS SUBROUTINE SOLVES THE CONSERVATION OF
C-   MASS EQUATION FOR THE LIQUID VELOCITIES IN THE HEAT PIPE.

```

C- THE BOUNDARY CONDITION USED IS THE VELOCITY IS ZERO AT THE  
 C- CONDENSER END OF THE HEAT PIPE. THE VELOCITIES ARE SOLVE FOR  
 C- AT THE EDGE OF THE NODAL CELLS.

C-  
 C-  
 C-----

C-  
 IMPLICIT REAL (A-H,O-Z)  
 COMMON /DENS/DENL1(100),DENL2(100),DENV1(100),DENV2(100)  
 COMMON /SPEED/SPELC1(100),SPELC2(100),SPELB1(100),SPELB2(100),  
 + SPEVC1(100),SPEVC2(100),SPEVB1(100),SPEVB2(100)  
 COMMON /SETUP/DELX(100),HETIN(100),HETOUT(100),SOURCE(100),  
 + SIGMA(100),XSAVE(100),FSAVE(100)  
 COMMON /INITIL/AMOLE,GASC,FLUDK,SHFLUD,DFLUD,VOLF,WICKP,WICKK,  
 + SHWICK,DWICK,RADI1,RADIN,RADBN,WALLK,SHWALL,DWALL,  
 + COOLK,PRCUL,VISCUL,TEMPC,CMFR,FDNUN,GRAV,THETA,  
 + SHREFV,SHREFL,ENREF,HDBCO,  
 + TTOL,DELT,PI,QSTC  
 COMMON /GEOMHP/EVAPL,ADIAL,CONDL,DELZL,DELZV,DELZ,DELY,VOLL,  
 + AREAL,AREAV,AREAC,WALLT,PWETV,PWETL,PWETC,  
 + POPEN,WDIA,FWAR,DELPV,DELPV,N,NE,NA,NC,LAYERS,  
 + NFAKE

C-  
 C- FIND THE AREA FOR FLOW

C-  
 AREA=DELY\*DELZL\*VOLF

C-  
 C- MARCH BACKWARDS THROUGH THE GRID TO FIND THE VELOCITIES

C-  
 DO 100 J=N,1,-1

C-  
 C- DETERMINE THE VOLUME OF THE CELL

C-  
 VV=DELX(J)\*AREA  
 IF(J.EQ.N) THEN

C-  
 C- APPLY BOUNDARY CONDITION (VELOCITY AT N+1/2= 0)

C-  
 SPELC2(J)=(-SOURCE(J)-VV\*(DENL2(J)-DENL1(J))/DELT)/  
 + (DENL2(J)\*AREA)  
 ELSE  
 SPELC2(J)=(DENL2(J+1)\*SPELC2(J+1)\*AREA-SOURCE(J)-VV\*  
 + (DENL2(J)-DENL1(J))/DELT)/(DENL2(J)\*AREA)  
 END IF

100 CONTINUE

C-  
 C- SET THE VELOCITY TO ZERO IF IT IS NEGATIVE. (RESULTS FROM TRUNCATION  
 C- ERROR)

C-  
 DO 200 I=1,N  
 IF(SPELC2(I).LT.0.0) SPELC2(I)=0.0

```

200 CONTINUE
    RETURN
    END
    SUBROUTINE CONMASV

C-
C-----
C-
C- SUBROUTINE CONMASV:
C-
C-           THIS SUBROUTINE SOLVES THE CONSERVATION OF
C- MASS EQUATION FOR THE VAPOR VELOCITIES IN THE HEAT PIPE.
C- THE BOUNDARY CONDITION USED IS THE VELOCITY IS ZERO AT THE
C- EVAPORATOR END OF THE HEAT PIPE. THE VELOCITIES ARE SOLVE FOR
C- AT THE EDGE OF THE NODAL CELLS.
C-
C-----
C-
    IMPLICIT REAL (A-H,O-Z)
    COMMON /DENS/DENL1(100),DENL2(100),DENV1(100),DENV2(100)
    COMMON /SPEED/SPELC1(100),SPELC2(100),SPELB1(100),SPELB2(100),
+           SPEVC1(100),SPEVC2(100),SPEVB1(100),SPEVB2(100)
    COMMON /SETUP/DELX(100),HETIN(100),HETOUT(100),SOURCE(100),
+           SIGMA(100),XSAVE(100),FSAVE(100)
    COMMON /INITIL/AMOLE,GASC,FLUDK,SHFLUD,DFLUD,VOLF,WICKP,WICKK,
+           SHWICK,DWICK,RAD11,RADIN,RADBN,WALLK,SHWALL,DWALL,
+           COOLK,PRCUL,VISCUL,TEMPC,CMFR,FDNUN,GRAV,THETA,
+           SHREFV,SHREFL,ENREF,HDBCO,
+           TTOL,DELT,PI,QSTC
    COMMON /GEOMHP/EVAPL,ADIAL,CONDL,DELZL,DELZV,DELZ,DELY,VOLL,
+           AREAL,AREAV,AREAC,WALLT,PWETV,PWETL,PWETC,
+           POPEN,WDIA,FWAR,DELPV,DELPL,N,NE,NA,NC,LAYERS,
+           NFAKE

C-
C- DETERMINE THE AREA FOR FLOW
C-
    AREA=DELZV*DELY

C-
C- MARCH THROUGH THE GRID TO FIND THE VELOCITIES
C-
    DO 100 I=1,N

C-
C- DETERMINE THE VOLUME OF THE NODAL CELL
C-
    VV=DELX(I)*DELZV*DELY
    IF(I.EQ.1) THEN

C-
C- APPLY BOUNDARY CONDITION (VELOCITY AT NODE -1/2 = 0.0)
C-
    SPEVC2(I) = (SOURCE(I) - VV*(DENV2(I) - DENV1(I)) / DELT) /
+              (DENV2(I) * AREA)
    ELSE

C-

```

```

C- DETERMINE IF DENSITY FROM TEMPERATURE IS CORRECT
C-
      SPEVC2(I) = (DENV2(I-1) * SPEVC2(I-1) * AREA + SOURCE(I) - VV *
+             (DENV2(I) - DENV1(I)) / DELT) / (DENV2(I) * AREA)
      END IF
100 CONTINUE
C-
C- SET VELOCITY TO ZERO IF NEGATIVE (RESULTS FROM TRUNCATION ERROR)
C-
      DO 200 I=1,N
          IF(SPEVC2(I).LT.0.0) SPEVC2(I)=0.0
200 CONTINUE
      RETURN
      END
      SUBROUTINE CONVAP

C-
C- -----
C-
C- SUBROUTINE CONVAP:
C-
C-           THIS SUBROUTINE CALCULATES THE CONDUCTIVITY OF
C- EACH VAPOR NODE AS A FUNCTION OF TEMPERATURE. A FOURTH DEGREE
C- LEAST SQUARES FIT IS USED. THE PROPERTY DATA USED IS FROM
C- COLLIER. IT IS VALID WITH LITTLE ERROR FOR TEMPERATURES BETWEEN
C- 273 K AND 473 K.
C-
C- -----
C-
      IMPLICIT REAL (A-H,O-Z)
      COMMON /TEMP/TEMPO1(100),TEMPO2(100),TEMPW1(100),TEMPW2(100),
+           TEMPL1(100),TEMPL2(100),TEMPV1(100),TEMPV2(100),
+           TEMPIN(1000),TEMPOUT(1000),NX
      COMMON /GEOMHP/EVAPL,ADIAL,CONDL,DELZL,DELZV,DELZ,DELY,VOLL,
+           AREAL,AREAV,AREAC,WALLT,PWETV,PWETL,PWETC,
+           POPEN,WDIA,FWAR,DELPV,DELPL,N,NE,NA,NC,LAYERS,
+           NFAKE
      COMMON /PROP/CONL(100),CONV(100),VISCOL(100),
+           VISCOV(100),REYNV(100),HDB(100),PRV(100)

C-
C- COEFFICIENTS FROM LEAST SQUARES FIT OF ORDER 5
C-
      A1=0.4983877220111E-01
      A2=(-0.5127775238422E-03)
      A3=0.2553818002239E-05
      A4=(-0.5198434805506E-08)
      A5=0.4172836216418E-11

C-
C- LOOP TO FIND CONDUCTIVITIES
C-
      DO 100 I=1,N
          T=TEMPV2(I)
          CONV(I)=A1+A2*T+A3*T**2.0+A4*T**3.0+A5*T**4.0

```

```

100 CONTINUE
    RETURN
    END
    SUBROUTINE DENSE
C-
C-----
C-
C- SUBROUTINE DENSE:
C-
C-           THIS SUBROUTINE CALCULATES THE DENSITY AT EACH
C- NODE FOR BOTH THE VAPOR AND LIQUID AS A FUNCTION OF TEMPERATURE.
C- THE FITS COME FROM THE ASME BOOK ON WATER PROPERTY DATA AND ARE
C- VALID THROUGHOUT THE STEAM DOME.
C-
C-----
C-
    IMPLICIT REAL (A-H,O-Z)
    COMMON /TEMP/TEMPO1(100),TEMPO2(100),TEMPW1(100),TEMPW2(100),
+         TEMPL1(100),TEMPL2(100),TEMPV1(100),TEMPV2(100),
+         TEMPIN(1000),TEMPOUT(1000),NX
    COMMON /DENS/DENL1(100),DENL2(100),DENV1(100),DENV2(100)
    COMMON /COEFF/RR1(25),CF1(9),CF2(9),CF3(9),CG1(12),
+         CG2(9),CG3(7),CT1(2,4),CT2(5,5),CT3(5,5),
+         CT4(5,5),CN1(3,5),CN2(4,3),AA1(5),AA2(7),
+         AA3(7),AK(9),AL(12),CLSH(6),CVSH(6),CLTC(6),
+         AZ(12),BBZ(9,6),BL(4),PCRIT,TEMPK,BETA1,
+         NYZ(8),LYZ(8),NZZ(8,3),LUZ(8,2)
    COMMON /GEOMHP/EVAPL,ADIAL,CONDL,DELZL,DELZV,DELZ,DELY,VOLL,
+         AREAL,AREAV,AREAC,WALLT,PWETV,PWETL,PWETC,
+         POPEN,WDIA,FWAR,DELPV,DELPL,N,NE,NA,NC,LAYERS,
+         NFAKE
    COMMON /FLAGS/IF1,IF2,IF3,IF4,IF5,IF6,IF7,IF8,IF9,IF10,IF11,IF12
C-
C- SET UP LOOP TO CALCULATE LIQUID DENSITIES
C-
    DO 100 I=1,N
        TR=TEMPL2(I)/647.3
        Y=1.0-AL(1)*TR**2-AL(2)*TR**(-6.0)
        SUM=0.0
        E=1.0-TR
        DO 10 J=1,5
            SUM=SUM+AK(J)*E**J
10    CONTINUE
C-
C- DETERMINE BETA FUNCTION
C-
        B=EXP(1.0/TR*SUM/(1.0+AK(6)*E+AK(7)*E**2)-(E/(AK(8)*E**2+
+         AK(9))))
        Z=Y+(AL(3)*Y**2-2.0*AL(4)*TR+2.0*AL(5)*B)**(0.5)
        X=AZ(1)*AL(5)*Z**(5.0/17.0*(-1.0))
        X=X+(AZ(2)+AZ(3)*TR+AZ(4)*TR**2+AZ(5)*(AL(6)-TR)**10.0+
+         AZ(6)*(AL(7)+TR**19.0)**(-1.0))

```

```

      X=X-((AL(8)+TR**11.0)**(-1.00)*(AZ(7)+2.0*AZ(8)*B+3.0*
+      AZ(9)*B**2))
      X=X-AZ(10)*TR**18.0*(AL(9)+TR**2)*(-3.0*(AL(10)+B)**
+      (-4.0)+AL(11))
      X=X+3.0*AZ(11)*(AL(12)-TR)*B**2.0+4.0*AZ(12)*TR**
+      (-20.0)*B**3
      SPL=X*0.00317
      DENL2(I)=1.0/SPL
100  CONTINUE
C-
C- FIND VAPOR DENSITIES FROM TEMPERATURE
C-
      DO 200 I=1,N
      TR=TEMPV2(I)/647.3
      E=1.0-TR
      SUM=0.0
      DO 110 J=1,5
      SUM=SUM+AK(J)*E**J
110  CONTINUE
C-
C- DETERMINE THE BETA FUNCTION
C-
      B=EXP(1.0/TR*SUM/(1.0+AK(6)*E+AK(7)*E**2)-(E/(AK(8)*E**2+
+      AK(9))))
      X=4.260321148*TR/B
      XX=EXP(7.63333333333E-1*E)
      ASUM=0.0
      DO 130 II=1,5
      JJ=NYZ(II)
      SUM=0.0
      DO 120 J=1,JJ
      SUM=SUM+BBZ(II,J)*XX**NZZ(II,J)
120  CONTINUE
      ASUM=ASUM+SUM*II*B**(II-1)
130  CONTINUE
      X=X-ASUM
      BSUM=0.0
      DO 160 II=6,8
      JJ=NYZ(II)
      SUM=0.0
      DO 140 J=1,JJ
      SUM=SUM+BBZ(II,J)*XX**NZZ(II,J)
140  CONTINUE
      SUM=SUM*(II-2)*B**(1-II)
      DSUM=0.0
      JK=LYZ(II)
      DO 150 J=1,JK
      DSUM=DSUM+BL(II+J-6)*XX**LUZ(II,J)
150  CONTINUE
      DSUM=(DSUM+B**(2-II))**(-2.0)
      BSUM=BSUM+SUM*DSUM
160  CONTINUE

```

```

X=X-BSUM
ESUM=BBZ(8,6)
DO 170 II=1,6
    ESUM=ESUM+BBZ(9,II)*XX**II
170 CONTINUE
BL1=1.574373327E1-3.417061978E1*TR+1.931380707E1*TR**2.0
ESUM=(B/BL1)**10.0*11.0*ESUM
X=X+ESUM
SPV=X*0.00317
DENV2(I)=1.0/SPV
200 CONTINUE
RETURN
END
SUBROUTINE ELIM(AA,NR,NP,NDIM)
C-
C-----
C-
C- SUBROUTINE ELIM :
C-           THIS SUBROUTINE SOLVES A SET OF LINEAR EQUATIONS
C- AND GIVE AN LU DECOMPOSITION OF THE COEFFICIENT MATRIX. THE GAUSS
C- ELIMINATION METHOD IS USED, WITH PARTIAL PIVOTING. MULTIPLE RIGHT
C- HAND SIDES ARE PERMITTED, THEY SHOULD BE SUPPLIED AS COLUMNS THAT
C- AUGMENT THE COEFFICIENT MATRIX.
C-
C-----
C-
C- PARAMETERS ARE:
C-
C- AA      -COEFFICIENT MATRIX AUGMENTED WITH R.H.S. VECTORS
C- NR      -NUMBER OF EQUATIONS
C- NP      -TOTAL NUMBER OF COLUMNS IN THE AUGMENTED MATRIX
C- NDIM    -FIRST DIMENSION OF MATRIX AA IN THE CALLING PROGRAM
C-
C- THE SOLUTION VECTOR(S) ARE RETURNED IN THE AUGMENTATION COLUMNS
C- OF AA
C-----
C-
C- IMPLICIT REAL (A-H,O-Z)
C- DIMENSION AA(NDIM,NP)
C-
C- BEGIN THE REDUCTION
C-
C- NM1=NR-1
C- DO 35 I=1,NM1
C-
C- FIND THE ROW NUMBER OF THE PIVOT ROW. WE WILL THEN INTERCHANGE ROWS
C- TO PUT THE PIVOT ELEMENT ON THE DIAGONAL.
C-
C- IPVT=I
C- IP1=I+1
C- DO 10 J=IP1,NR

```

```

        IF (ABS (AA (IPVT, I)) .LT. ABS (AA (J, I))) IPVT=J
10    CONTINUE
C-
C- CHECK FOR A NEAR SINGULAR MATRIX
C-
        IF (ABS (AA (IPVT, I)) .EQ. 0.0) THEN
            WRITE (8, 1010)
            RETURN
        END IF
C-
C- NOW INTERCHANGE, EXCEPT IF THE PIVOT ELEMENT IS ALREADY ON THE
C- DIAGONAL, DON'T NEED TO.
C-
        IF (IPVT.NE.I) THEN
            DO 20 JCOL=1, NP
                SAVE=AA (I, JCOL)
                AA (I, JCOL)=AA (IPVT, JCOL)
                AA (IPVT, JCOL)=SAVE
20    CONTINUE
        END IF
C-
C- NOW REDUCE ALL ELEMENTS BELOW THE DIAGONAL IN THE I-TH ROW. CHECK
C- FIRST TO SEE IF A ZERO ALREADY PRESENT. IF SO, CAN SKIP REDUCTION
C- ON THAT ROW.
C-
        DO 32 JROW =IP1, NR
            IF (AA (JROW, I) .EQ. 0.0) GO TO 32
            RATIO=AA (JROW, I) / AA (I, I)
            AA (JROW, I)=RATIO
            DO 30 KCOL=IP1, NP
                AA (JROW, KCOL)=AA (JROW, KCOL) -RATIO*AA (I, KCOL)
30    CONTINUE
32    CONTINUE
35    CONTINUE
C-
C- WE STILL NEED TO CHECK AA (NR, NR) FOR SIZE
C-
        IF (ABS (AA (NR, NR)) .EQ. 0.0) THEN
            WRITE (8, 1010)
            RETURN
        END IF
C-
C- NOW WE BACK SUBSTITUE
C-
        NP1=NR+1
        DO 50 KCOL=NP1, NP
            AA (NR, KCOL)=AA (NR, KCOL) / AA (NR, NR)
            DO 45 J=2, NR
                NVBL=NP1-J
                L=NVBL+1
                VALUE=AA (NVBL, KCOL)
                DO 40 K=L, NR

```

```

                VALUE=VALUE-AA (NVBL, K) *AA (K, KCOL)
40      CONTINUE
                AA (NVBL, KCOL) =VALUE/AA (NVBL, NVBL)
45      CONTINUE
50      CONTINUE
        RETURN
1010   FORMAT (1X, /, 'SOLUTION NOT FEASIBLE. A ZERO PIVOT OCCURED')
        END
        SUBROUTINE ENERI
C-
C-----
C-
C-   SUBROUTINE ENERI:
C-
C-           THIS SUBROUTINE SETS UP THE EQUATIONS FOR THE
C-   SIMPLIFIED ENERGY EQUATION TO BE SOLVED BY SUBROUTINE ELIM.
C-   ITS SOLUTION WILL GIVE THE INITIAL GUESS FOR THE TEMPERATURE-
C-   PRESSURE OF THE FIRST NODE IN BOTH THE VAPOR AND LIQUID AREAS.
C-   THIS SUBROUTINE IS ALSO USED TO DETERMINE THE TIME CONSTANT
C-   FOR THE EVAPORATION/CONDENSATION APPROXIMATION.
C-----
C-
        IMPLICIT REAL (A-H,O-Z)
        COMMON /SETUP/DELX(100), HETIN(100), HETOUT(100), SOURCE(100),
+           SIGMA(100), XSAVE(100), FSAVE(100)
        COMMON /EZENG/TT1(5), D1(5,6), A1(5), B1(5), CC1(5), TS(5), STORE(1000)
        COMMON /INITIL/AMOLE, GASC, FLUDK, SHFLUD, DFLUD, VOLF, WICKP, WICKK,
+           SHWICK, DWICK, RAD11, RADIN, RADBN, WALLK, SHWALL, DWALL,
+           COOLK, PRCUL, VISCUL, TEMPC, CMFR, FDNUN, GRAV, THETA,
+           SHREFV, SHREFL, ENREF, HDBCO,
+           TTOL, DELT, PI, QSTC
        COMMON /GEOMHP/EVAPL, ADIAL, CONDL, DELZL, DELZV, DELZ, DELY, VOLL,
+           AREAL, AREAV, AREAC, WALLT, PWETV, PWETL, PWETC,
+           POPEN, WDIA, FWAR, DELPV, DELPL, N, NE, NA, NC, LAYERS,
+           NFAKE
        COMMON /PFLAGS/IP1, IP2, IP3, IP4, IP5, IP6, IP7, IP8, IP9, IP10, IP11, IP12
C-
C- SET MATRIES EQUAL TO ZERO
C-
        DO 5 I=1,5
            A1(I)=0.0
            B1(I)=0.0
            CC1(I)=0.0
        DO 4 J=1,6
            D1(I,J)=0.0
4      CONTINUE
5      CONTINUE
C-
C- CALCULATE EQUATION OF FIRST NODE
C-
        A1(1)=WALLK/WALLT

```

```

      CC1 (1) = DWALL * SHWALL * WALLT / (2.0 * DELT)
C-
C- CALCULATE EQUATION OF SECOND NODE
C-
      WAVGK = (1.0 - VOLF) * WICKK + VOLF * FLUDK
      VTOL = DELZL * DELY * (EVAPL + ADIAL + CONDL)
      VLIQ = VOLF * VTOL
      VSST = (1.0 - VOLF) * VTOL
      WMAS = VLIQ * DFLUD
      SMAS = VSST * DWICK
      TMAS = WMAS + SMAS
      GAMA = WMAS / TMAS
      WAVGD = (1.0 - GAMA) * DWICK + GAMA * DFLUD
      WAVGSH = (1.0 - GAMA) * SHWICK + GAMA * SHFLUD
      A1 (2) = A1 (1)
      B1 (2) = WAVGK / DELZL
      CC1 (2) = (DWALL * SHWALL * WALLT + WAVGD * WAVGSH * DELZL) / (2.0 * DELT)
C-
C- CALCULATE EQUATION OF THIRD NODE
C-
      WIEGHT = (DELY * EVAPL + DELY * CONDL) / 2.0
      A1 (3) = WAVGK * DELY * EVAPL / (WIEGHT * DELZL)
      B1 (3) = WAVGK * DELY * CONDL / (WIEGHT * DELZL)
      CC1 (3) = WAVGD * WAVGSH * DELZL / DELT
C-
C- CALCULATE EQUATION OF FOURTH NODE
C-
      A1 (4) = B1 (2)
      B1 (4) = A1 (1)
      CC1 (4) = CC1 (2)
C-
C- CALCULATE EQUATION OF FIFTH NODE
C-
      HDIACO = 4.0 * AREAC / PWETC
      REYNCO = 4.0 * CMFR / (PI * HDIACO * VISCUL)
      IF (REYNCO .LT. 2.3E3) THEN
        CONUD = FDNUN
      ELSE
        CONUD = 0.023 * (REYNCO ** 0.8) * (PRCUL ** 0.4)
      END IF
      HDBCO = CONUD * COOLK / HDIACO
      A1 (5) = B1 (4)
      B1 (5) = HDBCO
      CC1 (5) = CC1 (1)
C-
C- SET UP MATRIX D TO BE SOLVED BY ELIM
C-
      DO 200 IROW = 1, 5
        DO 100 JCOL = 1, 5
          IF (IROW .NE. JCOL) GOTO 100
          IF (IROW .EQ. 1) THEN
            D1 (IROW, JCOL) = A1 (IROW) + CC1 (IROW)

```

```

D1(IROW,6)=CC1(IROW)*TT1(IROW)+HETIN(IROW)*NE/(EVAPL*DELY)
D1(IROW,JCOL+1)=A1(IROW)*(-1.0)
ELSE
  IF(IROW.EQ.5) THEN
    D1(IROW,JCOL)=A1(IROW)+B1(IROW)+CC1(IROW)
    D1(IROW,JCOL-1)=A1(IROW)*(-1.0)
    D1(IROW,6)=CC1(IROW)*TT1(IROW)+B1(IROW)*TEMPC
  ELSE
    D1(IROW,JCOL-1)=A1(IROW)*(-1.0)
    D1(IROW,JCOL)=A1(IROW)+B1(IROW)+CC1(IROW)
    D1(IROW,JCOL+1)=B1(IROW)*(-1.0)
    D1(IROW,6)=CC1(IROW)*TT1(IROW)
  END IF
END IF
100 CONTINUE
200 CONTINUE
C-
C- USE ELIM TO SOLVE MATRIX
C-
CALL ELIM(D1,5,6,5)
RETURN
END
SUBROUTINE ENERGY
C-
C-----
C-
C- SUBROUTINE ENERGY:
C-
C- THIS SUBROUTINE SETS UP THE ENERGY EQUATIONS
C- FOR EACH NODE OF THE HEAT PIPE. THERE ARE N AXIAL BY NY RADIAL
C- NODES. ONCE SET UP THE EQUATIONS ARE PUT IN A FORM TO BE
C- SOLVED BY THE GAUSS-SIEDEL METHOD . THE SOLUTION
C- WILL GIVE THE TEMPERATURE AT EACH NODE AND A NEW BOUNDARY
C- CONDITION FOR THE MOMENTUM EQUATION.
C-
C-----
C-
IMPLICIT REAL (A-H,O-Z)
COMMON /TEMP/TEMPO1(100),TEMPO2(100),TEMPW1(100),TEMPW2(100),
+ TEMPL1(100),TEMPL2(100),TEMPV1(100),TEMPV2(100),
+ TEMPIN(1000),TEMPOUT(1000),NX
COMMON /DENS/DENL1(100),DENL2(100),DENV1(100),DENV2(100)
COMMON /SPEED/SPELC1(100),SPELC2(100),SPELB1(100),SPELB2(100),
+ SPEVC1(100),SPEVC2(100),SPEVB1(100),SPEVB2(100)
COMMON /SPHEAT/SHLIQ1(100),SHLIQ2(100),SHVAP1(100),SHVAP2(100)
COMMON /PROP/CONL(100),CONV(100),VISCOL(100),
+ VISCOV(100),REYNV(100),HDB(100),PRV(100)
COMMON /SETUP/DELX(100),HETIN(100),HETOUT(100),SOURCE(100),
+ SIGMA(100),XSAVE(100),FSAVE(100)
COMMON /INITIL/AMOLE,GASC,FLUDK,SHFLUD,DFLUD,VOLF,WICKP,WICKK,
+ SHWICK,DWICK,RADI1,RADIN,RADBN,WALLK,SHWALL,DWALL,
+ COOLK,PRCUL,VISCOL,TEMPC,CMFR,FDNUN,GRAV,THETA,

```

```

+          SHREFV, SHREFL, ENREF, HDBCO,
+          TTOL, DELT, PI, QSTC
COMMON /GEOMHP/EVAPL, ADIAL, CONDL, DELZL, DELZV, DELZ, DELY, VOLL,
+          AREAL, AREAV, AREAC, WALLT, PWETV, PWETL, PWETC,
+          POPEN, WDIA, FWAR, DELPV, DELPL, N, NE, NA, NC, LAYERS,
+          NFAKE
COMMON /PFLAGS/IP1, IP2, IP3, IP4, IP5, IP6, IP7, IP8, IP9, IP10, IP11, IP12
C-
C- SET UP BOUNDRIES FOR THE PROBLEM
C-
      DZ1=WALLT/2.0
      DZ2=WALLT/2.0
      DZ3=DELZL
      DZ5=DELZV
C-
C- DETERMINE THE ENTHALPIES FOR THE LIQUID AND VAPOR
C-
      ENTHV=2556.0E3
      ENTHL=125.66E3
C-
C- LOOP THROUGH THE AXIAL NODES
C-
      DO 500 I=1, N
C-
C- WALL BOUNDARY NODE
C-
      V=DZ1*DELX(I)*DELY/2.0
      AK1=WALLK*DELX(I)*DELY/(DZ1*V)
C-
C- APPLY ADIABATIC BOUNDARY CONDITION FOR EVAPORATOR END
C-
      IF(I.EQ.1) THEN
          AK2=0.0
          A=0.0
      ELSE
          AK2=WALLK*DZ1*DELY*2.0/(V*(DELX(I-1)+DELX(I)))
          A=AK2*TEMPO2(I-1)
      END IF
C-
C- APPLY ADIABATIC BOUNDARY CONDITION FOR CONDENSER END
C-
      IF(I.EQ.N) THEN
          AK4=0.0
          E=0.0
      ELSE
          AK4=WALLK*DZ1*DELY*2.0/(V*(DELX(I+1)+DELX(I)))
          E=AK4*TEMPO2(I+1)
      END IF
C-
C- IF IN THE CONDENSER SECTION APPLY COOLANT TEMPERATURE BOUNDARY
C- CONDITION
C-

```

```

      IF (I.GT.NFAKE) THEN
        AK3=DELX(I)*DELY*HDBCO/V
      ELSE
        AK3=0.0
      END IF
      C=DWALL*SHWALL/DELT+AK1+AK2+AK4+AK3
      D=AK1*TEMPW2(I)
C-
C- DETERMINE RIGHT HAND SIDE OF THE EQUATION
C-
      F=HETIN(I)/V+DWALL*SHWALL*TEMPO1(I)/DELT+AK3*TEMPC
C-
C- FIND OUTER WALL TEMPERATURE FOR ITERATION J+1
C-
      TEMPO2(I)=(A+D+E+F)/C
C-
C- WALL INTERIOR NODE
C-
      V=DELX(I)*DELY*(DZ2+DZ1/2.0)
      WAVGK=CONL(I)*VOLF+WICKK*(1.0-VOLF)
      R1=DZ2/WALLK+DZ3/(2.0*WAVGK)
C-
C- FIND HEAT TRANSFER TO REGIONS ABOVE AND BELOW NODE
C-
      AK3=WALLK*DELX(I)*DELY/(V*DZ1)
      AK1=DELX(I)*DELY/(R1*V)
C-
C- APPLY ADIABATIC BOUNDARY CONDITION FOR EVAPORATOR END
C-
      IF (I.EQ.1) THEN
        AK2=0.0
        A=0.0
      ELSE
        AK2=WALLK*DZ2*DELY*2.0/(V*(DELX(I-1)+DELX(I)))
        A=AK2*TEMPW2(I-1)
      END IF
C-
C- APPLY ADIABATIC BOUNDARY CONDITION FOR CONDENSER END
C-
      IF (I.EQ.N) THEN
        AK4=0.0
        E=0.0
      ELSE
        AK4=WALLK*DZ2*DELY*2.0/(V*(DELX(I+1)+DELX(I)))
        E=AK4*TEMPW2(I+1)
      END IF
      B=AK3*TEMPO2(I)
      C=DWALL*SHWALL/DELT+AK1+AK2+AK3+AK4
      D=AK1*TEMPL2(I)
C-
C- DETERMINE RIGHT HAND SIDE OF THE EQUATION
C-

```

```

      F=DWALL*SHWALL*TEMPW1(I)/DELT
C-
C- FIND INNER WALL TEMPERATURE FOR ITERATION J+1
C-
      TEMPW2(I)=(A+B+D+E+F)/C
C-
C- LIQUID NODE
C-
      VL=DZ3*DELY*DELX(I)*VOLF
      VW=DZ3*DELY*DELX(I)*(1.0-VOLF)
C-
C- FIND HEAT TRANSFER TO REGIONS ABOVE AND BELOW NODE
C-
      CEFF=VOLF*CONL(I)+(1.0-VOLF)*WICKK
      R1=DELX(I)*DELY/VL/(DZ3/(2.0*CEFF)+DZ5/(2.0*CONV(I)))
      R3=DELX(I)*DELY/VL/(DZ2/WALLK+DELZL/(2.0*CEFF))
C-
C- DETERMINE STORED ENERGY TERMS
C-
      E=VW*DWICK*SHWICK/(VL*DELT)
      F=E*TEMPL1(I)
      CP2I=(SHLIQ2(I)+SHREFL)/2.0
      CP1I=(SHLIQ1(I)+SHREFL)/2.0
      G=DENL2(I)*CP2I/DELT
      P=DENL1(I)*CP1I*TEMPL1(I)/DELT
C-
C- FIND EVAPORATION/CONDENSATION HEAT TRANSFER
C-
      R=SOURCE(I)*ENTHV/VL
C-
C- APPLY ADIABATIC BOUNDARY CONDITION FOR EVAPORATOR END
C- AND THE VELOCITY BOUNDARY CONDITION
C-
      IF(I.NE.1) THEN
          CEFF4=(VOLF*CONL(I)+(1.0-VOLF)*WICKK+
+           VOLF*CONL(I-1)+(1.0-VOLF)*WICKK)/2.0
          R4=CEFF4*DELY*DELZL*2.0/(DELX(I)+DELX(I-1))/VL
          V=SPELC2(I)
          C=DENL2(I)*ENTHL*V/DELX(I)
          R4T=R4*TEMPL2(I-1)
      ELSE
          R4=0.0
          C=0.0
          R4T=0.0
      END IF
C-
C- APPLY ADIABATIC BOUNDARY CONDITION FOR CONDENSER END
C- AND THE VELOCITY BOUNDARY CONDITION
C-
      IF(I.NE.N) THEN
          CEFF2=(VOLF*CONL(I)+(1.0-VOLF)*WICKK+
+           VOLF*CONL(I+1)+(1.0-VOLF)*WICKK)/2.0

```

```

R2=CEFF2*DELY*DELZL*2.0/(DELX(I)+DELX(I+1))/VL
V=SPELC2(I+1)
A=DENL2(I+1)*ENTHL*V/DELX(I)
R2T=R2*TEMPL2(I+1)
ELSE
R2=0.0
A=0.0
B=0.0
R2T=0.0
END IF

C-
C- DETERMINE LEFT AND RIGHT HAND SIDES OF THE EQUATION
C-
AL=G+R1+R2+R3+R4+E
AR=F+P+R3*TEMPW2(I)+R1*TEMPV2(I)+R4T+R2T+A-C-R

C-
C- FIND LIQUID TEMPERATURE FOR ITERATION J+1
C-
TEMPL2(I)=AR/AL

C-
C- VAPOR NODE
C-
VV=DELX(I)*DELY*DZ5

C-
C- DETERMINE STORED ENERGY TERMS
C-
CHI2=DENV2(I)*GASC/AMOLE
CHI1=DENV1(I)*GASC/AMOLE
CPV1=(SHVAP1(I)+SHREFV)/2.0
CPV2=(SHVAP2(I)+SHREFV)/2.0
E=(DENV2(I)*CPV2-CHI2)/DELTA
G=(DENV1(I)*CPV1-CHI1)*TEMPV1(I)/DELTA

C-
C- DETERMINE HEAT TRANSFER FROM BELOW AND APPLY ADIABATIC B.C. ON TOP
C-
R3=DELX(I)*DELY/VV/(DZ5/(2.0*CONV(I))+DZ3/(2.0*CEFF))

C-
C- DETERMINE EVAPORATION/CONDENSATION HEAT TRANSFER
C-
R=SOURCE(I)*ENTHV/VV

C-
C- APPLY ADIABATIC BOUNDARY CONDITION FOR EVAPORATOR END
C- AND THE VELOCITY BOUNDARY CONDITION
C-
IF(I.NE.1) THEN
CEFF4=(CONV(I)+CONV(I-1))/2.0
R4=CEFF4*DELY*DELZV*2.0/(DELX(I)+DELX(I-1))/VV
V=SPEVC2(I-1)
A=DENV2(I-1)*ENTHV*V/DELX(I)
R4T=R4*TEMPV2(I-1)
ELSE
R4=0.0

```

```

      A=0.0
      R4T=0.0
    END IF

C-
C- APPLY ADIABATIC BOUNDARY CONDITION FOR CONDENSER END
C- AND THE VELOCITY BOUNDARY CONDITION
C-
      IF (I.NE.N) THEN
        CEFF2=(CONV(I)+CONV(I+1))/2.0
        R2=CEFF2*DELY*DELZV*2.0/(DELX(I)+DELX(I+1))/VV
        V=SPEVC2(I)
        C=DENV2(I)*ENTHV*V/DELX(I)
        R2T=R2*TEMPV2(I+1)
      ELSE
        R2=0.0
        C=0.0
        R2T=0.0
      END IF

C-
C- DETERMINE LEFT AND RIGHT HAND SIDES OF THE EQUATION
C-
      AL=E+R3+R2+R4
      AR=R4T+R3*TEMPL2(I)+R2T+G+A-C+R

C-
C- DETERMINE VAPOR TEMPERATURE AT ITERATION J+1
C-
      TEMPV2(I)=AR/AL
500 CONTINUE
      RETURN
      END
      SUBROUTINE EVAP

C-
C- -----
C-
C- SUBROUTINE EVAP:
C-
C-           THIS SUBROUTINE CALCULATES THE EVAPORATION OR
C- CONDENSATION FROM A NODE. THE SUBROUTINE IS NOW SET UP TO USE
C- THE STORED ENERGY APPROXIMATION. THE TIME CONSTANT IS GIVEN AS
C- QSTC.
C-
C- -----
C-
      IMPLICIT REAL (A-H,O-Z)
      COMMON /SETUP/DELX(100),HETIN(100),HETOUT(100),SOURCE(100),
+           SIGMA(100),XSAVE(100),FSAVE(100)
      COMMON /INITIL/AMOLE,GASC,FLUDK,SHFLUD,DFLUD,VOLF,WICKP,WICKK,
+           SHWICK,DWICK,RAD11,RADIN,RADBN,WALLK,SHWALL,DWALL,
+           COOLK,PRCUL,VISCUL,TEMPC,CMFR,FDNUN,GRAV,THETA,
+           SHREFV,SHREFL,ENREF,HDBCO,
+           TTOL,DELT,PI,QSTC
      COMMON /GEOMHP/EVAPL,ADIAL,CONDL,DELZL,DELZV,DELZ,DELY,VOLL,

```

```

+          AREAL, AREAV, AREAC, WALLT, PWETV, PWETL, PWETC,
+          POPEN, WDIA, FWAR, DELPV, DELPL, N, NE, NA, NC, LAYERS,
+          NFAKE
COMMON /OUTPU/RTIME, ERRMAX, NRE, ITER, ITIME, IREAD
COMMON /FLAGS/IF1, IF2, IF3, IF4, IF5, IF6, IF7, IF8, IF9, IF10, IF11, IF12
NE1=NE+NA+1

C-
C- DETERMINE THE ENTHALPIES OF THE VAPOR AND LIQUID AND THE
C- LATENT HEAT OF EVAPORIZATION
C-
    ENTHV=2556.0E3
    ENTHL=125.66E3
    HFG=ENTHV-ENTHL

C-
C- SET UP LOOP TO DETERMINE SOURCE IN EACH NODE
C-
    DO 100 I=1,NE
        SOURCE(I)=HETIN(I)*(1.0-EXP(-QSTC*RTIME))/HFG
100 CONTINUE
    DO 200 I=NE1,N
        SOURCE(I)=HETOUT(I)*(1.0-EXP(-QSTC*RTIME))/HFG*(-1.0)
200 CONTINUE
    RETURN
    END
    SUBROUTINE FINISH

C-
C-----
C-
C- SUBROUTINE FINISH:
C-
C-          THIS SUBROUTINE OUTPUTS ALL CONSTANTS AND HEAT
C- PIPE PARAMETERS FOR THE FINAL TIME STEP SO THAT THE CODE CAN
C- BE RESTARTED AGAIN FROM WHERE IT LEFT OFF.
C-
C-----
C-
    IMPLICIT REAL (A-H,O-Z)
    COMMON /TEMP/TEMPO1(100), TEMPO2(100), TEMPW1(100), TEMPW2(100),
+          TEMPL1(100), TEMPL2(100), TEMPV1(100), TEMPV2(100),
+          TEMPIN(1000), TEMPOUT(1000), NX
    COMMON /PRES/PRESL1(100), PRESL2(100), PRESV1(100), PRESV2(100),
+          DPLIQ(100), DPVAP(100)
    COMMON /DENS/DENL1(100), DENL2(100), DENV1(100), DENV2(100)
    COMMON /SPEED/SPELC1(100), SPELC2(100), SPELB1(100), SPELB2(100),
+          SPEVC1(100), SPEVC2(100), SPEVB1(100), SPEVB2(100)
    COMMON /SETUP/DELX(100), HETIN(100), HETOUT(100), SOURCE(100),
+          SIGMA(100), XSAVE(100), FSAVE(100)
    COMMON /INITIL/AMOLE, GASC, FLUDK, SHFLUD, DFLUD, VOLF, WICKP, WICKK,
+          SHWICK, DWICK, RAD11, RADIN, RADBN, WALLK, SHWALL, DWALL,
+          COOLK, PRCUL, VISUL, TEMPC, CMFR, FDNUN, GRAV, THETA,
+          SHREFV, SHREFL, ENREF, HDBCO,
+          TTOL, DELT, PI, QSTC

```

```

COMMON /GEOMHP/EVAPL, ADIAL, CONDL, DELZL, DELZV, DELZ, DELY, VOLL,
+ AREAL, AREAV, AREAC, WALLT, PWETV, PWETL, PWETC,
+ POPEN, WDIA, FWAR, DELPV, DELPL, N, NE, NA, NC, LAYERS,
+ NFAKE
COMMON /EZENG/TT1 (5), D1 (5, 6), A1 (5), B1 (5), CC1 (5), TS (5), STORE (1000)
COMMON /FLAGS/IF1, IF2, IF3, IF4, IF5, IF6, IF7, IF8, IF9, IF10, IF11, IF12
COMMON /PFLAGS/IP1, IP2, IP3, IP4, IP5, IP6, IP7, IP8, IP9, IP10, IP11, IP12
C-
C- SET FLAGS SO THE RESART FILE WILL RESPOND CORRECTLY
C-
IF1=1
IF2=1
IF3=1
IF4=1
IF5=2
IF6=1
C-
C- WRITE OUT FLAGS AND CONSTANTS
C-
WRITE (5, 1001) IF1, IF2, IF3, IF4, IF5, IF6, IF7, IF8, IF9, IF10, IF11, IF12
WRITE (5, 1001) IP1, IP2, IP3, IP4, IP5, IP6, IP7, IP8, IP9, IP10, IP11, IP12
WRITE (5, 1000) EVAPL, ADIAL, CONDL, DELT
WRITE (5, 1000) RTIME, QSTC
WRITE (5, 1000) DELZ, VOLL
WRITE (5, 1000) AMOLE, GASC, WICKP
WRITE (5, 1000) DELY
WRITE (5, 1000) GRAV, ACCEL, THETA, THETAP
WRITE (5, 1000) TTOL
WRITE (5, 1001) LAYERS
WRITE (5, 1000) POPEN, WDIA
WRITE (5, 1000) WALLK, WICKK, FLUDK, COOLK
WRITE (5, 1000) SHWALL, SHWICK, SHFLUD
WRITE (5, 1000) DWALL, DWICK, DFLUD
WRITE (5, 1000) PRUL
WRITE (5, 1000) VISCUL
WRITE (5, 1000) WALLT
WRITE (5, 1000) CMFR, AREAC, PWETC
WRITE (5, 1000) FDNUN, TEMPC
C-
C- WRITE OUT SIMPLE ENERGY EQUATION TEMPERATURE
C-
WRITE (5, 1000) (TT1 (I), I=1, 4)
WRITE (5, 1000) TT1 (5)
WRITE (5, 1000) FWAR, PI
WRITE (5, 1000) SHREFV, SHREFL, ENREF
C-
C- WRITE OUT VELOCITIES FOR EACH NODE FOR LAST TIME STEP
C-
DO 5 I=1, N

WRITE (5, 1000) SPELC1 (I), SPEVC1 (I)
5 CONTINUE

```

```

C-
C- WRITE OUT ENERGY INPUTS AND OUTPUTS
C-
      DO 20 INIT=1,N
        WRITE (5,1000) HETIN (INIT) , HETOUT (INIT)
20    CONTINUE
C-
C- WRITE OUT FINAL TEMPERATURES
C-
      DO 60 INIT=1,N
        WRITE (5,1000) TEMPO1 (INIT) , TEMPW1 (INIT)
60    CONTINUE
      DO 65 INIT=1,N
        WRITE (5,1000) TEMPL1 (INIT) , TEMPV1 (INIT)
65    CONTINUE
C-
C- WRITE OUT ALL SOURCES
C-
      DO 155 I=1,N
        WRITE (5,1000) SOURCE (I)
155   CONTINUE
      DO 160 I=1,N
        WRITE (5,1000) DENL1 (I) , DENV1 (I)
160   CONTINUE
      DO 170 I=1,N
        WRITE (5,1000) PRESL1 (I) , PRESV1 (I)
170   CONTINUE
      RETURN
1000  FORMAT (6 (E15.8))
1001  FORMAT (12 (I6))
      END
      SUBROUTINE GEO

C-
C-----
C-
C- SUBROUTINE GEO:
C-
C-           THIS SUBROUTINE CALCULATES THE PERMABILITY
C- OF THE WICK-LIQUID STRUCTURE. IT ASSUMES THAT THE WICK-LIQUID
C- REGION IS MADE UP OF A SERIES OF PARALLEL CHANNELS. IN ADDITION,
C- THE AREA AND HIEGHTS OF BOTH THE LIQUID AND VAPOR ARE CALCULATED.
C-
C-----
C-
      IMPLICIT REAL (A-H,O-Z)
      COMMON /INITIL/AMOLE,GASC,FLUDK,SHFLUD,DFLUD,VOLF,WICKP,WICKK,
+           SHWICK,DWICK,RAD11,RADIN,RADBN,WALLK,SHWALL,DWALL,
+           COOLK,PRCUL,VISCUL,TEMPC,CMFR,FDNUN,GRAV,THETA,
+           SHREFV,SHREFL,ENREF,HDBCO,
+           TTOL,DELT,PI,QSTC
      COMMON /GEOMHP/EVAPL,ADIAL,CONDL,DELZL,DELZV,DELZ,DELY,VOLL,
+           AREAL,AREAV,AREAC,WALLT,PWETV,PWETL,PWETC,

```

```

+           POPEN,WDIA,FWAR,DELPV,DELPL,N,NE,NA,NC,LAYERS,
+           NFAKE
COMMON /FLAGS/IF1,IF2,IF3,IF4,IF5,IF6,IF7,IF8,IF9,IF10,IF11,IF12
C-
C- CALCULATE WICK VOLUME
C-
      AREAP=(POPEN+WDIA)**2
      AREAW=AREAP-POPEN**2
      AREAT=(EVAPL+CONDL+ADIAL)*DELY
      PNUM=AREAT/AREAP
      WIRER=WDIA/2.0
      VWIRE=PI*WIRER**2.0*(2.0*POPEN+2.0*(POPEN+WDIA))/2.0
      VTWIRE=VWIRE*PNUM*LAYERS
C-
C- DETERMINE LIQUID AND TOTAL VOLUMES
C-
      VLIQ=VOLL*1.0E-3
      VTOT=VTWIRE+VLIQ
C-
C- DETERMINE THE VOLUME FRACTION
C-
      VOLF=VLIQ/VTOT
C-
C- DETERMINE LIQUID AND VAPOR HIEGHTS
C-
      DELZL=VTOT/AREAT
      DELZV=DELZ-DELZL
C-
C- DETERMINE CROSS SECTIONAL AREAS FOR FLOW AND WETTED PERIMETERS
C-
      AREAL=DELY*DELZL*VOLF
      AREAV=DELY*DELZV
      PWETL=2.0*(DELZL*DELY)
      PWETV=2.0*(DELZV*DELY)
C-
C- DETERMINE WICK ASPECT RATIO FUNCTION
C-
      WIDTH=AREAL/DELZL
      IF (DELZL.GE.WIDTH) THEN
        FWAR=FWAR
      ELSE
        FWAR=14.3
      END IF
C-
C- DETERMINE EFFECTIVE RADIUS OF OPENING AND WICK PERMABILITY
C-
      DELZO=DELZL-WDIA*(LAYERS)
      RADI=(2.0*WIDTH*DELZO/LAYERS)/(WIDTH+2.0*DELZO/LAYERS)
      IF (IF7.EQ.0) RETURN
      IF (IF7.EQ.1) THEN
        WICKP=2.0*VOLF*RADI**2.0/FWAR
      END IF

```

```

IF (IF7.EQ.2) THEN
  WICKP=2.0*VOLF*RADI**2.0
  WICKP=WICKP/FWAR
END IF
RETURN
END
SUBROUTINE GETPROP

```

```

C-
C-----
C-
C- SUBROUTINE GETPROP:
C-
C-           THIS SUBROUTINE CALCULATES THE DENSITY AND
C- SPECIFIC HEATS FOR BOTH THE VAPOR AND LIQUID AS A FUNCTION OF
C- TEMPERATURE. THIS IS DONE FOR THE INITIAL HEAT PIPE TEMPERATURES
C- BEFORE THE TRANSIENT BEGINS
C-
C-----
C-

```

```

IMPLICIT REAL (A-H,O-Z)
COMMON /TEMP/TEMPO1(100),TEMPO2(100),TEMPW1(100),TEMPW2(100),
+      TEMPL1(100),TEMPL2(100),TEMPV1(100),TEMPV2(100),
+      TEMPIN(1000),TEMPOUT(1000),NX
COMMON /DENS/DENL1(100),DENL2(100),DENV1(100),DENV2(100)
COMMON /SPHEAT/SHLIQ1(100),SHLIQ2(100),SHVAP1(100),SHVAP2(100)
COMMON /GEOMHP/EVAPL,ADIAL,CONDL,DELZL,DELZV,DELZ,DELY,VOLL,
+      AREAL,AREAV,AREAC,WALLT,PWETV,PWETL,PWETC,
+      POPEN,WDIA,FWAR,DELPV,DELPL,N,NE,NA,NC,LAYERS,
+      NFAKE
COMMON /COEFF/RR1(25),CF1(9),CF2(9),CF3(9),CG1(12),
+      CG2(9),CG3(7),CT1(2,4),CT2(5,5),CT3(5,5),
+      CT4(5,5),CN1(3,5),CN2(4,3),AA1(5),AA2(7),
+      AA3(7),AK(9),AL(12),CLSH(6),CVSH(6),CLTC(6),
+      AZ(12),BBZ(9,6),BL(4),PCRIT,TEMPK,BETA1,
+      NYZ(8),LYZ(8),NZZ(8,3),LUZ(8,2)
COMMON /FLAGS/IF1,IF2,IF3,IF4,IF5,IF6,IF7,IF8,IF9,IF10,IF11,IF12

```

```

C-
C- SET UP LOOP TO CALCULATE LIQUID DENSITIES
C-

```

```

DO 100 I=1,N
  TR=TEMPL1(I)/647.3
  Y=1.0-AL(1)*TR**2-AL(2)*TR**(-6.0)
  SUM=0.0
  E=1.0-TR
  DO 10 J=1,5
    SUM=SUM+AK(J)*E**J

```

```

10 CONTINUE

```

```

C-
C- CALCULATE THE BETA FUNCTION
C-

```

```

  B=EXP(1.0/TR*SUM/(1.0+AK(6)*E+AK(7)*E**2)-(E/(AK(8)*E**2+
+ AK(9))))

```

```

Z=Y+(AL(3)*Y**2-2.0*AL(4)*TR+2.0*AL(5)*B)**(0.5)
X=AZ(1)*AL(5)*Z**(5.0/17.0*(-1.0))
X=X+(AZ(2)+AZ(3)*TR+AZ(4)*TR**2+AZ(5)*(AL(6)-TR)**10.0+
+ AZ(6)*(AL(7)+TR**19.0)**(-1.0))
X=X-((AL(8)+TR**11.0)**(-1.00)*(AZ(7)+2.0*AZ(8)*B+3.0*
+ AZ(9)*B**2))
X=X-AZ(10)*TR**18.0*(AL(9)+TR**2)*(-3.0*(AL(10)+B)**
+ (-4.0)+AL(11))
X=X+3.0*AZ(11)*(AL(12)-TR)*B**2.0+4.0*AZ(12)*TR**
+ (-20.0)*B**3
SPL=X*0.00317
DENL1(I)=1.0/SPL
100 CONTINUE
C-
C- DETERMINE THE VAPOR DENSITIES
C-
DO 200 I=1,N
TR=TEMPV1(I)/647.3
E=1.0-TR
SUM=0.0
DO 110 J=1,5
SUM=SUM+AK(J)*E**J
110 CONTINUE
C-
C- CALCULATE THE BETA FUNCTION
C-
B=EXP(1.0/TR*SUM/(1.0+AK(6)*E+AK(7)*E**2)-(E/(AK(8)*E**2+
+ AK(9))))
X=4.260321148*TR/B
XX=EXP(7.633333333333E-1*E)
ASUM=0.0
DO 130 II=1,5
JJ=NYZ(II)
SUM=0.0
DO 120 J=1,JJ
SUM=SUM+BBZ(II,J)*XX**NZZ(II,J)
120 CONTINUE
ASUM=ASUM+SUM*II*B**(II-1)
130 CONTINUE
X=X-ASUM
BSUM=0.0
DO 160 II=6,8
JJ=NYZ(II)
SUM=0.0
DO 140 J=1,JJ
SUM=SUM+BBZ(II,J)*XX**NZZ(II,J)
140 CONTINUE
SUM=SUM*(II-2)*B**(1-II)
DSUM=0.0
JK=LYZ(II)
DO 150 J=1,JK
DSUM=DSUM+BL(II+J-6)*XX**LUZ(II,J)

```

```

150     CONTINUE
        DSUM=(DSUM+B**(2-II))**(-2.0)
        BSUM=BSUM+SUM*DSUM
160     CONTINUE
        X=X-BSUM
        ESUM=BBZ(8,6)
        DO 170 II=1,6
            ESUM=ESUM+BBZ(9,II)*XX**II
170     CONTINUE
        BL1=1.574373327E1-3.417061978E1*TR+1.931380707E1*TR**2.0
        ESUM=((B/BL1)**10.0)*11.0*ESUM
        X=X+ESUM
        SPV=X*0.00317
        DENV1(I)=1.0/SPV
200     CONTINUE
C-
C- SET UP LOOP TO CALCULATE THE SPECIFIC HEATS AT EACH NODE
C-
        DO 400 I=1,N
            SUM1=0.0
            SUM2=0.0
            DO 350 J=1,6
                SUM1=SUM1+CLSH(J)*TEMPL1(I)**(J-1)
                SUM2=SUM2+CVSH(J)*TEMPV1(I)**(J-1)
350     CONTINUE
C-
C- CONVECT SPECIFIC HEAT FROM KJ TO J
C-
        SHLIQ1(I)=SUM1*1.0E03
        SHVAP1(I)=SUM2*1.0E03
400     CONTINUE
        RETURN
        END
        SUBROUTINE HTCF
C-
C-----
C-
C- SUBROUTINE HTCF:
C-
C-             THIS SUBROUTINE CALCULATES THE HEAT TRANSFER
C- COEFFICIENT BETWEEN THE LIQUID AND VAPOR FOR EACH NODE. EACH NODE
C- IS TREATED AS A FLAT PLATE.
C-
C-----
C-
        IMPLICIT REAL (A-H,O-Z)
        COMMON /PROP/CONL(100),CONV(100),VISCOL(100),
+             VISCOV(100),REYNV(100),HDB(100),PRV(100)
        COMMON /SETUP/DELX(100),HETIN(100),HETOUT(100),SOURCE(100),
+             SIGMA(100),XSAVE(100),FSAVE(100)
        COMMON /GEOMHP/EVAPL,ADIAL,CONDL,DELZL,DELZV,DELZ,DELY,VOLL,
+             AREAL,AREAV,AREAC,WALLT,PWETV,PWETL,PWETC,

```

```

+           POPEN,WDIA,FWAR,DELPV,DELPL,N,NE,NA,NC,LAYERS,
+           NFAKE
C-
C- SET UP LOOP TO EVALUATE EACH NODE
C-
      DO 100 I=1,N
        IF (REYNV(I).LE.0.0) THEN
          HDB(I)=0.0
          GO TO 100
        END IF
        IF (REYNV(I).LT.5.0E5) THEN
C-
C- DETERMINE HEAT TRANSFER COEFFICIENT FOR LAMINAR FLOW
C-
          HDB(I)=0.664*REYNV(I)**(1.0/2.0)*PRV(I)**(1.0/3.0)*
+           CONV(I)/DELX(I)
          ELSE
C-
C- DETERMINE HEAT TRANSFER COEFFICIENT FOR TURBULENT FLOW
C-
          HDB(I)=0.0296*REYNV(I)**(4.0/5.0)*PRV(I)**(1.0/3.0)*
+           CONV(I)/DELX(I)
          END IF
100 CONTINUE
      RETURN
      END
      SUBROUTINE INCOF
C-
C- -----
C-
C- SUBROUTINE INCOF:
C-
C-           THIS SUBROUTINE GOES OUT TO FILE WATCOF
C- AND RETREIVES THE DATA NECESSARY FOR THE PROPERTY RELATIONSHIPS.
C-
C- -----
C-
      IMPLICIT REAL (A-H,O-Z)
      COMMON /COEFF/RR1(25),CF1(9),CF2(9),CF3(9),CG1(12),
+           CG2(9),CG3(7),CT1(2,4),CT2(5,5),CT3(5,5),
+           CT4(5,5),CN1(3,5),CN2(4,3),AA1(5),AA2(7),
+           AA3(7),AK(9),AL(12),CLSH(6),CVSH(6),CLTC(6),
+           AZ(12),BBZ(9,6),BL(4),PCRIT,TEMPK,BETA1,
+           NYZ(8),LYZ(8),NZZ(8,3),LUZ(8,2)
C-
C- READ IN DATA USING A STANDARD FORMAT AND IMPLICIT DO LOOPS.
C-
      READ(4,1001)PCRIT
      READ(4,1001)(CF1(I),I=1,9)
      READ(4,1001)(CF2(I),I=1,9)
      READ(4,1001)(CF3(I),I=1,9)
      READ(4,1001)(CG1(I),I=1,12)

```

```

READ (4,1001) (CG2 (I), I=1, 9)
READ (4,1001) (CG3 (I), I=1, 7)
READ (4,1001) ((CT1 (I, J), J=1, 4), I=1, 2)
READ (4,1001) ((CT2 (I, J), J=1, 5), I=1, 5)
READ (4,1001) ((CT3 (I, J), J=1, 5), I=1, 5)
READ (4,1001) ((CT4 (I, J), J=1, 5), I=1, 5)
READ (4,1001) ((CN1 (I, J), J=1, 5), I=1, 3)
READ (4,1001) ((CN2 (I, J), J=1, 3), I=1, 4)
READ (4,1001) (AA1 (I), I=1, 5)
READ (4,1001) (AA2 (I), I=1, 7)
READ (4,1001) (AA3 (I), I=1, 7)
READ (4,1001) TEMPK, BETA1
READ (4,1002) (RR1 (I), I=1, 25)
READ (4,1003) (AK (J), J=1, 9)
READ (4,1003) (AL (J), J=1, 12)
READ (4,1001) (CLSH (I), I=1, 6)
READ (4,1001) (CLTC (I), I=1, 6)
READ (4,1001) (CVSH (I), I=1, 6)
READ (4,1003) (AZ (I), I=1, 12)
DO 200 I=1, 9
    READ (4,1003) (BBZ (I, J), J=1, 4)
    READ (4,1003) (BBZ (I, J), J=5, 6)
200 CONTINUE
    READ (4,1004) (NYZ (I), I=1, 8)
    READ (4,1004) (LYZ (I), I=1, 8)
    DO 300 I=1, 8
        READ (4,1004) (NZZ (I, J), J=1, 3)
300 CONTINUE
    DO 400 I=1, 8
        READ (4,1004) (LUZ (I, J), J=1, 2)
400 CONTINUE
    READ (4,1003) (BL (J), J=1, 4)
    RETURN
1001 FORMAT (4 (E20.10))
1002 FORMAT (E23.16)
1003 FORMAT (4 (E15.6))
1004 FORMAT (12 (I6))
END
SUBROUTINE INITIAL
C-
C-----
C-
C- SUBROUTINE INITIAL:
C-
C- THIS SUBROUTINE SETS THE NEXT TIME STEP
C- VELOCITIES AND DENSITIES TO THE LAST TIME STEPS VALUES.
C-
C-----
C-
    IMPLICIT REAL (A-H,O-Z)
    COMMON /PRES/PRESL1(100), PRESL2(100), PRESV1(100), PRESV2(100),
+         DPLIQ(100), DPVAP(100)

```

```

COMMON /DENS/DENL1 (100) , DENL2 (100) , DENV1 (100) , DENV2 (100)
COMMON /SPEED/SPELC1 (100) , SPELC2 (100) , SPELB1 (100) , SPELB2 (100) ,
+       SPEVC1 (100) , SPEVC2 (100) , SPEVB1 (100) , SPEVB2 (100)
COMMON /GEOMHP/EVAPL, ADIAL, CONDL, DELZL, DELZV, DELZ, DELY, VOLL,
+       AREAL, AREAV, AREAC, WALLT, PWETV, PWETL, PWETC,
+       POPEN, WDIA, FWAR, DELPV, DELPL, N, NE, NA, NC, LAYERS,
+       NFAKE
C-
C- SET VALUES FOR THE VELOCITIES, DENSITIES, AND PRESSURES TO
C- OLD TIME VALUES TO USE AS THE FIRST GUESS
C-
DO 100 I=1,N
  DENV2 (I)=DENV1 (I)
  DENL2 (I)=DENL1 (I)
  PRESL2 (I)=PRESL1 (I)
  PRESV2 (I)=PRESV1 (I)
  SPELC2 (I)=SPELC1 (I)
  SPEVC2 (I)=SPEVC1 (I)
100 CONTINUE
RETURN
END
SUBROUTINE INPUT
C-
C-----
C-
C- SUBROUTINE INPUT:
C-
C-           THIS SUBROUTINE READS IN ALL CONSTANTS AND HEAT
C- PIPE PARAMETERS FOR TIME=0. ADDITIONALLY, IT READS IN THE
C- DIMENSIONS OF THE HEAT PIPE AND DETERMINES THE NODAL SPACING.
C-
C-----
C-
  IMPLICIT REAL (A-H,O-Z)
  COMMON /TEMP/TEMPO1 (100) , TEMPO2 (100) , TEMPW1 (100) , TEMPW2 (100) ,
+       TEMPL1 (100) , TEMPL2 (100) , TEMPV1 (100) , TEMPV2 (100) ,
+       TEMPIN (1000) , TEMPOUT (1000) , NX
  COMMON /PRES/PRESL1 (100) , PRESL2 (100) , PRESV1 (100) , PRESV2 (100) ,
+       DPLIQ (100) , DPVAP (100)
  COMMON /DENS/DENL1 (100) , DENL2 (100) , DENV1 (100) , DENV2 (100)
  COMMON /SPEED/SPELC1 (100) , SPELC2 (100) , SPELB1 (100) , SPELB2 (100) ,
+       SPEVC1 (100) , SPEVC2 (100) , SPEVB1 (100) , SPEVB2 (100)
  COMMON /SETUP/DELX (100) , HETIN (100) , HETOUT (100) , SOURCE (100) ,
+       SIGMA (100) , XSAVE (100) , FSAVE (100)
  COMMON /EZENG/TT1 (5) , D1 (5, 6) , A1 (5) , B1 (5) , CC1 (5) , TS (5) , STORE (1000)
  COMMON /INITIL/AMOLE, GASC, FLUDK, SHFLUD, DFLUD, VOLF, WICKP, WICKK,
+       SHWICK, DWICK, RADI1, RADIN, RADBN, WALLK, SHWALL, DWALL,
+       COOLK, PRCUL, VISCUL, TEMPC, CMFR, FDNUN, GRAV, THETA,
+       SHREFV, SHREFL, ENREF, HDBCO,
+       TTOL, DELT, PI, QSTC
  COMMON /GEOMHP/EVAPL, ADIAL, CONDL, DELZL, DELZV, DELZ, DELY, VOLL,
+       AREAL, AREAV, AREAC, WALLT, PWETV, PWETL, PWETC,

```

+ POPEN, WDIA, FWAR, DELPV, DELPL, N, NE, NA, NC, LAYERS,  
+ NFAKE

```

COMMON /OUTPU/RTIME,ERRMAX,NRE,ITER,ITIME,IREAD
COMMON /FLAGS/IF1,IF2,IF3,IF4,IF5,IF6,IF7,IF8,IF9,IF10,IF11,IF12
COMMON /PFLAGS/IP1,IP2,IP3,IP4,IP5,IP6,IP7,IP8,IP9,IP10,IP11,IP12
NFAKE=NE+NA

```

C-

C- READ IN CONSTANTS AND FLAGS

C-

```

READ (IREAD,1001) IF1,IF2,IF3,IF4,IF5,IF6,IF7,IF8,IF9,IF10,IF11,
+ IF12
READ (IREAD,1001) IP1,IP2,IP3,IP4,IP5,IP6,IP7,IP8,IP9,IP10,IP11,
+ IP12
READ (IREAD,1000) EVAPL,ADIAL,CONDL,DELT
READ (IREAD,1000) RTIME,QSTC
READ (IREAD,1000) DELZ,VOLL
READ (IREAD,1000) AMOLE,GASC,WICKP
READ (IREAD,1000) DELY
READ (IREAD,1000) GRAV,ACCEL,THETA,THETAP
READ (IREAD,1000) TTOL
READ (IREAD,1001) LAYERS
READ (IREAD,1000) POPEN,WDIA

```

C-

C- READ IN DATA FOR INITIAL SET UP OF HEAT PIPE

C-

```

READ (IREAD,1000) WALLK,WICKK,FLUDK,COOLK
READ (IREAD,1000) SHWALL,SHWICK,SHFLUD
READ (IREAD,1000) DWALL,DWICK,DFLUD

```

```

READ (IREAD,1000) PRCUL
READ (IREAD,1000) VISCUL
READ (IREAD,1000) WALLT
READ (IREAD,1000) CMFR,AREAC,PWETC
READ (IREAD,1000) FDNUN,TEMPC
READ (IREAD,1000) (TT1(I),I=1,4)
READ (IREAD,1000) TT1(5)
READ (IREAD,1000) FWAR,PI
READ (IREAD,1000) SHREFV,SHREFL,ENREF

```

C-

C- DETERMINE IF VELOCITIES SHOULD BE READ IN OR SET TO ZERO

C-

```

IF (IF6.EQ.1) THEN
  DO 5 I=1,N
    READ (IREAD,1000) SPELC1(I),SPEVC1(I)
5  CONTINUE

ELSE
  DO 10 INIT=1,N
    SPELC1(INIT)=0.0
    SPEVC1(INIT)=0.0
10 CONTINUE
END IF

```

C-

C- READ IN ENERGY INPUTS AND OUTPUTS

C-

```
      IF (IF1.EQ.1) THEN
        DO 20 INIT=1,N
          READ (IREAD,1000) HETIN (INIT) , HETOUT (INIT)
20      CONTINUE
      ELSE
        DO 30 INIT=1,N
          HETIN (INIT) =0.0
          HETOUT (INIT) =0.0
30      CONTINUE
          READ (IREAD,1000) HETIN (1) , HETOUT (NFAKE+1)
          DO 40 INIT=1,NE
            HETIN (INIT) =HETIN (1)
40      CONTINUE
          DO 50 INIT=1,NC
            HETOUT (INIT+NFAKE) =HETOUT (NFAKE+1)
50      CONTINUE
      END IF
```

C-

C- READ IN INTIAL TEMPERATURES

C-

```
      IF (IF4.EQ.1) THEN
        DO 60 INIT=1,N
          READ (IREAD,1000) TEMPO1 (INIT) , TEMPW1 (INIT)
60      CONTINUE
          DO 65 INIT=1,N
            READ (IREAD,1000) TEMPL1 (INIT) , TEMPV1 (INIT)
65      CONTINUE
      ELSE
        READ (IREAD,1000) TEMPO1 (1) , TEMPW1 (1)
        READ (IREAD,1000) TEMPL1 (1) , TEMPV1 (1)
        DO 70 INIT=1,N
          TEMPO1 (INIT) =TEMPO1 (1)
          TEMPW1 (INIT) =TEMPW1 (1)
          TEMPL1 (INIT) =TEMPL1 (1)
          TEMPV1 (INIT) =TEMPV1 (1)
70      CONTINUE
      END IF
```

C-

C- DETERMINE IF SOURCE SHOULD BE READ IN

C-

```
      DO 80 I=1,N
        SOURCE (I) =0.0
80      CONTINUE
      IF (IF5.EQ.2) THEN
        DO 85 I=1,N
          READ (IREAD,1000) XSAVE (I)
85      CONTINUE
      END IF
      IF (IF5.EQ.3) THEN
        READ (IREAD,1000) SOURCE (1) , SOURCE (NFAKE+1)
```

```

        DO 90 I=1,N
          IF (I.LE.NE) SOURCE(I)=SOURCE(1)
          IF (I.GT.NFAKE) SOURCE(I)=SOURCE(NFAKE+1)
90      CONTINUE
        END IF
C-
C- DETERMINE WIDTHS OF THE CELLS FROM NUMBER OF NODES
C- REQUIRED.
C-
        DO 130 I=1,N
          IF (I.GT.NE) GO TO 110
          DELX(I)=EVAPL/NE
          GO TO 130
110     IF (I.GT.NFAKE) GO TO 120
          DELX(I)=ADIAL/NA
          GO TO 130
120     DELX(I)=CONDL/NC
130     CONTINUE
          IF (IF2.EQ.1) THEN
            DO 160 I=1,N
              READ (IREAD,1000) DENL1(I), DENV1(I)
160      CONTINUE
            END IF
          IF (IF3.EQ.1) THEN
            DO 170 I=1,N
              READ (IREAD,1000) PRESL1(I), PRESV1(I)
170      CONTINUE
            END IF
C
C- INITIALIZE THE TEMPERATURES
C-
        DO 190 INIT=1,N
          TEMPO2 (INIT)=TEMPO1 (INIT)
          TEMPW2 (INIT)=TEMPW1 (INIT)
          TEMPL2 (INIT)=TEMPL1 (INIT)
          TEMPV2 (INIT)=TEMPV1 (INIT)
190     CONTINUE
        RETURNC1000 FORMAT (4 (E21.14))
1000  FORMAT (6 (E15.8))
1001  FORMAT (12 (I6))
        END
        SUBROUTINE MOMTUML
C-
C-----
C-
C- SUBROUTINE MOMTUML:
C-
C-           THIS SURROUTINE CALCULATES THE RESIDUALS OF
C- THE CONSERVATION OF MOMENTUM EQUATION WHEN VALUES FOR THE
C- VELOCITIES ARE GIVEN. THE BOUNDARY CONDITION USED IS THE VELOCITY
C- IS ZERO AT THE CONDENSER WALL.
C-

```

```

C-----
C-
  IMPLICIT REAL (A-H,O-Z)
  COMMON /PRES/PRESL1(100),PRESL2(100),PRESV1(100),PRESV2(100),
+       DPLIQ(100),DPVAP(100)
  COMMON /DENS/DENL1(100),DENL2(100),DENV1(100),DENV2(100)
  COMMON /SPEED/SPELC1(100),SPELC2(100),SPELB1(100),SPELB2(100),
+       SPEVC1(100),SPEVC2(100),SPEVB1(100),SPEVB2(100)
  COMMON /PROP/CONL(100),CONV(100),VISCOL(100),
+       VISCOV(100),REYNV(100),HDB(100),PRV(100)
  COMMON /SETUP/DELX(100),HETIN(100),HETOUT(100),SOURCE(100),
+       SIGMA(100),XSAVE(100),FSAVE(100)
  COMMON /INITIL/AMOLE,GASC,FLUDK,SHFLUD,DFLUD,VOLF,WICKP,WICKK,
+       SHWICK,DWICK,RADI1,RADIN,RADBN,WALLK,SHWALL,DWALL,
+       COOLK,PRCUL,VISCU,TEMPC,CMFR,FDNUN,GRAV,THETA,
+       SHREFV,SHREFL,ENREF,HDBCO,
+       TTOL,DELT,PI,QSTC
  COMMON /GEOMHP/EVAPL,ADIAL,CONDL,DELZL,DELZV,DELZ,DELY,VOLL,
+       AREAL,AREAV,AREAC,WALLT,PWETV,PWETL,PWETC,
+       POPEN,WDIA,FWAR,DELPV,DELPL,N,NE,NA,NC,LAYERS,
+       NFAKE
C-
C- FIND DELTA P'S FOR EACH NODE
C-
  DO 100 I=1,N
C-
C- DETERMINE XEFF FOR THE FRICTION PRESSURE DROP
C-
  XEFF=DELX(I)/2.0
  IF(I.GT.NE.AND.I.LE.NFAKE) XEFF=DELX(I)
C-
C- DETERMINE THE TRANSIENT PRESSURE DROP
C-
  TIME=DELX(I)*(DENL1(I)*SPELC1(I)-DENL2(I)*SPELC2(I))/DELT
C-
C- DETERMINE THE GRAVITY PRESSURE DROP
C-
  GRAVT=DENL2(I)*GRAV*SIN(THETA)*DELX(I)
C-
C- DETERMINE THE FRICTION PRESSURE DROP
C-
  FRICT=(-VISCOL(I)*SPELC2(I)*XEFF/(PI*WICKP))
  IF(I.EQ.N) THEN
C-
C- APPLY BOUNDARY CONDITION (VELOCITY=0 AT N+1)
C-
  ACCEL=(-DENL2(I)*SPELC2(I)**2.0)
  ELSE
  ACCEL=DENL2(I+1)*SPELC2(I+1)**2.0-DENL2(I)*SPELC2(I)**2.0
  END IF
C-
C- DETERMINE THE DELTA P ACROSS THE NODE

```

```

C-      DPLIQ(I)=TIME+ACCEL+GRAVT+FRICT
100 CONTINUE
      RETURN
      END
      SUBROUTINE MOMTUMV

C-
C-----
C-
C-      SUBROUTINE MOMTUMV:
C-
C-              THIS SUROUTINE CALCULATES THE DELTA P'S OF
C-      THE CONSERVATION OF MOMENTUM EQUATION WHEN A VALUE FOR THE
C-      VELOCITIES ARE GIVEN. THE BOUNDARY CONDITON USED IS THE VELOCITY
C-      IS ZERO AT THE EVAPORATOR WALL
C-----
C-
      IMPLICIT REAL (A-H,O-Z)
      COMMON /PRES/PRESL1(100),PRESL2(100),PRESV1(100),PRESV2(100),
+          DPLIQ(100),DPVAP(100)
      COMMON /DENS/DENL1(100),DENL2(100),DENV1(100),DENV2(100)
      COMMON /SPEED/SPELC1(100),SPELC2(100),SPELB1(100),SPELB2(100),
+          SPEVC1(100),SPEVC2(100),SPEVB1(100),SPEVB2(100)
      COMMON /PROP/CONL(100),CONV(100),VISCOL(100),
+          VISCOV(100),REYNV(100),HDB(100),PRV(100)
      COMMON /SETUP/DELX(100),HETIN(100),HETOUT(100),SOURCE(100),
+          SIGMA(100),XSAVE(100),FSAVE(100)
      COMMON /INITIL/AMOLE,GASC,FLUDK,SHFLUD,DFLUD,VOLF,WICKP,WICKK,
+          SHWICK,DWICK,RADI1,RADIN,RADBN,WALLK,SHWALL,DWALL,
+          COOLK,PRCUL,VISCU,TEMPC,CMFR,FDNUN,GRAV,THETA,
+          SHREFV,SHREFL,ENREF,HDBCO,
+          TTOL,DELT,PI,QSTC
      COMMON /GEOMHP/EVAPL,ADIAL,CONDL,DELZL,DELZV,DELZ,DELY,VOLL,
+          AREAL,AREAV,AREAC,WALLT,PWETV,PWETL,PWETC,
+          POPEN,WDIA,FWAR,DELPV,DELPL,N,NE,NA,NC,LAYERS,
+          NFAKE

C-
C- FIND DELAT P, S FOR EACH NODE
C-
      DO 100 I=1,N

C-
C- DETERMINE XEFF FOR THE FRICTION PRESSURE DROP
C-
      XEFF=DELX(I)/2.0
      IF(I.GT.NE.AND.I.LE.NFAKE) XEFF=DELX(I)

C-
C- DETERMINE THE TRANSIENT PRESSURE DROP
C-
      TIME=DELX(I)*(DENV1(I)*SPEVC1(I)-DENV2(I)*SPEVC2(I))/DELT

C-
C- DETERMINE THE GRAVATATIONAL PRESSURE DROP

```

```

C-          GRAVT=(-DELX(I)*DENV2(I)*GRAV*SIN(THETA))
C-
C- DETERMINE IF TURBULENT OR LAMINAR FLOW; THEN FIND FRICTION PRESSURE
C- DROP
C-
          HYD=4.0*DELY*DELZV/(2.0*(DELY+DELZV))
          REYNOLD=DENV2(I)*SPEVC2(I)*HYD/VISCOV(I)
          IF(REYNOLD.LT.2.1E3) THEN
            FRICT=(-8.0*VISCOV(I)*SPEVC2(I)*DELY*DELZV*XEFF)/(PI*
+              (HYD/2.0)**4.0)
          ELSE
            FFACT=0.079/(REYNOLD**(0.25))
            FRICT=(-FFACT*DENV2(I)*SPEVC2(I)**2.0*XEFF/(HYD/2.0))
          END IF
          IF(I.EQ.1) THEN
C-
C- APPLY BOUNDARY CONDITION (VELOCITY=0 AT NODE 0)
C-
            ACCEL=(-DENV2(I)*SPEVC2(I)**2.0)
          ELSE
            ACCEL=DENV2(I-1)*SPEVC2(I-1)**2.0-DENV2(I)*SPEVC2(I)**2.0
          END IF
C-
C- DETERMINE THE DELTA P ACROSS THE NODE
C-
            DPVAP(I)=TIME+ACCEL+GRAVT+FRICT
100 CONTINUE
            RETURN
            END
            SUBROUTINE NEXTTS
C-
C- -----
C-
C- SUBROUTINE NEXTTS:
C-
C-           THIS SUBROUTINE SETS THE VALUES FROM THE NEW
C- TIME STEP TO THE OLD TIME STEP, THUS ALLOWING THE PROGRAM TO
C- MARCH THROUGH TIME.
C-
C- -----
C-
            IMPLICIT REAL (A-H,O-Z)
            COMMON /TEMP/TEMPO1(100),TEMPO2(100),TEMPW1(100),TEMPW2(100),
+              TEMPL1(100),TEMPL2(100),TEMPV1(100),TEMPV2(100),
+              TEMPIN(1000),TEMPOUT(1000),NX
            COMMON /PRES/PRESL1(100),PRESL2(100),PRESV1(100),PRESV2(100),
+              DPLIQ(100),DPVAP(100)
            COMMON /DENS/DENL1(100),DENL2(100),DENV1(100),DENV2(100)
            COMMON /SPEED/SPELC1(100),SPELC2(100),SPELB1(100),SPELB2(100),
+              SPEVC1(100),SPEVC2(100),SPEVB1(100),SPEVB2(100)
            COMMON /SPHEAT/SHLIQ1(100),SHLIQ2(100),SHVAP1(100),SHVAP2(100)

```

```

COMMON /SETUP/DELX(100),HETIN(100),HETOUT(100),SOURCE(100),
+ SIGMA(100),XSAVE(100),FSAVE(100)
COMMON /GEOMHP/EVAPL,ADIAL,CONDL,DELZL,DELZV,DELZ,DELY,VOLL,
+ AREAL,AREAV,AREAC,WALLT,PWETV,PWETL,PWETC,
+ POPEN,WDIA,FWAR,DELPV,DELPL,N,NE,NA,NC,LAYERS,
+ NFAKE
COMMON /FLAGS/IF1,IF2,IF3,IF4,IF5,IF6,IF7,IF8,IF9,IF10,IF11,IF12
COMMON /PFLAGS/IP1,IP2,IP3,IP4,IP5,IP6,IP7,IP8,IP9,IP10,IP11,IP12

```

C-  
C- SET UP LOOP TO EXCHANGE VALUES FOR EACH NODE BETWEEN TIME STEPS  
C-

```

60 DO 100 I=1,N
    DENL1(I)=DENL2(I)
    DENV1(I)=DENV2(I)
    SPELC1(I)=SPELC2(I)
    SPEVC1(I)=SPEVC2(I)
    TEMPO1(I)=TEMPO2(I)
    TEMPW1(I)=TEMPW2(I)
    TEMPL1(I)=TEMPL2(I)
    TEMPV1(I)=TEMPV2(I)
    SHLIQ1(I)=SHLIQ2(I)
    SHVAP1(I)=SHVAP2(I)
    PRESL1(I)=PRESL2(I)
    PRESV1(I)=PRESV2(I)
    XSAVE(I)=SOURCE(I)

```

```

100 CONTINUE
    RETURN
    END
    SUBROUTINE OUTCONT

```

C-  
C-----  
C-  
C- SUBROUTINE OUTCONT:  
C-  
C- THIS SUBROUTINE IS USED TO OUTPUT ALL THE  
C- IMPORTANT VARIABLES AFTER THE TRANSIENT HAS EXECUTED. THIS IS  
C- A GOOD CHECK FOR CHANGES OCCURING DURING THE RUN AND FOR MAKING  
C- SURE THE INPUT DECK WAS CORRECT.  
C-  
C-----  
C-

```

IMPLICIT REAL (A-H,O-Z)
COMMON /TEMP/TEMPO1(100),TEMPO2(100),TEMPW1(100),TEMPW2(100),
+ TEMPL1(100),TEMPL2(100),TEMPV1(100),TEMPV2(100),
+ TEMPIN(1000),TEMPOUT(1000),NX
COMMON /INITIL/AMOLE,GASC,FLUDK,SHFLUD,DFLUD,VOLF,WICKP,WICKK,
+ SHWICK,DWICK,RAD11,RADIN,RADBN,WALLK,SHWALL,DWALL,
+ COOLK,PRCUL,VISCUL,TEMPC,CMFR,FDNUN,GRAV,THETA,
+ SHREFV,SHREFL,ENREF,HDBCO,
+ TTOL,DELT,PI,QSTC
COMMON /GEOMHP/EVAPL,ADIAL,CONDL,DELZL,DELZV,DELZ,DELY,VOLL,
+ AREAL,AREAV,AREAC,WALLT,PWETV,PWETL,PWETC,

```

```

+           POPEN,WDIA,FWAR,DELPV,DELPL,N,NE,NA,NC,LAYERS,
+           NFAKE
COMMON /FLAGS/IF1,IF2,IF3,IF4,IF5,IF6,IF7,IF8,IF9,IF10,IF11,IF12
COMMON /PFLAGS/IP1,IP2,IP3,IP4,IP5,IP6,IP7,IP8,IP9,IP10,IP11,IP12
C-
C- WRITE OUT PHYSICAL PARAMETERS OF THE HEAT PIPE
C-
WRITE (IP1,1010) NE,NA,NC,NFAKE,N,NX
WRITE (IP1,1011) EVAPL,ADIAL,CONDL
WRITE (IP1,1012) DELY,WALLT,DELZL,DELZV,DELZ
WRITE (IP1,1013) AREAL,AREAV,AREAC,PWETL,PWETV,PWETC
WRITE (IP1,1014) POPEN,WDIA,FWAR,LAYERS,VOLL
WRITE (IP1,1015) VOLF,TEMPC,CMFR,AMOLE,GASC
WRITE (IP1,1016) FLUDK,SHFLUD,DFLUD
WRITE (IP1,1017) WICKP,WICKK,SHWICK,DWICK
WRITE (IP1,1018) WALLK,SHWALL,DWALL
WRITE (IP1,1019) COOLK,PRCUL,VISCUL,FDNUN,HDBCO
WRITE (IP1,1020) SHREFL,SHREFV,ENREF
WRITE (IP1,1021) GRAV,THETA,PI,QSTC
WRITE (IP1,1022) TTOL,DELT
WRITE (IP1,1023) IF1,IF2,IF3,IF4,IF5,IF6,IF7,IF8,IF9,IF10,
+           IF11,IF12
WRITE (IP1,1024) IP1,IP2,IP3,IP4,IP5,IP6,IP7,IP8,IP9,IP10,
+           IP11,IP12
RETURN
1010 FORMAT(1X,///,1X,130('*'),/,1X,48('*'),
+          '***** HEAT PIPE VARIABLES *****',48('*'),/,1X,130('*'),
+          //,' NUMBER OF EVAPORATOR NODES = ',T50,I6,/,
+
+          ' NUMBER OF ADIABATIC NODES = ',T50,I6,/,
+          ' NUMBER OF CONDENSER NODES = ',T50,I6,/,
+          ' NUMBER OF EVAP + ADIA NODES = ',T50,I6,/,
+          ' TOTAL NUMBER OF AXIAL NODES = ',T50,I6,/,
+          ' TOTAL NUMBER OF NODES = ',T50,I6,/)
1011 FORMAT(1X,'EVAPORATOR LENGTH = ',T50,1PE15.8,T68,'M',/,
+          ' ADIABATIC LENGTH = ',T50,1PE15.8,T68,'M',/,
+          ' CONDENSER LENGTH = ',T50,1PE15.8,T68,'M',/)
1012 FORMAT(1X,'WIDTH OF HEAT PIPE = ',T50,1PE15.8,T68,'M',/,
+          ' HEAT PIPE WALL THICKNESS = ',T50,1PE15.8,T68,'M',/,
+          ' LIQUID REGION THICKNESS = ',T50,1PE15.8,T68,'M',/,
+          ' VAPOR REGION THICKNESS = ',T50,1PE15.8,T68,'M',/,
+          ' TOTAL WIDTH FOR FLOW = ',T50,1PE15.8,T68,'M',/)
1013 FORMAT(1X,'CROSS-SECTIONAL AREA FOR LIQUID FLOW = ',T50,1PE15.8,
+          T68,'M2',/, ' CROSS-SECTIONAL AREA FOR VAPOR FLOW = ',T50,
+          1PE15.8,T68,'M2',/, ' CROSS-SECTIONAL AREA FOR COOLANT',
+          ' FLOW = ',T50,1PE15.8,T68,'M2',/, ' LIQUID WETTED',
+          ' PERIMETER = ',T50,1PE15.8,T68,'M',/, ' VAPOR WETTED',
+          ' PERIMETER = ',T50,1PE15.8,T68,'M',/, ' COOLANT WETTED',
+          ' PERIMETER = ',T50,1PE15.8,T68,'M',/)
1014 FORMAT(1X,'WIDTH OF PORE OPENING = ',T50,1PE15.8,T68,'M',/,
+          ' WIRE DIAMETER IN MESH = ',T50,1PE15.8,T68,'M',/,
+          ' WICK ASPECT RATIO FUNCTION = ',T50,1PE15.8,/,

```

```

+      ' NUMBER OF WIRE MESH LAYERS = ',T50,1PE15.8,/,
+      ' VOLUME OF LIQUID INTRODUCED = ',T50,1PE15.8,
+      T68,'LITER',//)
1015 FORMAT(1X,'LIQUID VOLUME FRACTION = ',T50,1PE15.8,/,
+      ' COOLANT TEMPERATURE = ',T50,1PE15.8,T68,'K',/,
+      ' COOLANT MASS FLOW RATE = ',T50,1PE15.8,T68,'KG/S',/,
+      ' MOLECULAR WIEGHT OF WORKING FLUID = ',T50,1PE15.8,/,
+      ' GAS CONSTANT = ',T50,1PE15.8,T68,'J/(KG-MOLE-K)',//)
1016 FORMAT(1X,'LIQUID CONDUCTIVITY = ',T50,1PE15.8,T68,'W/M-K',/,
+      ' SPECIFIC HEAT OF LIQUID = ',T50,1PE15.8,T68,'J/KG-K',/,
+      ' DENSITY OF LIQUID = ',T50,1PE15.8,T68,'KG/M3',//)
1017 FORMAT(1X,'WICK PERMABILITY = ',T50,1PE15.8,T68,'M2',/,
+      ' WICK CONDUCTIVITY = ',T50,1PE15.8,T68,'W/M-K',/,
+      ' WICK SPECIFIC HEAT = ',T50,1PE15.8,T68,'J/KG-K',/,
+      ' WICK DENSITY = ',T50,1PE15.8,T68,'KG/M3',//)
1018 FORMAT(1X,'WALL CONDUCTIVITY = ',T50,1PE15.8,T68,'W/M-K',/,
+      ' WALL SPECIFIC HEAT = ',T50,1PE15.8,T68,'J/KG-K',/,
+      ' WALL DENSITY = ',T50,1PE15.8,T68,'KG/M3',//)
1019 FORMAT(1X,'COOLANT CONDUCTIVITY = ',T50,1PE15.8,T68,'W/M-K',/,
+      ' COOLANT PRANDLT NUMBER = ',T50,1PE15.8,/,
+      ' COOLANT VISCOSITY = ',T50,1PE15.8,T68,'N-S/M',/,
+      ' COOLANT NUSSELT NUMBER = ',T50,1PE15.8,/,
+      ' COOLANT HEAT TRANSFER COEFFICIENT = ',T50,1PE15.8,
+      T68,'W/M2-K',//)
1020 FORMAT(1X,'LIQUID REFERENCE SP. HEAT = ',T50,1PE15.8,T68,
+      'J/KG-K',/, ' VAPOR REFERENCE SP. HEAT = ',T50,1PE15.8,
+      T68,'J/KG-K',/, ' VAPOR REFERENCE ENTHALPY = ',T50,1PE15.8,
+      T68,'J/KG',//)
1021 FORMAT(1X,'LOCAL ACCELERATION = ',T50,1PE15.8,T68,'M/S2',/,
+      ' ANGLE OF TILT = ',T50,1PE15.8,T68,'RADIANS',/,
+      ' VALUE OF PI = ',T50,1PE15.8,/,
+      ' STORED ENERGY CONSTANT = ',T50,1PE15.8,T68,'1/S',//)
1022 FORMAT(1X,'TOLERANCE ALLOWED ON TEMPERATURE = ',T50,1PE15.8,/,
+      ' TIME STEP = ',T50,1PE15.8,T68,'S',//)
1023 FORMAT(1X,T50,'***** VALUE OF FLAGS *****',/,4X,12(I6,4X))
1024 FORMAT(4X,12(I6,4X))

```

```

END
SUBROUTINE OUTPUTE

```

C-

-----

C-

C- SUBROUTINE OUTPUTE:

C-

C- THIS SUBROUTINE PRINTS TO FILE IP1 ALL  
C- INFORMATION BETWEEN ITERATIONS.

C-

-----

C-

```

IMPLICIT REAL (A-H,O-Z)
COMMON /TEMP/TEMPO1(100),TEMPO2(100),TEMPW1(100),TEMPW2(100),
+      TEMPL1(100),TEMPL2(100),TEMPV1(100),TEMPV2(100),
+      TEMPIN(1000),TEMPOUT(1000),NX

```

```

COMMON /PRES/PRESL1 (100), PRESL2 (100), PRESV1 (100), PRESV2 (100),
+
DPLIQ (100), DPVAP (100)
COMMON /DENS/DENL1 (100), DENL2 (100), DENV1 (100), DENV2 (100)
COMMON /SPEED/SPELC1 (100), SPELC2 (100), SPELB1 (100), SPELB2 (100),
+
SPEVC1 (100), SPEVC2 (100), SPEVB1 (100), SPEVB2 (100)
COMMON /SPHEAT/SHLIQ1 (100), SHLIQ2 (100), SHVAP1 (100), SHVAP2 (100)
COMMON /PROP/CONL (100), CONV (100), VISCOL (100),
+
VISCOV (100), REYNV (100), HDB (100), PRV (100)
COMMON /SETUP/DELX (100), HETIN (100), HETOUT (100), SOURCE (100),
+
SIGMA (100), XSAVE (100), FSAVE (100)
COMMON /OUTPU/RTIME, ERRMAX, NRE, ITER, ITIME, IREAD
COMMON /INITIL/AMOLE, GASC, FLUDK, SHFLUD, DFLUD, VOLF, WICKP, WICKK,
+
SHWICK, DWICK, RAD11, RADIN, RADBN, WALLK, SHWALL, DWALL,
+
COOLK, PRCUL, VISCOL, TEMPC, CMFR, FDNUN, GRAV, THETA,
+
SHREFV, SHREFL, ENREF, HDBCO,
+
TTOL, DELT, PI, QSTC
COMMON /GEOMHP/EVAPL, ADIAL, CONDL, DELZL, DELZV, DELZ, DELY, VOLL,
+
AREAL, AREAV, AREAC, WALLT, PWETV, PWETL, PWETC,
+
POPEN, WDIA, FWAR, DELPV, DELPL, N, NE, NA, NC, LAYERS,
+
NFAKE
COMMON /PFLAGS/IP1, IP2, IP3, IP4, IP5, IP6, IP7, IP8, IP9, IP10, IP11, IP12
C-
C- DETERMINE IF THE INITIAL CONDITIONS SHOULD BE PRINTED OUT
C-
IF (ITIME.EQ.0) THEN
C-
C- CALCULATE THE TIME
C-
TIME=0.0
C-
C- SET UP LOOP TO WRITE OUT PARAMETERS FOR EACH NODE
C-
WRITE (IP1, 1010) TIME, ERPMAX, NRE, ITER
WRITE (IP1, 1011)
C-
C- PRINT OUT INITIAL TEMPERATURES
C-
DO 10 I=1, N
WRITE (IP1, 1012) I, TEMPO1 (I), TEMPW1 (I), TEMPL1 (I), TEMPV1 (I)
10 CONTINUE
C-
C- PRINT OUT PROPERTIES
C-
WRITE (IP1, 1013)
DO 20 I=1, N
WRITE (IP1, 1014) I, PRESL1 (I), DENL1 (I), SPELC1 (I), SHLIQ1 (I),
+
PRESV1 (I), DENV1 (I), SPEVC1 (I), SHVAP1 (I), SOURCE (I)
20 CONTINUE
WLMASS=0.0
VMASS=0.0
DO 30 I=1, N
WLMASS=WLMASS+DENL1 (I) *DELX (I) *DELY*DELZL* (1.0-VOLF)

```

```

          VMASS=VMASS+DENV1 (I) *DELX(I) *DELY*DELZV
30      CONTINUE
          TTMAS=WLMASS+VMASS
          WRITE (IP1,1015)WLMASS,VMASS,TTMAS
          RETURN
      END IF
C-
C- WRITE OUT FIRST TIME STEP CONDITIONS
C-
          IF (ITIME.EQ.1) GO TO 50
C-
C- DETERMINE IF THER SHOULD BE OUTPUT
C-
          DDT=FLOAT (ITIME) /FLOAT (IP2)
          IDT=ITIME/IP2
          ADT=DDT-IDT
          IF (ADT.NE.0.0) THEN
              RETURN
          END IF
C-
C- CALCULATE THE TIME
C-
          50  TIME=RTIME
C-
C- SET UP LOOP TO WRITE OUT PARAMETERS FOR EACH NODE
C-
          WRITE (IP1,1010) TIME,ERRMAX,NRE,ITER
          WRITE (IP1,1011)
C-
C- WRITE OUT CONVERGED TEMPERATURES FOR TIME = TIME
C-
          DO 60 I=1,N
              WRITE (IP1,1012) I,TEMPO2 (I) ,TEMPW2 (I) ,TEMPL2 (I) ,TEMPV2 (I)
60      CONTINUE
C-
C- WRITE OUT PROPERTIES FOR TIME = TIME
C-
          WRITE (IP1,1013)
          DO 70 I=1,N
              WRITE (IP1,1014) I,PRESL2 (I) ,DENL2 (I) ,SPELC2 (I) ,SHLIQ2 (I) ,
+
              PRESV2 (I) ,DENV2 (I) ,SPEVC2 (I) ,SHVAP2 (I) ,SOURCE (I)
70      CONTINUE
C-
C- DETERMINE TOTAL HEAT PIPE MASS AND PRINT IT OUT
C-
          WLMASS=0.0
          VMASS=0.0
          DO 80 I=1,N
              WLMASS=WLMASS+DENL2 (I) *DELX(I) *DELY*DELZL* (1.0-VOLF)
              VMASS=VMASS+DENV2 (I) *DELX(I) *DELY*DELZV
80      CONTINUE
          TTMAS=WLMASS+VMASS

```

```

WRITE (IP1,1015)WLMASS,VMASS,TTMAS
RETURN
1010 FORMAT(1X,///,1X,130('$'),/,1X,T5,'TIME = ',1PE12.5,T32,
+         'MAXIMUM RELATIVE ERROR = ',1PE12.5,2X,'OCCURED AT NODE',
+         1X,'(',I4,')',T105,'NUMBER OF ITERATIONS ',I2,
+         /,1X,130('$'))
1011 FORMAT(1X,/,1X,T5,'NODE',T17,'OUTER WALL',T41,'INNER WALL',T67,
+         'LIQUID',T87,'VAPOR',/,1X,T2,
+         132('-'))
1012 FORMAT(1X,T2,I6,4X,4(3PE20.13,4X))
1013 FORMAT(1X,/,1X,T12,'LIQUID',T25,'LIQUID',T38,'LIQUID',
+         T51,'LIQUID',T65,'VAPOR',T78,'VAPOR',T91,'VAPOR',T104,
+         'VAPOR',/,1X,T5,'NODE',T11,'PRESSURE',T25,'DENSITY',T37,
+         'VELOCITY',T49,'SPEC. HEAT',T63,'PRESSURE',T77,'DENSITY',
+         T89,'VELOCITY',T101,'SPEC. HEAT',T116,'SOURCE',/,1X,
+         130('-'))
1014 FORMAT(1X,T2,I6,1X,9(1PE12.5,1X))
1015 FORMAT(1X,/,1X,'LIQUID TOTAL MASS =',1PE15.8,5X,
+         'VAPOR TOTAL MASS =',1PE15.8,5X,
+         'TOTAL MASS =',1PE15.8)

```

END

SUBROUTINE OUTPUTI

C-

C-----

C-

C- SUBROUTINE OUTPUTI:

C-

C-

C-

C-

C-----

C-

IMPLICIT REAL (A-H,O-Z)

COMMON /TEMP/TEMPO1(100),TEMPO2(100),TEMPW1(100),TEMPW2(100),

+ TEMPL1(100),TEMPL2(100),TEMPV1(100),TEMPV2(100),

+ TEMPIN(1000),TEMPOUT(1000),NX

COMMON /PRES/PRESL1(100),PRESL2(100),PRESV1(100),PRESV2(100),

+ DPLIQ(100),DPVAP(100)

COMMON /DENS/DENL1(100),DENL2(100),DENV1(100),DENV2(100)

COMMON /SPEED/SPELC1(100),SPELC2(100),SPELB1(100),SPELB2(100),

+ SPEVC1(100),SPEVC2(100),SPEVB1(100),SPEVB2(100)

COMMON /SPHEAT/SHLIQ1(100),SHLIQ2(100),SHVAP1(100),SHVAP2(100)

COMMON /PROP/CONL(100),CONV(100),VISCOL(100),

+ VISCOV(100),REYNV(100),HDB(100),PRV(100)

COMMON /SETUP/DELX(100),HETIN(100),HETOUT(100),SOURCE(100),

+ SIGMA(100),XSAVE(100),FSAVE(100)

COMMON /OUTPU/RTIME,ERRMAX,NRE,ITER,ITIME,IREAD

COMMON /INITIL/AMOLE,GASC,FLUDK,SHFLUD,DFLUD,VOLF,WICKP,WICKK,

+ SHWICK,DWICK,RADIL,RADIN,RADBN,WALLK,SHWALL,DWALL,

+ COOLK,PRCUL,VISCU,TEMPC,CMFR,FDNUN,GRAV,THETA,

+ SHREFV,SHREFL,ENREF,HDBCO,

+ TTOL,DELT,PI,QSTC

```

COMMON /GEOMHP/EVAPL, ADIAL, CONDL, DELZL, DELZV, DELZ, DELY, VOLL,
+
+ AREAL, AREAV, AREAC, WALLT, PWETV, PWETL, PWETC,
+ POPEN, WDIA, FWAR, DELPV, DELPL, N, NE, NA, NC, LAYERS,
+ NFAKE
COMMON /PFLAGS/IP1, IP2, IP3, IP4, IP5, IP6, IP7, IP8, IP9, IP10, IP11, IP12
C-
C- DETERMINE IF THERE SHOULD BE OUTPUT
C-
IF (IP5.EQ.1) THEN
RETURN
END IF
IF (ITER.EQ.0.OR.ITER.EQ.1) GO TO 50
DDT=FLOAT(ITER)/FLOAT(IP4)
IDT=ITER/IP4
ADT=DDT-IDT
IF (ADT.NE.0.0) THEN
RETURN
END IF
C-
C- CALCULATE THE TIME
C-
50 TIME=RTIME
C-
C- SET UP LOOP TO WRITE OUT PARAMETERS FOR EACH NODE
C-
WRITE (IP3, 1010) ITER, ERRMAX, NRE, TIME
WRITE (IP3, 1011)
C-
C- WRITE OUT ITERATION TEMPERATURES
C-
DO 100 I=1, N
WRITE (IP3, 1012) I, TEMPO2 (I), TEMPW2 (I), TEMPL2 (I), TEMPV2 (I)
100 CONTINUE
C-
C- WRITE OUT PROPERTIES FOR THE GIVEN ITERATION
C-
WRITE (IP3, 1013)
DO 200 I=1, N
WRITE (IP3, 1014) I, PRESL2 (I), DENL2 (I), SPELC2 (I), SHLIQ2 (I),
+ PRESV2 (I), DENV2 (I), SPEVC2 (I), SHVAP2 (I), SOURCE (I)
200 CONTINUE
RETURN
1010 FORMAT (1X, ///, 1X, 130 ('*'), /, 1X, T5, 'ITERATION NUMBER ', I6, T35,
+ 'MAXIMUM RELATIVE ERROR = ', 1PE12.5, 2X, 'OCCURED AT NODE',
+ 1X, '(', I4, ')', T110, 'TIME = ', 1PE12.5, /, 1X, 130 ('*'))
1011 FORMAT (1X, /, 1X, T5, 'NODE', T17, 'OUTER WALL', T41, 'INNER WALL', T67,
+ 'LIQUID', T87, 'VAPOR', /, 1X, T2,
+ 132 ('-'))
1012 FORMAT (1X, T2, I6, 4X, 4 (3PE20.13, 4X))
1013 FORMAT (1X, /, 1X, T12, 'LIQUID', T25, 'LIQUID', T38, 'LIQUID',
+ T51, 'LIQUID', T65, 'VAPOR', T78, 'VAPOR', T91, 'VAPOR', T104,
+ 'VAPOR', /, 1X, T5, 'NODE', T11, 'PRESSURE', T25, 'DENSITY', T37,

```

```

+          'VELOCITY',T49,'SPEC. HEAT',T63,'PRESSURE',T77,'DENSITY',
+          T89,'VELOCITY',T101,'SPEC. HEAT',T116,'SOURCE',/,1X,
+          130('-')
1014 FORMAT(1X,T2,I6,1X,9(1PE12.5,1X))
      END
      SUBROUTINE PRANDLT
C-
C-----
C-
C-   SUBROUTINE PRANDLT:
C-
C-           THIS SUBROUTINE CALCULATES THE PRANDLT NUMBER
C-   FOR THE VAPOR AS A FUNCTION OF TEMPERATURE. THE FIT WAS DONE
C-   USING A FOURTH ORDER LEAST SQUARES FIT FOR PROPERTY DATA FOUND
C-   IN COLLIER.
C-----
C-
      IMPLICIT REAL (A-H,O-Z)
      COMMON /TEMP/TEMPO1(100),TEMPO2(100),TEMPW1(100),TEMPW2(100),
+          TEMPL1(100),TEMPL2(100),TEMPV1(100),TEMPV2(100),
+          TEMPIN(1000),TEMPOUT(1000),NX
      COMMON /PROP/CONL(100),CONV(100),VISCOL(100),
+          VISCOV(100),REYNV(100),HDB(100),PRV(100)
      COMMON /GEOMHP/EVAPL,ADIAL,CONDL,DELZL,DELZV,DELZ,DELY,VOLL,
+          AREAL,AREAV,AREAC,WALLT,PWETV,PWETL,PWETC,
+          POPEN,WDIA,FWAR,DELPV,DELPL,N,NE,NA,NC,LAYERS,
+          NFAKE
C-
C- SET UP COEFFICIENTS FROM FIT
C-
      A1=(-0.3341460060758E01)
      A2=0.4249353324688E-01
      A3=(-0.1604024352477E-03)
      A4=0.2668579216012E-06
      A5=(-0.1578478304355E-09)
C-
C- SET UP LOOP TO FIND THE PRANDLT NUMBER FOR EACH NODE
C-
      DO 100 I=1,N
          T=TEMPV2(I)
          PRV(I)=A1+A2*T+A3*T**2.0+A4*T**3.0+A5*T**4.0
100  CONTINUE
      RETURN
      END
      SUBROUTINE PREGES
C-
C-----
C-
C-   SUBROUTINE PREGES:
C-
C-           THIS SUBROUTINE SOLVES FOR LIQUID AND VAPOR

```

C- PRESSURE DISTRIBUTION IN THE HEAT PIPE FOR THE NEW TIME STEP.  
 C- THE BOUNDARY CONDITIONS USED ARE THE VAPOR PRESSURE AT THE  
 C- EVAPORATOR EDGE IS GIVEN BY THE SATURATION TEMPERATURE OF THE  
 C- FIRST NODE AND AT THE END OF THE CONDENSER THE LIQUID  
 C- PRESSURE IS EQUAL TO THE VAPOR PRESSURE.

C-  
 C-----  
 C-

```

    IMPLICIT REAL (A-H,O-Z)
    COMMON /PRES/PRESL1(100),PRESL2(100),PRESV1(100),PRESV2(100),
+         DPLIQ(100),DPVAP(100)
    COMMON /GEOMHP/EVAPL,ADIAL,CONDL,DELZL,DELZV,DELZ,DELY,VOLL,
+         AREAL,AREAV,AREAC,WALLT,PWETV,PWETL,PWETC,
+         POPEN,WDIA,FWAR,DELPV,DELPL,N,NE,NA,NC,LAYERS,
+         NFAKE
  
```

C-  
 C- SET UP LOOP TO ADD DIFFERENTIAL PRESSURES FOR THE VAPOR  
 C-

```

    DO 100 I=1,N
      IF (I.NE.1) THEN
        PRESV2(I)=PRESV2(I-1)+(DPVAP(I-1)+DPVAP(I))/2.0
      ELSE
        PRESV2(I)=PRESV2(I)+DPVAP(I)/2.0
      END IF
    100 CONTINUE
  
```

C-  
 C- SET UP LOOP TO ADD DIFFERENTIAL PRESSURES FOR THE LIQUID  
 C-

```

    PLASTV=PRESV2(N)+DPVAP(N)/2.0
    PLASTL=PLASTV
    DO 200 I=N,1,-1
      IF (I.NE.N) THEN
        PRESL2(I)=PRESL2(I+1)+(DPLIQ(I+1)+DPLIQ(I))/2.0
      ELSE
        PRESL2(I)=PLASTL+DPLIQ(I)/2.0
      END IF
    200 CONTINUE
  
```

```

    RETURN
    END
    SUBROUTINE PRESFT
  
```

C-  
 C-----

C-  
 C- SUBROUTINE PRESFT:  
 C- THIS SUBROUTINE CALCULATES THE SATURATION  
 C- PRESSURE FROM THE TEMPERATURE USING COEFFICIENTS GIVEN IN ASME  
 C- STEAM TABLES. THIS IS USED AS THE BOUNDARY CONDITION FOR THE  
 C- MOMENTUM EQUATION.

C-  
 C-----  
 C-

```

    IMPLICIT REAL (A-H,O-Z)
  
```

```

COMMON /TEMP/TEMPO1(100),TEMPO2(100),TEMPW1(100),TEMPW2(100),
+      TEMPL1(100),TEMPL2(100),TEMPV1(100),TEMPV2(100),
+      TEMPIN(1000),TEMPOUT(1000),NX
COMMON /PRES/PRESL1(100),PRESL2(100),PRESV1(100),PRESV2(100),
+      DPLIQ(100),DPVAP(100)
COMMON /COEFF/RR1(25),CF1(9),CF2(9),CF3(9),CG1(12),
+      CG2(9),CG3(7),CT1(2,4),CT2(5,5),CT3(5,5),
+      CT4(5,5),CN1(3,5),CN2(4,3),AA1(5),AA2(7),
+      AA3(7),AK(9),AL(12),CLSH(6),CVSH(6),CLTC(6),
+      AZ(12),BBZ(9,6),BL(4),PCRT,TEMPK,BETA1,
+      NYZ(8),LYZ(8),NZZ(8,3),LUZ(8,2)
COMMON /GEOMHP/EVAPL,ADIAL,CONDL,DELZL,DELZV,DELZ,DELY,VOLL,
+      AREAL,AREAV,AREAC,WALLT,PWETV,PWETL,PWETC,
+      POPEN,WDIA,FWAR,DELPV,DELPL,N,NE,NA,NC,LAYERS,
+      NFAKE

```

C-

C- FIND THE VAPOR PRESSURE OF NODE 1

C-

```

TR=TEMPV2(1)/647.3
Y=1.0-AL(1)*TR**2.0-AL(2)*TR**(-6.0)
SUM=0.0
E=1.0-TR
DO 10 I=1,5
    SUM=SUM+AK(I)*E**I

```

10 CONTINUE

C-

C- DETERMINE BETA FUNCTION

C-

```

BB=EXP(1.0/TR*SUM/(1.0+AK(6)*E+AK(7)*E**2.0)-(E/(AK(8)*
+ E**2.0+AK(9))))
PRESV2(1)=BB*22120000.0
RETURN
END
SUBROUTINE REYN

```

C-

C-----

C-

C- SUBROUTINE REYN:

C-

C- THIS SUBROUTINE CALCULATES THE REYNOLDS NUMBER  
C- FOR EACH VAPOR NODE AS IF IT WERE A FLUID FLOWING OVER A FLAT  
C- PLATE.

C-

C-----

C-

```

IMPLICIT REAL (A-H,O-Z)
COMMON /DENS/DENL1(100),DENL2(100),DENV1(100),DENV2(100)
COMMON /SPEED/SPELC1(100),SPELC2(100),SPELB1(100),SPELB2(100),
+      SPEVC1(100),SPEVC2(100),SPEVB1(100),SPEVB2(100)
COMMON /PROP/CONL(100),CONV(100),VISCOL(100),
+      VISCOV(100),REYNV(100),HDB(100),PRV(100)
COMMON /SETUP/DELX(100),HETIN(100),HETOUT(100),SOURCE(100),

```

```

+           SIGMA(100), XSAVE(100), FSAVE(100)
COMMON /GEOMHP/EVAPL, ADIAL, CONDL, DELZL, DELZV, DELZ, DELY, VOLL,
+           AREAL, AREAV, AREAC, WALLT, PWETV, PWETL, PWETC,
+           POPEN, WDIA, FWAR, DELPV, DELPL, N, NE, NA, NC, LAYERS,
+           NFAKE
C-
C- SET UP LOOP TO EVALUATE EACH NODE
C-
DO 100 I=1,N
    REYNV(I)=DELX(I)*DENV2(I)*SPEVC2(I)/VISCOV(I)
100 CONTINUE
    RETURN
    END
SUBROUTINE SIEDEL
C-
C-----
C-
C- SUBROUTINE SIEDEL:
C-
C-           THIS SUBROUTINE DETERMINES TEMPERATURE ERRORS
C- BETWEEN ITERATIONS AND SAVES THE NEW VALUES OF TEMPERATURE.
C- THIS IS PART OF THE GAUSS SIEDEL SOLUTION.
C-
C-----
C-
    IMPLICIT REAL (A-H,O-Z)
COMMON /TEMP/TEMPO1(100), TEMPO2(100), TEMPW1(100), TEMPW2(100),
+           TEMPL1(100), TEMPL2(100), TEMPV1(100), TEMPV2(100),
+           TEMPIN(1000), TEMPOUT(1000), NX
COMMON /INITIL/AMOLE, GASC, FLUDK, SHFLUD, DFLUD, VOLF, WICKP, WICKK,
+           SHWICK, DWICK, RAD11, RADIN, RADBN, WALLK, SHWALL, DWALL,
+           COOLK, PRCUL, VISCU, TEMPC, CMFR, FDNUN, GRAV, THETA,
+           SHREFV, SHREFL, ENREF, HDBCO,
+           TTOL, DELT, PI, QSTC
COMMON /GEOMHP/EVAPL, ADIAL, CONDL, DELZL, DELZV, DELZ, DELY, VOLL,
+           AREAL, AREAV, AREAC, WALLT, PWETV, PWETL, PWETC,
+           POPEN, WDIA, FWAR, DELPV, DELPL, N, NE, NA, NC, LAYERS,
+           NFAKE
COMMON /OUTPU/RTIME, ERRMAX, NRE, ITER, ITIME, IREAD
C-
C- SET UP SOLUTION VECTOR
C-
DO 40 I=1,N
    TEMPOUT((I-1)*4+1)=TEMPO2(I)
    TEMPOUT((I-1)*4+2)=TEMPW2(I)
    TEMPOUT((I-1)*4+3)=TEMPL2(I)
    TEMPOUT((I-1)*4+4)=TEMPV2(I)
40 CONTINUE
C-
C- CHECK FOR CONVERGENCE AND RESET GUESS
C-
    ERRMAX=0.0

```

```

IR=0
DO 110 I=1,NX
  RELCONV=ABS ((TEMPIN(I)-TEMPOUT(I))/TEMPOUT(I))
  IF (RELCONV.GT.ERRMAX) THEN
    ERRMAX=RELCONV
    NRE=I
  END IF
C-
C- RESET TEMPERATURES
C-
  TEMPIN(I)=TEMPOUT(I)
110 CONTINUE
RETURN
END
SUBROUTINE SPECHT
C-
C-----
C-
C- SUBROUTINE SPHEAT:
C-
C- THIS SUBROUTINE CALCULATES THE SPECIFIC HEAT OF
C- THE VAPOR AND LIQUID AS A FUNCTION OF THE TEMPERATURE. THIS FIT
C- WAS DONE USING A FIFTH DEGREE LEAST SQUARES FIT TO PROPERTY DATA
C- FOUND IN COLLIER.
C-
C-----
C-
  IMPLICIT REAL (A-H,O-Z)
  COMMON /TEMP/TEMPO1(100),TEMPO2(100),TEMPW1(100),TEMPW2(100),
+      TEMPL1(100),TEMPL2(100),TEMPV1(100),TEMPV2(100),
+      TEMPIN(1000),TEMPOUT(1000),NX
  COMMON /SPHEAT/SHLIQ1(100),SHLIQ2(100),SHVAP1(100),SHVAP2(100)
  COMMON /GEOMHP/EVAPL,ADIAL,CONDL,DELZL,DELZV,DELZ,DELY,VOLL,
+      AREAL,AREAV,AREAC,WALLT,PWETV,PWETL,PWETC,
+      POPEN,WDIA,FWAR,DELPV,DELPL,N,NE,NA,NC,LAYERS,
+      NFAKE
  COMMON /COEFF/RR1(25),CF1(9),CF2(9),CF3(9),CG1(12),
+      CG2(9),CG3(7),CT1(2,4),CT2(5,5),CT3(5,5),
+      CT4(5,5),CN1(3,5),CN2(4,3),AA1(5),AA2(7),
+      AA3(7),AK(9),AL(12),CLSH(6),CVSH(6),CLTC(6),
+      AZ(12),BBZ(9,6),BL(4),PCRIT,TEMPK,BETA1,
+      NYZ(8),LYZ(8),NZZ(8,3),LUZ(8,2)
  COMMON /PFLAGS/IP1,IP2,IP3,IP4,IP5,IP6,IP7,IP8,IP9,IP10,IP11,IP12
C-
C- SET UP LOOP TO CALCULATE THE SPECIFIC HEATS AT EACH NODE
C-
  DO 200 I=1,N
    SUM1=0.0
    SUM2=0.0
C-
C- APPLY COEFFICIENTS FROM THE FIT
C-

```

```

DO 100 J=1,6
    SUM1=SUM1+CLSH(J)*TEMPL2(I)**(J-1)
    SUM2=SUM2+CVSH(J)*TEMPV2(I)**(J-1)
100 CONTINUE
C-
C- CONVECT SPECIFIC HEAT FROM KJ TO J
C-
    SHLIQ2(I)=SUM1*1.0E03
    SHVAP2(I)=SUM2*1.0E03
200 CONTINUE
RETURN
END
SUBROUTINE TGUSS

C-
C-----
C-
C- SUBROUTINE TGUSS:
C-
C- THIS SUBROUTINE SETS THE VALUES FROM ENERGI TO
C- THE NEXT TIME STEP TEMPERATURES. THIS ALLOWS THE PROPERTIES TO
C- BE EVALUATED BEFORE ENTERING ENERGY.
C-
C-----
C-
    IMPLICIT REAL (A-H,O-Z)
    COMMON /TEMP/TEMPO1(100),TEMPO2(100),TEMPW1(100),TEMPW2(100),
+         TEMPL1(100),TEMPL2(100),TEMPV1(100),TEMPV2(100),
+         TEMPIN(1000),TEMPOUT(1000),NX
    COMMON /GEOMHP/EVAPL,ADIAL,CONDL,DELZL,DELZV,DELZ,DELY,VOLL,
+         AREAL,AREAV,AREAC,WALLT,PWETV,PWETL,PWETC,
+         POPEN,WDIA,FWAR,DELPV,DELPL,N,NE,NA,NC,LAYERS,
+         NFAKE
    COMMON /EZENG/TT1(5),D1(5,6),A1(5),B1(5),CC1(5),TS(5),STORE(1000)
    COMMON /PFLAGS/IP1,IP2,IP3,IP4,IP5,IP6,IP7,IP8,IP9,IP10,IP11,IP12

C-
C- DETERMINE IF THIS IS A RESTART JOB
C-
    IF (IREAD.EQ.5) THEN
        DO 50 I=1,N
            TEMPO2(I)=TEMPO1(I)
            TEMPW2(I)=TEMPW1(I)
            TEMPL2(I)=TEMPL1(I)
            TEMPV2(I)=TEMPV1(I)
            TEMPIN((I-1)*4+1)=TEMPO1(I)
            TEMPIN((I-1)*4+2)=TEMPW1(I)
            TEMPIN((I-1)*4+3)=TEMPL1(I)
            TEMPIN((I-1)*4+4)=TEMPV1(I)
50 CONTINUE
RETURN
END IF

C-
C- SET TEMPERATURES FROM MATRIX SOLUTION

```

```

C-
      DO 60 ITEMP=1,5
          TT1(ITEMP)=D1(ITEMP,6)
60    CONTINUE
C-
C- SET UP TEMPERATURE FROM SOLUTION
C-
      DO 70 I=1,N
          IF(I.GT.NE) THEN
              TEMPO2(I)=TT1(5)
              TEMPW2(I)=TT1(4)
              TEMPL2(I)=TEMPL1(I)
              TEMPV2(I)=TEMPV1(I)
          ELSE
              TEMPO2(I)=TT1(1)
              TEMPW2(I)=TT1(2)
              TEMPL2(I)=TT1(3)
              TEMPV2(I)=TEMPV1(I)
          END IF
70    CONTINUE
C-
C- SET UP ITERATION VECTOR
C-
      DO 80 I=1,N
          TEMPIN((I-1)*4+1)=TEMPO2(I)
          TEMPIN((I-1)*4+2)=TEMPW2(I)
          TEMPIN((I-1)*4+3)=TEMPL2(I)
          TEMPIN((I-1)*4+4)=TEMPV2(I)
80    CONTINUE
      RETURN
      END
      SUBROUTINE TIMCON

C-
C-----
C-
C- SUBROUTINE TIMCON:
C-
C-           THIS SUBROUTINE CALCULATES THE TIME CONSTANT
C- TO BE USED FOR EVAPORATION AND CONDENSATION MODEL.
C-
C-----
C-
      IMPLICIT REAL (A-H,O-Z)
      COMMON /EZENG/TT1(5),D1(5,6),A1(5),B1(5),CC1(5),TS(5),STORE(1000)
      COMMON /SETUP/DELX(100),HETIN(100),HETOUT(100),SOURCE(100),
+           SIGMA(100),XSAVE(100),FSAVE(100)
      COMMON /INITIL/AMOLE,GASC,FLUDK,SHFLUD,DFLUD,VOLF,WICKP,WICKK,
+           SHWICK,DWICK,RADI1,RADIN,RADBN,WALLK,SHWALL,DWALL,
+           COOLK,PRCUL,VISCUL,TEMPC,CMFR,FDNUN,GRAV,THETA,
+           SHREFV,SHREFL,ENREF,HDBCO,
+           TTOL,DELT,PI,QSTC
      COMMON /GEOMHP/EVAPL,ADIAL,CONDL,DELZL,DELZV,DELZ,DELY,VOLL,

```

```

+          AREAL, AREAV, AREAC, WALLT, PWETV, PWETL, PWETC,
+          POPEN, WDIA, FWAR, DELPV, DELPL, N, NE, NA, NC, LAYERS,
+          NFAKE
C-
C- SET UP CONSTANTS
C-
      TIMES=DELT
      DELT=1.0
      WIEGHT=(DELY*EVAPL+DELY*CONDL)/2.0
      DO 10 I=1,5
          TS(I)=TT1(I)
10  CONTINUE
C-
C- SET UP LOOP TO FIND THE CHANGE IN STORED ENERGY WITH TIME
C-
      DO 100 IJ=1,1000
          CALL ENERI
C-
C- DETERMINE STORED ENERGY IN EACH NODE
C-
          Q1=CC1(1)*(D1(1,6)-TT1(1))*DELY*EVAPL
          Q2=CC1(2)*(D1(2,6)-TT1(2))*DELY*EVAPL
          Q3=CC1(3)*(D1(3,6)-TT1(3))*WIEGHT
          Q4=CC1(4)*(D1(4,6)-TT1(4))*DELY*CONDL
          Q5=CC1(5)*(D1(5,6)-TT1(5))*DELY*CONDL
          STORE(IJ)=Q1+Q2+Q3+Q4+Q5
          DO 20 ITEMP=1,5
              TT1(ITEMP)=D1(ITEMP,6)
20  CONTINUE
100 CONTINUE
C-
C- DETERMINE THE TIME CONSTANT
C-
      G1=LOG(STORE(1000)/STORE(1))/(-999.0)
      G2=LOG(STORE(900)/STORE(100))/(-800.0)
      G3=LOG(STORE(995)/STORE(990))/(-5.0)
      AVG=(G1+G2+G3)/3.0
      QSTC=AVG
C-
C- SET VALUES BACK
C-
      DELT=TIMES
      DO 200 I=1,5
          TT1(I)=TS(I)
200 CONTINUE
      RETURN
      END
      SUBROUTINE TTP
C-
C-----
C-
C- SUBROUTINE TTP:

```

```

C-           THIS SUBROUTINE CALCULATES THE SATURATION
C- PRESSURE FROM THE TEMPERATURE USING COEFFICIENTS GIVEN IN ASME
C- STEAM TABLES.
C- -----
C-
C-     IMPLICIT REAL (A-H,O-Z)
C-     COMMON /TEMP/TEMPO1(100),TEMPO2(100),TEMPW1(100),TEMPW2(100),
+         TEMPL1(100),TEMPL2(100),TEMPV1(100),TEMPV2(100),
+         TEMPIN(1000),TEMPOUT(1000),NX
C-     COMMON /PRES/PRESL1(100),PRESL2(100),PRESV1(100),PRESV2(100),
+         DPLIQ(100),DPVAP(100)
C-     COMMON /GEOMHP/EVAPL,ADIAL,CONDL,DELZL,DELZV,DELZ,DELY,VOLL,
+         AREAL,AREAV,AREAC,WALLT,PWETV,PWETL,PWETC,
+         POPEN,WDIA,FWAR,DELPV,DELPL,N,NE,NA,NC,LAYERS,
+         NFAKE
C-     COMMON /COEFF/RR1(25),CF1(9),CF2(9),CF3(9),CG1(12),
+         CG2(9),CG3(7),CT1(2,4),CT2(5,5),CT3(5,5),
+         CT4(5,5),CN1(3,5),CN2(4,3),AA1(5),AA2(7),
+         AA3(7),AK(9),AL(12),CLSH(6),CVSH(6),CLTC(6),
+         AZ(12),BBZ(9,6),BL(4),PCRIT,TEMPK,BETA1,
+         NYZ(8),LYZ(8),NZZ(8,3),LUZ(8,2)
C-     COMMON /FLAGS/IF1,IF2,IF3,IF4,IF5,IF6,IF7,IF8,IF9,IF10,IF11,IF12
C-
C- SET UP LOOP TO CALCULATED THE PRESSURES OF EACH LIQUID NODE
C-
C-     DO 100 I=1,N
C-         TR=TEMPL1(I)/647.3
C-         SUM=0.0
C-         E=1.0-TR
C-         DO 10 II=1,5
C-             SUM=SUM+AK(II)*E**II
C-     10 CONTINUE
C-
C- DETERMINE BETA FUNCTION
C-
C-         BB=EXP(1.0/TR*SUM/(1.0+AK(6)*E+AK(7)*E**2.0)-(E/(AK(8)*
+         E**2.0+AK(9))))
C-         PRESL1(I)=BB*22120000.0
C-     100 CONTINUE
C-
C- DETERMINE VAPOR PRESSURES
C-
C-     DO 200 I=1,N
C-         TR=TEMPV1(I)/647.3
C-         SUM=0.0
C-         E=1.0-TR
C-         DO 150 II=1,5
C-             SUM=SUM+AK(II)*E**II
C-     150 CONTINUE
C-
C- DETERMINE BETA FUNCTION

```

```

C-
      BB=EXP(1.0/TR*SUM/(1.0+AK(6)*E+AK(7)*E**2.0)-(E/(AK(8)*
+      E**2.0+AK(9))))
      PRESV1(I)=BB*22120000.0
200  CONTINUE
      RETURN
      END
      SUBROUTINE VISFT

C-
C-----
C-
C-   SUBROUTINE VISFT:
C-
C-           THIS SUBROUTINE CALCULATES THE VISCOSITY OF THE
C-   LIQUID AND VAPOR FOR EACH NODE FROM A SIXTH DEGREE POLYNOMIAL
C-   FIT WITH TEMPERATURE USING PROPERTY DAT FROM COLLIER.
C-----
C-
      IMPLICIT REAL (A-H,O-Z)
      COMMON /TEMP/TEMPO1(100),TEMPO2(100),TEMPW1(100),TEMPW2(100),
+           TEMPL1(100),TEMPL2(100),TEMPV1(100),TEMPV2(100),
+           TEMPIN(1000),TEMPOUT(1000),NX
      COMMON /PROP/CONL(100),CONV(100),VISCOL(100),
+           VISCOV(100),REYNV(100),HDB(100),PRV(100)
      COMMON /GEOMHP/EVAPL,ADIAL,CONDL,DELZL,DELZV,DELZ,DELY,VOLL,
+           AREAL,AREAV,AREAC,WALLT,PWETV,PWETL,PWETC,
+           POPEN,WDIA,FWAR,DELPV,DELPL,N,NE,NA,NC,LAYERS,
+           NFAKE
      COMMON /COEFF/RR1(25),CF1(9),CF2(9),CF3(9),CG1(12),
+           CG2(9),CG3(7),CT1(2,4),CT2(5,5),CT3(5,5),
+           CT4(5,5),CN1(3,5),CN2(4,3),AA1(5),AA2(7),
+           AA3(7),AK(9),AL(12),CLSH(6),CVSH(6),CLTC(6),
+           AZ(12),BBZ(9,6),BL(4),PCRIT,TEMPK,BETA1,
+           NYZ(8),LYZ(8),NZZ(8,3),LUZ(8,2)

C-
C- SET UP LOOP TO CALCULATE VISCOSITY IN EACH NODE
C-
      DO 200 I=1,N
          SUML=0.0
          SUMV=0.0

C-
C- APPLY COEFFICIENTS FROM FIT
C-
          DO 100 J=1,7
              SUML=SUML+AA2(J)*TEMPL2(I)**(J-1)
              SUMV=SUMV+AA3(J)*TEMPV2(I)**(J-1)
100    CONTINUE
          VISCOL(I)=SUML
          VISCOV(I)=SUMV

C-
C- CONVERT VISCOSITY OF LIQUID FROM CENTIPOISE TO N-S/M2

```

C-

VISCOL(I)=VISCOL(I)\*1.0E-3

C-

C- CONVERT VISCOSITY OF VAPOR FROM CP\*1.0E-2 TO N-S/M2

C-

VISCOV(I)=VISCOV(I)\*1.0E-5

200 CONTINUE

RETURN

END

## APPENDIX F

### ENERGY EQUATION TERM DEFINITIONS

In the outer wall region energy equation, Equation 73, the terms are defined as

$$a = \frac{K_w}{\Delta x_{j-1}^2}$$

$$c = \frac{\rho_w C_{p_w}}{\Delta t} + \frac{K_w}{\Delta x_{j-1}^2} + \frac{K_w}{\Delta x_{j+1}^2} + \frac{2K_w}{\Delta z_1^2}$$

$$d = \frac{2K_w}{\Delta z_1^2}$$

$$e = \frac{K_w}{\Delta x_{j+1}^2}$$

$$f = \frac{\rho_w C_{p_w}}{\Delta t} T_{1,j}^n - H_{BC}$$

In the inner wall region energy equation, Equation 83, the terms are defined as

$$a = \frac{K_w}{\Delta x_{j-1}^2}$$

$$b = \frac{2K_w}{3\Delta z_1^2}$$

$$c = \frac{\rho_w C_p}{\Delta t} + \frac{2K_w}{3\Delta z_1^2} + \frac{K_w}{\Delta x_{j-1}^2} + \frac{K_w}{\Delta x_{j+1}^2} + \frac{2R}{3\Delta z_1}$$

$$d = \frac{2R}{3\Delta z_1}$$

$$e = \frac{K_w}{\Delta x_{j+1}^2}$$

$$f = \frac{\rho_w C_p}{\Delta t}$$

In the liquid region energy equation, Equation 91, the terms are defined as

$$a = \frac{K_{wL}^n}{\epsilon \Delta x_{j-1}^2}$$

$$b = \frac{R}{\epsilon \Delta z_2}$$

$$c = \frac{\rho_{Lj}^n C_{pLj}^n}{\Delta t} + \left(\frac{1-\epsilon}{\epsilon}\right) \frac{\rho_{wk} C_{p_{wk}}}{\Delta t} + \frac{R}{\epsilon \Delta z_2} + \frac{K_{wL_{j-1}}^n}{\epsilon \Delta x_{j-1}^2} + \frac{K_{wL_{j+1}}^n}{\epsilon \Delta x_{j+1}^2} + \frac{R_v}{\epsilon \Delta z_2}$$

$$d = \frac{R_v}{\epsilon \Delta z_2}$$

$$e = \frac{K_{wL_{j+1}}^n}{\epsilon \Delta x_{j+1}^2}$$

$$f = \left( \left(\frac{1-\epsilon}{\epsilon}\right) \frac{\rho_{wk} C_{p_{wk}}}{\Delta t} + \frac{\rho_{Lj}^n C_{pLj}^n}{\Delta t} \right) T_{3,j}^n + \frac{\rho_{L_{j+1}}^n h_{L_{j+1/2}}^{n+1} - \rho_{L_j}^n h_{L_{j-1/2}}^{n+1}}{\Delta x} - \frac{S_j^{n+1} h_v}{V_L}$$

In the vapor region energy equation, Equation 97, the terms are defined as

$$a = \frac{K_{v,j-1}^n}{\Delta x_{j-1}^2}$$

$$b = \frac{R_v}{\Delta z_3}$$

$$c = \frac{\rho_{vj}^n C_{vj}^n}{\Delta t} + \frac{R_v}{\Delta z_3} + \frac{K_{v,j-1}^n}{\Delta x_{j-1}^2} + \frac{K_{v,j+1}^n}{\Delta x_{j+1}^2}$$

$$e = \frac{K_{v,j+1}^n}{\Delta x_{j+1}^2}$$

$$f = \frac{\rho_{vj}^n C_{vj}^n T_{4,j}^n}{\Delta t} + \frac{S_j^{n+1} h_v}{V_v} + \frac{\rho_{vj-1}^n h_v v_{j-1/2}^{n+1} - \rho_{vj}^n h_v v_{j+1/2}^{n+1}}{\Delta x}$$

## APPENDIX G

### NOMENCLATURE

Symbol	Description	SI Units
A	area	m <sup>2</sup>
C <sub>p</sub>	specific heat at constant pressure	J/kg-K
C <sub>v</sub>	specific heat at constant volume	J/kg-K
D <sub>h</sub>	hydraulic diameter	m
e	total energy	J/kg
f	friction factor	-----
f(f <sub>1</sub> , R <sub>el</sub> )	wick aspect ratio	-----
F	body force per unit mass	m/s <sup>2</sup>
g	gravity	m/s <sup>2</sup>
h	enthalpy	J/kg
h <sub>fg</sub>	latent heat of evaporation	J/kg
h <sub>t</sub>	coolant heat transfer coefficient	W/m <sup>2</sup> -K
i	internal energy	J/kg
K	permeability	m <sup>2</sup>
K	thermal conductivity	W/m-K
l <sub>eff</sub>	effective length	m
L	liquid area	m <sup>2</sup>
m	mass flow rate	kg/s
M	molecular weight	kg/(kg-mole)
P	pressure	N/m <sup>2</sup>
P <sub>cmax</sub>	maximum capillary pumping head	N/m <sup>2</sup>

$\Delta P_g$	gravitational pressure drop	N/m <sup>2</sup>
$\Delta P_l$	liquid pressure drop	N/m <sup>2</sup>
$\Delta P_v$	vapor pressure drop	N/m <sup>2</sup>
Pr	Prandlt number	-----
P <sub>w</sub>	wetted perimeter	m
q"	energy flux	W/m <sup>2</sup>
Q	input thermal power	W
Q <sub>store</sub>	stored thermal power	W
r <sub>crit</sub>	minimum radius of curvature	m
R	universal gas constant	J/(kg-mole)K
Re	Reynolds number	-----
S	evaporation/condensation mass flow rate	kg/s
t	time	s
T	temperature	K
v	velocity	m/s
V	volume	m <sup>3</sup>
w	width of flow channel	m
W	wall area	m <sup>2</sup>
x	horizontal distance	m
z	vertical distance	m

GREEK

$\delta$	height of flow channel	m
$\epsilon$	liquid volume fraction	-----
$\rho$	density	kg/m <sup>3</sup>
$\mu$	viscosity	N-s/m <sup>2</sup>

$\lambda$	stored energy time constant	$s^{-1}$
$v$	specific volume	$m^3/kg$
$\sigma$	surface tension	$N/m$
$\theta$	angle measured from the heat pipe to the horizontal axis	radian

#### SUBSCRIPTS

b	bulk coolant
bcl	liquid boundary condition
bcv	vapor boundary condition
BC	boundary
c	coolant
g	gravity
j	axial node location
l	liquid
m	number of axial nodes
sat	saturation
v	vapor
w	wall
wick	wick
wL	wick-liquid
x	horizontal position
z	vertical position
1	outer wall node
2	inner wall node
3	liquid node
4	vapor node

## SUPERSCRIPTS

n            time step

→            vector notation